INVESTIGATION OF DNA DAMAGE RESPONSE AT INTERSTITIAL TELOMERIC SITES IN CHINESE HAMSTER CELL LINES

A thesis submitted for a degree of Doctor of Philosophy

by

Sheila Matta Castillo

College of Health and Life Sciences
Department of Life Sciences
Brunel University

July 2018

Declaration

I hereby declare that the research presented in this thesis is my own work, except where otherwise specified, and has not been submitted for any other degree.

Sheila Matta

July 2018

Abstract

Telomeres are highly specialised structures that protect the ends of linear chromosomes from damage. Telomeric DNA consists of tandem repeats of a specific sequence (TTAGGG)n that varies in length depending on the species. Two telomere maintenance mechanisms are known to exist. Telomerase, an enzyme that synthesises new tandem repeats onto the end of linear chromosome and ALT (Alternative Lengthening of Chromosomes), which uses recombination to lengthen telomeric sequences. In some mammalian species, both mechanisms are known to co-exist. Telomeric DNA that is found at non-telomere sites are referred to as interstitial telomeric sequences (ITS). Several studies have shown that ITS sites in the Chinese hamster are preferred sites for radiation and spontaneous chromosomal damage. Once damage occurs, repair mechanisms such as HR (homologous recombination) and NHEJ (non-homologous end joined) are activated. However, the contribution to this repair by telomerase and ALT is unknown. The aim of this work therefore is to investigate the contribution that above mention mechanisms (HR, NHEJ, telomerase and ALT) make to ITS repair in Chinese hamster cells.

Classical cytogenetic techniques such as Giemsa staining, chromosomal aberration analysis, FISH (Fluorescence in situ hybridazation, IHC (Immunohistochemistry), TIF (Telomere dysfunction induced foci), were used to quantify chromosomal damage after IR (ionising radiation) treatment of normal and repair deficient (HR and NHEJ) Chinese

hamster cell lines. Molecular analysis employed the TRAP assay, and C-circle analysis to look at telomerase expression and ALT activity. Finally, siRNA was used to look at two genes which are important in the telomere maintenance pathways, ATRX and HDAC9, were knocked down using siRNA and cells were analysed using Western blotting and qPCR for the effects this had on telomerase and ALT.

Our results show that chromatid breaks within ITSs sites were higher than expected in repair deficient cell lines. In addition, repair deficient cells recover more slowly to IR chromosomal damage than control cells, suggesting that HR and NHEJ play a part in the repair of ITS in Chinese hamster cells. siRNA knockdown revealed that ATRX and HDAC9 affected the expression of ALT and telomerase respectively in our cell lines. Taken together, our work provides evidence that show for the first time the co-existence of both telomerase and ALT activity in Chinese hamster cells.

TABLE OF CONTENTS

LIST OF FIGURES

LIST OF TABLES

Acknowledgements

This thesis would not have been possible without the help and great support of the kind people around me. I would like to express my deepest gratitude to my supervisor, Dr Predrag Slijepcevic for his unfailing guidance, support and advice throughout my research project. He has shared his expertise and knowledge with me through insightful discussions and has always encouraged me to think independently on this project. I would like to thank my second supervisor Dr Uday Kishore for his advices and positive comments.

I would also like to extend my gratitude to Dr Terry Roberts for his expert advice on RT-PCR that was a milestone in the completion of this project and sharing his priceless troubleshooting tips with me. I want to thank Dr Thomas Hoefken for his comprehensive Western blot training and his helpful advised on transfer big size proteins without losing my nerves.
I would like to acknowledge friends and colleagues I have met throughout this long journey for keeping a refreshing working atmosphere. I would especially like to thank my generous friends, Chrissi, Haroon, and Ezgi for their endless jokes, optimisms and tough me how to be resilient and kept a smile despite the experiment outcomes and continue trying to learn.

Finally, I would like to thank my family, Mercedes, Jaime and Harold for their constant support, unconditional love, patience and encouragement. They have faith in me and always trying to understand when I missed important moments. I know I always have my family to count on when times are tough and I love them very much.

ABREBIATIONS

ALT	Alternative lengthening of telomeres
ATR	ATM and Rad3 related proteins
ATRX	Alpha Thalassemia X-linked mental retardation syndrome
BSA	Bovine serum albumin
cDNA	complementary DNA
DDR	DNA damage response
DMEM	Dulbecco modified eagle medium
DMSO	Dimethylsulfoxide
dNTP	Deoxynucleotide triphosphate
CA	Chromosome aberrations
DSB	Double strand break
HR	Homologous recombination
NHEJ	Non-homologous end-joined
DNA-PKcs	DNA dependent protein kinases catalytic subunits
TRF1	Telomeric repeat-binding factor 1
TRF2	Telomeric repeat-binding factor 2
POT1	Protection of telomeres 1
TPP1	TIN2-interacting protein
RAP1	Repressor and activator protein 1
TIN2	The TRF1-interacting nuclear protein 2
TIFs	Telomere dysfunction induce foci
TERT	Telomerase reverse transcriptase
TERC	Telomerase RNA
DKc1	Dyskeratosis congenita 1
hTERT	Human telomerase reverse transcriptase
IR	Ionising radiation
H+	Hydrogen
OH-	Hydroxyl ions
H_2O_2	Hydrogen peroxides
MRN	MRE1-RAD50-NBS1 complex
RPA	Replication protein A
BRCA2	Breast cancer type 2
Pol	lambda DNA polymerase lambda
ITRS	Interstitial telomeric repeat sites
FISH	Fluorescence in situ hybridization
Rb	Robertsonian
ATM	Ataxia telangiectasia mutated protein
PNA	Peptide nucleic acid
PBS	Phosphate buffer saline

PD	Population doubling
PCR	Polymerase chain reaction
RNA	Ribonuclei acid
RPA	Replication protein A
RPM	Rotations per minute
RT-PCR	Reverse transcriptase polymerase chainreaction
SDS	Sodium dodecyl sulphate
siRNA	short interfering ribonucleic acid
SSB	Single strand breaks
TBST	Tris-buffered saline tween-20
TERT	Telomerase reverse transcriptase
TIFs	Telomere dysfunction
T-loop	Telomere loop

"No puedes poner los pies en la tierra hasta que no has tocado el cielo…
y las historias solo suceden a quienes son capaces de contarlas"

Paul Auster

Chapter 1.

General Introduction

1. Introduction

This dissertation is focused on mechanisms of DNA damage and repair at interstitial telomeric sites (ITSs). As their name suggests, ITSs are derived from DNA sequences present at chromosome ends or telomeres. This introductory section is divided into two parts. The first part deals with the biology of telomeres, mechanisms behind telomere maintenance and the origin of ITSs. The second part deals with mechanisms of DNA damage response and how telomere maintenance integrates with these mechanisms. Of particular concern is the specificity of DNA damage processing at ITSs, which differs from DNA damage processing in other regions of the genome. It is important to stress that ITSs are universally present in mammalian genomes. In this project we used exclusively cells from Chinese hamster (Cricetulus griseus) because their ITSs are cytological markers and are well defined and can be easily visualized by standard cytogenetic analysis.

1.1 Telomeres: caps at the linear ends

Telomeres were described more than 70 years ago by Herman J. Muller and Barbara McClintock as “terminal gene” or “natural ends” located at the end of chromosomes (review by Gall, 1995). Muller coined the term “telomeres” that derives from two Greek words telos (end) and meros (part) (Muller, 1938). Muller’s (1938) and McClintock’s (1941) pioneer studies on Drosophila melanogaster and Zea mays respectively, showed chromosomal deletions, inversions and fusions after X-ray irradiation (McClintock, 1941). These observations suggested that telomeres are specialized structures that protect or “cap “chromosome linear ends from fusion and recombination and thus must be essential for chromosomal stability.

1.2 Telomere structure

Telomeres overcome the end-replication problem with telomerase, a reverse transcriptase enzyme that uses its own RNA template to synthesis the G-rich telomeric DNA strand of the telomeres. Telomerase was first identified in the ciliate, Tetrahymena (Fernández and Gosálvez, 2002). In humans, telomere length is estimated at about 5 to 15kb in primary cells, while in mouse and rat cells telomere length usually ranges from 20 to 50kb (Wu, Lee and Chen, 2000; Balakin, Smith and Fournier, 1996). Telomeric DNA consists of a stretch of tandem (TTAGGG)n repeats that are conserved among eukaryotes (Blackburn, 1991) (Figure1.1). These repeats are guanosine and cytosine-rich strands; double stranded G-rich is oriented 5' to 3' towards the chromosomal terminus and elongates and forms single stranded 3' DNA overhang structure known as G-rich tail (Henderson and Blackburn, 1989). The G-strand overhangs length varies between species such as in ciliated protozoans about 16 bp (Rapić-Otrin et al., 2003), and S.Cerevisiae with 30bp, whereas in humans G-strand overhang is estimated at between 45 and 275bp (Hemann and Greider, 1999; Makarov, Hirose and Langmore, 1997). The G-strand overhang invades into double strand DNA forming a D-loop, and then the telomere ends folds back on itself and forms a large telomeric loop known as T-loop structure (Griffith et al., 1999), stabilized by G-quadruplexes (Phan and Mergny, 2002). A visual representation of a T-loop is presented in Figure 1.1. It is important to emphasize that the T-loop structure was discovered only when it became possible to analyze telomeric chromatin by electron microscopy after extensive biochemical preparation (Griffith et al. 1999). The t-loop allows the sequestration of the G-strand overhang and prevents the DNA ends to be recognized as broken ends thus preventing the activation of DNA damage repair signaling (Griffith et al., 1999). T-loop formation and stabilization are mediated by the telomeric binding proteins (Figure 1.1 B) (Griffith et al., 1999).

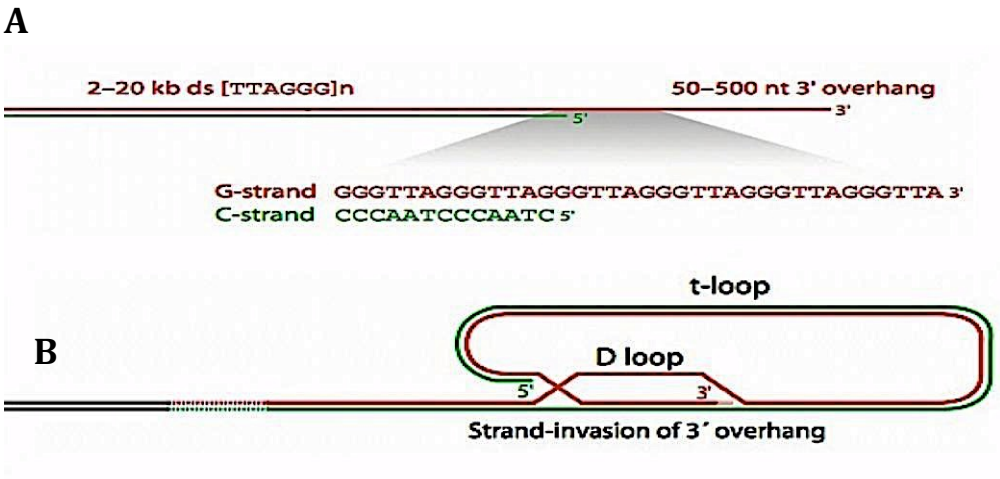

Figure 1.1 A) Schematic representation of human telomeres end showing the 3'G-rich overhang, which varies from 50 to 500 nucleotides in length. **B)** A schematic image of telomere invasion into DNA double strand and fold back on itself and gives rise to T-loop structure. Image taken from Palm and de Lange, (2008).

1.3 G-quadruplex structure

The G-quadruplex is comprised of four guanines that are associated by cyclic Hoogsteen hydrogen bonding in a planar configuration, and the structure strongly depends on monocations, such as K^+ and Na^+ (Figure 1.2) (Knight et al., 1999). These G-quadruplex structures are found as parallel and antiparallel depending on the number of G-tracts in the strand; four strands or the dimerization of two strands, respectively (Han and Hurley, 2000; Rhodes and Giraldo, 1995). Therefore, G-quadruplexes have been involved in telomere protection, suppression of recombination and they inhibit the access of telomerase to telomeres (Wang and Meier, 2004). Recently, G-quadruplex studies have identified a small molecule ligand based on ruthenium (Ru) that bind and stabilize the G-quadruplexes structures, and by doing so prevent telomerase access to telomeres with profound effects on cancer cells (Li et al., 2014).

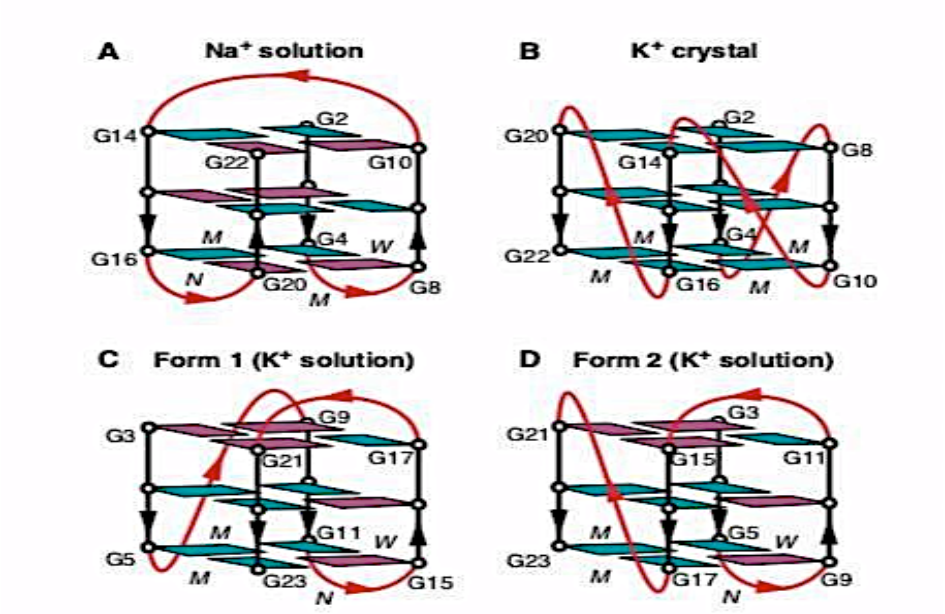

Figure 1.2 Schematic representation of intramolecular G-quadruplexes formed by human telomeric DNA. It has been reported multiple human G-quadruplex forms in physiological K^+ solution conditions. **A)** $AGGG(TTAGGG)_3$ in Na^+ solution; **B)** $AGGG(TTAGGG)_3$ in K^+ containing crystal; **C)** $AGGG(TTAGGG)_3$ in K^+ solution (natural form 1) and **D)** $AGGG(TTAGGG)_3$ TT in K^+ solution (natural form 2). Image obtained **from** Phan et al., (2007).

1.4 Telomere function

Telomeres are nucleoprotein complexes located at the ends of linear eukaryotic chromosomes (Bessler, Wilson and Mason, 2004). These nucleoprotein structures have essential functions, including, protection from recombination, exonuclease degradation and they prevent end-to-end fusions between chromosomes (Blasco et al., 1997; Blackburn, 1991). Telomeric sequences progressively shorten with each cell cycle, due to end replication problem. The loss amounts to approximately 50 to 100 nucleotide base pairs per cell division and eventually causes cells to enter replicative senescence (Harley, 1991). Conventional DNA polymerases are unable to replicate the 3'end of the linear duplex DNA. Telomeres overcome the end-replication problem with telomerase, a reverse transcriptase enzyme that uses its own RNA template to synthesis the G-rich telomeric DNA strand of the telomeres. Telomerase was first identified in the ciliate, Tetrahymena (Fernández and Gosálvez, 2002).

1.4.1 Telomeres and Shelterin complex

Mammalian telomeres are stabilized and specifically bound to a group of six proteins known as the shelterin complex (de Lange, 2005; van Steensel, Smogorzewska and de Lange, 1998). This complex is composed of six proteins; TRF1, TRF2, TIN2, Rap1, TPP1 and POT1 (Figure 1.3). Three of the shelterin proteins have shown specificity and direct binding to TTAGGG tandem repeats (Donate and Blasco, 2011). The telomeric repeat-binding factor 1 and 2 (TRF1 and TRF2) directly bind to doublestranded telomeric DNA, while the protection of telomeres 1 (POT1) binds to the single-stranded G-strand overhang of telomeres (Nandakumar and Cech, 2013; Palm and de Lange, 2008). TRF1 and TRF2 have been initially identified at mammalian telomeres (Meier, 2005). Both TRF1 and TRF2 proteins specifically bind the doublestranded telomeric DNA through a conserved C-terminal Myb DNA binding domain and can form homodimers (Figure 1.3) (Balakin, Smith and Fournier, 1996). However, TRF1 and TRF2 clearly differ in their N-terminus residues acidic and basic, respectively. TRF1 is ubiquitously expressed throughout the cell cycle and it is located only at telomeres (Balakin, Smith and Fournier, 1996). TRF1 protein is capable of bending its telomeric site to an angle of 120^{o}, hence promotes the formation of the Tloop structure (Venteicher et al., 2008).

In addition, TFR1 is a cis acting inhibitor of telomerase activity; it performs this function by limiting its access to the G-strand overhang. Therefore, TRF1 acts as a negative regulator of telomere length maintenance through telomerase inhibition at telomeres (Wu, Lee and Chen, 2000). Interestingly, the TRF1 defective mouse model (mTRF1-/-) exhibits telomere shortening, apoptosis or senescence, along with end-toend fusions between chromosomes (Iwano et al., 2004).

The key role of TRF2 at telomeres is to stabilize and maintain the unpaired G-strand overhang, thereby protecting chromosome ends from end-to-end fusion (van Steensel, Smogorzewska and de Lange, 1998). TRF2 protects short telomeres from end-to end fusion and delays entry into senescence (New et al., 1998). In addition, TRF2 similarly to TRF1 act as negative regulator of telomere length when overexpressed in human and mouse cells (Wu, Lee and Chen, 2000; Stuurman et al., 1992). For example, TRF2 overexpressing transgenic mice show telomere shortening and loss of G-strand overhang (Munoz et al., 2005), an effect similar to a defect in XPF, a protein responsible for the genetic disease Xerdorema pigmentosum (XP) (Wood et al., 2001). Cells from XP patients have defect in NER (nucleotide excision repair) (Rapić-Otrin et al., 2003; Cleaver, 1968). In human cells, deletion of TRF2 from telomeres leads to chromosome abnormalities such as, anaphase bridges and multiple chromosome end fusions, due to the degradation of the G-rich overhang that leads to the activation of the DNA damage response (van Steensel, Smogorzewska and de Lange, 1998). It has also been shown that TRF2 is capable of moving from telomeres at internal non-telomeric genomic regions after exposure of cells to DNA damage (Baker et al., 2011; de Lange, 2005). This suggests a potential active involvement of TRF2 in DNA damage response.

In humans, POT1 is regulated by TRF1. POT1 forms a complex with TIN2-interacting protein (TPP1). The POT1-TPP1 complex increases its affinity for binding to the G-rich tail (Chen, Liu and Songyang, 2007; Colgin et al., 2003). POT1 has affinity for a single stranded telomeric repeat $(TTAGGG)_n$, it binds the G-rich tail and protects telomeres from degradation (Colgin et al., 2003), and regulates telomere length and telomere capping (Pearson et al., 2000).

POT1 in mouse contains two subtypes, Pot1a and Pot1b. Double knock-down in mouse cells causes increased telomere dysfunction and chromosome reduplication, possibly as a dysfunction of 5' single strand DNA end at telomeres (Guo et al., 2000; Mu et al., 1997). Additionally, POT1 prevents the activation of ATM/ATR pathway by repressing the binding of RPA to telomeres (Bailey, Brenneman and Goodwin, 2004; Loayza and de Lange, 2003).

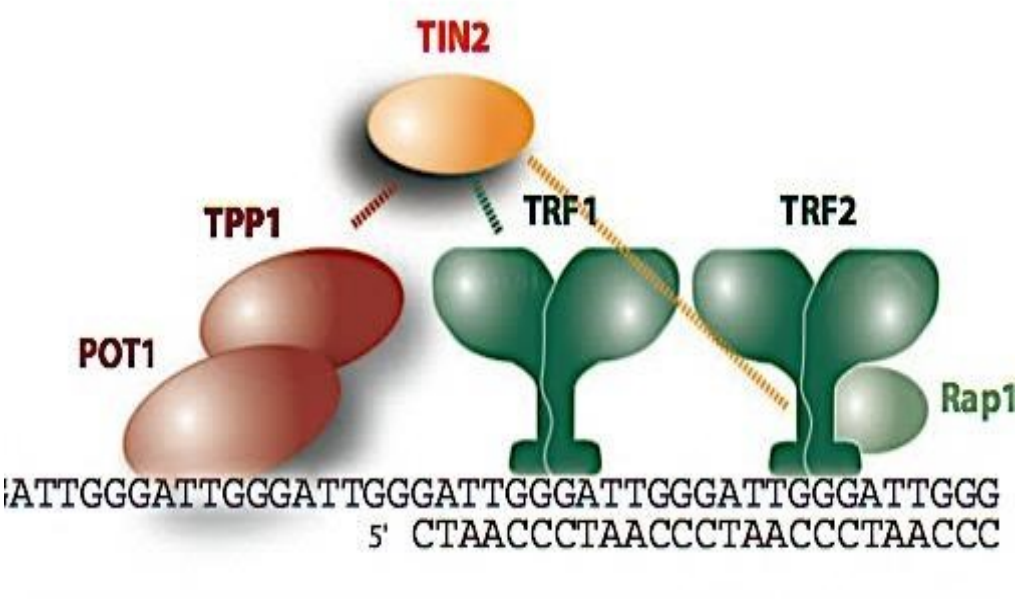

Figure 1.3. Schematic representation of the six telomeric proteins, shelterin, assemble and it can be observed that TRF1 and TRF2 bind to the double strand of telomeric DNA, while POT1 binds to the single telomeric strand. Image taken from Palm and de Lange, (2008).

The repressor and activator protein 1 (RAP1) is a protein that forms a stable complex with TRF2, due to its lack of DNA binding domain (Moyzis et al., 1988). In humans, RAP1 (hRAP1) complex controls telomere length and prevents telomere fusions by inactivating DNA damage response pathways, homologous recombination (HR) and non-homologous end joined (NHEJ) (Bae and Baumann, 2007). Rap1 deficient transgenic mice show that Rap1 is not necessary for mouse viability but instead Rap1 is required for HR repression (Allshire et al., 1988).

The TRF1-interacting nuclear proteins 2 (TIN2) binds to the TRF1 homodimerization domain, and also associates with the TRF2 protein and together modulate and limit the access of telomerase to telomeres, thus regulating telomere elongation (S. H. Kim et al., 2003).

TIN2 overexpression inhibits telomere elongation in human cells, while the TIN2 N-terminal deletion shows aberrant telomere elongation (Chiang et al., 2004). In addition, the TIN2 knockout mouse suffers from embryonic lethality, which suggest that TIN2 is required during embryogenesis (Chiang et al., 2004).

TPP1 is a multi-domain protein which contains an OB-fold domain that facilitates the interaction of telomerase with telomeres by forming a heterodimer complex with POT1 (Rajavel, Mullins and Taylor, 2014). The POT1-TPP1 complex recruits and enhances telomerase activity and influences telomere length (Rajavel, Mullins and Taylor, 2014; Yang et al., 2013). In addition, TPP1 is required in the formation and stabilization of the TRF1-TIN2 and TF2 complex. Interestingly, in relation to TPP1 interaction with telomerase, deletion of Tpp1 in MEFs (mouse embryonic fibroblasts) result in decreased TERT (telomerase catalytic component) binding to telomeres that cause an increase in telomere shortening (Hastie and Allshire, 1989). Moreover, Tpp1 deletion induces a robust DNA damage response at telomeres mediated by ataxia telangiectasia and rad3 related (ATR) and leads to an excess of single G-strand overhang (Flint et al., 1994).

1.4.2 The end replication problem

Telomere physical configuration with its 3' single strand end poses a challenge to the DNA replication machinery. Conventional DNA polymerases cannot replicate the very end of the linear chromosome and this is known as the end-replication problem (Lamb et al., 1993). During the conventional DNA replication, the 3'end is synthesized by the leading strand synthesis, while the 5'end is synthesized by the lagging strand synthesis. The lagging strand synthesis involves RNA primers that are extended by DNA polymerase to form the Okazaki fragments (Bouffler et al., 1993). After removal of RNA primers, DNA ligase and DNA polymerase enzymes ligate the Okazaki fragments to form a continuous DNA strand (Silver and Cox, 1993). The removal of the distal RNA primer leaves a small region at the chromosome termini, in which no complementary strand can be synthesized (Ohki, Tsurimoto and Ishikawa, 2001). The size of this gap has been estimated at 8-12 bp, which roughly corresponds to the size of an RNA primer. However, the size of a single-stranded overhang at telomeres is in the region of up to 200 bp (Counter et al., 1992; Harley, Futcher and Greider, 1990). This suggests that additional enzymatic activity is required to convert a short overhang (8-12 bp) into a much longer one (up to 200 bp). Such an activity has been identified in the form of an exonuclease capable of degrading an opposite single strand (Makarov, Hirose and Langmore, 1997). As a result of exonuclease activity specific for telomeres, all chromosome ends possess long single strand overhangs. A diagrammatic representation of end replication problem is shown in Figure 1.4.

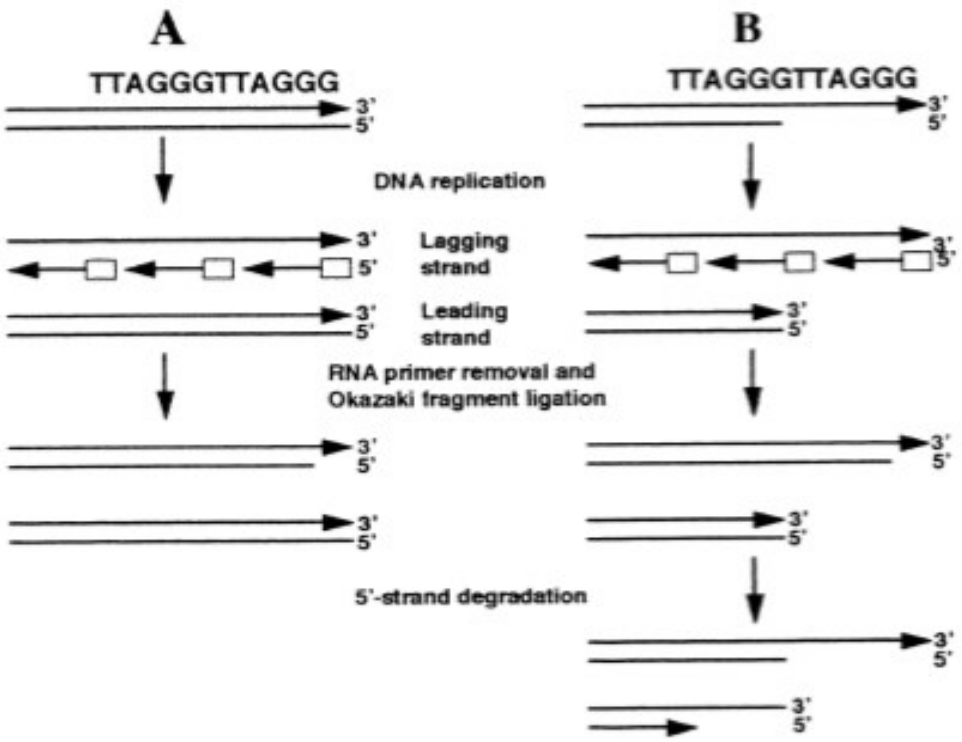

Figure 1.4 Schematic representation of telomere replication. **A)** Conventional model (Lingner et al. 1995) and **B)** Revised model (Makarov et al. 1997). The lagging strand synthesis produces a series of Okazaki fragments attached to short RNA primers. The conventional model suggests that degradation of primers; gap repair and ligation would result in a gap at 5'end so-called end replication problem. The revised models show that DNA is lost from both ends of the chromosomes and leads in long 3'end overhangs at both ends. Image obtained from P. Slijepecevic, (1997).

1.5 Telomerase

The de novo synthesis of telomeric sequences is accomplished by the reverse transcriptase ribonucleoprotein enzyme, telomerase. Greider and Blackburn discovered telomerase in tetrahymena thermophile ciliate protozoa (Fernández and Gosálvez, 2002). Telomerase is highly conserved among eukaryotes and consists of two major subunits, telomerase reverse transcriptase (TERT) a catalytic subunit and telomerase RNA (TERC) that serves as an RNA template for TERT (Mosquera et al., 2005). Furthermore, several smaller telomerase components have been identified.

1.5.1 Telomerase structure and functions

1.5.2 hTERT (human TElomerase Reverse Transcriptase)

hTERT protein is encoded by the hTERT gene located at chromosome 5p15.33 and consists of 16 exons and 15 introns spanning about 40kb of genomic DNA (Simonet et al., 2011). The hTERT promoter is GC-rich and lacks TATA or CAAT boxes (Rovatsos et al., 2011), but contains binding sites for several transcription factors, including binding sites for the c-Myc oncogene (Aksenova et al., 2013). hTERT is highly regulated and absent or present at low levels in somatic cells but expressed in germ cells, embryonic cells and in a subset of stem cells (Gazy and Kupiec, 2013; F. T. Kao and Puck, 1968). In addition, regulatory elements have been found at the 5' end of the hTERT genomic region extending from 330bp upstream of the ATG and 37 bp of exon 2 of the gene (Zakian, 1995). Interestingly, the myc oncogene induces hTERT expression and elevates telomerase levels in malignant tumours (Aksenova et al., 2013; Kim et al., 1994).

1.5.3 hTERC (human TElomerase RNA Component)

hTERC gene maps to the 3q26.3 region of chromosome 3 and is 451 nucleotides in length (Soder et al., 1997; Zhao et al., 1998). hTERC consists of three conserved structural domains; the template or pseudoknot domain which contains the template for telomeric DNA synthesis, stem loop CR4-CR5 (Chen, Blasco and Greider, 2000), and the small Cajal body RNA domain (Sijen et al., 2001; Jordan, Oroskar and Sedita, 1995). The hTERC is ubiquitously expressed in both the normal and tumour cells (Feng et al., 1995), but appears to be up-regulated in tumour cells (Heiss et al., 1998). Interestingly, inhibition of hTERC down-regulates glycolytic pathway genes and alter cellular morphology (Bagheri et al., 2006). Other components of telomerase include a protein called Dyskerin, encodes by the DKC1 gene and it is a highly conserved protein

(Knight et al., 1999). Dyskerin binds to the hairpin H/ACA motifs and mediates pseudouridylation of ribosomal RNA, which is needed for hTERC nuclear accumulation (Wang and Meier, 2004). Mutations in DKC1 gene cause dyskeratosis congenita (DC) syndrome, which is an inherited disorder characterized by bone marrow failure and hypersensitivity to cancer (Bessler, Wilson and Mason, 2004; Heiss et al., 1998). Therefore, dyskerin is essential for nuclear accumulation of hTERC and for the formation of the telomerase complex. In addition to dyskerin, three small basic proteins, NOP10, GAR1 and NHP2 are associated with H/ACA motif (reviewed by Meier, 2005). These proteins are located in the nucleoli and Cajal bodies of mammalian cells. Together they interact with the telomerase complex where they are involved in its maturation. Another two ATPase enzymes have been identified to be associated with telomerase, reptin and Pontin. Both enzymes interact directly with dyskerin and hTERT to form a TERT-pontin-reptin complex. Pontin and reptin have been shown to be critical for telomerase activity and for accumulation of dyskerin and hTERC (Venteicher et al., 2008). These proteins interact with telomerase complex and they are involved in its maturation and trafficking.

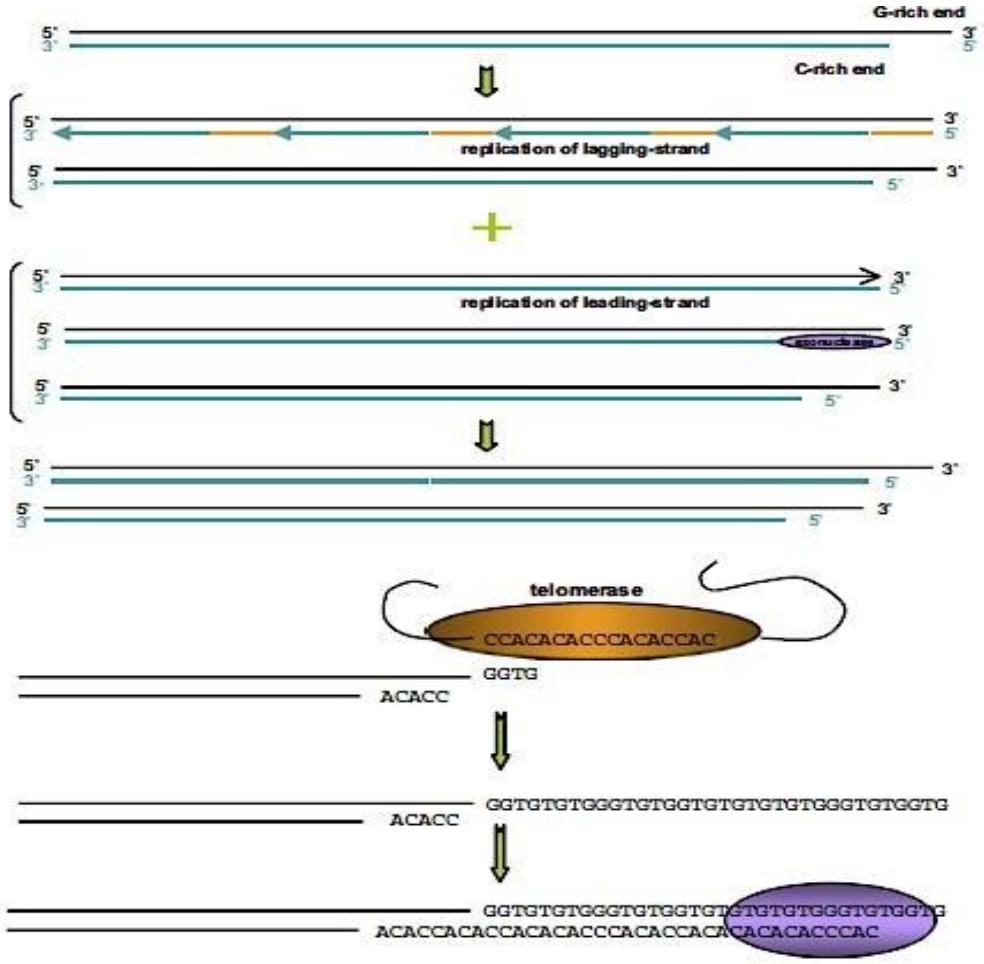

Figure 1.5 Schematic representation of the telomere replication. In the upper-middle, the linear ends cannot be replicated by the DNA polymerase machinery and results in the single 3'overhang lagging strand due to lack of RNA primer. To leads to the synthesis of the Okazaki fragment at the linear end during the generation of a new daughter cell, which is know as the end replication problem. In lower-middle shows a holoenzyme telomerase that binds to the 3'overhang, which is complementary to its own RNA template and extend the 3'single strand by adding nucleotides, which are joined and sealed by the DNA polymerases at the linear ends. Image obtained from Grandin and Charbonneau, (2008).

1.6 Telomerase and cancer

In humans, telomerase activity is tightly regulated by TERT and telomerase is mainly detected in stem cells compartments and embryonic cells, whereas telomerase expression is low or absent in somatic or differentiated cells (Gazy and Kupiec, 2013; Zakian, 1995). A positive correlation between TERT mRNA expression and telomerase activity indicates that telomerase activity is tightly regulated by the rate of transcription of the TERT gene (Zakian, 1995). One of

the hallmarks of cancer is the evasion of replicative senescence and proliferation that leads to immortalisation through reactivation or up-regulation of telomerase in somatic cells (Liu et al., 2004). In the majority of cancers (approximately 85 to 90%) telomerase is active and it stabilizes the shortening of telomeres, and thus provides an indefinite proliferative potential to cancer cells (Kim et al., 1994). However, a small number of cancer cells (10 to 15%) use a telomerase independent system, alternative lengthening of telomere (ALT), based on recombination mechanisms (Neumann and Reddel, 2002). Telomerase role in cancer has been unravelled through the use of mutated telomerase components such as mutant hTERT that shows telomere loss and limited cell growth in cancer cells, leading to senescence and apoptosis (Hahn et al., 1999). A mutant TERC (Terc $^{-/-}$) mouse model has shown telomere shortening, proliferative tissues defects, short lifespan and chromosomal instability in each generation until it reaches infertility, due to defect in meiosis caused by shortening of telomeres (Blasco et al., 1997). The re-introduction of the TERC gene into mutant Terc-/- mouse has rescued cells from replicative senescence and stabilized telomere length and corrected the ageing phenotype in mice (Samper, Flores and Blasco, 2001).

1.7 Ectopic expression of telomerase in human cells

It has been shown experimentally that restoration of hTERT allows human fibroblast to proliferate beyond senescence limit, despite telomere elongation (Mason, Wilson and Bessler, 2005). hTERT immortalized cells exhibit shorter telomeres than normal cells. However, telomerase activation results in a stable and homogenous telomeres length in spite of telomeres being short relative to normal somatic cells (Vaziri and Benchimol, 1999). For example, ectopic expression of hTERT induces proliferation in HMEC cell lines through up-regulating the levels of epidermal growth factor receptor (EGFR) signalling (Smith, Coller and

Roberts, 2003). In addition, hTERT in HMEC antagonizes transforming growth factor (TGF) and down-regulates the expression of antigrowth factor (Geserick et al., 2006; Stampfer et al., 2001). Therefore, hTERT enhances cell proliferation and promotes cellular resistance to antigrowth signalling.

1.8 Alternative lengthening of telomeres (ALT)

Telomerase negative cancer cells maintain their telomere length by an alternative lengthening of telomeres mechanism (Bryan and Reddel, 1997). ALT mechanism uses recombination mediated DNA replication. It was first observed in S. cerevisiae cells that completely lacked telomerase (Lundblad and Blackburn, 1993). These yeast cells have a poor cellular phenotype that resembles human ALT cells. It is known that ALT is dependent on homologous recombination genes such as RAD50 and RAD52 (Teng and Zakian, 1999). The ALT activity has been found in a small proportion of human immortalized cancer cells and telomerase null mouse cell lines (Henson et al., 2002; T. M. Bryan et al., 1995). The ALT cancer cells usually originate from mesenchymal tissues, including bone, soft tissues, neuroendocrine systems and central nervous system (Dilley and Greenberg, 2015; Heaphy et al., 2011; Henson and Reddel, 2010). It is not known why ALT tumours are of a mesenchymal origin. However, it has been speculated that a tight regulation of telomerase in mesenchymal tissue may force the cells to activate ALT (Dilley and Greenberg, 2015; Zimmermann et al., 2003). Human ALT cells are characterized by specific telomeric phenotype that includes heterogeneous telomere lengths ranging from very short (1kb) to very long (40kb) (T. M. Bryan et al., 1995).

1.8.1 Alternative lengthening of telomeres hallmark

The hallmark of the ALT mechanism is the presence of APBs. APBs are detected in ALT cell lines and tumours. APBs contain PML proteins that colocalize with telomeric DNA and telomere binding protein hTRF1 and hTRF2 (Yeager et al., 1999). PML nuclear bodies (PNBs) are nuclear protein structures that are present in many tissues (Stuurman et al., 1992), and are involved in a wide range of cellular processes, including tumour suppression, cell cycle regulation, senescence, apoptosis and inflammatory response (Pearson et al., 2000; Guo et al., 2000; Mu et al., 1997). PNBs function by releasing and sequestering proteins close to the site of action and enhancing protein-protein interactions (Henson et al., 2002). In contrast to PNBs, APBs contain proteins associated with DNA repair, recombination and replication, such as replication factor A, RAD51, RAD52, NSB1, SP100, BML, WRN as well as TRF1 and TRF2 (Wu, Lee and Chen, 2000; Yeager et al., 1999; New et al., 1998). In addition, APBs appear in ALT cells with heterogeneous telomere length but disappear when ALT activity is repressed in somatic hybrid cells (Perrem et al., 2001; Yeager et al., 1999).

ALT-associated PML bodies (APBs) are found in most ALT positive human cells and present themselves as distinct PML foci and telomeric DNA (Yeager et al., 1999). Mutations in the ATRX gene (Tang et al., 2004), and increased frequencies of T-SCEs (Londono-Vallejo et al., 2004), are also characteristics of ALT positive cells. Furthermore, ALT cells contain extrachromosomal telomeric DNA, which adopts many forms such as double stranded telomeric circles (t-circles) and the single stranded circles (C-circles) (Nabetani and Ishikawa, 2009; Cesare and Griffith, 2004).

Several studies have shown a limited coexistence of telomerase and ALT in vitro in human cells (Cerone, Londono-Vallejo and Bacchetti, 2001; Perrem et al., 2001). It has been shown that the ectopic expression of hTERT in the ALT positive cell line, GM847, contributes to telomere homeostasis together with ALT (Perrem et al., 2001). However, reduced ALT activity and repressed APBs foci along with disappearance and reduction of telomere length occurred when GM847 cells were fused with telomerase positive or normal fibroblast cells. This means that ALT repression factors are potentially present in these cells (Perrem et al., 2001; Perrem et al., 1999).

ALT positive cells are characterized by elevated frequency of telomere recombination which can be assessed by measuring frequencies of telomere sister chromatid exchanges (T-SCEs). These T-SCEs are detected by a strand specific in situ hybridization technique known as chromosome orientation FISH (CO)-FISH (Bailey, Brenneman and Goodwin, 2004). This technique yields a distinct telomere signals pattern, one on each end of the chromatids for lagging and leading strands (Bailey et al., 2001). High rate of T-SCEs splits the hybridization probe between sister chromatids, generating a three-telomere hybridization pattern (Bailey, Brenneman and Goodwin, 2004; Bailey et al., 2001). It is thought that a lesion in the replication fork may trigger recombinational repair in one of the parental strands. This leads to unequal exchanges of telomeric DNA between chromatids (Bailey, Brenneman and Goodwin, 2004).

The mechanism and causes of ALT are still not well known. It has been shown that specific proteins may trigger ALT activation. A typical example is mutation in the gene encoding for the alpha thalassemia-mental retardation syndrome X- linked protein (ATRX). The ATRX is a chromatin-remodelling factor of the Snf2 family and it is closely related to RAD54 (Gibbons et al., 1995). ATRX binds to Death-Domain Associated protein (DAXX), which acts as specific

chaperon protein for histone H3.3 and together form the ATRX/DAXX/H3.3 complex (Drane et al., 2010). The majority of ALT cancer cells have shown recurrent mutations in genes encoding the ATRX/DAXX complex have been shown to influent ALT activation and maintenance (Heaphy et al., 2011). However, siRNA ATRX in human immortalized cell cultures and tumour cells is not enough to generate ALT phenotype, therefore suggesting that additional genetic or epigenetic modifications are required for cells to begin ALT (Wong et al., 2010; Fling et al., 2015). In this regard, transient ATRX expression repressed ALT mechanism and thus indicates that loss of ATRX function is necessary but not sufficient to trigger ALT (Napier et al., 2015).

Recent studies in mice have shown that the alterations in telomeric and subtelomeric heterochromatin lead to an increase frequency of T-SCE and telomere elongation, thus inducing phenotypic characteristic of ALT (Conomos et al., 2013; Gonzalo et al., 2006). For example, Dnmt (DNA methyltransferases) deficient and telomerase deficient Terc-/-mice have shown DNA hypomethylation at chromosome ends and exhibit ALT phenotype accompanied with high frequency of telomere recombination (Naderlinger, 2017; Benetti, Roberta 2007; Gonzalo et al., 2006).

In addition, Tert-/- deficient mouse model has been shown that telomere shortening results in epigenetic changes in telomeric chromatin, such as low levels of trimethylated H3K9 and H4K20 and decreased binding of HP1 (Benetti, Roberta 2007; Blasco, 2007). Consistent with these observations of chromatin modification, Atkinson et al., (2005) found that the lack of expression of hTERT and hTR in ALT cells is associated with histone H3 and H4 hypoacetylation and methylation of Lys^9 histone H3.

In contrast to ALT cells, hyperacetylation of H3 and H4 and methylation of Lys^4 residue have been found to play a role in hTR and hTERT expression in telomerase positive cells. Moreover,

methylation of Lys^{20} H4 has been shown to be specific to hTR and hTERT promoters of ALT cells (Blasco, 2007; Atkinson et al., 2005). Based on these observations, similar ALT phenotypes were observed in human telomerase positive cancer cells when cells were given DNA-demethylating drugs, and thus increased telomere recombination and elongation. These studies suggested that loss of heterochromatic features resulted in the emergence of ALT mechanism in telomerase positive cells (Jung et al., 2013; Vera, 2008).

Interestingly, Conomos et al., (2014) have reported that ALT cells maintain and favour their environment of telomere- telomere recombination by recruiting the nucleosome remodelling and histone deacetylase (NuRD) complex to their telomeres. This interaction is mediated by the N-terminal of zinc finger protein, ZNF827 with NuRD, when the NuRD-ZNF827 complex binds to ALT telomeres causes reduction of chromatin compactation through partial inhibition of shelterin binding and through histone deacetylation and together promote HR activity at ALT telomeres (Conomos et al., 2014). In addition, it has been shown that disruption of NuRD complex results in loss of ALT cell viability and ALT activity (Yang, 2018). In fact, ALT cells are shown chromatin decondensation that is associated with a global decrease in telomeric H3K9me3, which promotes telomeric recombination at ALT telomeres (Episkopou et al., 2014).

A group of histone deacetylases (HDACs) among to the class IIa HDAC have been reported to interact with ALT pathway. Histone deacetylase 5 (HDAC5) has been shown to play a role in the maintenance of long telomeres of osteosarcomas cell lines, depletion of HDAC5 by siRNA leaded in the shortening of longer telomeres and homogenous telomere length in cells that can use telomerase or ALT mechanism for telomere maintenance (Novo et al., 2013). In addition, HDAC9 is up-regulated in ALT cells and modulates ALT activity through the formation of the APBs and C-circle in ALT positive cells and HDAC9 depletion leads to a decrease in telomere replicative capacity in ALT cells (Jamiruddin et al., 2016).

1.9 Ionising radiation induced DNA damage

Ionising radiation (IR) can be defined as radiation energy capable to remove tightly bound electrons from the orbit of an atom and this energy can be propagated in rays or waves (Morgan et al, 1988; Ward, 1988). The atoms exposed to IR source can gain or lose electrons and obtain a net electrical charge (Marcu, Bezak and Allen, 2012). The DNA is a large double helix structure composed of four nucleotides bases: adenine, thymine, guanine and cytosine that are bound together by hydrogen bonds (Crick and Watson, 1954). When it is exposed to IR it suffers a range of lesions including double strand breaks shown below (Fig 1.6).

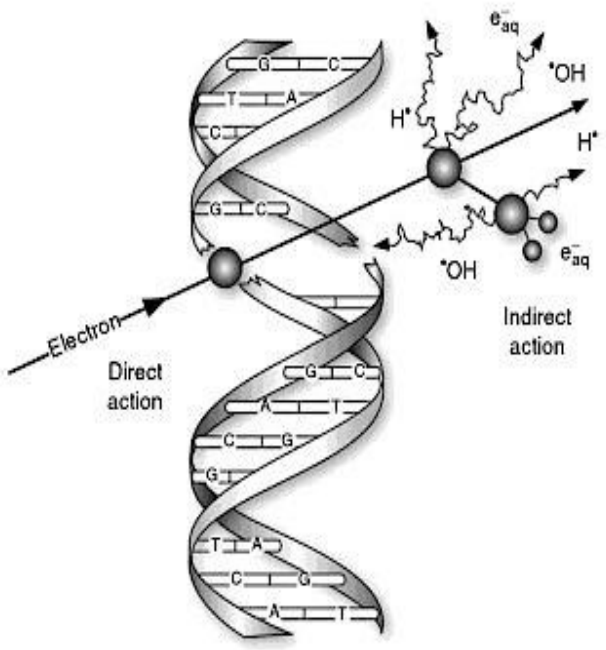

Figure 1.6 Schematic representation of DNA double strand helix that absorbs ionising radiation directly or indirectly ionising which results in structural biological changes and generation of charged particles, respectively. The indirect action effects in DNA molecules cause the dissociation of hydrogen bonds and free radicals' formation during radiolysis. Image taken from Lehnert, (2007).

IR exhibits different effects on cells; cells absorb the IR energy and this causes radiolysis of water molecules:

This may involve breaks of hydrogen bonds and release of hydrogen (H^+), hydroxyl ions (OH-), and radicals such as hydrogen peroxides (H_2O_2). They diffuse far away and may contribute to double strand breaks (DSBs) in DNA (Figure 1.5) (Hall and Giaccia, 2006).

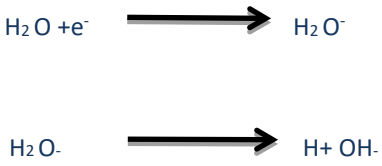

These oxidative agents and free radicals interaction with DNA structure induce an atomic reorganization that results in structural and chemical changes in DNA molecules, including strand scission and cross-linking between DNA strands, therefore the indirect action effects of IR are significant (Marcu, Bezak and Allen, 2012).

1.10 Chromosomal aberrations

IR is known to be a potent inducer of chromosomal aberrations. The mechanisms behind formation of chromosome aberrations are different and depend on the chromosome site of breakage and on the type of repair of these breaks. There are two main theories dealing with the mechanisms of chromosome aberrations; breakage and reunion (Sax, 1940), and the exchange theory (Revell, 1959). The breakage and reunion theory indicate that DSBs are generated at single or multiple sites on many chromosomes and the nature of the repair mechanism, (e.g. NHEJ which is error prone) leads to chromatid or chromosome break type aberrations that appear in the next mitosis (Conforth, 2006; Nagasawa et al., 2010). The exchange theory, suggests that the primary lesion may not be a DSB, but instead two interacting lesions whose identity is not known at that time. When the two lesions are closed together in space and time they may begin the exchange initiation (Revell, 1959). A single site of DNA damage starts the exchange of an undamaged DNA strand (Goodhead, 1995). Today we know, based on the work of Bryant (1984) and Natarajan and Obe (1984) that the key molecular lesion that leads to IR induced chromosomal aberrations is the DNA DSB. Furthermore, chromosomal aberrations induced by IR can be divided into terminal deletions, intra-chromosomal and inter-chromosomal exchanges. The majority of aberrations observed in solid staining appear from the interaction of two chromosome breaks. When the breaks are situated in the arms of different chromosomes they are referred to as interchanges, while if the breaks are in the same chromosome can be classified as intra-changes. However, some aberrations appear to rise from a single break in one arm and are called breaks or discontinuities (Savage, 1976). Given that the lesion responsible for IR induced chromosomal aberrations is DNA DSB, I will next review mechanisms behind DSB repair.

1.11 DNA damage response pathways activation

DSBs are considered major lesions that may lead to genome rearrangements and chromosome aberrations, carcinogenesis and mutations, resulting in chromosomal instability or cell death (Chapman, Taylor and Boulton, 2012). IR effectively induces DSBs in all stages of the cell cycle leading to chromosome-type and chromatid-type chromosomal aberration (Edwards, Virsik-Peuckert and Bryant, 1996). DSBs are repaired through two major pathways: HR and NHEJ, and these are cell cycle dependent (Natarajan, 2002). The HR repairs the broken DNA strand with high fidelity and uses an undamaged homologous sister chromatid as a template for its DNA synthesis. The HR repair pathway is conditioned to specific stages of the cell cycle, S-phase and G2-phase. It involves a range of proteins including Rad51, Rad52, Rad54, various nucleases and helicases, DNA polymerases and ligases (Natarajan and Palitti, 2008). The HR repair mechanism begins with the detection of a DSB by the MRN complex (MRE1RAD50-NBS1 complex). This is followed by the resection of the DSB to form the 3'end overhang strand, which is mediated by nucleases and helicases (Chapman, Taylor and Boulton, 2012). Then, the 3'single strand is coated by replication protein A (RPA) and serves as a dock for the binding of Rad51, which results in the formation of presynaptic filament. Rad52 mediates the interaction between RPA and Rad51 proteins (Figure 1.7) (Thacker, 2005). The Rad51 is recruited to DBSs by the BRCA2 protein through the binding of its BRC domains and then Rad54 protein enhances Rad51 catalyses that searches and invades onto homologous sister chromatid strand, forming a D loop structure. This represents a template for the new synthesis of DSBs and then the strand dissociates and anneals to sister chromatid DNA end to complete the DSB repair (San Filippo, Sung and Klein, 2008).

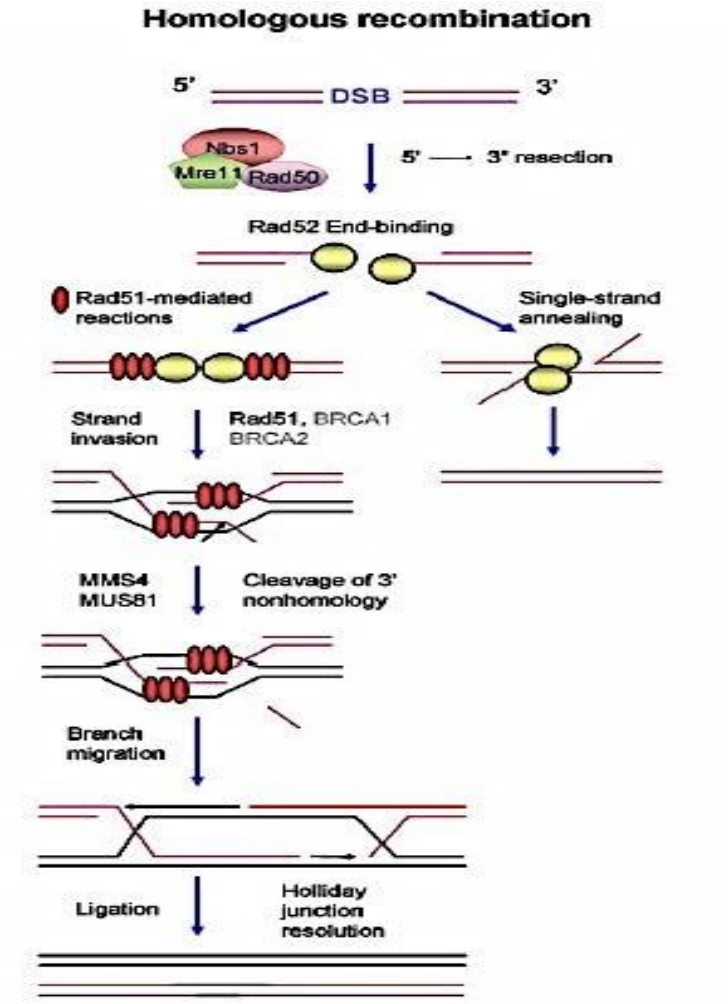

Figure 1.7 Schematic representation of HR repair which is an error free pathway and uses a homologous sister chromatid as template for the DNA synthesis. This repair pathway requires many key components, including Rad52, Rad51, DNA polymerases and ligases. Image taken from Sancar et al, (2004).

In contrast to HR, the NHEJ pathway repairs DSBs mainly in the G1-phase of the cell cycle and it is an error prone pathway that may cause DNA deletions, small insertions and substitutions at the break sites (Figure 1.8) (Chapman, Taylor and Boulton, 2012). It requires a heterodimer complex, Ku70 and Ku80 that shows a high binding affinity to DNA ends and stabilized the broken ends by recruiting the DNA-dependent protein kinases (DNA-PKs), which promotes the juxtaposition of the two broken DNA ends (Kanaar, Hoeijmakers and van Gent, 1998). Then, endonuclease Artemis is recruited to the DNA broken end and interacts with the DNA-PKs forming a complex. Artemis/DNA-PKs complex cleaves 3'overhang strand or removes the damage bases and then interacts with three DNA polymerases including: TdT, pol lambda and pol mu. The final step of rejoining and sealing the broken DNA strand and reshaping the ends are mediated by DNA ligase IV and XRCC4 and protein XLF (Wyman and Kanaar, 2006).

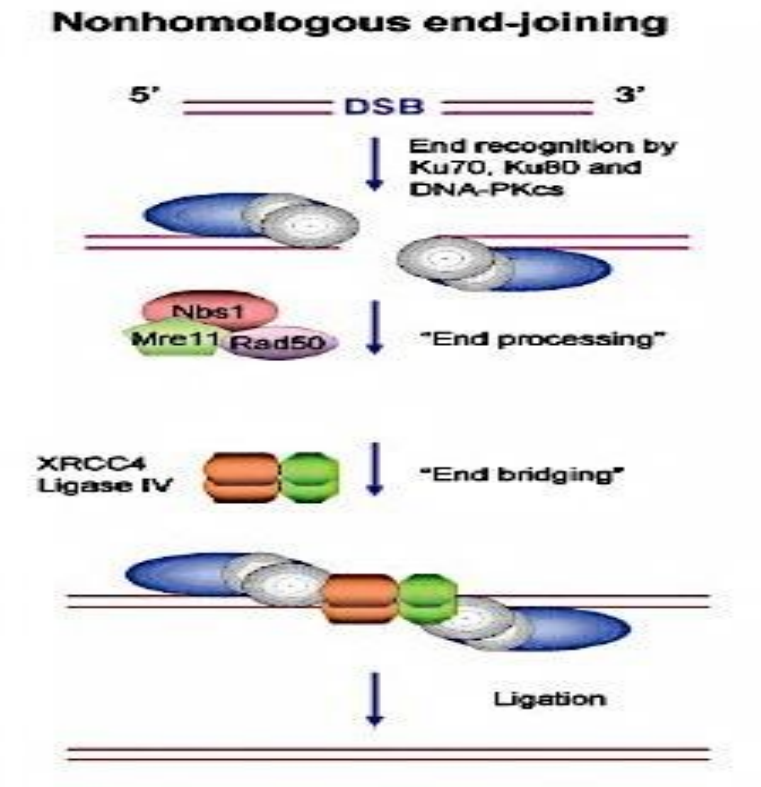

Figure 1.8. Schematic representation of the NHEJ pathway repair DSB through the binding of the Ku heterodimers to broken ends and recruits the DNA-PKcs, and the broken ends are ligated by the DNA ligase IV, XRCC4 and XLF. Image taken from Sancar et al, (2004).

1.12 Telomeres and interstitial telomere sites

Telomeric repeat sequences, located at the end of linear chromosomes, have been found at non-telomeric or intrachromosomal sites and these sequences are known as interstitial telomeric sites (ITSs) (Meyne et al., 1990). In 1988, Allshire and co-workers demonstrated the presence of ITSs in the human genome and showed telomeric probe hybridized to discrete bands of human chromosomes using Southern blot (Allshire et al., 1988). They detected that these bands, in human and mouse genome long stretches of telomeric repeats, were insensitive to exonuclease Bal31 and FISH indicated that they derived from interstitial chromosome sites (Hastie et al., 1989). Consistent with these findings, Well et al., (1990) studied the distribution of Bal31 fragments and screened the human genomic cosmid library and they estimated at least 20 hybridizing fragments were presented per haploid genome (Well et al.1990; Allshire et al., 1988). The hybridization signal was detected at interstitial location, in the region 2q13-2q14 and thought to represent a fusion of two chromosomes and also harboured a fragile site, FRA2B (Sutherland and Mattei, 1987). It has been proposed that ITSs originated from telomeric fusion of ancentral chromosomes during evolution (Hastie and Allshire, 1989).

1.12.1 Characterization of ITSs

Meyne et al. (1990) characterized ITSs in numerous vertebrate species ranging from fish to humans and detected ITSs predominantly in the pericentromeric regions of chromosomes using the newly developed FISH method for detecting telomeric sequences (Meyne et al., 1990). It has been shown that the human telomeric sequences located at chromosome ends (true telomeres) are tightly associated with nuclear matrix, thus EcoRI nuclease can not degrade DNA loop of human chromatin. In contrast to humans, Chinese hamster large ITSs blocks are located in loop regions and the EcoRI nuclease removed most of the ITSs from the loop chromatin region. Therefore, ITSs do not represent functional telomeres as these ITS sequences are not associated with nuclear matrix (Balajee et al., 1996; Meyne et al., 1990). For instances, in the human genome, chromosome 2q13 contains a well characterized ITS that derives from fusion of head-to-head of two ancestral ape chromosomes (IJdo et al., 1991). The human chromosome 2 is formed by two individual chromosomes 2a and 2b (primates) and the fusion point between chromosomes results in ITSs at 2q13 during karyotype evolution (IJdo et al., 1991).

Azzalin et al. (2001) cloned six human ITS fragments by screening a human cosmid library with synthetic probes representing telomeric sequences (Azzalin, Nergadze and Giulotto, 2001; Azzalin et al., 1997). Based on detailed analysis they identified three types of ITSs: (i) short ITSs made of few $(TTAGGG)_n$ repeats; (ii) subtelomeric ITSs formed by large tandem array of $(TTAGGG)_n$ dispersed with degenerated telomere-like repeats, and (iii) fusion ITSs composed of two stretches of ITSs that are oriented head to head (Azzalin, Nergadze and Giulotto, 2001). Surprisingly, there are over 50 short ITSs present in the human genome but the chromosome 2q13 region remains the only fusion ITS in humans (Azzalin et al., 1997).

A fourth type of ITS has been described in non-human species, heterochromatic ITSs, consisting of extended blocks of ITSs at pericentromeric region of most chromosomes, including Chinese hamster chromosomes (Bertoni et al., 1996). In Chinese hamster cells, ITSs range from 250-500 kb on each chromosome (Faravelli et al., 1998). These ITSs represent the main DNA satellite in the Chinese hamster genome and are organized as uninterrupted telomeric-like DNA arrays, which do not contain restriction enzyme sites, therefore are not transcriptionally active (Ruiz-Herrera et al., 2008; Faravelli et al., 2002). In addition, short ITSs estimate at about 20 hexamers have been identified in Chinese hamster chromosomes (Azzalin, Nergadze and Giulotto, 2001; Faravelli et al., 1998). These short ITSs are AT-rich DNA sequences that posses low duplex stability and are associated with fragile sites (Palin et al., 1998). They suggested that these ITSs might be inserted within AT-rich regions (unstable DNA) during evolution. For example, short ITSs have been identified in mouse chromosome 8 and 13 (Yen et al., 1996; Yen et al., 1997).

Interestingly, these short ITSs have been classified into five subclasses based upon their flanking sequences: class A, telomeric array is flanked by the same repetitive elements on both sides, such as short interspersed nuclear element (SINE), long terminal repeat (LTR) or long interspersed element (LINE); class B, telomeric array is flanked by the same direct repeat on both side; class C telomeric array is flanked by unique sequence; class D telomeric array is flanked by transposable elements on one side and unique sequence on the other side, and class E, telomeric array is inserted at the junction between two different repetitive elements (Azzalin, Nergadze and Giulotto, 2001).

Recent studies in yeast model, Saccharomyces cerevisiae has shown genome instability caused by interstitial yeast telomeric (Ytel). Aksenova et al., (2013) used a reporter gene, URA3, to detect changes within the Ytel and found high rates of small insertions and deletions of interstitial repeats. Interestingly, they have also found chromosome rearrangements that involved an interaction between the Ytel and canonical telomeres of yeast chromosomes (Aksenova et al., 2013). Later, Aksenova et al., (2015) reported the likelihood of yeast ITSs for expansion when C-rich strand served as lagging strand template for DNA replication, and HR as potential mechanism for Ytel expansion. Recently, Aksenova et al., (2018) has shown that the constructed URA3 gene from class1 yeast strains are displayed mutations in the coding sequences flanking the ITSs insertion. These findings suggest that ITS in yeast may be account for point mutations, chromosomal rearrangements that result in yeast genome instability.

Interestingly, a characterization of ITSs during meiosis in Mongolian gerbil (Meriones unguiculatus) has shown different chromatin conformation than true telomeres, ITSs recruit TRF1 and RAP1 binding proteins to late prophase I stages and also detectable levels of MLH1, protein involved in mismatch repair, are present. This interaction between ITSs and Shelterin binding proteins is mediated through a nuclear envelope, SUN1 protein and together provide genetic stability to the specie (De la Fuente et al., 2014). In some species, the origin of ITSs remains puzzling. It is thought that ITSs present in vertebrate chromosomes is explained by presuming that ITSs reflect remnants of chromosomal rearrangements during karyotype evolution such as Robertsonian-like fusion (reviewed by Bolzan, 2017).

1.12.2 Telomere binding proteins and ITSs

ITSs have been associated with specific telomere binding proteins, TRF1 and TRF2. Both, TRF1 and TRF2 have been found to co-localize with ITSs in Chinese hamster chromosomes (Krutilina et al., 2001; Smogorzewska et al., 2000). In addition, inhibition of TRF1 causes high levels of spontaneous chromosomal breakages (Krutilina et al., 2003). This suggests the TRF1 association with ITSs in Chinese hamster cells may protect hamster chromosomes from rearrangements.

The mechanism(s) behind ITS formation in mammalian chromosomes are not fully understood. Some studies suggest that ITSs are the result of head-to head telomeric fusions resulting from evolutionary chromosome rearrangements. For example, the fusion site at chromosome arm 2q13 that includes a folate sensitive fragile site (FRA2B) would be a good example. It has been shown that ITSs and subtelomeric repeats sequences are present as inverted repeat rearrangements (Azzalin, Nergadze and Giulotto, 2001; IJdo et al., 1992). Interestingly, Azzalin et al. (2001) have proposed that short ITSs present at interstitial chromosome regions may represent a repair event of DNA DSBs occurring in the germ line during evolution. The NHEJ pathway may repair the breakage and the interrupting sequences, SINEs or LINEs, indicate that ITSs are inserted during the break repair (Azzalin, Nergadze and Giulotto, 2001). However, another possibility for ITS formation is the involvement of telomerase to heal broken chromosome ends, which adds telomeric repeat to the 3'end of DSBs and stabilizes breaks during evolution (Flint et al., 1994). For example, it has been shown that telomerase was responsible for adding TTTAGG repeats directly to the breakpoint resulting in the chromosome deletion at 16p in alpha thalassemia patients (Lamb et al., 1993b; Wilkie et al., 1990).

1.13 Radiation induced instability at ITSs

Several cytogenetic studies of Chinese hamster chromosomes have shown that ITSs are preferential sites for spontaneous and radiation induced breakages (Slijepcevic et al., 1996; Fernández, Gosálvez and Goyanes, 1995a; Alvarez et al., 1993), recombination (Bertoni et al., 1994), and amplification (Day, Limoli and Morgan, 1998). Moreover, these heterochromatic ITSs coincide at pericentromeric regions with fragile sites, folate-sensitive fragile sites, and are prone to chromosomal breakages (Simi et al., 1998; Simi et al., 1990). It has also been speculated that the presence of short ITSs in rodent's genome arise from chromosome healing mediated by telomerase during the germ line evolution, such as the short ITSs insertion in mouse chromosome 8 and few shorts ITSs in Chinese hamster chromosomes (Lin and Yan, 2008; Nergadze et al., 2004; Yen, Pazik and Elliott, 1996).

In contrast to Chinese hamster cells, short ITSs in human cells are not preferential sites for spontaneous breakages or chromosomal rearrangements (Desmaze et al., 2004). However, a recent human study has identified more than 100 insertions of short ITSs in the human genome (Lin and Yan, 2008; Nergadze et al., 2004). Similarly, in cells from human gastric carcinomas chromosome 17 exhibits high rate of ITSs, 2.1 % in cancer specimens, accompanied with telomere loss (Kashima et al., 2006). Cytogenetic analysis suggests that ITSs, when present at internal locations, behave as radiation-induced "hot spots" and are hypersensitive for IR induced chromosomal breakages in Chinese hamster cells (Alvarez et al., 1993).

Furthermore, a similar observation presented in CBA/H mice in which ITSs were associated with IR induced acute myeloid leukaemia (AML) due to rearrangements in chromosome 2 (Finnon et al., 2002; Bouffler et al., 1993; Silver and Cox, 1993). Therefore, the high incidence of break

sites within ITSs in the CBA/H mouse indicates that ITSs may undergo deletions or rearrangements that leads to AML in mouse.

In addition to IR, Chinese hamster ITSs also show sensitivity to radiomimetic compounds. For example, FISH studies using bleomycin (BLM) and streptonigrin (STN) drugs have shown induction of chromosomal aberrations preferentially within pericentromeric regions containing ITSs.

These breakages involving ITSs caused acentric interstitial fragments, which were stained with the telomeric probe in their entire length. Also, some chromosome regions showed amplification of ITS bands following treatment with BLM and STN (Bolzán, Páez and Bianchi, 2001). Moreover, spontaneous amplification of ITSs in sub-clone of the CHO cell lines has been observed and proposed mechanisms of amplification included unequal crossing over between sister chromatids, breakage fusion bridge cycles and replication slippage (reviewed by Bolzan, 2017).

1.14. AIMS and OBJECTIVES

The ITSs are recognized as “fragile sites” or “hot spots” and are radiation sensitivity regions where chromosomal breakage occurs preferentially in Chinese hamster cells (Alvarez et al., 1993). Several cytogenetic studies have highlighted the higher than expected frequencies of breakage involving ITSs in Chinese hamster cells (Slijepcevic et al., 1996; Fernández, Gosálvez and Goyanes, 1995b; Alvarez et al., 1993).

The aim of my project is to investigate the DNA damage repair within ITSs in Chinese hamster cells with a view to identifying potential mechanisms.

In order to achieve this aim, my objectives are as follows:

- To investigate repair kinetics at ITSs in normal and mutant Chinese hamster cell lines using classical cytological methods and immunocytochemistry markers.
- To investigate the contribution of telomerase activity and the ALT pathway towards ITS sensitivity by employing siRNA approaches to target key ALT regulator proteins.

Chapter 2.

Materials and Methods

2.1 Cell lines and tissue culture

2.1.1 Chinese hamster cell lines

In 1957, Theodore Puck and colleagues isolated the first Chinese hamster (Cricetulus griseus) ovary cell line, CHO from a biopsy of an ovary of an adult female Chinese hamster (Puck, Cieciura and Robinson, 1958). Since then, many subclones have been derived from CHO and Chinese hamster cells are widely used in laboratories all over the world (see table 2.1). Chinese hamster cells grow as monolayer adherent cells and have a fibroblast-like morphology (Figure 2.1). The modal chromosome number is 2n=22. These Chinese hamster cells spontaneously transformed and cell doubling time is approximately 17 hours to 19 hours (Kao and Puck, 1968). The Chinese hamster cell lines used in this thesis were grown in HAM-F10 media (Gibco) supplemented with 10% fetal calf serum (FBS) and 1% of Penicillin- Streptomycin (Gibco) was added to the media. The list of all Chinese hamster cell lines used in this study is presented in Table 2.1 below.

Table 2.1 List of cell lines used in this project

Cell lines	Species	Defect protein	Origin	Source
CHOK-1	Chinese hamster	Control	Ovary fibroblast	Dr S. Ermler (Institute of the Enviroment, Brunel University)
V79B	Chinese hamster	Control	Lung fibroblast	Leiden University (Dr M. Zdzienicka's group)
CHE	Chinese hamster	Control	Embryonic fibroblast	Professor Natarajan (University of Leiden)
AA8	Chinese hamster	Control	Ovary fibroblast	Professor Jeggo (University of Sussex)
Irs-1	Chinese hamster	XRCC2	Lung fibroblast	Professor Jeggo (University of Sussex)
Irs1-SF	Chinese hamster	XRCC3	Lung fibroblast	Professor Jeggo (University of Sussex)
Xrs-5	Chinese hamster	Ku86	Ovary fibroblast	Professor Jeggo (University of Sussex)
Xr-1	Chinese hamster	XRCC4	Ovary fibroblast	ECC (European Collection of cell cultures)
V3	Chinese hamster	DNA-PKcs	Ovary fibroblast	Professor Jeggo (University of Sussex)
HeLA	Human		Cervical Carcinoma	ATCC (American Tissue culture collection)
U2OS	Human		Osteosarcoma	ECC (European Collection of cell cultures)
PC-3hTERT	Human		Prostate adenocarcinoma	Professor Newbold's group
GM08399	Human	Control	Skin fibroblast	Coriell Cell Repositories

2.1.2 Human cancer cell lines

HeLA cell line was established from a cervical cancer in a patient with adenocarcinoma of the cervix (Gey et., 1952), U2OS cell line was established from mesenchymal tumour in a patient with osteosarcoma (Saksela et al., 1964) and PC-3 cell line was derived from a prostatic adenocarcinoma (Kaighn, 1979). HeLA cells were cultured in Dulbecco's modified Eagle medium (DMEN) (Gibco, Invitrogen), U2OS cells were cultured in McCoy`s 5a medium (Gibco, Invitrogen) and PC3 cells were cultured in RPMI 1640 (Gibco, Invitrogen). Growth medium was supplemented with 10% FBS (Gibco, Invitrogen) and 1% of Penicillin-Streptomycin (Gibco). These human cancer cells were grown as semi-confluent monolayer and cells were subcultured at the ratio 1:5 every 3 days (Figure 2.1).

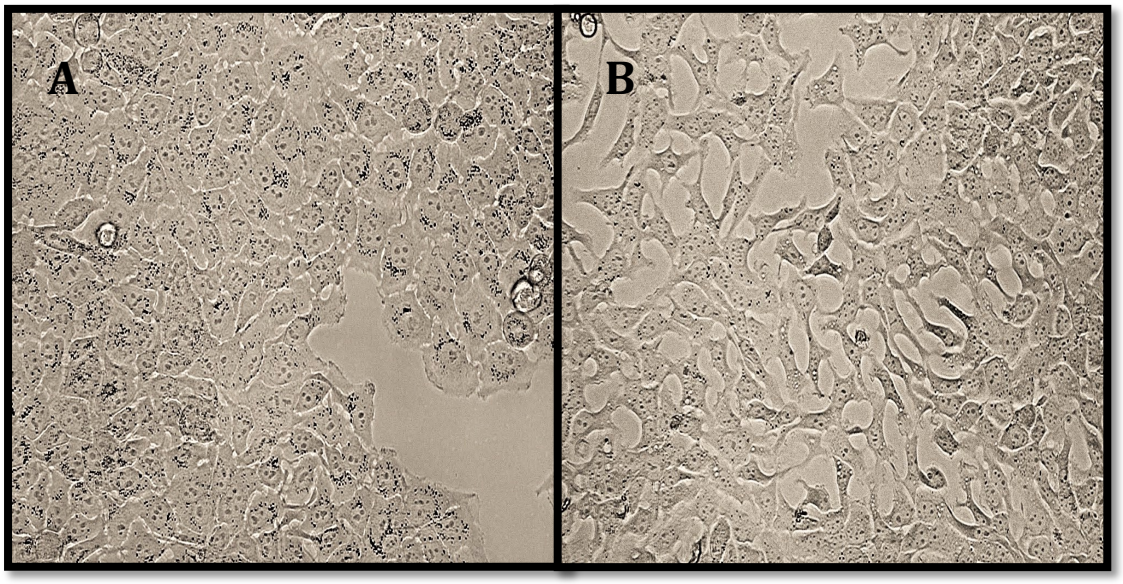

Figure 2.1 Representative images of cellular morphology in human and hamster cell (X100 magnification). **A)** HeLA cell line exhibits a typical epithelial morphology. **B)** V79 Chinese hamster cells show normal fibroblast- like morphology.

2.2 Tissue Culture procedure

A HeraSafe safety cabinet class II (Heraeus, Germany) hood was used to culture cells and UV filter prior and after culture was used to keep the hood sterile. All cell lines vials were kept frozen in liquid nitrogen. When required vials of frozen cells were thawed and set up in 25cm^2 or 75cm^2 flask with lid filter (Nunc). Human cancer cells were cultured with their specific medium and incubated at 37^{o}C with 10% CO_2 in a HeraCell 150 (Heraeus, Germany) incubator. Chinese hamster cells were cultured and incubated at 37^{o}C with 5% CO_2 in a HeraCell 150 (Heraeus, Germany) incubator. All cells prior to subculture were washed with 4ml of warm PBS (Gibco) and gently trypsinized with 1ml of trypsin-EDTA (Gibco, Invitrogen) for five minutes in the incubator. Cells were gently re-suspended in fresh media and transferred to a 15ml falcon tube and spun down in a centrifuge (Megafuge 1.0, Heraeus) at 1200rpm for 5 minutes. Cells supernatants were aspirated and cell pellets were gently flicked and re-suspended in 1ml fresh media. Human cells were subcultured at the ratio of 1:5 in a way that 200µl of suspended cells was put in a new flask with 5ml of fresh media. Chinese hamster cells were subcultured at the ratio of 1:6 in a way that 170µl of suspended cells pellet was put in a new flask with 5ml of fresh media at 37^{o}C. Human and hamster cells were subcultured every two or three days at 80% confluence, preferably before the medium colour changed to yellow.

2.2.1 Cryopreservation of cells

Stock cells were generated from each cell line and stored for long-term storage in liquid nitrogen (-196^{o}C). Cell freezing solution consisted of 90% FBS (Gibco, Invitrogen). Cell freezing solution consisted of 90% FBS (Gibco, Invitrogen) and 10% of DMSO (dimethylsulfoxide, Gibco). Cells were harvested and collected as decribed above. Cell pellets were resuspended in 1ml of freeszing solution and were aliquoted into cryogenic vials and kept in a freezing container rack (Nalgene) at -80oC for 24 hours. Finally, cells were transferred into liquid nitrogen for long-term storage.

2.2.2 Thawing of cryopreserved cells

The cryopreserved cells were warmed for three minutes at 37^{o}C in water bath. Cells were resuspended in 5ml of complete medium and centrifuged at 1200rpm for 5 minutes. After removed DMSO traces, the cell pellet was gently re-suspended and transferred into a 25cm^{2} flask.

2.2.3 Cell counting

Cell counting was carried out using Countess automated cell counter (Invitrogen). After cells were trypsinized cells pellet were resuspended in 1ml fresh medium. The cell suspension was placed in a 1.5ml Eppendorf tube then in a new 1.5ml Eppendorf, a mix of 10µl of Trypan blue and 10µl of cell suspension was prepared and mixed well. A total of 10µl of the mixture was taken and added onto each side of the countess slide and inserted into the slot of the Countess machine. The machine screen shows the total number of cells per ml and viability (live, dead and total cells).

2.2.4 Irradiation of cells

Brunel University has a 60Co radiation facility, where all gamma irradiation experiments were conducted. Cells were exposed to ionising radiation using 60Co source, Chinese hamster cells at 70-80 % confluence, growing in log-phase, were irradiated either in 25cm^2 flasks for metaphase preparation or poly-lysine slides (Sigma) for immunocytochemistry. Cells were irradiated with a dose of 1 Gy gamma irradiation and a distance of 25cm from the gamma source. The calculation of radiation dosages was measured in Gy per minutes. The formula was used to calculate the time required for irradiation was:

$$\text{Time (mins)} = \frac{\textit{Dose Needed (Gy)}}{\textit{Dose Rate (Gy min}^{-1}\textit{)}}$$

2.3 Cytogenetic Analysis

2.3.1 Metaphase preparation using Chinese hamster cells

When Chinese hamster cells were about 70% to 80% confluence they were treated with Demecolcine (0.1µg/ml, Gibco) for 1 hour. Demecolcine inhibits mitosis at metaphase by inhibiting tubulin polymerization into microtubules that leads to cell cycle arrest at metaphase and preventing cell division. Cells were washed once with pre-warmed 1X PBS and trypsinized for 5 minutes and then spun down at 1200rpm for five minutes. Cell pellet was resuspended with 5ml of hypotonic buffer KCl (75mM) drop-by-drop and mixed gently, and incubated for 20 minutes in a 37^{o}C water bath. This hypotonic buffer causes cells to swell and burst while the nuclear membrane remains intact. After KCl incubation, a fresh fixative solution

(3 methanol: 1 acetic acid) was added in a drop-by-drop fashion and the cell suspension was spun down at 1000 rpm for 5 minutes. The fixation process was repeated at least 3 times and then cells pellet were resuspended in 1ml fresh fixative and 20µl of this suspension was dropped onto precleaned slides. The slides were dried for 4 minutes at room temperature and checked under a phase contrast microscope for metaphases.

2.3.2 Giemsa staining

Next, metaphase cells were stained with 4% (v/v) Giemsa (Sigma-Aldrich) for 5 minutes. Then slides were rinsed gently with dH_2O and left to air dry. Finally, slides were mounted with DPX (BDH laboratories) and sealed with cover slip, and left for maximum 2 hours to dry (Figure 2.2). Analysis of metaphases was conduced using a Zeiss Axioplan light microscope and images captured using Metasystem software (Altlussheim, Germany).

2.3.3 Chromosomal aberration analysis

Chromosomal aberrations are microscopically visible part of a wide spectrum of DNA changes generated by repair mechanism of DSBs (Obe *et al.*, 2002). The G2 chromosomal radiosensitity assay 'G2 assay' is a cell cycle-based technique that mesuares the frequency of chromatid aberrations in cells (Scott et al., 1994; Bryant, 2001). G2 assay involves irradiating cells in vitro during G2 phase of the cell cycle to induce DNA damage, which can be observed as chromatid gaps or breaks in the first mitosis. To detect chromatid type aberrations in Chinese hamster cells, metaphase chromosome spreads were stained using Giemsa (light microscopy) or DAPI (fluorescence microscopy).

Cells were irradiated as semi-confluent (70%) and were harvested at different time points over 4 hours after irradiation to examine repair kinetics. In each slide, 100 metaphase cells were counted to determine the chromosome aberrations.

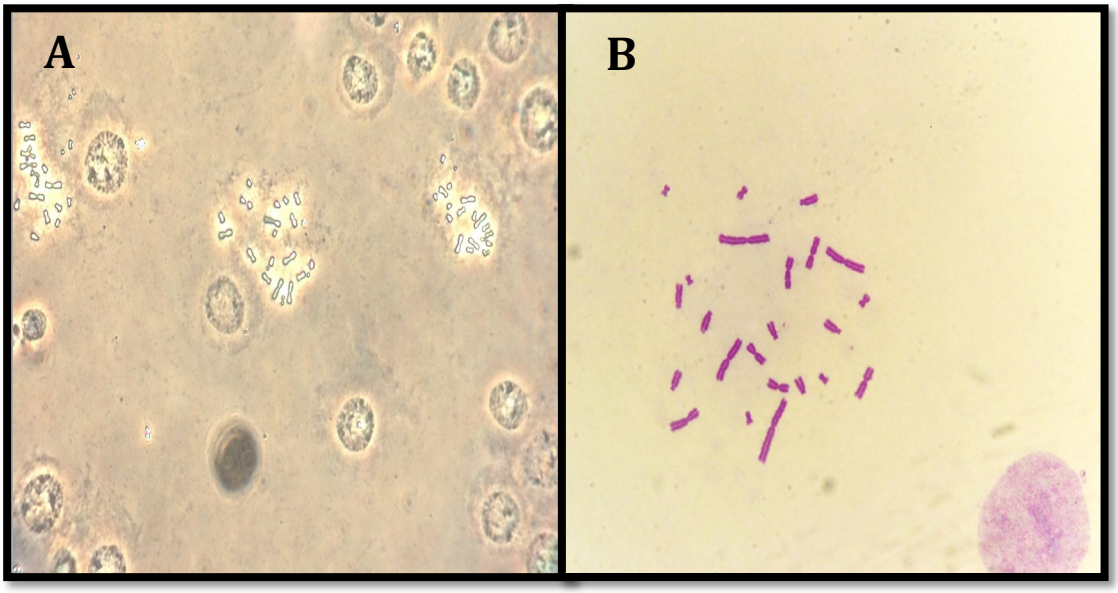

Figure 2.2 Typical Chinese hamster chromosome metaphase spreads. **A)** Representative images of chromosome metaphases spread prior staining under contrast microscope X 40 magnification. **B)** Representative image of V79 metaphase spread stained with 4% Giemsa.

2.3.4 Metaphase Fluorescence *in situ* Hybridization

Metaphase chromosomes were prepared from the G2 assay and cells suspension were then dropped onto clean slides. Slides were air-dried and aged in hybridizing box for one week to harden chromosomal DNA matrix, therefore aging of slides is essential to obtain good FISH signal. After a week the slides were washed with 2XSSC buffer for 5 minutes on the shaker. Then chromosomes were fixed with 4% formaldehyde for 7 minutes and followed by 3 washed of PBS for 5 minutes on the shaker. Slides were treated with pepsin to digest the cell cytoplasm, which surrounded the chromosomes. A total of 50µl of pepsin (10% pepsin, Sigma) was mixed

with 50ml of dH_2O (pH2 49.5ml of dH_2O and added 0.5ml HCl) and incubated at 37°C in water bath for 7 minutes. Next, slides were washed 3 times with PBS for 5 minutes on the shaker. Then slides were fixed for second time with 4% formaldehyde for 5 minutes followed by 2 washed with PBS for 5 minutes.

2.3.5 Hybridisation

A total of 20µl of telomeric DNA sequence $(CCCTAA)_3$ PNA probe labelled with Cy3 fluorophore was added onto the slide and covered with coverslip. Then slides were put on the heating block for 3 minutes at 75°C to denature. Slides were left to hybridize for at least 2 hours in a slide moisture chamber.

2.3.6 Post-hybridisation washes

The slides were dipped in PBS to remove the coverslip. Slides were washed twice, each time for 7 minutes with hybridization stringent washes (50% formamide, 2X SCC) followed by 2 washes with TBST for 5 minutes and one more with PBS. Next, slides were dehydrated with ethanol series (70%, 90% and 100%) and left to air dry protected from light. Finally, 15µl of Vectra shield anti-fade (DAPI) mount was added to each slide and slides were sealed by nail varnish (Figure 2.3).

2.3.7 Image Analysis

Image of metaphase chromosomes were acquired by Zeiss fluorescence microscope equipped with CCD camera and the ISIS capture software (in situ imaging system ISIS, Meta system-Altlusshim, Germany). For the G2 assay we counted 100 metaphases per each time point (1- 4 hours) for every Chinese hamster cell line.

2.3.8 Analysis of the ITSs in percentage

The relative chromosome lengths were calculated by printing a metaphase spread image in paper and chromosomes length and ITRS length were measuring by ruler per each hamster cell line. The chromosomes and ITRS length measures were taken in millimetres (mm) and were converted into percentage (%) by dividing the total ITSs value by chromosome length value in the three Chinese hamster lines. For example, CHOK-1 the total sum up of all 22 chromosomes length was 387.5 mm and the ITSs lengths of all chromosomes were 32.5mm. It was divided the 387.5/32.5= 8.3% of ITSs present in CHOK-1 cell line.

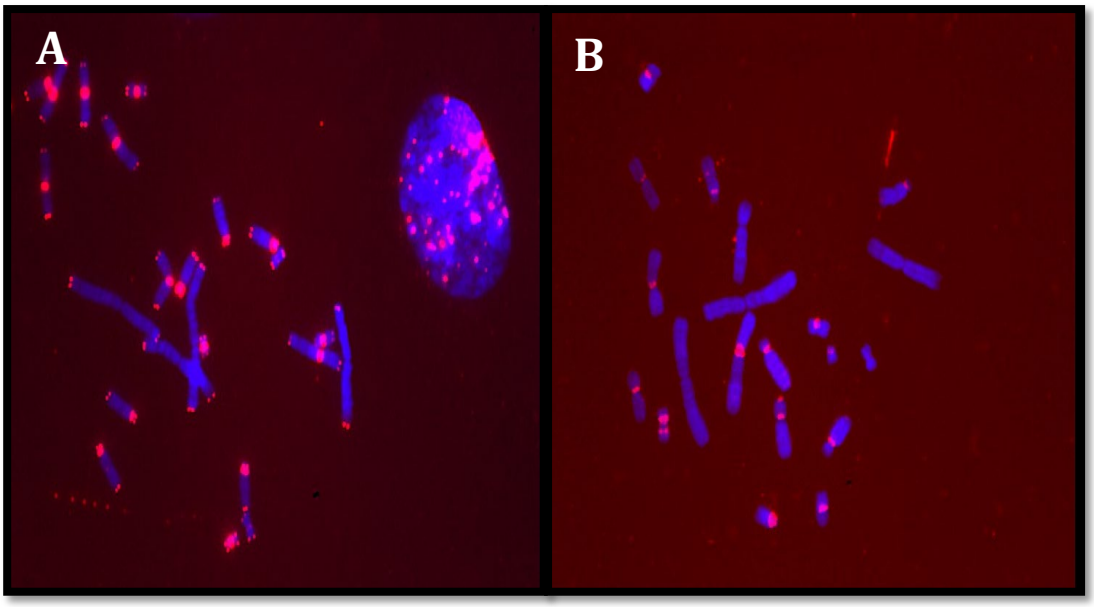

Figure 2.3 Hybridisation of telomeric DNA probe labelled Cy3 (red) in Chinese hamster metaphase spreads. **A)** CHE metaphase FISH showed large blocks of ITSs pattern at pericentromeric regions and also strong hybridization signal at telomeres. **B**) CHOK-1 cell line exhibited no hybridization at telomeres but ITSs hybridization signal at centromeres in the metaphase spread.

2.4 Immunocytochemistry

2.4.1 Immunofluorescence detection of γ-H2AX foci

Ionizing radiation induced DSBs and can be detected using a specific DNA damage marker, γ-H2AX. Cells were grown on poly-L lysine coated slides for 24 hours prior to irradiation (1Gy). After irradiation slides were put back in the incubator at 37^{o}C to for 30 minutes fro cells to recover. The cells were washed with warm PBS to remove any media left and immediately fixed in 2% formaldehyde for 10 minutes. Cells were washed 3 times in PBS for 5 minutes on the shaker. Then cells were permeabilized with 0.5% Triton X-100 solution (Sigma-Aldrich) in PBS for 10 minutes at 4^{o}C. Next, cells were blocked to reduce non-specific antibody binding in 5% BSA blocking buffer (5% BSA in PBS-Tween). A total of 100µl of blocking buffer was added to each slide, covered with parafilm and incubated for 1 hour in the slide moisture chamber. Slides were rinsed in PBS. A total of 120µl primary monoclonal anti-phosphohistone H2AX (γ-H2AX, Millipore) antibody at 1:500 dilutions was added to each slide and incubated for 1 hour in the slide moisture chamber at room temperature. Slides were washed 3 times in PBS-T for 5 minutes on the shaker and incubated with 120µl of secondary antibody anti-mouse IgG FITC conjugated antibody (Invitrogen) at 1:1000 for 1 hour in the slide moisture chamber at room temperature. Slides were washed 3 times in PBS-T for 5 minutes on orbital shaker. Slides were left to air dry in dark and then 15µl DAPI was added, slides covered with coverslip and sealed with nail varnish. Cells were analysed using Axioskop Zeiss fluorescence microscope. In each slide, 100 interphase cells were scored per slide to determine the DNA damage repair kinetics in hamster cells.

2.4.2 Telomere dysfunction-induced foci (TIF) assay

TIF assay is a technique based on the co-localization detection of DNA damage by antibody, γ-H2AX, and specific telomere antibody or probe, such as telomeric probe (Cy3) to detect DNA damage at telomeres. Cells were stained for γ-H2AX (Chapter 2.13) and then fixed with 2% formaldehyde for 10 minutes. Cells were washed 3 times in PBS for 5 minutes on shaker. Next, cells were hybridized with PNA Cy3 probe (see Chapter 2.4) and incubated for 2 hours in slide moisture chamber followed by hybridization washes. Cells were counterstained with DAPI and then cells were analysed using Axioskop Zeiss fluorescence microscope. 100 interphase cells were scored and TIFs foci were counted per each time point (30 min to 48 hours) per Chinese hamster cell line (Figure 2.4).

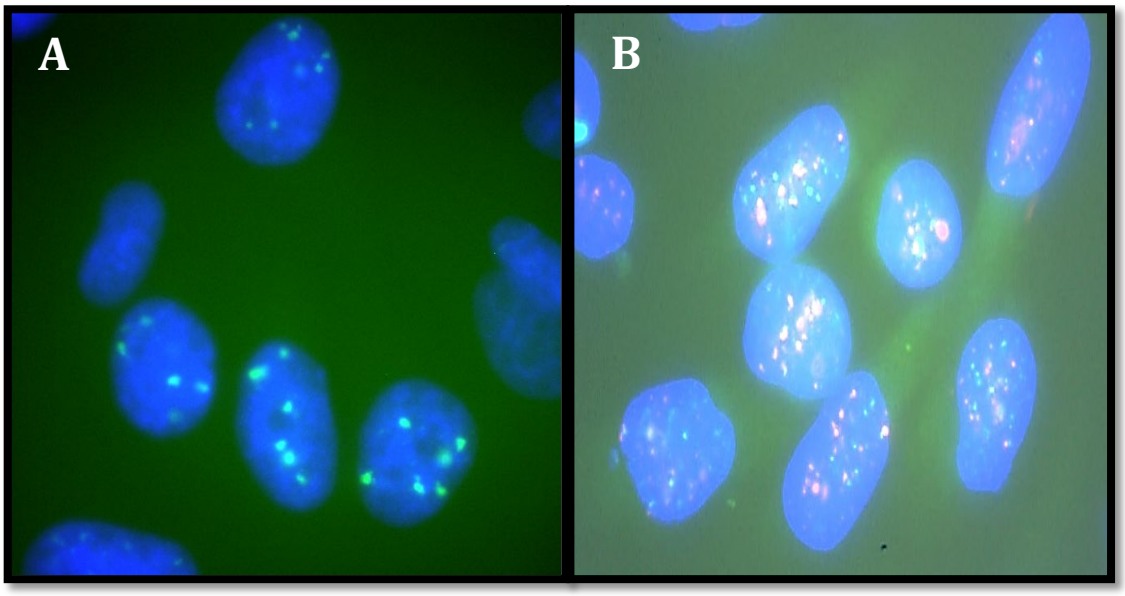

Figure 2.4 Immunohistochemistry detection of DNA damage and telomere damage in Chinese hamster interphase cells. **A)** Positive detection of γ-H2AX foci (green) at 24 hours after exposure to 1Gy irradiation in CHOK-1. **B)** Representative images of TIFs foci that showed as yellow foci, co-localisation of γ-H2AX (green) and Cy3 pna probe (red) post-radiation.

2.4.3 Immunofluorescence detection of ATRX foci

Chinese hamster cells were plated on poly-L-lysine coated slides and washed in PBS for 3 minutes and fixed in 2% formaldehyde for 10 minutes. Cells were washed 3 times with PBS for 5 minutes on the shaker and permeabilised with 0.5% Triton X-100 at 4^{o}C for 10 minutes. Then cells then were washed 3 times with PBS-T for 5 minutes on shaker. Next, cells were blocked in 100µl of 5% BSA and covered with parafilm and incubated for 1 hour in the slide moisture chamber at room temperature. Cells were washed with 1X PBS for 5 minutes and added 100µl of the ATRX primary antibody (ab97508, Abcam) diluted (1:100) according to the manufacture's instructions and incubated for 1 hour in the slide moisture chamber. Then cells were washed 3 times with PBS-T for 5 minutes on the shaker and later incubated with 100µl of Alexa Fluor 488 secondary antibody (A-11034, Invitrogen) for 45 minutes in the slide moisture chamber. Finally, cells were washed 3 times in PBS-T for 5 minutes on the shaker and added 15µl of DAPI, and covered with cover slip and sealed with nail varnish.

2.5 Quantification of Telomere Repeat Amplification protocol (TRAP) assay

All Chinese hamster and human cell lines were harvested at 70- 80% confluence and the total number of cells counted. Then cell pellets were washed once in cold 1X PBS and spun down. Cell pellets were lysed by adding 200µl/10x^{5}-10x^{6} cells of TRAPeze 1XCHAPS lysis buffer (S7705, Millipore) and mixed vigorously with a syringe. Cells were incubated on ice for 20 minutes and centrifuged at 12,000xg for 20 minutes at 4^{o}C. A total of 150µl of supernatant was transferred into a fresh tube and immediately stored at -80oC until required. A total of 20µl of suspension was reserved for to determine the protein concentration for all the samples.

2.5.1 Protein concentration

The protein concentration of each sample was determined using CB-X protein assay (G-Biosciences). The CB-X assay is highly sensitive and uses a protein dye that is an improvement on the Bradford Coomassie dye reagent, which changes colour according to the amount of protein with the samples. A serial dilution of BSA (2mg/ml) ranging from 0.05 to 2µg/µl was produced and CHAP buffer was used to dilute BSA. The BSA standard curve was used to determine the protein concentration of sample extracts (Figure 2.5). Samples were prepared for quantification by transferring 10µl of BSA dilutions of sample extracts to a 96 well microplate, followed by 200µl of CB-X assay dye. The protein extracts and CB-X dyes were incubated for 5 minutes at room temperature, and the absorbance values at 595nm determined. Sample extracts and BSA standards were read in duplicated. The 1XCHAPS buffer was subtracted the from the sample average.

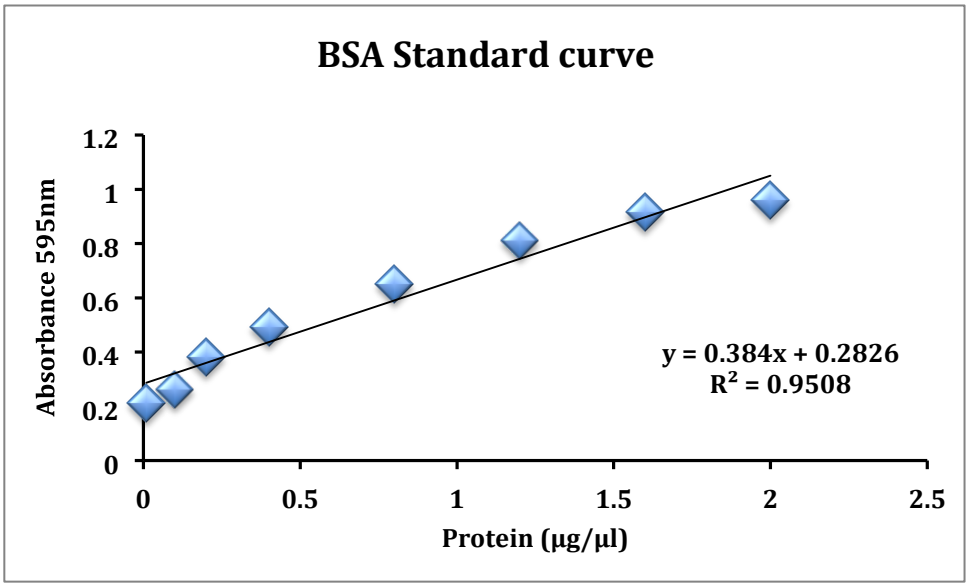

Figure 2.5 Standard calibration curve of BSA protein diluted in CHAPS lysis buffer.

2.5.2 TRAP PCR reaction set-up

Telomerase activity was determined using a qRT-PCR based TRAP protocol adapted from Wege et al. (2003). Protein samples extracts were thawed on ice and diluted in 1X CHAPS buffer to desirable concentration. A serial dilution of telomerase positive, PC-3 hTERT protein extract was made to prepare a standard curve ranging from 50ng-500ng protein. Negative control was generated by heat-inactivating telomerase HeLA extract at 85°C for 10 minutes and also non-template control (NTC) consisting of 1X CHAPS buffer instead of protein extract, both were included in the plate. TRAP reaction required for each sample two set of primers; ACX (0.05 µg/µl) and TS primer (0.1 µg/µl) (Table 2.2), 250ng sample extract, iTaq Universal SYBR (Biorad), and nuclease free water to bring the total volume to 25ul per well. In a separate tube a stock master mix was prepared containing all reaction components except the protein extracts. A total of 20µl of the master mix in triplicates was loaded into 96 well microplates (MicroAmp, ABI) and protein extracts were added last. The master mix reaction was prepared as follow:

Mater mix reaction 1X:

SYBR	12.5µl		
ACX	1µl	+	5µl of protein extract
TS	1µl		
RNAse free water	5.5µl		
	20µl		

Table 2.2 Primer sequences used in the qRT-PCR TRAP assay

Primer Name	Sequence (5'-3')
Telomerase Substrate (TS)	AATCCGTCGAGCAGAGTT
Anchored Return Primer (ACX)	GCGCGG$(CTTACC)_3$CTAACC

QuantStudio software V1.3 program was used to set up the QuantStudio 7 Flex RT-PCR system (AB, Invitrogen) consisting of an initial incubation step at 25°C for 20 minutes to enable endogenous telomerase to elongate the TS primer substrate molecule, followed by PCR amplification of extended fragments at 95°C for 10 minutes and 35 cycles of 95°C for 30 seconds and 60°C for 90 seconds. Once the thermal cycling program had completed, amplification plots of positive and negative control samples were inspected for telomerase amplification. Telomerase activity was quantified by taken the average of quantity mean values of PC-3 hTERT protein standard and QuanStudio V1.3 software was used to plot the standard curve (Figure 2.6). These values were exported and presented as bar graph with error bars SEM.

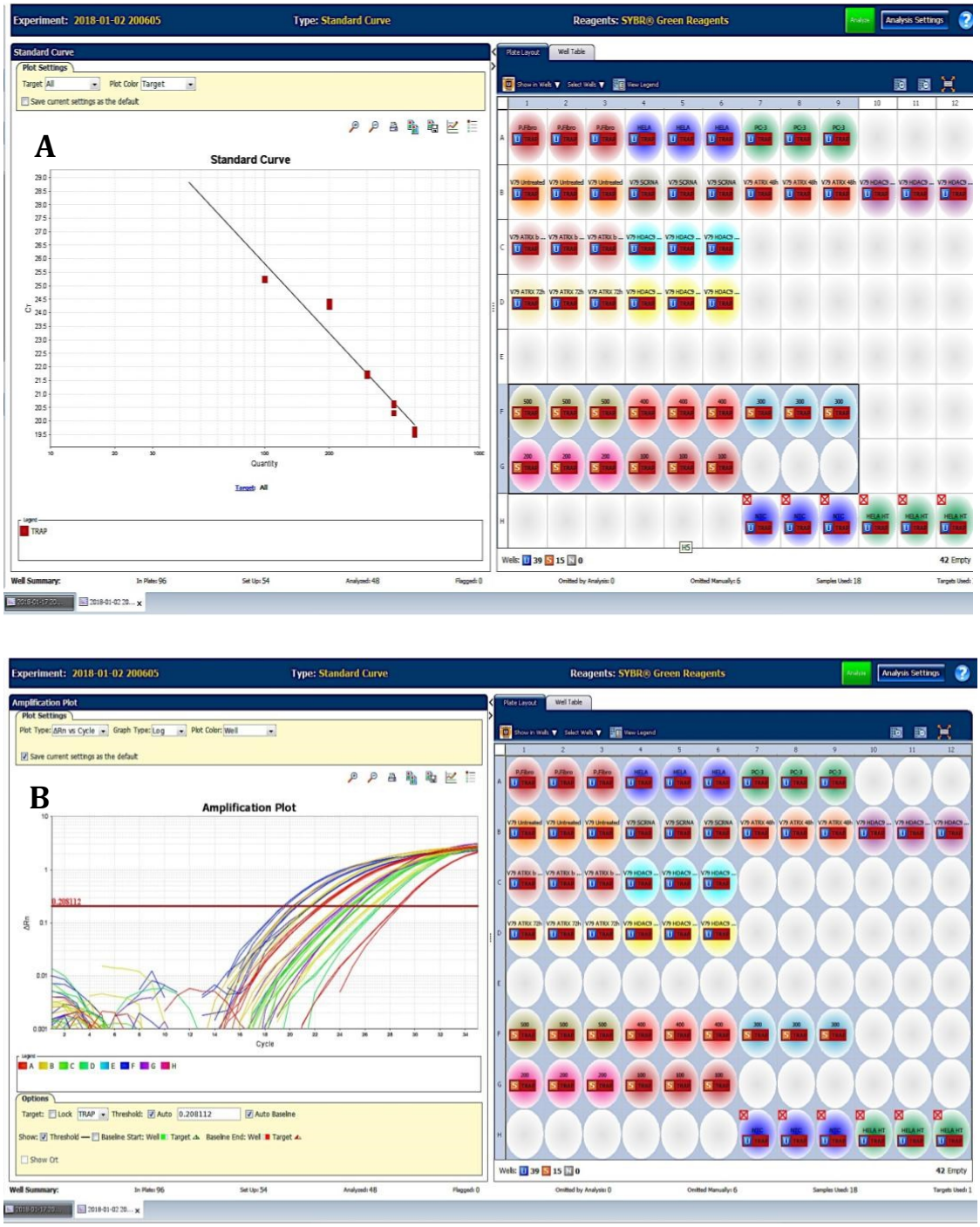

Figure 2.6 Representative images of TRAP amplification. **A)** PC-3 hTERT standard curve plots of five serial dilution standards **B)** Telomerase activity in Chines hamster cell lines, positive and negative controls, HELA inactivated, NTC samples.

2.6 Alternative lengthening of telomeres (ALT) C-circle assay

C-circle (CC) assay is a sensitive and quantitative test that measures alternative lengthening of telomeres (ALT) mechasnim (Henson and Reddel, 2010). ALT positive cell lines and tumours phenotype is characterized by the presence of heterogeneous telomere length, high frequency of APBs foci, high frequency of T-SCE and circular c-rich single stranded telomeric DNA. The CC levels are measured through two steps process: DNA amplification using phi29 DNA polymerase and probed by radioisotope (P^{32}) and hybridization using $(CCCTAA)_3$ oligonucleotides.

2.6.1 Genomic DNA extraction

Chinese hamster cells and human cells were grown (80-90% confluence) and were harvested to obtain cell pellets. A DNA Mini kit (Qiagen QIAmp) was used to extract genomic DNA according to manufacturer's instructions. The DNA Mini kit uses column-based technique in which DNA specifically binds to QIAmp silica membrane.

The detail step of DNA extraction in shown below:

1- Cell pellets are suspended in 200µl of PBS. 20µl of protein K followed by 4µl of RNAse A. These enure that RNAs and protein are degraded in the cell pellets.
2- Add 200µl of nuclear lysis solution (Buffer AL) and the sample were vortex for 15 seconds intermittently.
3- The samples are then heated for 10 minutes at 56°C in a heating block.
4- Spin down the samples for 10 seconds at 6000xg to remove drops from the inside of the lid.
5- Add 200µl ethanol 100% to precipitate the nuclei acid from the samples followed by short spin for 10 seconds at 6000xg

6- The supernatant is then transferred into QIAmp column attached to a collection tube and spin down for 60 seconds at 6000x g. gDNA is attached to the silica-based membrane and flow through discarded.

7- The DNA is now washed with 500µl of solution AW1 and spin down the column at 6000x g for 1 minute.

8- DNA is washed with 500µl of solution AW2 and spin down the column at 20,000x g for 3 minutes.

9- Next, collection 1.5ml tubes are placed under each column and spin down at 20,000x for 60 seconds.

10- Finally, DNA is eluted with 50µl of elution buffer (AE) and incubates at room temperature for 1 minute and then centrifuge at 6000x g for 1 minute.

11- Samples are stored at -20^{o}C.

2.6.2 DNA quantification

The concentration of sample DNA was determined using NanoDrop 2000 UV/Spectrophotometer (Thermo Scientific). The spectrophotometer was calibrated using the AE buffer, the absorbance wavelengths at 260nm and 280nm. Only, sample with high DNA quality and purity at ratio around 1.8 were kept for C-circle analysis.

2.6.3 C-circle amplification

The first step of the CC assay involves amplification of C-circles using the rolling circular amplification (RCA) of a partially double stranded C-circle by Phi 29 DNA polymerase (M0269L, NEB) is auto-primed by the G-strand (TTAGGG)n (Henson *et al.*, 2009). gDNA samples were diluted to a concentration of 30ng/µl in 10mM TRIS (pH7.6) buffer and made up to final volume of 10µl.

Table 2.3 Phi 29 DNA polymerase master mix reaction as follow:

Stock concentration	Volume (µl)	Final concentration
1M DTT	0.8	4mM
10x phi29 buffer	2	1x Conc
10mg/ml BSA	0.4	0.2mg/ml
10% Tween	0.2	0.10%
1mM dTTTP	0.8	0.1mM
Phi 29 DNA polymerase (10, 000 U/ml)	1.5	15U
Nuclease Free water	4.3	
Total Volume	**10µl**	

The reaction master mixture components (table 2.3) were added to a 1.5ml Eppendorf tube and centrifuged. 10ul of DNA polymerase master mix was added to PCR microtubes and then 10ul of the gDNA (30ng/µl) samples followed by gently vortex. Samples were spun down for 10 seconds and put in the thermocycler to incubate at 30^{o}C for 8 hours followed by 65^{o}C for 20 minutes incubation, to inactivate phi 29 DNA polymerase. Samples were immediately store at -20^{o}C.

2.6.4 Slot-blotting

Samples were slot-blotted using a nylon membrane (Hybond-N, Amersham Biosciences) and blotting paper were cut according to the size of slot blot apparatus, and then the membrane and blotting paper were hydrated in 2x SSC buffer for 5 minutes. Samples were gently thawed on ice and spun down for 10 seconds and were diluted with 40µl of 2xSSC and vortex for 15 seconds at 2500 rpm. The slot blot apparatus was assembled by placing the pre-soaked blotting paper in the base and on top the nylon membrane and seal the apparatus by tightening the O-rings. The DNA samples were gently loaded on each slot according to template position slots and then turn on the vacuum until sample liquids were sucked through the membrane. Next, the membrane containing the DNA samples was washed with 100µl of 2x SCC buffer to remove any residual sample and turn off the vacuum was gently removed the membrane from the slot blot apparatus. After membrane was let air dried, the membrane was immediately cross-linked using UV cross-linker box (GE, Healthcare) at 1,200 J twice.

2.6.5 Hybridization P^{32} end labelled telomeric probe

Preparation of P^{32} probe

The C-rich telomeric specific $(CCCTAA)_3$ (Invitrogen) oligonucleotide was end-labelled with ATP [Y-^{32}P] 3000Ci/mmol (NEG002A250UC, Perkin Elmer) using DNA 5' end labeling system (U2010, Promega) as follows:

Stock concentration 2	Volume (µl)
Oligonucleotide 100uM	10
T4 polynucleotide kinase buffer 10X	2
T4 polynucleotide kinase enzyme	2
ATP	5
Total Volume	**19µl**

Incubate the above mixture at 37°C for 20 minutes in block heater. The reaction was stopped by adding 2µl of 0.5M EDTA and then added 40µl of TE buffer and spun down for 15 seconds.

2.6.6 Purification of P^{32} probe

The newly prepared probe was washed to remove any unbounded nucleotide through a column resin base chromatography (GE, Healthcare). The column was vortex for few seconds to re-suspend the resin and snap off the bottom cap and spun down for 1 minute at 1000rpm. Next the column is placed into a new 1.5ml Eppendorf tube and P^{32}probe mixture was then immediately added into the resin column before resin bed dried and spun down for 2 minutes at 1000rpm. Finally, the purified probe is then stored at -20°C or used to hybridise the samples in the membrane.

2.6.7 Hybridization buffer

Prior to purification of P^{32} probe, the nylon membrane contained the DNA samples was placed in a glass hybridization bottle and incubated with 10ml of pre-warmed PerfectHyb Plus hybridization buffer (H7033, Sigma) at 37°C for 20 minutes to block the membrane for unspecific binding. The fresh prepared P^{32} probe was added to the hybridization bottle and allowed to hybridize overnight at 37°C. The next day, nylon membrane was washed three times with 10ml of 0.5x SCC and 0.1% SDS buffer for 15 minutes at 37°C. The membrane was wrapped in a hybridization bag and exposed overnight onto X-ray film (Kodak) in darkness at -80°C. Then the film was developed using automated system (Xograph) and images were scanned for analysis.

2.6.8 Image analysis of CC assay

The X-ray film was analysed by Image J software (NIH) and the intensity of the slot blots generated peaks (Figure 2.7).

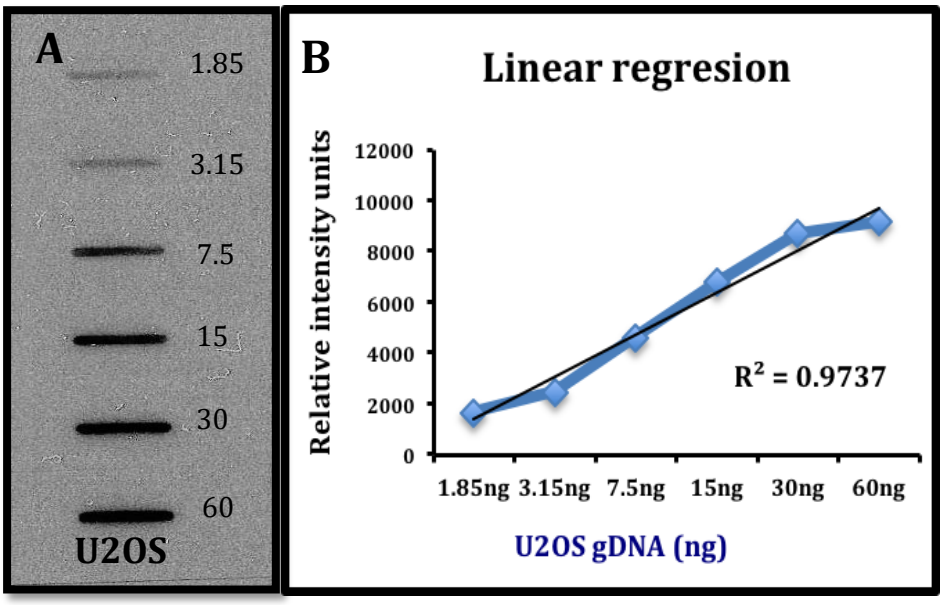

Figure 2.7. ALT activity and U2OS standard curve. **A)** The vertical dashed lines represented the C-circle positive signal of U2OS, an ALT positive cell line, and the concentration of gDNA is proportional to the intensity of the vertical lines. **B)** The graph showed the absolute values of U2OS serial dilutions measured by using Image J, which is used to normalize the telomeric signal to the total amount of gDNA. The linear regression analysis R= 0.9737.

2.7 Small interference RNA (siRNA)

RNA interference (RNAi) is a process of sequence specific, post-translational gene expression silencing in mammalian cultured cells, initiated by double stranded RNA (dsRNA) (Elbashir, Sayda 2001). The sequences specific messenger RNA degradation are 21 and 22 bp length, small interfering RNAs (siRNAs), which are homologous in sequence to target gene and specifically supress gene expression (Sijen *et al.*, 2001). All siRNAs oligonucleotides for Chinese hamster cells were purchased from Microsynth AG (Switzerland) and arrived in suspension.

Table 2.4 List of siRNAs nucleotide sequences 5' to 3'

Names	Sequences
ATRX_siRNA_1	AAA GGG UGU UUC ACA UAA A
ATRX_scRNA	GAGACAACTAGGTTAATAT
HDAC9_siRNA_1	UUC UGA AUG UUG CGU UUA A
GAPDH_siRNA_1	AGC UUG UCA UCA ACG GGA A

2.7.1 siRNA Optimization transfection procedure

siGLO transfection indicator (D-001630-01, Dharmacon) was used to optimize transfection conditions. siGLO green fluorescent oligonucleotide can be used to monitor how efficient cells uptake siRNA, as the green dye localize to the nucleus of the cell. It also can be used to optimize the cell number, viability and siRNA concentration. In order to determine the optimal concentration of siGLO green (non-targeting labelled siRNA) was diluted ranging from 10nM, 20nM, 50nM, 100nM and 150nM. CHOK-1 cells were seeded at the density of $1.5x10^5$-$2.0x10^5$ cells in 6 well plate with complete medium overnight. 24 hours later complete medium was removed and added fresh Opti-MEM I (31985070, Invitrogen).

Cells were transfected with 10nM, 20nM, 50nM, 100nM and 150nM concentrations of siGLO green siRNAs using Lipofectamine RNAiMAX (Invitrogen) and diluted in Opti-MEM I (Invitrogen) and incubated at 37^{o}C. The following day, cells were visualized under Floid cell imaging station, fluorescence microscopy, and images were taken to assess the efficiency of siGLO green uptake into mammalian cells (Figure 2.8). The green fluorescence signal emitted from the transfected cells represents positive transfection of siRNA.

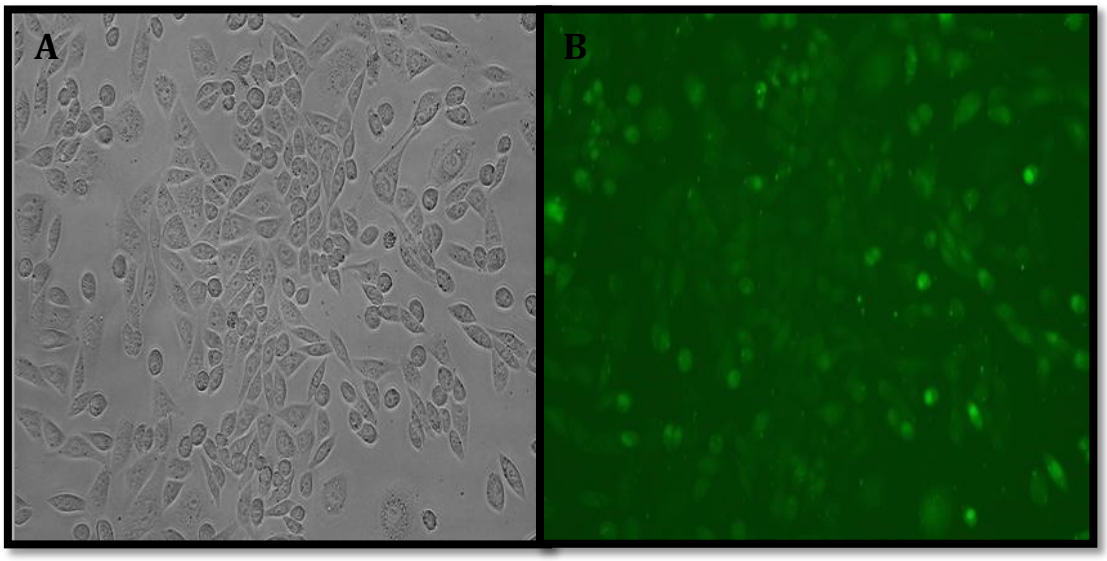

Figure 2.8 Representative images of transfection efficiency in Chinese hamster cell. **A)** Representative image of CHOK-1 line after 24 hours post-transfection with 100nM siGLO green indicator (x40 magnification). **B)** CHOK-1 cells showed green fluorescence staining that represented efficient uptake of siRNA within the target cell and indicated a successful transfection.

2.7.2 siRNA mediated knockdown in Chinese hamster cells

Prior to transfection, Cells (2.0 x10^5) were seeded in a 6 well plate containing complete medium without antibiotics. On the day of transfection, Cells were gently washed with Opti-MEM I (Invitrogen) to remove any FBS trace and added 1.6ml of Opti-MEM I (Invitrogen). All siRNAs stock concentrations were supplied as 40µM (Table 2.4), and were diluted to a final concentration of 100nM of each siRNAs. In a sterile 1.5ml Eppendorf tube (tube A) was transfer 5µl of siRNA and added Opti-MEM I to a final volume of 200µl and incubated for 5 minutes. Next, a second sterile 1.5ml Eppendorf tube (tube B) was prepared with 6µl of Lipofectamine RNAiMAX (13778030, Invitrogen) and added Opti-MEM I (Invitrogen) to a final volume of 200µl and incubated for 5 minutes. Both tube A and tube B mixture were incubated at room temperature for 30 minutes. Transfection siRNA mixture 400µl were then added drop-wise onto cells and gently swirled to avoid concentration in the middle of the plate. After 24 hours of incubation, the transfection media was removed and replenished with fresh 2ml of OPT-MEMI and incubated for another 24 hours in the incubator at 37^{o}C with 5% CO_2. Transfected cells were harvested and pelleted at different time points for knockdown gene expression analysis at 48 hours and 72 hours post-transfection.

2.7.3 RNA extraction

Total RNA is extracted using the RNeasy Plus kit (Qiagen) according manufacture's instructions. Chinese hamster cells were grown (80-90% confluence) and were harvested to obtain cell pellets (Chapter 2.3). Cells were disrupted by adding RLT buffer plus and 10µl Beta-mercaptoethanol and vortex for 15 seconds. The lysate was homogenized using a syringe and passed at least 5 times. The lysate cells were transferred to a gDNA filter column and spun down

for 30 seconds at 10,000rpm to remove any gDNA residue. One volume of 70% RNA free ethanol was added to the flow-through. The samples were transferred to a RNeasy spin column placed in a 2ml collection tube and spun down for 15 seconds at 10,000rpm. The flow through was discarded and added 700µl of RW1 buffer to the RNeasy spin column and spun down for 15 seconds at 1000rpm. Then added 500µl of RPE buffer to the RNeasy spin column and spun down for 15 seconds at 10,000rpm and discarded the flow through, this step was repeated twice. Placed the RNeasy spin column in a new collection tube and added 40µl of RNase free water directly to the spin column membrane and spun down for 1 minute at 10,000rpm to elute the RNA.

2.7.4. RNA quantification

The concentration of sample DNA was measured using NanoDrop 2000C UV/Spectrophotometer (Thermo Scientific). The spectrophotometer was calibrated using the AE buffer, the absorbance wavelengths at 260nm. Only, sample with high DNA quality and purity at ratio around 1.8 were kept for C-circle analysis.

2.7.5 Purification of RNA extracts from DNA

Removal of DNA from RNA sample extracts was achieved using Deoxyribonuclease I (DNAse I) amplification grade enzyme (Invitrogen). Each reaction mixture contained 1µg of RNA, 1µl of 10X DNase I reaction buffer and 1µl of DNAse I enzyme was added nuclease free water to final volume of 10µl. Samples were incubated at room temperature for 30 minutes. Then added 1µl of 25mM EDTA to the mixture and incubated for 10 minutes at 65^{o}C to deactivate the DNAse I enzyme.

2.7.6. Reverse transcription of RNA to complementary (cDNA)

The high capacity cDNA reverse transcription kit (4368814, AB) to synthesize single stranded cDNA from total RNA.

Table 2.5 Master mix reaction for cDNA synthesis

Stock concentration	Volume (µl)
10X RT buffer	2
25X dNTP Mix (100mM)	0.8
10X RT Random primers	2
MultiScribe reverse Transcriptase	1
Rnase Inhibitor	1
Nuclease Free water	3.2
Total Volume	**10µl**

Labelled PCR microtubes and placed in cooler rack then added 10µl of cDNA reaction mix to each tube and 11µl of the purified RNA and spun down for 20 seconds. cDNA synthesis was carried out by incubating the reaction mixture at 25 ^{o}C for 10 minutes, followed by 37^{o}C for 120 minutes and then at 85 ^{o}C for 5 minutes using a thermal cycler. cDNA samples were diluted in 20ul nuclease free water (1:1) and stored at-20^{o}C.

2.7.7 Analysis of gene expression by qRT-PCR

Gene expression levels were determined using QuantStudio 7 Flex RT-PCR system (AB, Invitrogen). The reaction mixtures for ATRX and HDAC9 genes consisted of 5µl 10 iTaq Universal probes (1725131, Bio-Rad), 1µl of forward TaqMan primer (10mM), 1µl of TaqMan reverse primer (10mM), 2µl of cDNA and nuclease free water up to 10µl. The reaction mix was spun down for 15 seconds and added to a 96 well plate (MicroAmp fast optical, AB) in triplicated per each sample and then sealed the microplate with clear adhesive film, followed by short centrifugation for at 1000rpm for 30 seconds. The microplate was loaded into the QuantStudio

7 Flex RT-PCR and parameters were selected for both the ATRX and HDC9 target genes and the GAPDH endogenous control were TaqMan assay, which were labeled with FAM dye label on the 5'end (Table 2.6).

Table 2.6 List of TaqMan primer and probe sequences

Name	Orientation	Length	Sequences
ATRX	Forward	19	GTGGACAACAGGTCAATCA
ATRX	Reverse	19	CCTTCTGCACACCATCTAC
ATRX	FAM 5'end	28	TTCATCCATTCCATCTG5AGTCACGGCT
HDAC9	Forward	19	GGGAATGTCACCGAAAATG
HDAC9	Reverse	18	GAGCAGGTTCATGGAGTC
HDAC9	FAM 5'end	21	CACGCCGCATCCTGAGCAACT
GAPDH	Forward	20	GGAGAAACCTGCCAAGTATG
GAPDH	Reverse	18	GTGGAAGAGTGGGAGTCA
GAPDH	FAM 5'end	23	ACAACCTGGTCCTCGGTGTAGCC

Figure 2.9 Representative image of qRT-PCR amplification using siRNA ATRX in CHOK-1. It can be observed the between of ATRX mRNA levels between untreated vs siRNA treated after 48 hours. The red curve represents the siRNA ATRX and the green curve represents the endogenous control gene, GAPDH.

2.8 Western Blots

Western blot is a technique that is used to detect specific proteins from cell extract or tissue. It is based on the separation of proteins molecular weight through gel electrophoresis. Proteins are transferred to a membrane and then incubated with an antibody specific to the protein of interest and detected on an x-ray film. Cells were grown, harvested and trypsinized, then after washed with ice cold-1X PBS for 5 minutes at 4°C. Cell pellets were lysed with 80µl RIPA lysis buffer (Sigma) containing protease inhibitor and vortex for 20 seconds. Cells were centrifuged at 14,000rpm for 15 minutes and supernatants aliquoted in several Eppendorf tubes and stored at -80°C. Protein extract concentrations were 30ug of protein and prepared in 2x Laemmli buffer and boiled in 100°C for 10 minutes to denature the globular structure of the proteins and loaded onto a 7.5% SDS casted gel.

2.8.1 Protein gel electrophoresis

The interior of the tank was filled with 1x running buffer composed (3g tris base, 14g glycine, 1g SDS and distilled water). The 30ug of sample proteins were loaded onto each well. The protein marker was loaded in the first lane and followed by sample proteins and allowed to run at 25mA with a constant of 100 volts for 1 hour 30 minutes until protein located near the bottom of the gel.

2.8.2 Blotting and transfer

Once proteins were separated in the gel based on their size and mobility (heavier move slower and hence at the top of the gel, while smaller proteins move faster and found near the bottom of the gel), proteins were transferred to a blotting membrane. Polyvinylidine fluoride (PVDF) (1620174, Bio-Rad) is a non-reactive membrane that offers high signal with low background.

The PVDF membrane was activated by soaking in 100% methanol for 10 seconds. The proteins were transferred onto PVDF membrane and assembled into a transfer sandwich system as followed: 1x filter pad, 1x filter paper, membrane, gel, 1x filter paper and 1x filter pad and locked into a transfer cassette as a sandwich. Then cassette was put in the tank and filled with transfer buffer up to 1litre and ran at 60 volts for 45 minutes and also an ice pad was placed inside the tank to prevent overheating of the buffer solution.

2.8.3 Blocking and antibody incubation

Once the proteins were transferred from the SDS gel onto the PVDF membranes and blocked in 5% blocking solution (5g non-fat milk, Marvel diluted in 100ml of TBST buffer) for 1 hour on shaker at room temperature to block unspecific binding of the antibody. Blocked membranes were gently rinsed in TBST and then incubated with primary antibodies ATRX (ab97508) 1:500 or HDAC9 (ab109446) 1:10000 were diluted in blocking solution and incubated overnight at 4^{o}C on shaker. After 24 hours incubation, membranes were washed 3 times in TBST for 5 minutes each and then incubated with the secondary antibody for 1 hour on the shaker at room temperature.

2.8.4 Protein detection with chemiluminescence

After incubation membranes were washed three times with TBST for 5 minutes each. ECL plus kit (GE healthcare) was used for detection based on the size of the membrane according to the manufacturer's instructions. The kit contained chemical A (HRP, a stable peroxidase detection reagent) and chemical B (luminol solution) and a mixture of both A and B reagents was prepared as follow; 2ml of reagent A mixed with 50µl of reagent B. The mixture was then added onto the

membrane and covered with Saran wrap for 5 minutes in the developer room. The excess of the ECL was tipped off onto a paper towel and membrane was placed in an x-ray cassette and ECL plus hyperfilm (GE healthcare) was put on top of the membrane and cassette closed and left for exposure for 5 minutes. The x-ray film was developed using an automatic machine (Xograph). If the protein bands were faint then a second film was exposed for a longer period, as ECL was active for at least 1 hour.

2.9 Statistical Analysis

Statistical analysis was done using student t-test in Microsoft Excel 2013 software. For chapters 3, 4, 5 and 6 t-tests were done at 95%, 99% and 99.9% confidences, where alpha value was set at 0.05, 0.01 and 0.001 respectively. For chapter 5, Anova test was done to compare to control samples for our test sample. Alpha was set at 0.05, 0.01 and 0.001 for 95% 99% and 99.9% confidences, respectively.

Chapter 3.

Analysis of chromatid type aberrations at interstitial telomeric sites in DNA repair proficient Chinese hamster cell lines

3.1. Introduction

Telomeres are specialized structures consisting of double stranded $(TTAGGG)_n$ telomeric sequences present at the termini of chromosomes in all vertebrates (Blackburn, 1991). In addition, telomeric sequences at intra-chromosomal sites known as interstitial telomeric sequences (ITSs) have also been identified in numerous vertebrate species (Meyne et al., 1990). Cytogenetic studies using FISH have shown that ITSs are located mostly in the pericentromeric regions and rarely inside chromosome arms (Multani et al., 2001; Azzalin et al., 1997; Bertoni et al., 1996). The ITSs have been associated with karyotype evolution during speciation in many vertebrate species (Meyne et al., 1990). For example, a well characterized ITS has been detected in human chromosome 2q13 and interpreted as a head-to-head telomere fusion of two ancestral ape chromosomes (IJdo et al., 1991). In Chinese hamster, ITSs can be divided into two ITSs types: heterochromatic ITSs (het-ITS) (Ruiz-Herrera et al., 2008), which constitute the major satellite DNA and comprise between 250- 500kb, and short ITSs contain short stretches of telomeric repeats (s-ITS) up to 20 hexamers in the same orientation (Faravelli et al., 2002; Azzalin, Nergadze and Giulotto, 2001; Faravelli et al., 1998). These s-ITSs sites are considered to be AT-rich DNA regions (Faravelli et al., 2002). It is known that AT-rich DNA regions display low duplex stability and are associated with aphidicolin-sensitive fragile sites in mammalian species (Faravelli et al., 2002; Palin et al., 1998; Yu et al., 1997).

Several cytogenetic studies have demonstrated that ITSs in Chinese hamster are considered to be “hot spots” (Ashley and Ward, 1993), for spontaneous chromosome breakage (Slijepcevic et al., 1996), as well as induced breakage by IR (Fernández, Gosálvez and Goyanes, 1995; Alvarez et al., 1993), and chemical compounds (Bolzán, Páez and Bianchi, 2001). In addition, ITSs in pericentromeric regions coincide with fragile site regions. Six folate-sensitive fragile sites have been detected in the Chinese hamster ITSs (Simi et al., 1998; Simi et al., 1990). Moreover, ITSs-associated fragile sites behave as recombination hot spots that lead to CAD gene amplification in Chinese hamster cells (Bertoni et al., 1994).

Furthermore, ITSs located at 2q14 on human chromosome 2 behaves as common fragile site, sensitive to aphidicolin, and requires TRF1 for its stabilization (Bosco and de Lange, 2012). Consistent with these findings, Bolzán et al. (2001) observed high incidence of breakage within ITSs in CHE and CHO cells treated with radiomimetic compounds, such as BLM, a well-known chemotherapeutic drug, and also reported additional chromosome areas of hybridisation in CHE, suggesting amplification events through breakage fusion-bridge cycles. Interestingly, Bolzán et al. (2013) demonstrated that chemically induced ITSs are not preferentially involved in the formation of chromosome type aberrations given that STZ, an antibiotic and antineoplastic drug, induces breaks outside pericentromeric regions in CHO cells. These results indicate that the association of telomeric sequences and the induction of chromosome breakage can be segregated further depending on the type of ITSs (het or s) and also the type of inducing clastogen.

One of the aims of this thesis is to examine DSB repair kinetics at the ITSs in Chinese hamster cell lines. A large body of evidence suggests that ITSs are preferential sites for IR-induced chromosome breakage and recombination in Chinese hamster cells. It is generally accepted that IR causes DSBs, which are considered to be critical lesions with cytotoxic effects, such as chromosome aberrations, apoptosis and cell death (Pfeiffer, Goedecke and Obe, 2000). In mammalian cells, DSBs are repaired by two main DNA repair mechanisms, NHEJ and HR.

In this chapter, we investigate the frequency of repair kinetics at ITSs in DNA repair proficient hamster. This will set up the basis for the analysis in later chapters, which will be focus on well-known Chinese hamster DNA repair deficient cell lines. We employed three Chinese control hamster cell lines; CHOK-1 line is originally derived from Chinese hamster ovary (CHO) and this subclone is proline deficient (Kao, 1967). V79 line is derived from lung tissue of a young male hamster (Sinclair, 1966). CHE line is originated from a female embryo.

3.2 Analysis of chromatid type aberrations in Chinese hamster control cell lines

Chromosome aberrations (CAs) are changes in chromosome number and chromosome structure (Savage, 1976). CAs can be classified as intra-chromosomal aberrations and involve a single chromosome, and inter-chromosomal aberrations comprising rearrangements between two or more chromosomes (Pfeiffer, Goedecke and Obe, 2000). IR induces CAs at all stages of the cell cycle; chromosome type aberrations occurs when cells are exposed in G1 or G0 phases of the cell cycle, whereas chromatid type aberrations arise when cells are exposed during S or G2 phase of the cell cycle (Bryant, 1985; Natarajan and Obe, 1984; Bender, Griggs and Bedford, 1974). The molecular lesion responsible for CAs is DSB.

Bryant (1998) proposed a "signal" model to explain conversion of DSBs into chromatid breaks. The signal model suggests that chromatid break is formed via chromatin strand rearrangement initiated by a signal caused by a single "hit" DSB induced within a loop chromatin domain. The rearrangement would involve strand scission and follow by mis-joining of the DNA strand at the crossover point of the chromatin loop (Bryant, 2004; Bryant, Peter and Slijepcevic, 1998). The disappearance or re-joining of chromatid breaks over time (in hours) begins with DSBs isolation in a loop configuration that disrupts topoisomerase IIα activity during deconcatenation of the sister chromatids in the G2 phase, leading to excision, re-joining and sealing of the chromatid ends at the crossover point (Terry, Riches and Bryant, 2008; Bryant, 2004). This leads to an exponential decline of the chromatid breaks with time, as the intra or inter-chromatid rearrangements and take place at the crossover point of the chromatid loop. The signal model is shown in Figure 3.1.

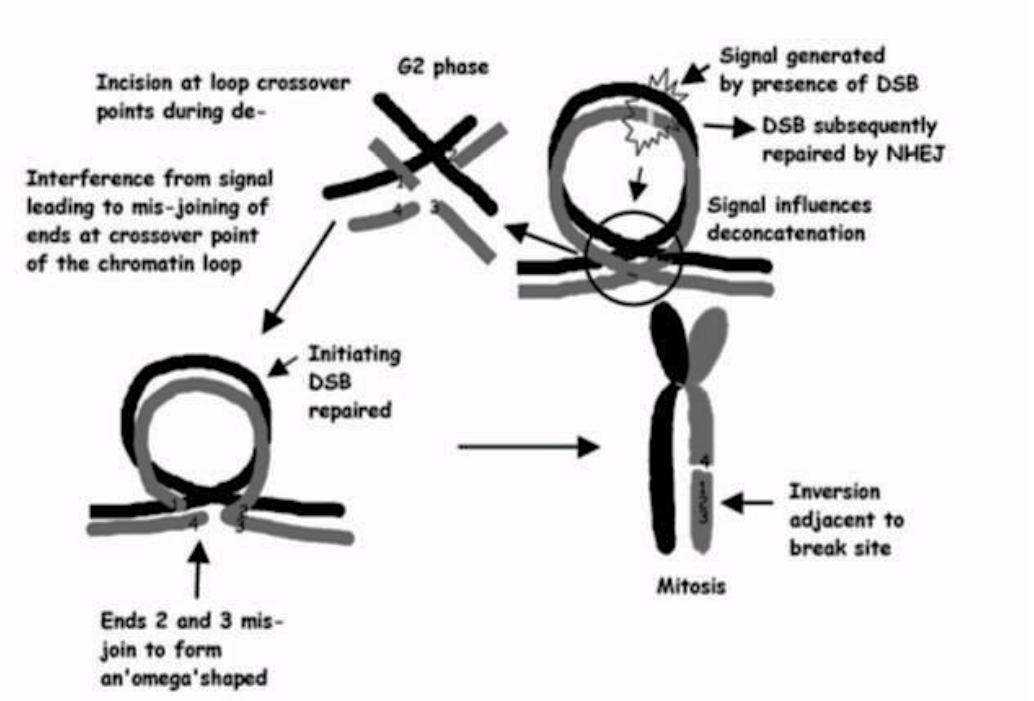

Figure 3.1 Schematic representation of the signal model for chromatid breakage. The DSBs within the chromatin loop domain results in the mis-joining of DNA ends through the deconcatenation of chromatids at G2 phase. The rearrangement of DNA strands at the crossover point would lead to the chromatid break disappearances over time. Image obtained from P. Bryant, (2004).

One of the aims of this chapter is to determine whether chromatid breaks exhibited repair kinetics response. We have used the G2 assay in three repair proficient Chinese hamster cell lines to study the chromatid type aberrations induced by gamma rays in unsynchronised cells. We used solid staining to detect CAs, which appear as chromatid gaps or chromatid breaks as shown in Figure 3.2.

Chromatid type aberrations in Chinese hamster control cell lines

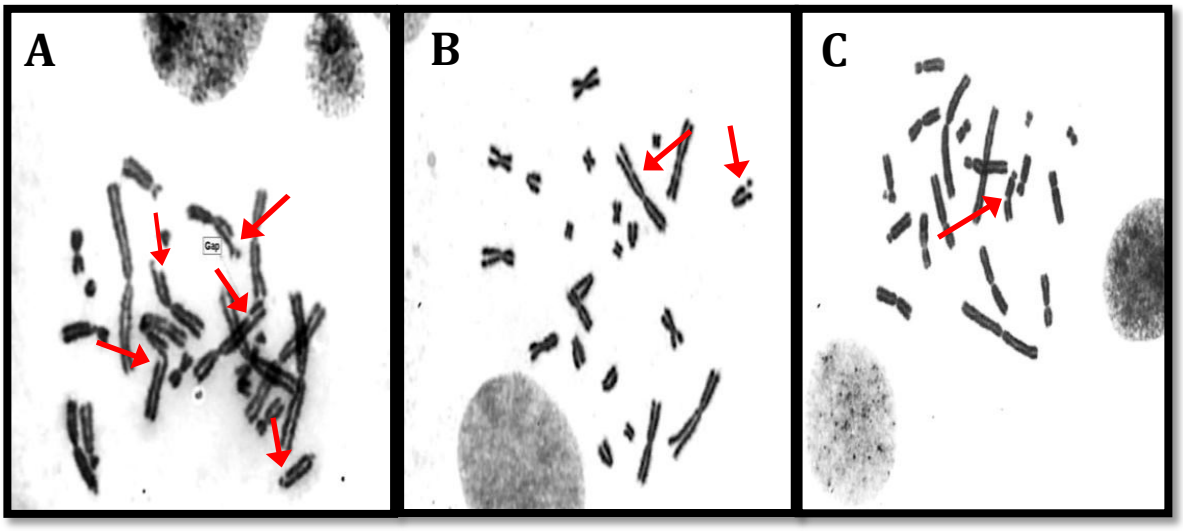

Figure 3.2. Representative images of chromosome metaphases spread in solid Giemsa staining post-radiation in three DNA repair proficient Chinese hamster cell lines. **A).** CHOK-1 metaphase spread and red arrows show chromatid breaks. **B).** CHE metaphase arrows indicate a break and a gap in the chromatids. **C).** V79 metaphase shows a break.

The highest number of breaks observed was at 1-hour post-radiation in all three cell lines, CHO-K1, CHE and V79 (Figure 3.3 and Figure 3.4). CHOK-1 cells showed higher frequency of chromatid breaks (2.53/cell) than CHE and V79 cells (1.88/cell and 1.35/cell respectively). At 2 hours all lines showed reduction in chromatid breaks by 0.70/cell (CHO-K1), 0.60/cell (CHE) and 0.50/cell (V79). The trend in the reduction of chromatid type aberrations continued at leading to the lowest frequencies in all cell lines at 4 hours post IR exposure (0.51/cell CHO-K1;0.34/cell CHE; and 0.21/cell V79) (Figure 3.3 and Figure 3.4). Overall, all three cell lines showed a steady reduction in the number of chromatid breaks, suggesting re-joining of DSBs (Figure 3.3). Furthermore, the kinetic followed a linear quadratic response (Figure 3.4). The statistical analysis showed significant differences (t-test **P<0.01, ***P<0.001) between un-irradiated samples and irradiated samples at each time points (1h-4hrs) in these three cell lines. The experiment was repeated twice under same conditions and the results averaged, thus ensuring that the random errors were minimised. Our results are in line with previous cytogenetic studies. Mateos et al. (1994) showed the kinetics of chromatid breaks disappearance or re-joining of DSBs with time. Slight differences between kinetic curves observed in different cell lines may be related to the stages of cell cycle progression, or differences in DNA repair proficiencies between cell lines. An important factor to consider is chromatin structure (euchromatin and heterochromatin). IR induced DSBs are higher in euchromatin than heterochromatin regions. However, DSBs in euchromatin repair faster than their counterparts in heterochromatin and this difference can be attributed to their chromatin compaction status between cell lines (Slijepcevic and Natarajan, 1994). Given that the only cell line with the normal karyotype and therefore the normal pattern of euchromatin/heterochromatin distribution is CHE, differences observed could be attributed to difference chromatin distribution in these three cell lines.

Chromatid type aberrations in Chinese hamster control cell lines

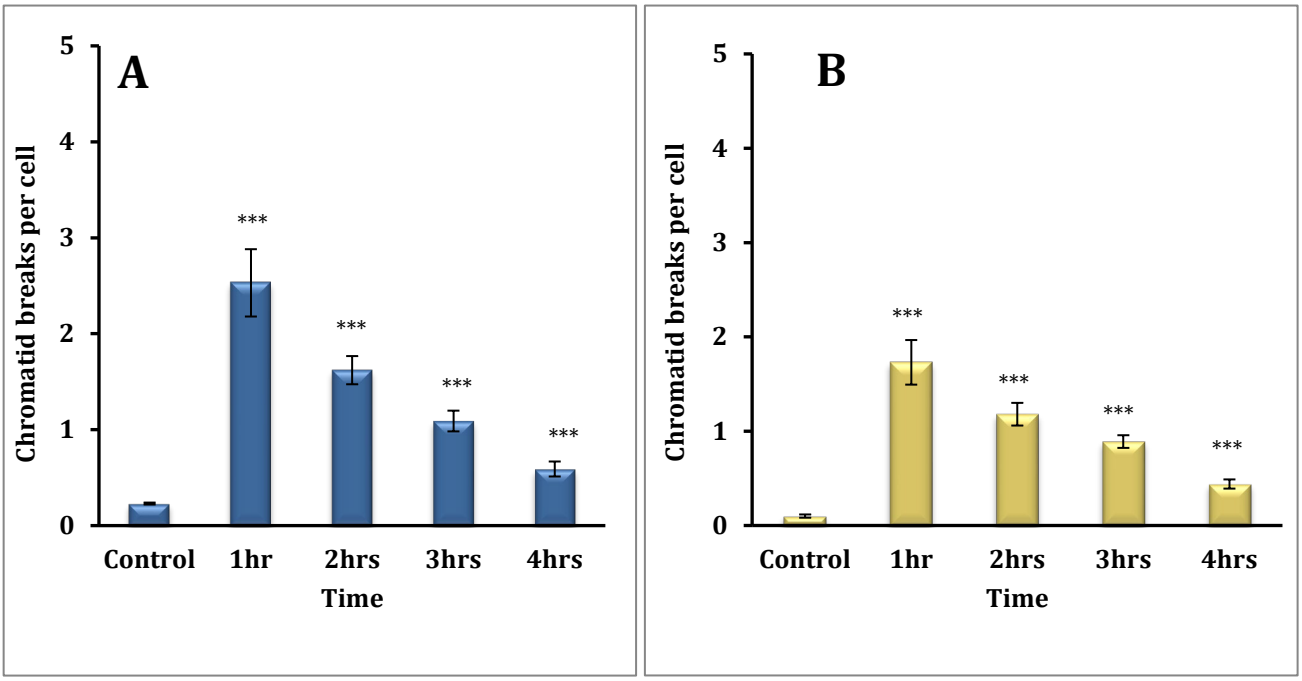

Figure 3.3 Frequencies of chromatid breaks and repair kinetics in Chinese hamster cell lines. **A).** CHOK-1 showed a frequency of 2.5 chromatid breaks per cells at 1 hour and the number of breaks decreased significantly with around 0.6 breaks at 4 hours. It can be observed breaks repair kinetics. **B)**. CHE cell line shows high frequency of breaks at 1 hour and chromatid breaks decreased over 4 hours with 2 breaks and 0.5 breaks, respectively. Experiment was performed twice and each time 100 cells were analysed. Error bars indicate SEM. The statistical significant the frequencies of chromatid breaks between untreated and treated in CHOK-1 and CHE cells at each time point, evaluated by unpaired student's t-test *P<0.05, **P<0.01, ***P<0.001.

Chromatid type aberrations in Chinese hamster control cell lines

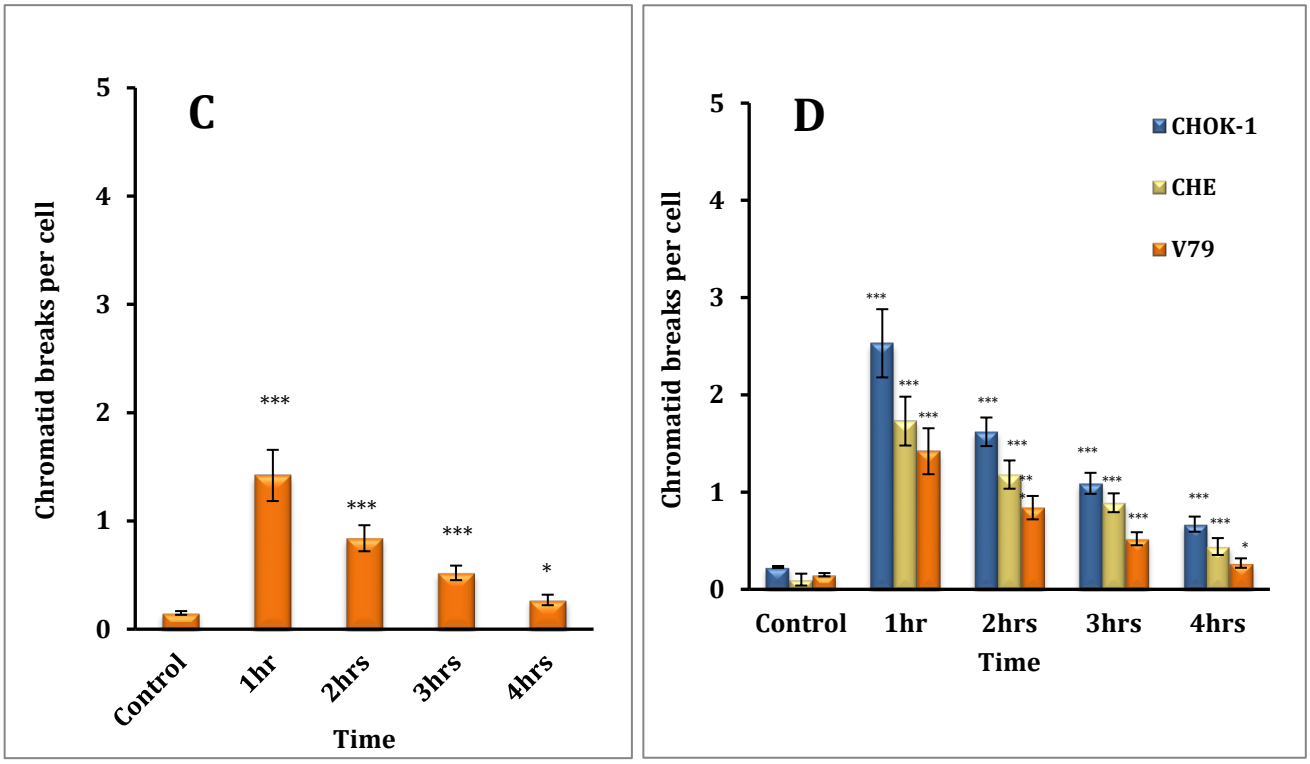

Figure 3.4 Frequencies of chromatid breaks and repair kinetics in Chinese hamster cell lines **C).** V79 showed a high frequency of chromatid breaks and the subsequence decline of break at 4 hours. **D).** The graph represented the chromatid breaks observed in the three cell lines. Error bars indicate SEM. The statistically significant of the frequencies of chromatid breaks between untreated and treated in V79 cells at each time point, evaluated by unpaired student's t-test *P<0.05, **P<0.01, ***P<0.001.

3.3 Analysis of chromatid break distribution at the ITSs in Chinese hamster control cell lines

Having established DBSs repair kinetics of chromatid break repair in Giemsa stained chromosomes we next wanted to establish distribution of chromatid breaks in ITS chromosome regions relative to the rest of the genome. To this end we employed FISH and used a PNA telomeric probe. In Chinese hamster chromosomes ITSs are located at the heterochromatic pericentromeric regions (Faravelli et al., 1998), and hamster genome contains a total of 18 large 500 kb blocks of ITSs in chromosomes 3-10 and X (Faravelli et al., 2002; Slijepcevic and Hande, 1999). Several cytogenetic studies have shown strong FISH hybridization signals at ITSs in Chinese hamster cell lines (Bertoni et al., 1996; Meyne et al., 1990). Interestingly, CHOK-1 cells lack hybridization signal at chromosome ends suggesting telomere length below 1kb (Slijepcevic and Bryant, 1995), and also a new sensitive method that measures the shortest telomere length, TeSLA has detected CHOK-1 telomere length below 1kb (Lai et al., 2017). By contrast, CHE and V79 cells showed visible terminal telomeric signals (Figure 3.5). As expected, all three control cell lines exhibited a strong ITS hybridization signal at pericentric regions in the majority of chromosomes, except in chromosomes 1 and 2. Moreover, a specific pattern of amplification events occurs on chromosome 10 in CHO-K1 cells Figure 3.5. (Slijepcevic et al., 1997; Slijepcevic et al., 1996).

To investigate whether the chromatid breaks occur at ITSs and kinetics of repair take place over time in three control hamster cells, we have analysed 50 metaphases per cell line and repeated the experiment twice to ensure consistency Figure 3.5.

The chromatid breaks were grouped into two categories: breaks inside or outside of the ITS regions. Results of this analysis are shown in Figure 3.6. In addition, to show results in a more detailed way, we produced a table with observed and expected values for all cell lines and performed the statistical analysis (Table 3. 1). From Figure 3.6 and Table 3. 1 it can be Chinese hamster chromosomes. In line with our results Bolzán et al. (2001) have shown that het-ITSs are involved in breakage more frequently than expected.

Chromatid aberrations at the ITSs in Chinese hamster control cell lines using FISH

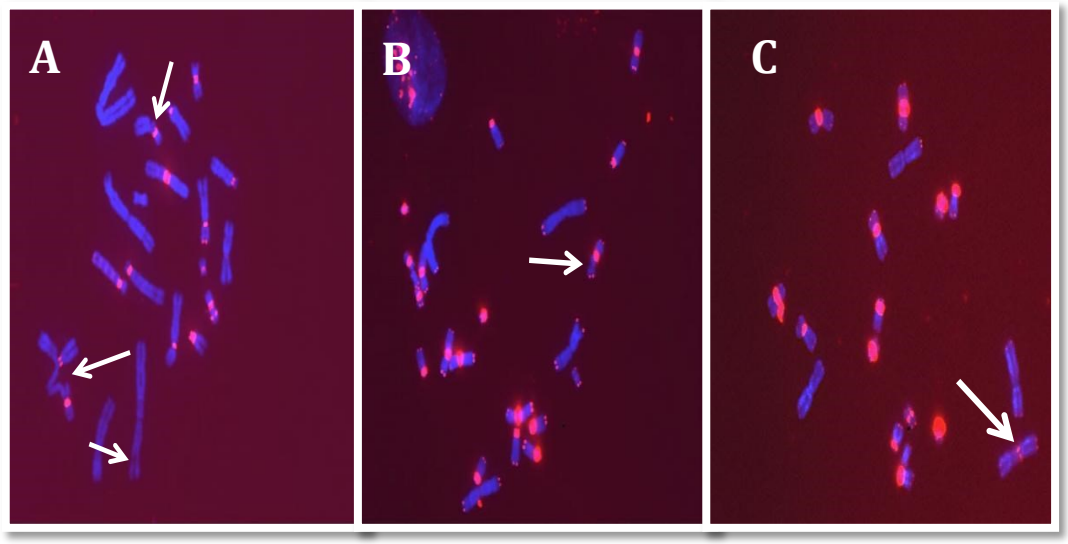

Figure 3.5 Representative image of FISH hybridization of ITSs signal at the pericentric regions in the Chinese hamster cell lines. **A).** CHOK-1 chromosomes metaphase showed breaks and an exchange (white arrows) and no signal at the chromosome ends. **B).** CHE metaphase exhibited strong telomere hybridization at the chromosome ends and pericentric regions and white arrow indicated a break within ITSs. **C).** V79 metaphases showed very strong hybridization at the centromeres and less strong at the chromosome ends, white arrows showed a break within ITSs and short ITS in one set of chromosomes 1.

Analysis of chromatid aberrations at ITSs in Chinese hamster control cell lines using FISH

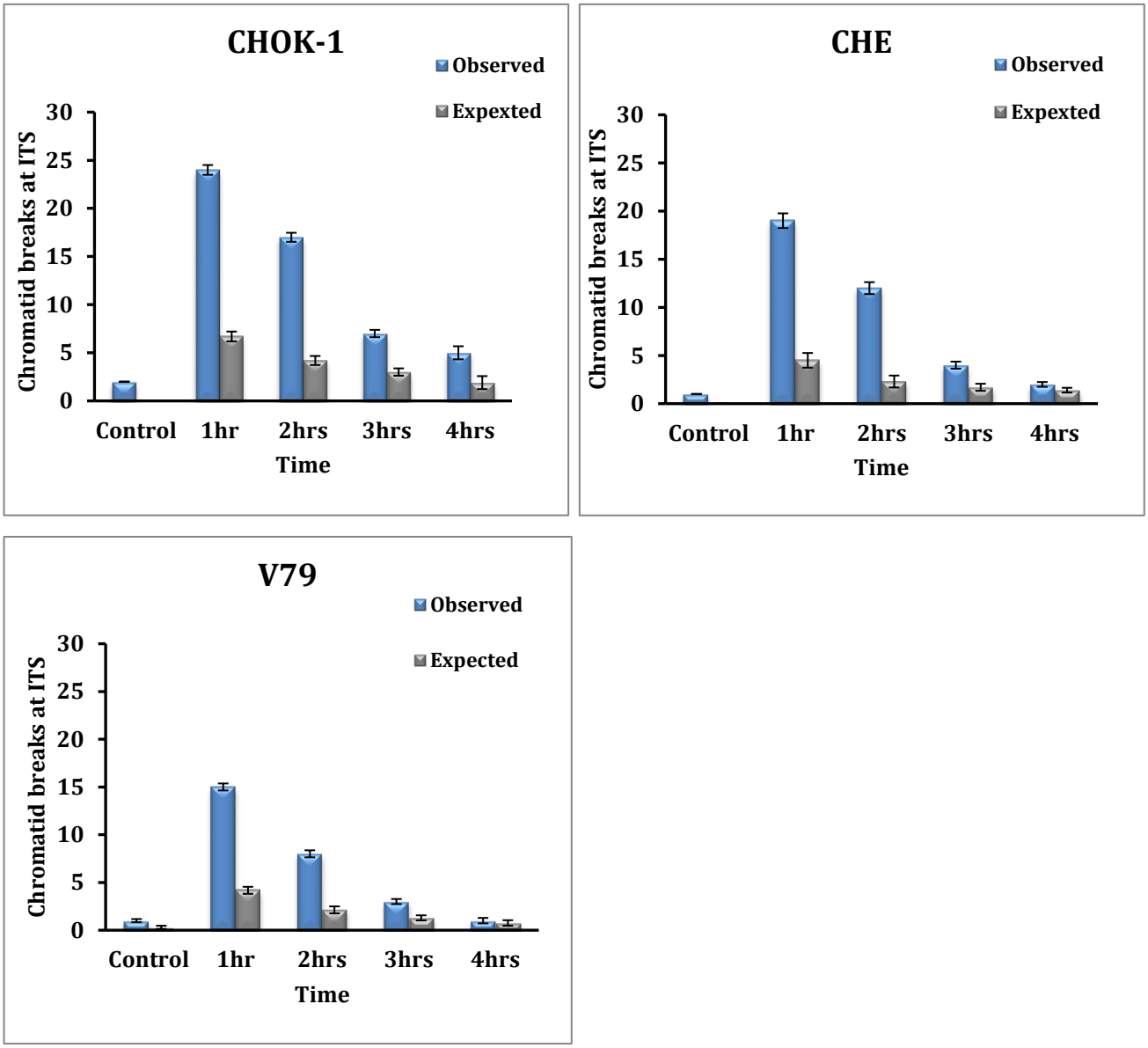

Figure 3.6 Chromatid breaks observed within the ITSs in three DNA repair proficient Chinese hamster cell lines. CHOK-1 shows the number of observed and expected breaks within ITSs. CHE shows total number of observed and expected breaks at ITSs. V79 shows chromatid breaks observed and expected over four hours. Error bars indicate SEM.

Table 3.1 Distribution of chromatid breaks within ITSs and DSBs repair kinects among DNA repair proficient Chinese hamster cells after 4 hours.

			0h		1hr		2hr		3hr		4hr		
Cell lines	**Score cells**	**ITS (%) Ch. Length**	**Obs.**	**Exp.**	**Obs.**	**Exp.**	**Obs.**	**Exp.**	**Obs.**	**Exp.**	**Obs.**	**Exp.**	***p-value (0.05)***
CHOK-1	100	8.4	2	0	24	6.7	17	4.2	7	3	5	1.9	p<0.05
CHE	100	6.3	1	0.1	19	4.5	12	2.3	4	1.7	2	1.4	p<0.05
V79	100	9.3	1	0.1	15	5.1	8	2.1	3	1.6	1	0.9	p<0.05

The difference between observed and expected frequencies of breaks and gaps were based on total ITSs (%) distribution on chromosome length and calculated by X^2 analysis.

3.4 Analysis of DNA DSBs in Chinese hamster control cell lines by γ-H2AX foci

Next, we wanted to investigate if what we observed at the cytogenetic level can be reproduced when analysing IR induced damage in interphase cells. γ-H2AX assay is a sensitive marker to assess DNA DSBs damage and repair in the nuclei of cells (Dickey et al., 2009). DSBs are recognized by sensor proteins and the MRN complex, BRCA and 53BP1 that activate the transducer proteins, ATM and ATR. These kinases phosphorylate histone H2AX on Serine residue 139, which becomes phosphorylated (γ-H2AX) (Rogakou et al., 1998). γ-H2AX induction is rapid and half the maximal levels are reached within 1-3 minutes post-radiation and the maximal yield levels are reached within 10- 30 minutes (Sedelnikova et al., 2002). DSBs can be detected and quantified by γ-H2AX marker and γ-H2AX foci number is proportional to the number of DSBs in a cell. We analysed 100 interphase cells per cell line and performed two independent experiments to ensure consistency.

The results of our analysis are shown in Figures 3.7 and 3.8. In line with results in Figure 3.8, which shows disappearance of chromatid breaks with time, which is presumably reflective of effective repair kinetics, analysis of DNA damage repair kinetics using a well-known DNA damage marker shows a similar trend of repair kinetics. The difference between untreated samples and treated samples were statistically significant (t-test **P<0.01, ***P<0.001) at each time points in the three cell lines in Figure 3.8.

γ-H2AX assay to investigate DNA DSB repair in Chinese hamster control cells

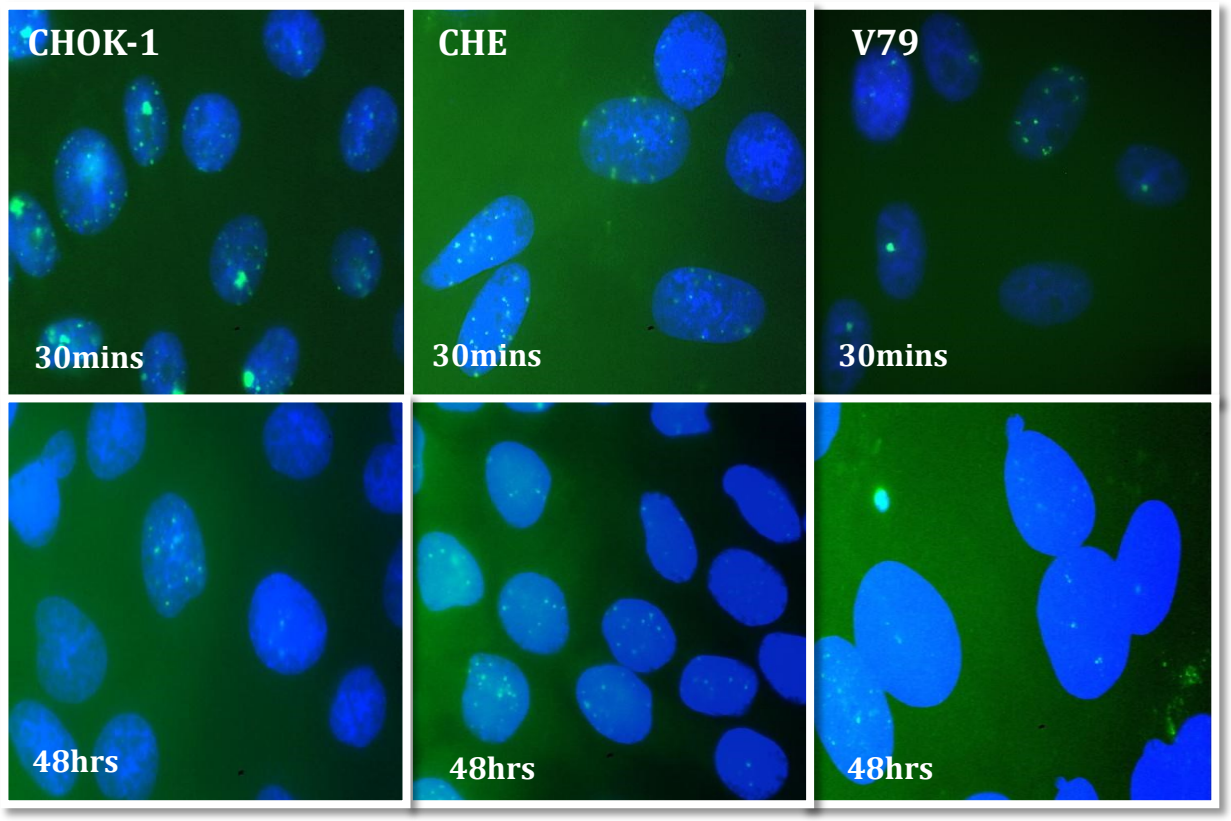

Figure 3.7 Representative image of DNA DSB damage detected by γ-H2AX antibody. The upper column represented the 30 minutes post-radiation and the γ-H2AX (green foci) corresponded to the DSB damage sites in interphase cells from three DNA repair proficient Chinese hamsters. The lower column showed the disappearance of γ-H2AX, which is proportional to the DNA damage repair at 48hrs.

Frequencies of DNA DSBs in Chinese hamster control cell lines using γ-H2AX foci

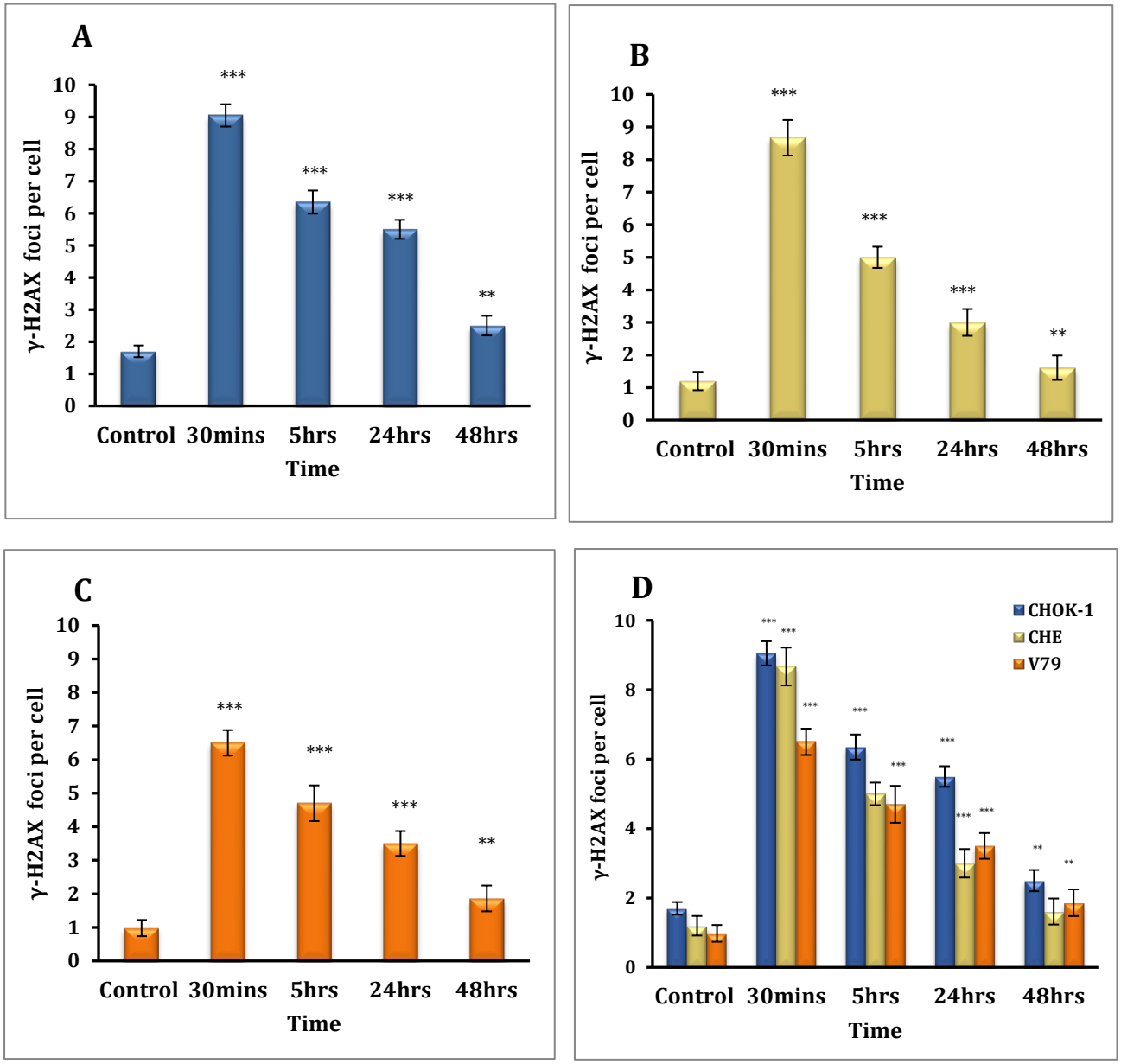

Figure 3.8 γ-H2AX repair kinetics in DNA repair proficient Chinese hamsters. **A).** CHOK-1 showed high frequencies of γ-H2AX foci at 30mins post-radiation and DSBs disappearance with time. **B).** CHE displayed less sensitivity to DSB induction compared to CHOK-1, but high levels of γ-H2AX were observed at 30mins post-radiation. **C).** V79 cells were shown γ-H2AX repair kinetics that correlated with the disappearance of γ-H2AX foci with time. **D).** The graphs showed the average of γ-H2AX foci number in three Chinese hamster cells. It can be observed that these cells lines had different sensitivity to DSB induction and also differences in the DSB repair response. It is clear that these three hamsters show a significant decreased in the number foci after 5 hours and 24 hours post-radiation. Error bars represent SEM and calculated from the total of 100 cells scored. Statistical analysis between untreated and treated in CHOK-1, CHE and V79 cells at each time point, evaluated by unpaired student's test *P<0.05, **P<0.01, ***P<0.001.

3.5 Analysis of telomere dysfunction in Chinese hamster control cell lines

In order to investigate whether DSBs occur at the telomeres and whether the repair kinetics of DSB takes place at telomeres in these control cell lines. We used telomere dysfunction induced foci (TIF) assay. The co-localization of both, γ-H2AX antibody and Cy3 PNA probe would result in double staining colour, representing TIFs foci formation, at interphase cells. Telomeres progressively shorten after cell division and since telomerase is absence from most somatic cells, this would result in telomere dysfunction (Callén and Surrallés, 2004; Blasco et al., 1997). When telomeres capping functions is impaired at the terminal ends, chromosomes end can be recognized by DNA repair mechanisms that leads to end-to-end fusion, causing chromosomal instability (d'Adda di Fagagna et al., 2003; de Lange, 2002). We analysed 100 interphase cells per cell line and counted TIFs as foci that showed double staining, green dye for γ-H2AX and red for Cy3.two independent experiments were performed to ensure consistency. The results of our TIFs analysis are shown in Figure 3.9 and 3.10. The highest levels of TIFs foci number was at 30 minutes post-radiation in all three cell lines, CHOK-1 (4.21/cell), CHE (3.74/cell) and V79 (2.6/cell). However, at 48 hours CHOK-1 (0.85/cell), CHE (0.67/cell) and V79 (0.57/cell) cell lines showed a decreased in the number of TIFs foci. The difference between untreated samples and treated samples were statistically significant (t-test **P<0.01, ***P<0.001) in the three cell lines. Despite the decrease of foci at 48 hours, the number of foci remained higher compared to untreated.

Telomere dysfunction and detection in Chinese hamster control cell lines by TIFs

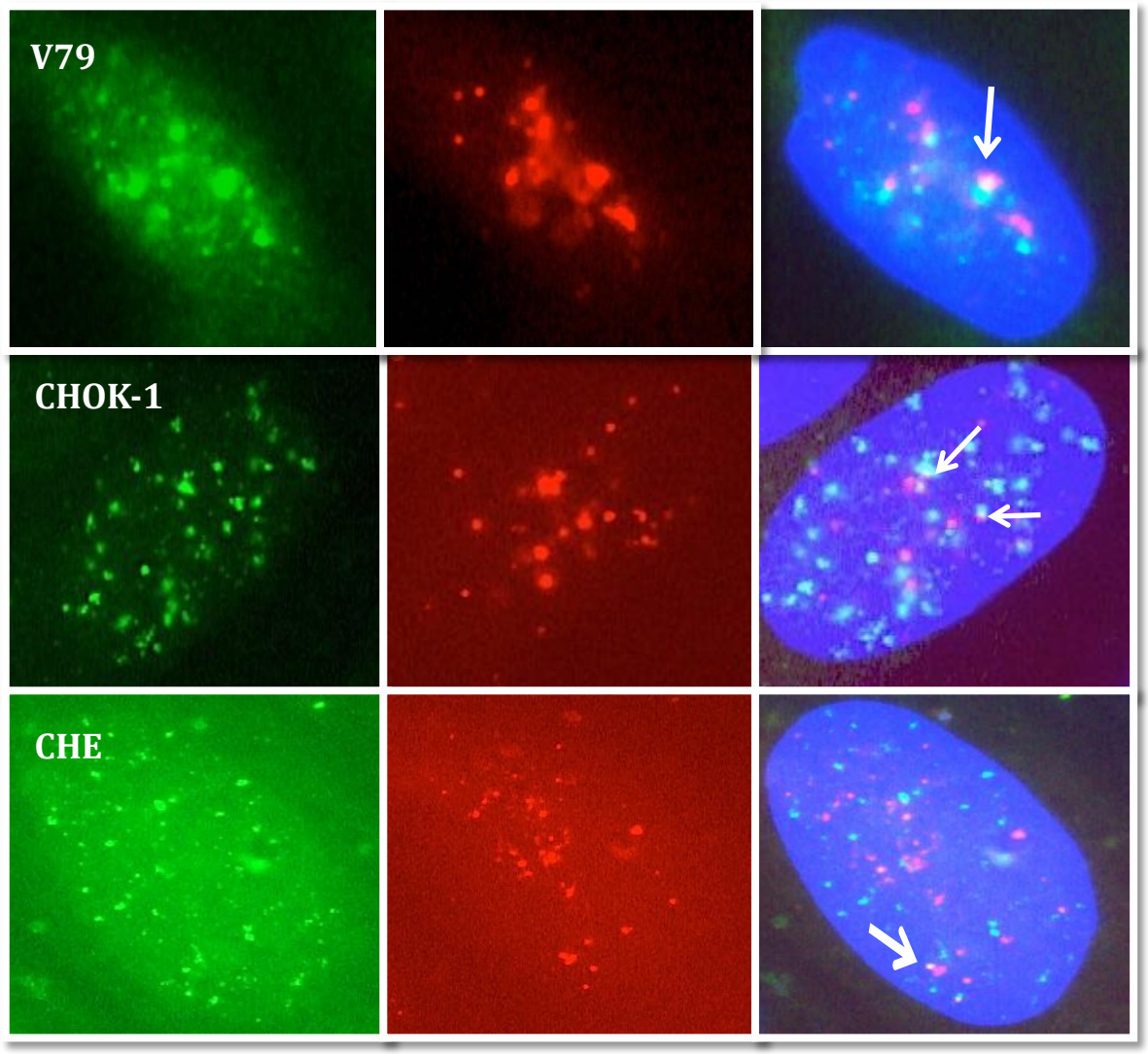

Figure 3.9 Representative images of TIFs in DNA repair proficient Chinese hamster cells. The first vertical column (green fluorescence) represented positive γ-H2AX foci, which accumulates at the DSB sites followed 1Gy radiation. The second column (red) corresponded to telomere specific PNA probe, Cy3 and since ITSs are telomere-like repeats the strong hybridization observed would represent ITSs contained within hamster cells. Third column showed the co-localization of γH2AX (DSBs) and Cy3 probe and double staining (yellow) foci represent DSBs within ITSs (white arrows) in hamster interphase cells.

Telomere dysfunction in Chinese hamster control cell lines using TIFs foci

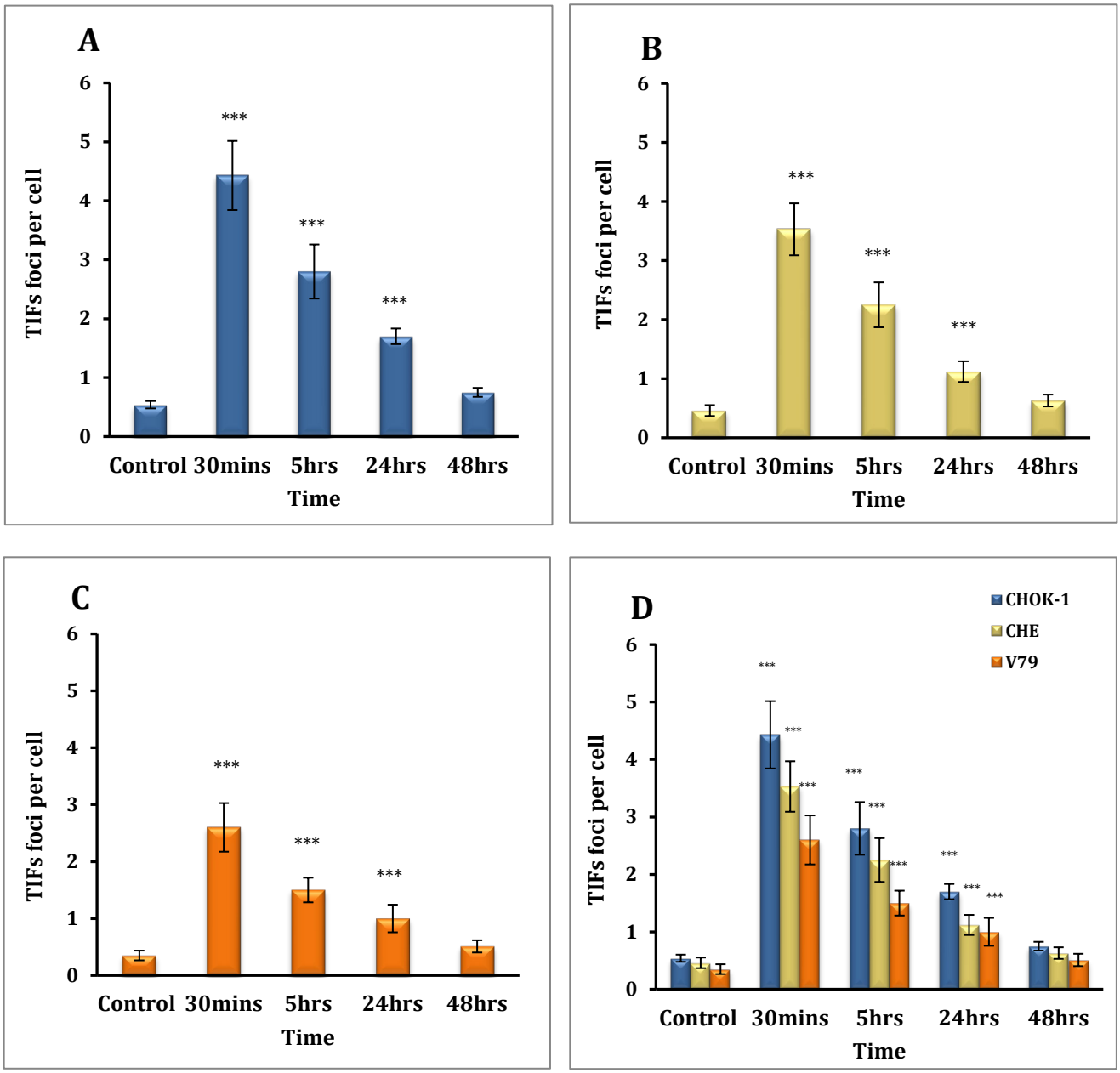

Figure 3.10 Frequencies of TIFs foci in Chinese hamster cell lines. **A).** CHOK-1 showed higher frequencies of TIFs levels at 30 mins post-irradiation and TIFs levels remained high throughout the 24 hours. **B).** CHE exhibited the second highest TIFs levels after CHOK-1. However, the disappearance of TIFs foci in CHE cells were faster compared with CHOK-1 and V79 cells. **C).** V79 cells were shown the lowest frequencies of TIFs induction throughout the 48hrs. **D).** The graph represented the total number of TIFs foci between the three cell lines. Error bars represent SEM and calculated from the total of 100 cells scored. Statistical analysis between untreated and treated in CHOK-1, CHE and V79 (cells at each time point, evaluated by unpaired student's t-test *P<0.05, **P<0.01, ***P<0.001.

3.6 Discussion

In 1993, Alvarez and colleagues demonstrated chromosomal radios-sensitivity at the ITSs in Chinese hamster cells (Alvarez et al. 1993). They concluded that breaks at ITSs were significantly higher than expected based on the proportion of ITSs within the Chinese hamster genome. Several cytogenetic FISH studies have shown ITSs as "hot spots" or preferential sites for chromosomal breakage, spontaneous or IR-induced, other genomic rearrangements and amplifications that resulted in chromosomal aberrations (Slijepcevic et al., 1996; Ashley and Ward, 1993).

The aim of our study was to investigate the frequency of breaks and repair kinetics at the ITSs and assess the kinetics of repair in three repair-proficient Chinese hamster cell lines. In line with Mateos et al., (1994) our results based on plain Giemsa staining of chromosomes (G2 assay) suggested a linear relationship between the disappearances of chromatid breaks with time (Figure 3.3 and Figure 3.4), although slight differences in chromosome repair kinetics between cell lines were observed (Figure 3.4). A possible explanation of the differences between chromatid break disappearances in these repair-proficient cell lines may be related to chromatin conformation. Therefore, the differences in the rate of chromatid breaks induction and repair response between cell lines may corresponded to their heterochromatin distribution within individual chromosomes. Natarajan et al., (1971) and Slijepcevic et al., (1994) have shown higher frequencies of chromosomal aberrations in heterochromatic regions than euchromatic regions in individual hamster chromosomes after irradiation.

Studies have suggested that DSBs in heterochromatin slow down the competence of DNA repair, because chromatin is compacted and DNA repair proteins cannot access to the DNA damage site (Storch et al., 2010). Since, heterochromatin is condensed and transcriptional inactive and predominantly by histone hypoacetylation and tri-methylation on Lys 9 histone H3. It can be further divided into constitutive and facultative heterochromatin (Schueler and Sullivan, 2006). Constitutive heterochromatin is comprised at centromeric, pericentric and telomeres regions and these constitutive heterochromatins are shared by all cells of a given specie and usually do not contain genes. While, facultative heterochromatin refers to regions where genes are kept silenced or developmental regulated (Saksouk, Simboeck and Déjardin, 2015).

It is known that chromosome aberrations are non-randomly distributed in the genome, and these chromosomal breakpoints have been localised at heterochromatic regions such as pericentromeric regions and telomeres regions, in humans, plants and animals (Trojer and Reinberg, 2007; Obe et al., 2002; Puerto et al., 2001; Tucker and Senft, 1994). Moreover, it has been shown that radiation-induced chromatid breaks tend to localize within heterochromatic blocks of Chinese hamster chromosomes (Slijepcevic and Natarajan 1994). Having established the repair kinetics, we then analysed the distribution of chromatid breaks and repair at the ITSs in the three Chinese hamster cell lines (Figure 3.6). FISH results showed higher frequencies of breaks at ITSs than expected based on the percentage of the genome covered by ITSs (Figure 3.5 and table 3.1). These results were in good agreement with previous cytogenetic FISH studies (Figure 3.6). (Bolzán, Páez and Bianchi, 2001; Slijepcevic et al., 1996; Fernández, Gosálvez and Goyanes, 1995).

A method called DNA Breakage Detection-FISH (DBD-FISH) is a procedure that allows intragenomic and intercellular heterogeneity in DNA breakage induction and repair to be assayed. The DBD-FISH incorporates the microgel technique that is used in nuclear halo or comet tail test (Fernández and Gosálvez, 2002). Rivero et al., (2004) DBD-FISH results have shown different patterns of single and double strand breaks repair kinetics at ITSs in Chinese hamster cell lines and reported that ITSs exhibit high alkali-sensitivity regions enriched with unrepaired DNA segments (Rivero et al., 2004). Therefore, results of the disappearance of chromatid break within ITSs in Chinese hamster contrast with those presented by Rivero et al., (2004).

The heterogeneity of DSB repair within the ITS regions can be associated to their chromatin conformation; the high dense chromatin compaction at long ITSs (pericentric) may result from an increase of the torsional stress that causes a high frequency of short unrepaired DNA segments, thus torsional stress of DNA loops during the process of chromatin packing in Chinese hamster cells, possibly may confers sensitivity to breakage and recombination within ITS regions (Mosquera et al., 2005; Rivero et al., 2004). In addition, Revaud et al., (2009) has reported that ITSs shares common structural features with true telomeric chromatin, and also high nucleosome density than bulk chromatin. Furthermore, there is some evidence to suggest the contribution of C-NHEJ mechanism in the repair of spontaneous and IR-induced DSB within pericentric and non-pericentric ITS in CHO cells. It has been shown that DNA-PKcs stabilizes spontaneous DSBs within ITSs from chromosome 9 long arms and results in terminal deletions, and the NHEJ is capable to restore the IR-induced DSBs within ITSs (Revaud et al., 2011).

It is known that chromatin compaction provides resistance to radiation effects and limited the DSBs formation events (Storch et al., 2010). These findings suggested that DNA-PKcs dependent C-NHEJ promotes DNA DSB repair at pericentromeric regions in CHO cells, but the difference in the sensitivity of heterochromatin to DNA damage is intrinsically related to the levels of chromatin compaction (Falk, Lukášová and Kozubek, 2008). However, since TRF2 protein colocalize with ITSs in CHO cells, this may inhibits DNA-PKcs (C-NHEJ) in favour of A-NHEJ repair, as an alternative mechanism of DSB repair for pericentromeric ITS regions in CHO model (Revaud et al., 2011; Krutilina et al., 2003).

Interestingly, recent studies have demonstrated a particular chromosome structural organization involving ITSs in humans. The shelterin protein, TRF2 (dependent t-loop) associates with ITSs and form an interstitial t-loop (ITL), this interaction is mediated by lamin A/C, nuclear intermediate filament protein (Wood et al., 2014). They proposed the interaction between with TRF2, lamin A/C and ITSs in normal cells is a regulated process and the binding of TFR2 and lamin A/C to ITSs varies between cell types, but also chromatin compaction status influences this interaction (Wood et al., 2014). Moreover, it has been suggested that alteration of ITL structure by disruption on its components leads to expose chromosome ends to DNA repair pathways, therefore a reduction or sequestration in ITL could be a preceded step before telomere instability (Wood et al., 2015; Wood et al., 2014).

We asked whether our cytogenetic results could be reproducible to assess DNA damage by other immunostaining means. To investigate the DSB repair kinetics we used immunocytochemistry and our results showed the disappearance of γ-H2AX foci with time in repair-proficient hamster cells (Figure 3.7 and Figure 3.8).

All three hamster cells were exhibited higher frequencies of γ-H2AX positive foci at 30 minutes post-radiation and the kinetics of γ-H2AX foci disappearances correlated with DSB repair that were noticeable at 48 hours in all cell lines, hence hamster cells may use both HR and NHEJ as repair mechanisms. Given that our three cell lines are DNA repair proficient we presumed that disappearance or re-joining of DSBs are carried out by both HR and NHEJ repair pathways. NHEJ is thought to be the predominant mechanism for DSB repair throughout the cell cycle and commonly used to repair DSBs induced by IR (Sancar et al., 2004). Interestingly, it has been reported that G2 phase exhibited a rapid kinetics of DSB repair due to NHEJ repair pathway. A slower repair component is due to HR (Shibata et al., 2011), suggesting that MRE11 endonuclease activity initiates the resection of 3' to 5' towards the DSB end, which is critical in the switch from NHEJ to HR repair (Shibata et al., 2014). Furthermore, changes in chromatin structure, acetylation of H4, allows decondensation of chromatin, and may favour DNA repair at different speeds (Dellaire, Kepkay and Bazett-Jones, 2009).

A number of studies have reported that human and mouse telomeres pose a challenge to DNA machinery and cause replication dependent abnormalities that resemble to aphidicolin induced fragile sites (Bosco and de Lange, 2012; Sfeir et al., 2009). For example, wild type mouse cells exposed to aphidicolin show fragile telomere phenotype in metaphase followed by TRF1 deletion. In fact, human telomeric repeats present at chromosome 2q14 are capable to form common fragile sites when aphidicolin exposure (Bosco and de Lange, 2012; Sfeir et al., 2009).

It has been demonstrated that telomeres are targets of a persistence DNA damage response in ageing and senescence. Telomeres ends are hidden from NHEJ or HR mechanism to prevent end-to-end fusion due to the binding of TRF2 to telomeres (Hewitt et al., 2012; Bae and Baumann, 2007).

In addition, Fumagalli et al., (2012) have found persistent DNA damage at telomeres in senescent cells. They found that in differentiated tissue of old primates a DNA damage marker, γ-H2AX, accumulates and preferential localized at telomeres that are not particular short. Interestingly, they proposed that linear genomes are not homogenously reparable and damage at telomeres are irreparable and would trigger persistent DNA damage response and cellular senescence (Fumagalli et al., 2012).

It is of interest to examine whether DSBs at telomeric sequences in hamster cells show repair kinetics or remain unrepaired. We reasoned that DSBs repair would have no involve canonical telomeres, since telomere length in hamster cells is approximately 1kb, thus the strong telomeric probe (Cy3) hybridization signal will be corresponded to large blocks of ITSs, therefore TIFs positive foci will represent hamster ITSs (Figure 3. 9).

As shown in Figure 3.10, the DSBs within ITSs are repaired and that correlate with the decrease in number of TIFs foci in Chinese hamster cells. Our observation of DNA DSBs exhibited kinetics of repair up to 4hours in all three DNA repair proficient hamsters. However, these Chinese hamster cells showed differences in the frequency of TIFs foci and that can be attributed to their percentage of ITSs present in each cell line.

For instance, CHOK-1 has the highest percentage of ITSs compared with CHE and V79. Similarly, Dr Yaghoub Gozaly (unpublished data) at Brunel University has observed TIFs foci disappearance in Chinese hamster cells.

Apart from our results there are no other published data examining directly DSB repair kinetics within ITSs in Chinese hamster cell lines. However, a recent study shows that telomeric DSBs are efficiently repaired in proliferating cells, including normal and cancer cells, but are irreparable in senescent human cells, where DNA damage response persists, and suggested that DSB repair in telomeric DNA involves HR between sister chromatid and non-sister chromatids (Mao et al., 2016).

In conclusion, the results presented within this chapter show that (a) the three repair proficient cell lines exhibit higher levels of chromatid breaks within ITSs than expected and that (b) ITSs, telomeric like-repeats, show chromatid break repair kinetics in three repair proficient Chinese hamster cell lines.

Chapter 4.

Analysis of chromatid type aberrations at interstitial telomeric sites in NHEJ deficient Chinese hamster cell lines

4.1 Introduction

Results presented in the previous chapter indicate that breakages involved the ITSs in repair-proficient Chinese hamster cell lines were higher than expected based on the percentage of the genome covered by telomeric repeats. Several cytogenetic studies have demonstrated the ITSs in the Chinese hamster genome; located mostly at pericentromeric regions are known as preferential breakage sites or "hot spot" for breakages, recombination and amplification (Slijepcevic *et al.*, 1996; Balajee *et al.*, 1996; Ashley and Ward, 1993; Alvarez *et al.*, 1993). Consistent wit this finding, Slijepcevic and Natarajan (1994) showed that the euchromatin regions are more susceptible to DNA damage than heterochromatic regions, and the repair of DNA damage appears to be more efficient in euchromatin than heterochromatin regions (Slijepcevic and Natarajan, 1994). In addition, Johnson and colleagues (1999) demonstrated that chromosome breakpoints are non-randomly distributed throughout the human genome with prevalence at heterochromatic regions and/or telomeres (Johnson *et al.*, 1999). For example, an association of chromosomal breakpoints with copy number variations (CNVs) have shown genomic amplification and translocation on chromosome 8q and is one the most frequently gained chromosomal arms in colorectal cancer (Camps *et al.*, 2008). It has been observed that chromosomal breakpoint coincided with CNV loci and these regions are more prone to chromosome breakage in primary colon cancer (Ben Marine, 2010; Camps *et al.*, 2008; Padilla-Nash *et al.*, 2001). Moreover, the non-randomly distribution of chromosomal breakpoints may be associated with gene density and chromatin structure (Rivero *et al.*, 2004; Slijepcevic and Natarajan, 1994).

It is known that the chromatin complex is a dynamic structure that plays an important role in DNA damage response and modulates the access to DNA damage sites that lead to structural chromosome modifications. The biochemical processes included acetylation, phosphorylation, deacetylation and ubiquitylation of various histones, which influence the access of DNA repair enzymes to DNA damage sites and thus modulate the DNA repair response (de la Fuente *et al.*, 2014; Falk, Lukášová and Kozubek, 2008). For example, H2AX, a well-known histone protein, is rapidly phosphorylated in response to DNA damage and facilitate the accumulation of DNA signalling and repair proteins to the DNA damage sites (Fernandez-Capetillo *et al.*, 2004; Lewandowska and Szumiel, 2002; Rogakou *et al.*, 1998). Interestingly, studies from yeast also found that the acetylation of H3 and H4 histones on the N-terminal lysine's contributes to NHEJ and HR DNA repair pathways, possibly by opening or relaxing the nucleosomal structures close to sites of DNA damage (Van Attikum and Gasser, 2005; Bird *et al.*, 2002).

In human and rodent cells, linker histone H1 is present at telomeres and it is involved in chromatin condensation. There is usually a linear relationship between histone 1 nucleosome ratio and nucleosome repeat length. However, this ratio is often higher at pericentromeric chromatin regions than in telomeres (Pisano, Galati and Cacchione, 2008; Gurley *et al.*, 1978). Interestingly, Revaud *et al.*, (2009) have reported that interstitial telomeric chromatin (centromeres) shares similarity with true telomeric chromatin (terminal ends), and presents high nucleosome density than bulk chromatin (Revaud *et al.*, 2009). It has been shown that binding factors, TRF1 and TRF2 stabilize and protect ITSs, and these factors can compete with linker histone, thus stabilizing the nucleosome repeat length (NRL) chromatin structure in CHO telomeric sequences in (Revaud *et al.*, 2011; Krutilina *et al.*, 2003).

Therefore, these findings suggest that TRF1 and TRF2 have a potential role in the organization and function of heterochromatic ITSs.

Mammalians cells have evolved two main DNA repair pathways, NHEJ and HR to remove DSBs, and thus guard genome integrity (Christmann *et al.*, 2003). The fate of NHEJ and HR pathways is cell cycle dependent NHEJ is mainly expressed in G0-G1, while HR occurs during late S and G2 phases (Takata *et al.*, 1998). NHEJ is thought to be the predominant mechanism to repair DSBs throughout the cell cycle and commonly used to repair DSBs induced by IR (Sancar *et al.*, 2004). The NHEJ is an error prone repair mechanism that repairs broken DNA ends with little or no sequence homology (Rothkamm and Lobrich, 2002). NHEJ can be classified into two subtypes: classical NHEJ (C-NHEJ) which joins the broken ends directly and relies on protein factors associated with this pathway, and alternative NHEJ (A-NHEJ) which is independent of C-NHEJ and shows deletions with microhomology at the repair junctions (Bennardo *et al.*, 2008; M. Wang *et al.*, 2006).

The C-NHEJ involves a set of core proteins such as Ku heterodimer (Ku70/Ku80) complex that binds two broken ends (Jeggo, 1998), recruits a catalytic subunit of DNA-PKcs which together form the active DNA-PK holoenzyme (Weaver, 1995). This process activates XRCC4/DNA ligase IV heterodimer, which ligates the broken DNA ends together (Christmann *et al.*, 2003). By contrast, A-NHEJ requires different proteins and enzymes such as PARP1, XRCC1, ligase III and Flap endonuclease1, it shows slow repair kinetics and it is active when C-NHEJ is repressed (M. Wang *et al.*, 2006).

The key role of NHEJ mechanism in resolving DSB damage has been identified through studies with mammalian cell lines that encoded NHEJ components. Chinese hamster Ovary (CHO) cell lines have been used to generate many mammalian cell mutants. For example, there are a large number of CHO cell mutants deficient in DNA repair for NHEJ and HR pathways. CHOK-1 is the parental cell line for repair deficient mutants (Kao and Puck, 1967), and AA8 is a parental cell line of V3 (Thompson, 1980) and both, CHOK-1 and AA8 cell lines are subclones derived from CHO cell line. For example, one cell line, xrs-5 is an X-ray sensitive cell line derived from CHOK-1 and is defective in DSB rejoining and V(D)J recombination. The xrs-5 defective phenotype is complemented by 86kDA subunit of Ku antigen (Jeggo and Kemp, 1983). XR-1 mutant cell line is derived from CHOK-1 and is hypersensitive to killing by gamma rays (Giaccia *et al.*, 1990). The XR-1 is complemented by the human XRCC (x-ray cross complementing) 4 gene, XRCC4 which forms a tight complex with DNA Ligase IV in the final ligation step in the classical NHEJ (Roy et al., 2012). V-3 cell line is sensitive to ionising radiation and has DSB repair defect, and derived from AA8 parental line (Whitmore, Varghese and Gulyas, 1989). Human DNA-PKcs complement the DNA DSB repair defects in V3 and rescues mutant phenotype (Kurimasa *et al.*, 1999). Therefore, their sensitivity to IR is directly associated to their impairment in DSB repair (Liang *et al.*, 1996; Darroudi *et al.*, 1990).

The aim in this chapter is to investigate DSB repair kinetics within ITSs in the three NHEJ deficient Chinese hamster cell lines indicated above. My aim is to evaluate the DSB induction and repair kinetics in the whole genome, as well as ITSs.

4.2 Analysis of chromatid type aberrations in NHEJ deficient Chinese hamster cell lines

Having evaluated the frequency of repair kinetics of chromatid breaks (G2 assay) and DSBs (immunocytochemistry) in repair-proficient Chinese hamster cell lines (Chapter 3), we next wanted to reproduce the same experiments in their NHEJ deficient counterparts (xrs5, xr-1 and v3) with a view to detecting potential differences in DNA damage responses at ITSs. We started by analysing the G2 assay, which effectively identifies induction and repair of G2 chromatid breaks (see previous chapter). Examples of chromatid type aberrations are shown in Figure 4.1. Frequencies of chromatid breaks in defective cell lines and their control counterparts are presented in Figure 4.2 and Figure 4.3. The xrs-5 cells showed higher frequency of breaks (4.04/cell) than v3 and xr-1 cells (3.24/cell and 3.1/cell respectively). Break frequencies in control cells were significantly lower (Figure 4.2 and Figure 4.3) and in line with the values observed in the previous chapter (Figures 3.2). Re-joining of breaks was slower in DSB deficient lines at 3 hours and 4 hours post irradiation (Figure 4.2 and 4.3). Overall, NHEJ deficient cell lines exhibited hypersensitivity to IR and slower DSB repair kinetics compared to control cell lines, and this is in line with published data. (Mateos *et al.*, 1994; MacLeod and Bryant, 1990). The statistical analysis showed significant differences (*t*-test *P<0.05, **P<0.01, ***P<0.001) between samples taken at different time intervals. Each experiment was repeated twice under the same conditions and the results averaged, thus ensuring that the random errors were minimised. These results indicated that the deficiency in the core components of NHEJ pathways significantly reduced DSBs repair in NHEJ deficient hamster cell lines.

However, despite the radiation sensitivity of these deficient cell lines we observed a moderate DSB repair activities at 3 hours and 4 hours post-irradiation (Figure 4.2 and Figure 4.3). Results suggested that an additional repair pathway might participate in the slow DSB repair observed in these NHEJ deficient cell lines. In support of this, Wu *et al.,* (2008) identified similar efficiency of DSBs repair in wild-type cells and mutant Chinese hamster cells. They reported that a pulsed-field gel electrophoresis study showed a pronounce DSBs repair in G2 than G1 cell phase in hamster DNA-PKcs, Ku80 and XRCC4 mutant cells (Wu *et al.,* 2008). These observations suggest that increased DSBs repair observed in G2 cells may rely on independence C-NHEJ pathway.

In line with this possibility, when C-NHEJ sub-pathway is impaired, the A-NHEJ sub-pathway becomes functional and DSBs are repaired (Iliakis *et al.*, 2004a; Pfeiffer, Goedecke and Obe, 2000). For example, the A-NHEJ sub-pathway is active in Ku80 deficient yeast and it shows efficient DSB repair generated by restriction enzymes (Boulton and Jackson, 1996). Moreover, a mouse embryo fibroblast (MEF) mutant defective in DNA-PKcs and xrcc4 deficient murine cells show increased activity of A-NHEJ that result in DSBs repair during class switching recombination (Wu *et al.*, 2008; Yan *et al.*, 2007).

Chromatid type aberrations in NHEJ deficient Chinese hamster cell lines

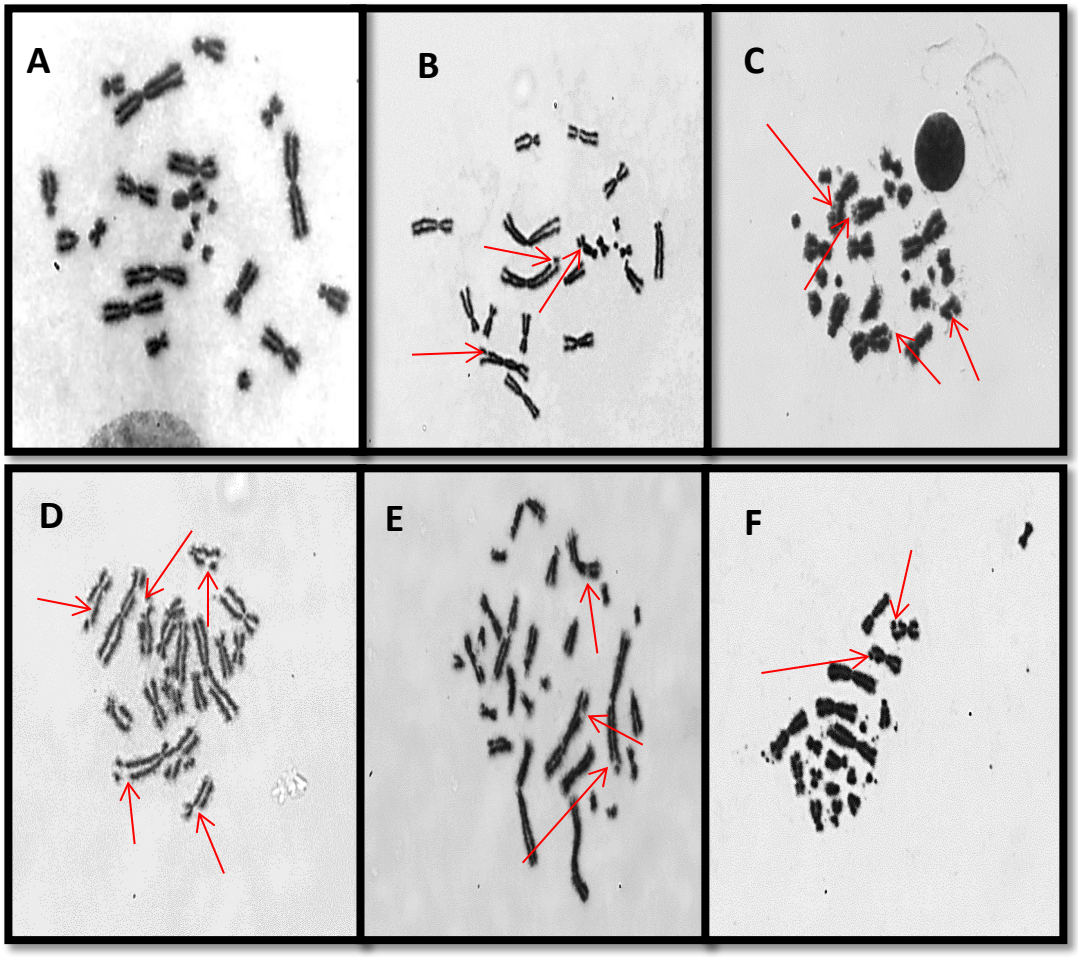

Figure 4.1. Representative images of NHEJ deficient and control Chinese hamster metaphase solid staining. **A)** Normal metaphase spread of control CHOK-1, **B)** CHOK-1 showed chromatid breaks (red arrows). **C)** XRS-5, Ku86 deficient cells were shown condensed chromosomes and breaks indicated with red arrows, **D)** V3, DNA-PKcs deficient cells were shown a significant number of chromatid breaks indicated with red arrows. **E)** XR-1, XRCC4 deficient line exhibited breaks and gaps indicated with red arrows. **F)** AA8 control cell line and break are indicated in red arrows.

Chromatid type aberrations in NHEJ deficient Chinese hamster cell lines

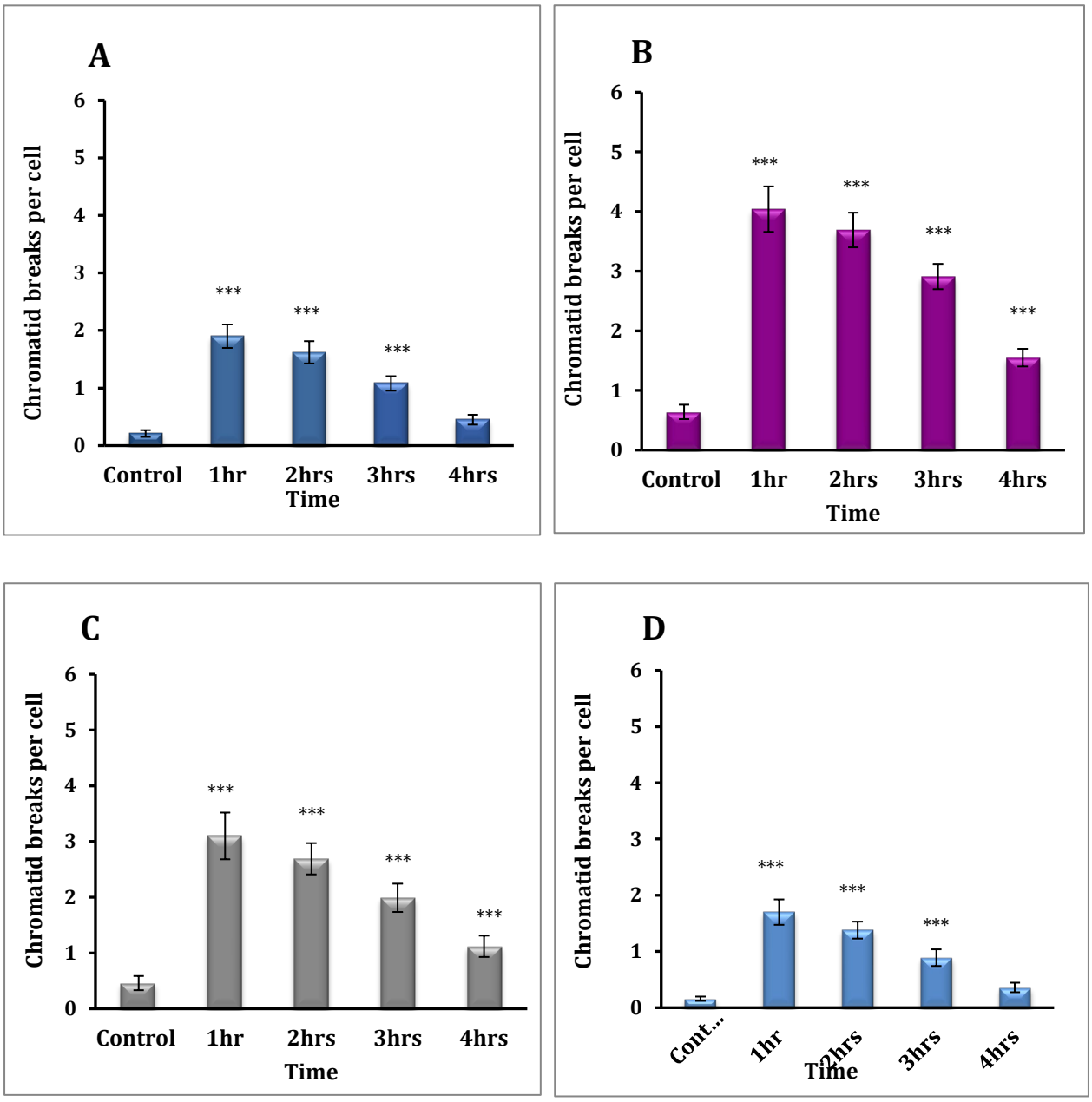

Figure 4.2. Frequencies of chromatid breaks in NHEJ deficient Chinese hamster cell lines. **A).** CHOK-1 control showed DSB repair kinetics throughout 4 hrs. **B).** Xrs-5 cell line exhibited higher frequencies of breaks compared with V3, Xr-1 hamster cells. **C).** Xr-1 hamster cells were shown higher levels of chromatid breaks but moderate repair kinetics between 2 to 3 hrs. **D).** AA8 control cells showed less breaks than CHOK-1 cells.

Frequencies of chromatid aberrations in NHEJ deficient Chinese hamster cells

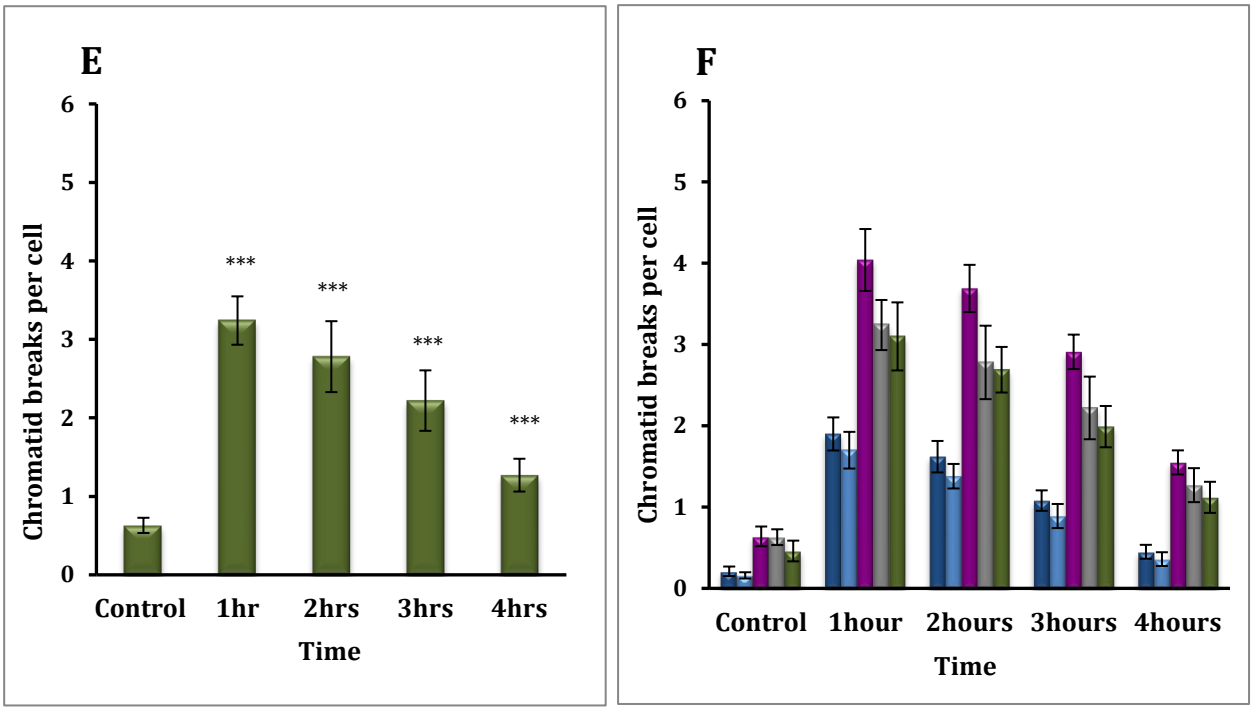

Figure 4.3. Frequencies of chromatid breaks in NHEJ deficient Chinese hamster cell lines. **E).** V3 cells showed elevated frequency of chromatid breaks compared to their control AA8. **F).** The graph showed the frequnecies of breaks between different NHEJ deficient Chinese hamster cell lines. Error bars indicate SEM. The statistical significant the frequencies of chromatid breaks between untreated and treated in all five cells at each time point, evaluated by student's t-test *P<0.05, **P<0.01, ***P<0.001.

4.3 Analysis of chromatid breaks at the ITSs in NHEJ deficient Chinese hamster cells

We next wanted to examine the chromatid break repair within ITSs in NHEJ deficient Chinese hamster cells. It has been suggested that ITSs constitute "hotspot" for chromosomal breakage, amplification and recombination and that these sequences coincide with fragile sites (Day, Limoli and Morgan, 1998; Slijepcevic *et al.*, 1996; Fernández, Gosálvez and Goyanes, 1995). Therefore, an investigation of repair kinetics at ITSs is important for understanding mechanisms behind genome stability maintenance in mammalian cells.

To investigate frequencies of chromatid breaks at ITSs we used FISH with the telomeric PNA probe. Representative examples of chromatid breaks detected by FISH are shown in Figure 4.4. The frequencies of chromatid break in control and NHEJ defective cell lines are presented in Figure 4.5 and Figure 4.6. Furthermore, Table 4.1 shows frequencies of observed and expected value for chromatid breaks in each cell line.

Overall, frequencies of chromatid breaks within ITSs were higher than expected in all cell lines (Table 4.1; Figure 4.5 and Figure 4.6). Our results are in line with previous studies by Fernandez *et al.*, (1995) and Bolzan *et al.*, (2001). However, we observed a degree of re-joining of breaks, with slow repair kinetics, over time (Figure 4.5 and Figure 4.6). Similarly, Rivero *et al.*, (2004) found a slow DSBs repair kinetics within ITSs in DNA-PKcs deficient hamster cells. In addition, they have reported that the ITSs exhibit a particular chromatin structure; enriched in short unrepaired DNA segments, and are alkali sensitive.

Moreover, Miller *et al.*, (2011) have shown increased frequency of large deletions during DSB repair near telomeres and interstitial sites in the human tumour cell line EJ-30 cell line, is a bladder carcinoma, in which DSBs repair is primarily mediated by A-NHEJ. Consistent with this notion, A-NHEJ is a predominant mechanism to repair DSBs at heterochromatin regions, near telomeres and interstitial sites, and accumulation of PARP 1 correlates with A-NHEJ activity (Miller *et al.*, 2011). Interestingly, TRF2 colocalizes and binds to ITSs in Chinese hamster cells, however TRF2 naturally represses C-NHEJ and this way favours A-NHEJ repair (Revaud *et al.*, 2011; Bae and Baumann, 2007).

Chromatid breaks at ITS in NHEJ deficient Chines hamster cell lines using FISH

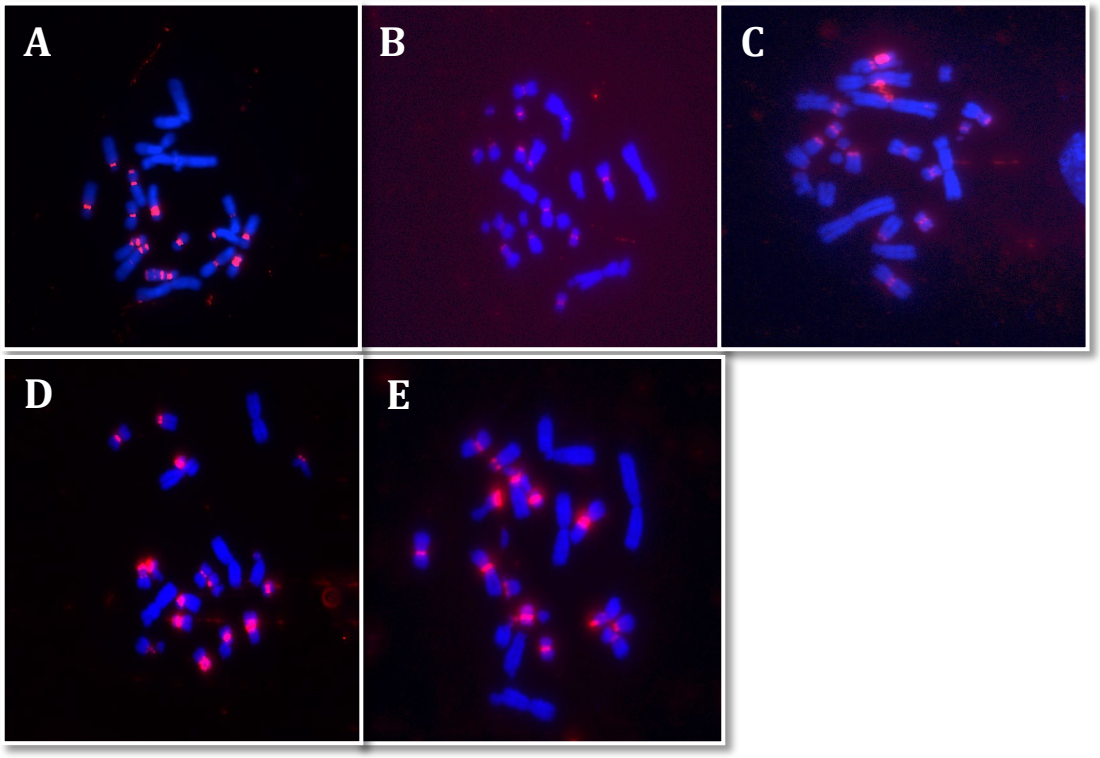

Figure 4.4. Representative FISH image of NHEJ deficient hamster metaphase spreads. **A).** CHOK-1 control cells showed strong centromeric ITSs signal. **B)-C)** Xrs-5 and Xr-1 metaphase spreads showed weak hybridization signal at centromeres but breaks can be observed in both cell lines. **D).** AA8 control line exhibited hibridization at centromeres and no detectable signal at telomeres. **E).** V3 line displayed strong signal within ITS and breaks can be observed in metaphase spread.

Analysis of chromatid breaks at ITSs in NHEJ deficient Chinese hamster cell lines

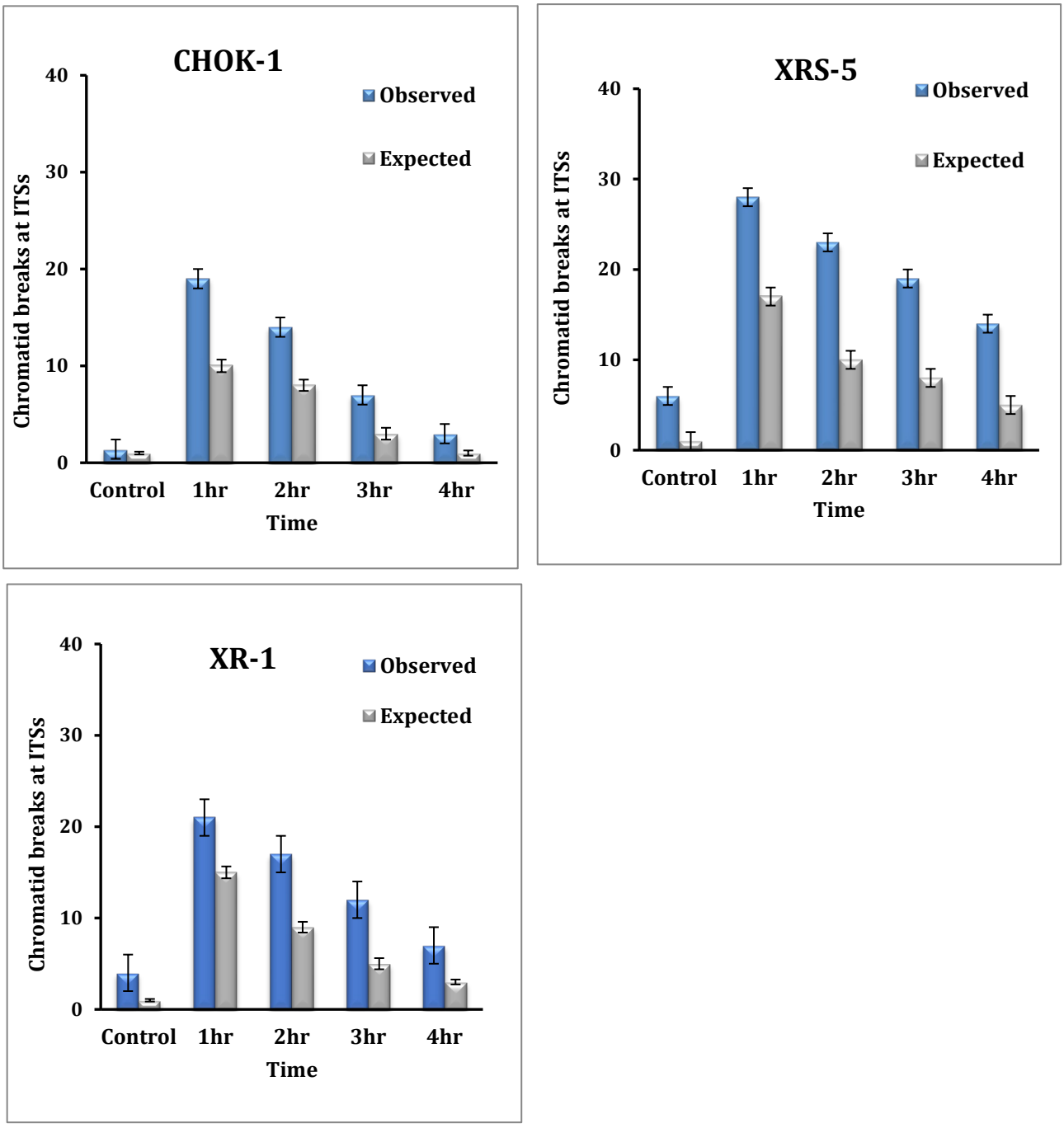

Figure 4.5 Frequencies of chromatid breaks within ITSs in NHEJ deficient and control Chinese hamster cell lines. The blue bars represented the total number of observed breaks within ITSs and the grey bars show the expected breaks within ITSs per hour (1-4 hours). The NHEJ deficient cells, xrs-5 and xr-1 exhibited a significant number of breaks within the ITSs than their control counterpart.

Analysis of chromatid breaks at ITSs in NHEJ deficient Chinese hamster cell lines

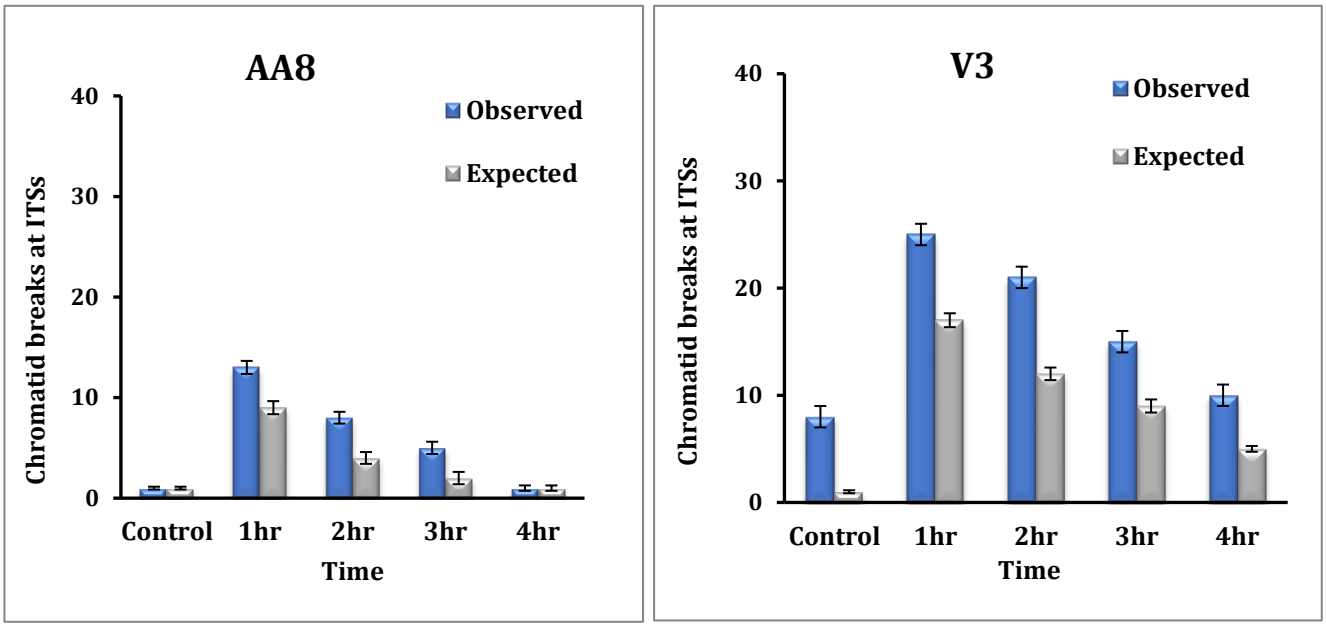

Figure 4.6. Frequencies of break within ITSs in NHEJ deficient and control Chinese hamster cells. The number of chromatids breaks within the ITSs in Chinese hamster cells is greater than expected. The blue bars in V3 showed greater number of 25 breaks within ITSs than AA8 control at 1 hour. However, it can be observed in both, V3 and AA8 cell lines DBS repair kinetics throughout 4 hours.

			0h		1hr		2hr		3hr		4hr		
Cell Lines	**Score cells**	**ITS % Ch. Length**	**Obs.**	**Exp.**	**Obs.**	**Exp.**	**Obs.**	**Exp.**	**Obs.**	**Exp.**	**Obs.**	**Exp.**	***p-value (0.05)***
CHOK-1	100	8.4	1	0	19	10	14	8	7	3	3	1	p<0.05
xrs-5	100	12	6	1	28	17	23	10	19	8	14	5	p<0.05
xr-1	100	10	4	2	21	15	17	9	12	5	7	3	p<0.05
AA8	100	9	1	0	13	9	8	4	5	2	1	1	p<0.05
V3	100	11	8	2	25	17	21	12	15	9	10	5	p<0.05

Table 4.1 Distribution of chromatid breaks within ITSs and DSBs repair kinects among NHEJ deficient Chinese hamster cells.

4.3. Analysis of DNA DSBs in deficient NHEJ Chinese hamster cells by γ-H2AX foci

In previous chapter we have shown frequencies of γ-H2AX foci in DSB repair-proficient cells and we observed γ-H2AX foci disappearance with time, evidencing a competent DNA damage repair mechanisms. In this chapter we repeated the analysis using the NHEJ deficient cell lines. Results of our analysis are shown in Figure 4.7. Examples of γ-H2AX foci are shown in Figure 4.9. As expected, NHEJ defective cells exhibited higher frequencies of γ-H2AX foci relative to control cell lines. The most sensitive cell line was xrs-5 (20.16/cell). The second highest was the v3 cell line (19.24/cell), followed by xr-1 (18.64/cell) (Figure 4.7 and Figure 4.8). The difference between untreated and treated samples were statistically significant (*t*-test **P<0.01, ***P<0.001) at each time points in the three cell lines. Our results are in good agreement with those of Rothkamm *et al*. (2003), which showed reduced DSB kinetics in defective Chinese hamster cells. The persistence of DNA damage foci in these mutant lines is significantly higher throughout the studied time interval (30 minutes to 48hours). Overall, our results showed the DSB repair system in the NHEJ mutants are impaired and those deficient cells exhibited radiosensitivity phenotype that result in high levels of γ-H2AX foci throughout the 48hrs. However, the discreet disappearing of DNA damage foci might suggest DNA repair by two possible scenarios either by HR or NHEJ. The HR repair is active in S/G2 phase and relies on its catalytic protein, RAD51, whereas NHEJ mediates DSB repair by facilitating chromatin relaxation through CBP and p300 histone proteins that leads to repair proteins such as ku70/80 or Mre11 to access the DNA DSB site (Ogiwara *et al.*, 2011).

DSBs damage detection in NHEJ deficient Chinese hamster cell lines using γ-H2AX

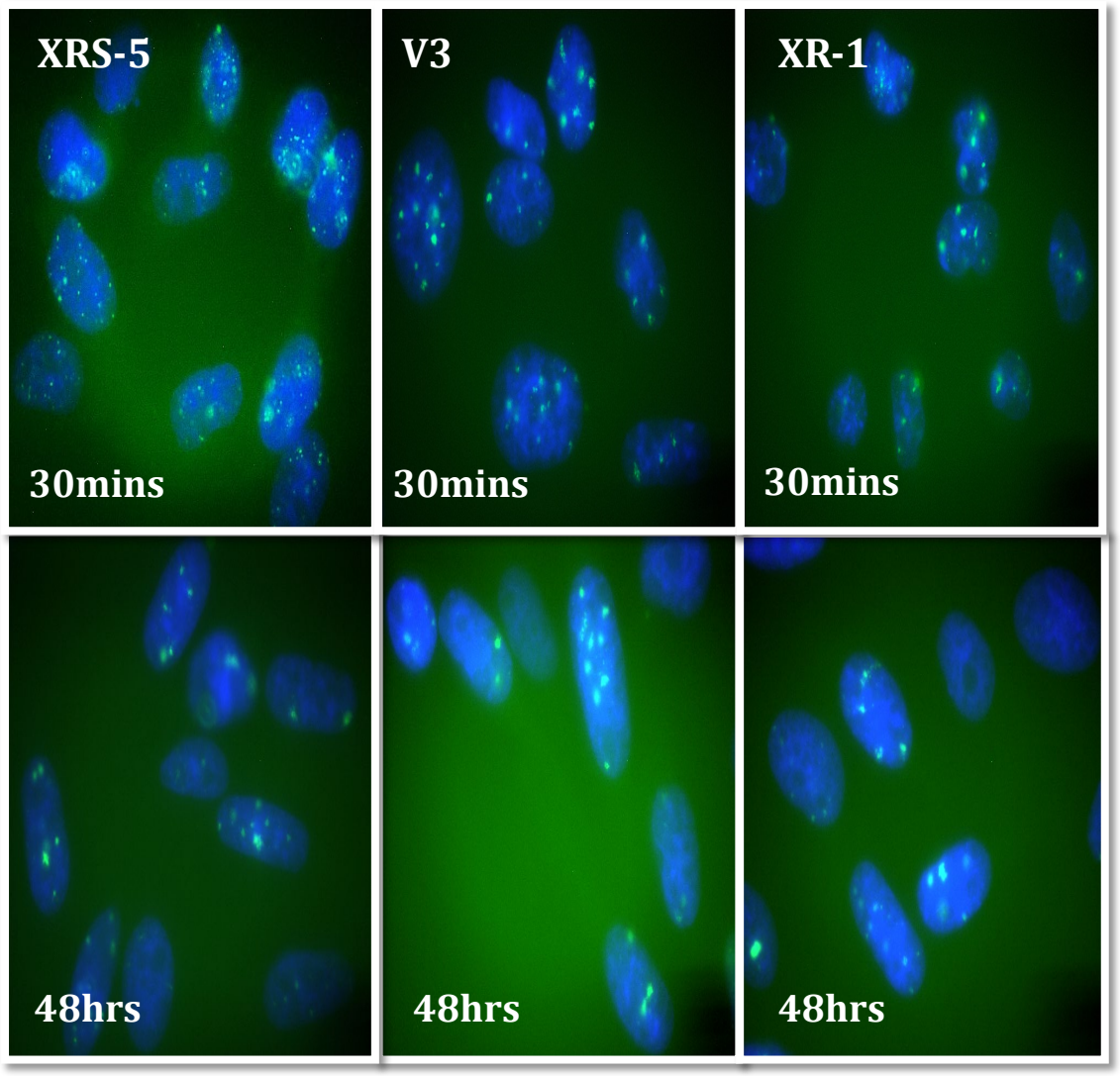

Figure 4.7. Represenative image of γ-H2AX detection in NHEJ deficient Chinese hamster cell lines. The upper column represents DSB induced 30 minutes post-radiation in three NHEJ deficient Chinese hamster cells. The bottom column corresponds to the disappearance of γ-H2AX foci at 48hrs that correlates with DSB repair in NHEJ deficient cells. However, it can be observed that the number of γ-H2AX remained higher at 48hrs in these cells.

DNA DSBs in deficient NHEJ Chinese hamster cell lines using γ-H2AX

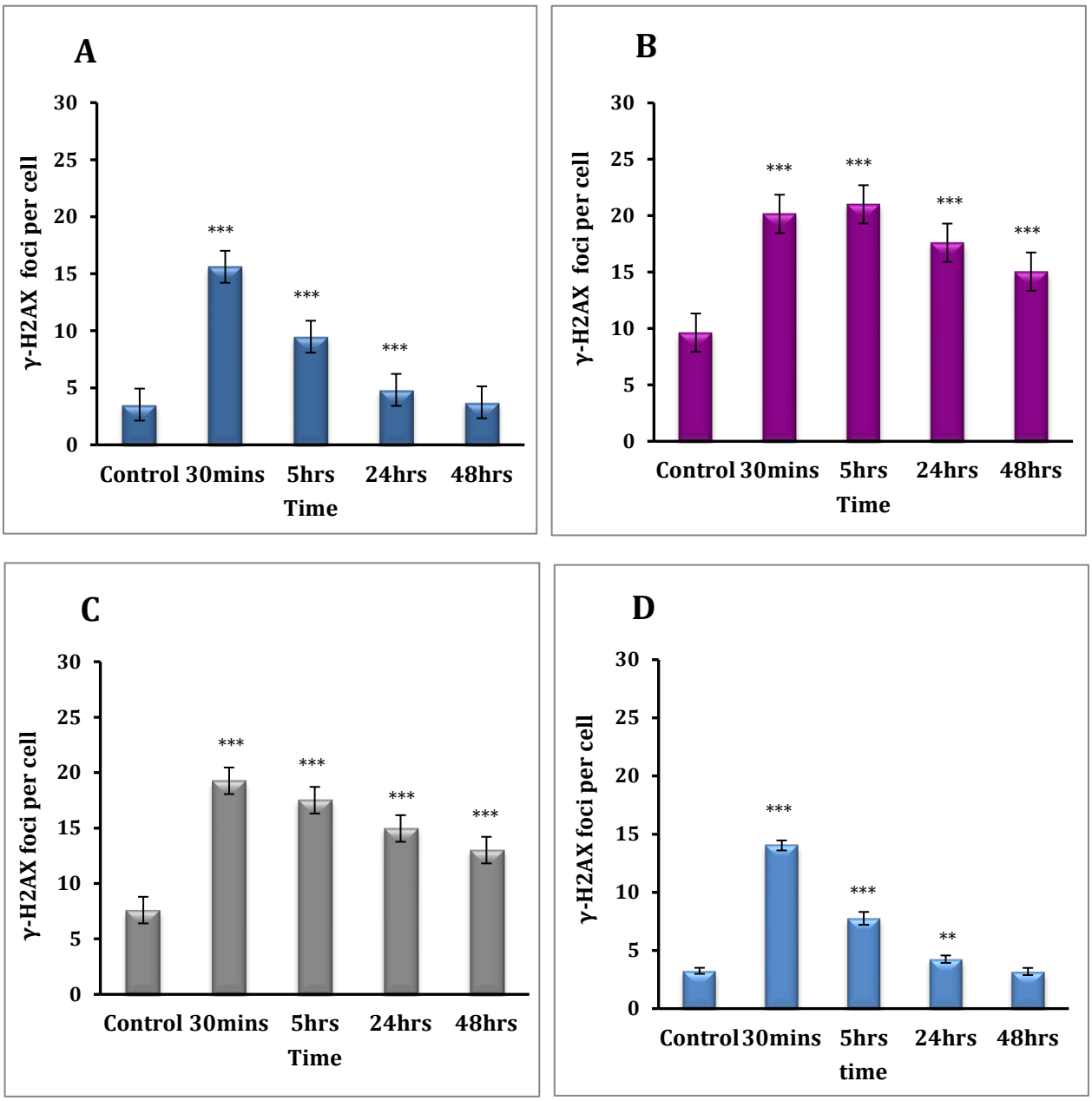

Figure 4.8 Frequencies of γ-H2AX in NHEJ deficient and control hamster cell lines. **A).** CHOk-1 control cells were shown an efficient DSB reapir kinetics with the disappareance of γ-H2AX foci with time **B).** Xrs-5 cells were shown higher γ-H2AX foci number and DSB repair was signicantly decreased throughout the 48hrs. **C).** Xr-1 cells displayed higher frequencies of γ-H2AX foci and exhibited a moderate DSBs repair at 24hrs and 48hrs. **D).** AA8 control cells showed lower γ-H2AX foci compared with V3 cells.

DNA DSBs in deficient NHEJ Chinese hamster cell lines using γ-H2AX

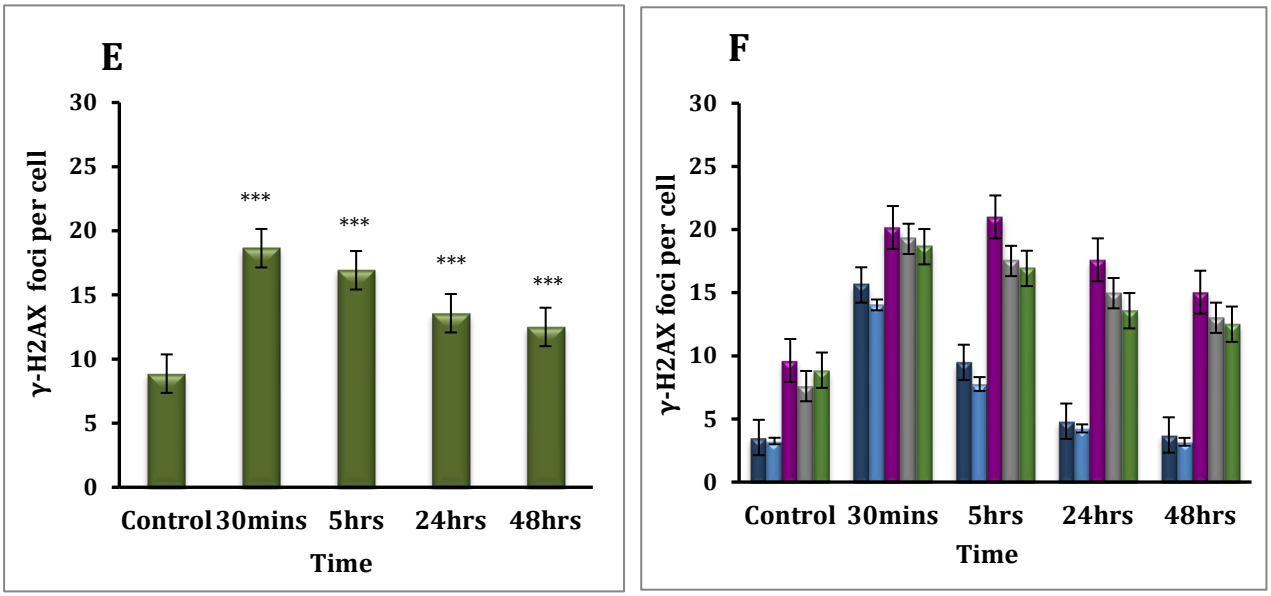

Figure 4.9. Frequencies of γ-H2AX in NHEJ deficient and control hamster cell lines. **E).** V3 cells showed elevated frequencies of γ-H2AX post-radiation and the DSB remained high after 48hrs. **F).** The graph showed the difference in the frequencies of γ-H2AX foci induction and foci disappearance in NHEJ deficient Chinese hamster cells at differences time points. However, it can be appreciated a discreet repair of DBSs in NHEJ deficient hamster compared to control counterparts.

4.4 Analysis of telomere dysfunction induced foci (TIF) in deficient NHEJ hamster cell lines

In the previous chapter we presented results of repair kinetics analysis within TIFs in repair-proficient Chinese hamster cell lines (Figures 3.9). As far as we know this is the first analysis of this type attempted in Chinese hamster cells. Next, we performed TIF assay to examine repair kinetics in NHEJ deficient Chinese hamster cell lines (two independent experiments to ensure consistency of results).

The results of our analysis are shown in Figure 4.10 to Figure 4.12. It is clear the high frequencies of TIFs foci in NHEJ deficient Chinese hamster cell lines. However, these deficient hamster cells showed different profiles of radiation sensitivity, therefore their DSB correlated with the TIFs number. For example, xrs-5 (13.2/cell) showed the highest number of TIFs foci compared with v3 (10.6/cell) and xr-1 (8.3/cell) Figure 4.10 and Figure 4.11. However, at 48 hours deficient NHEJ deficient cells showed a mild decreased in the number of TIFs, but the frequencies were still higher compared to control cell lines. The difference between untreated samples and treated samples were statistically significant (*t*-test **P<0.01, ***P<0.001).

Telomere dysfunction in NHEJ deficient Chinese hamster cell lines using TIFs foci

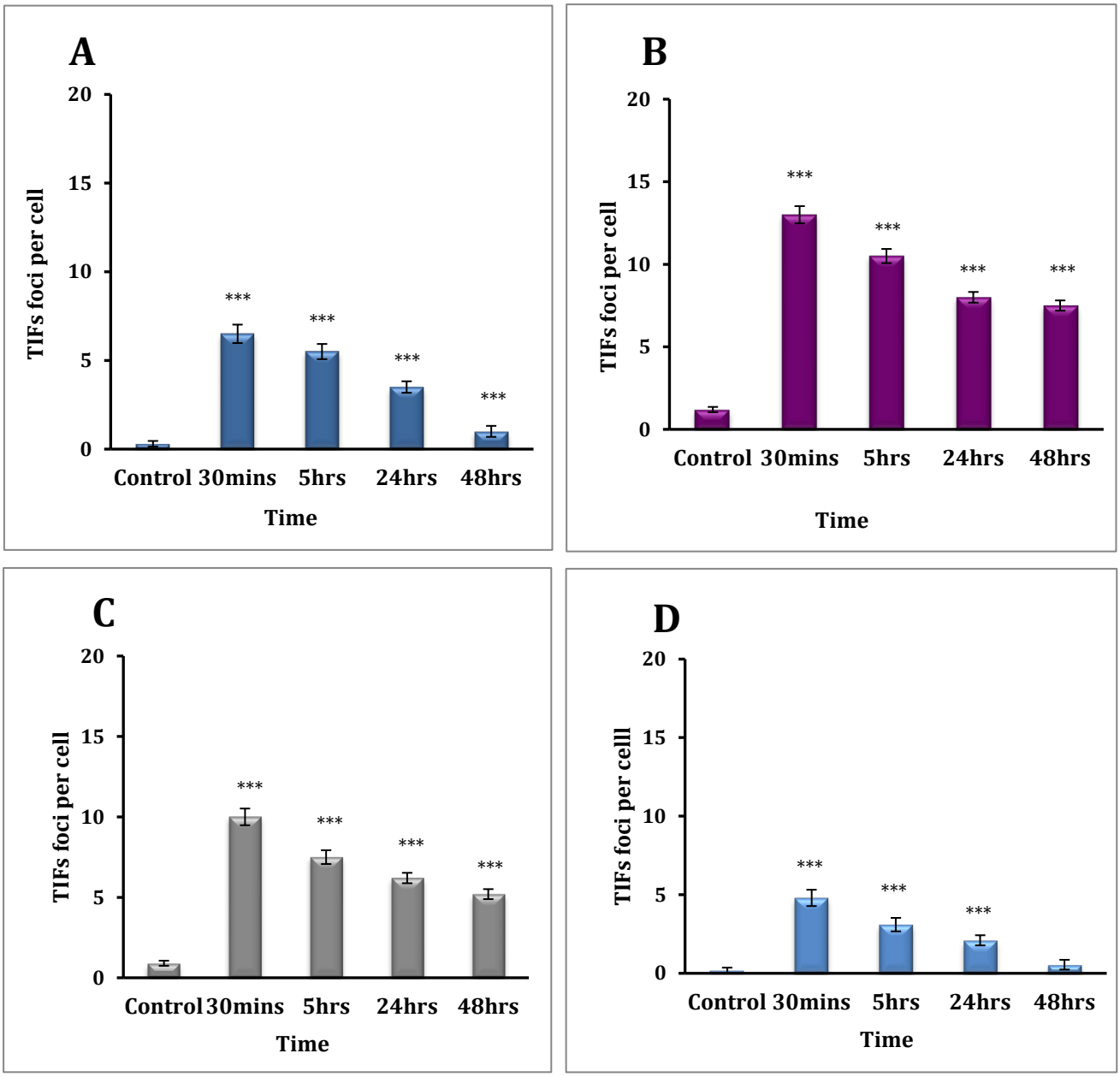

Figure 4.10. Frequencies of TIFs foci in NHEJ deficient Chinese hamster cell lines. **A).** CHOK-1 control cells were shown a lower number of TIFs foci compared with NHEJ deficient cells. **B).** Xrs-5 exhibited higher frequencies of TIFs foci post-radiation but foci decreased by half at 48hrs. **C).** Xr-1 cells were shown the second highest to exhibited increased TIFs foci and can be observed disappearance of DSB over time, 48hrs. **D).** AA8 control cells displayed slightly less TIFs levels than CHOK-1 cells.

Telomere dysfunction in NHEJ deficient Chinese hamster cell lines using TIFs foci

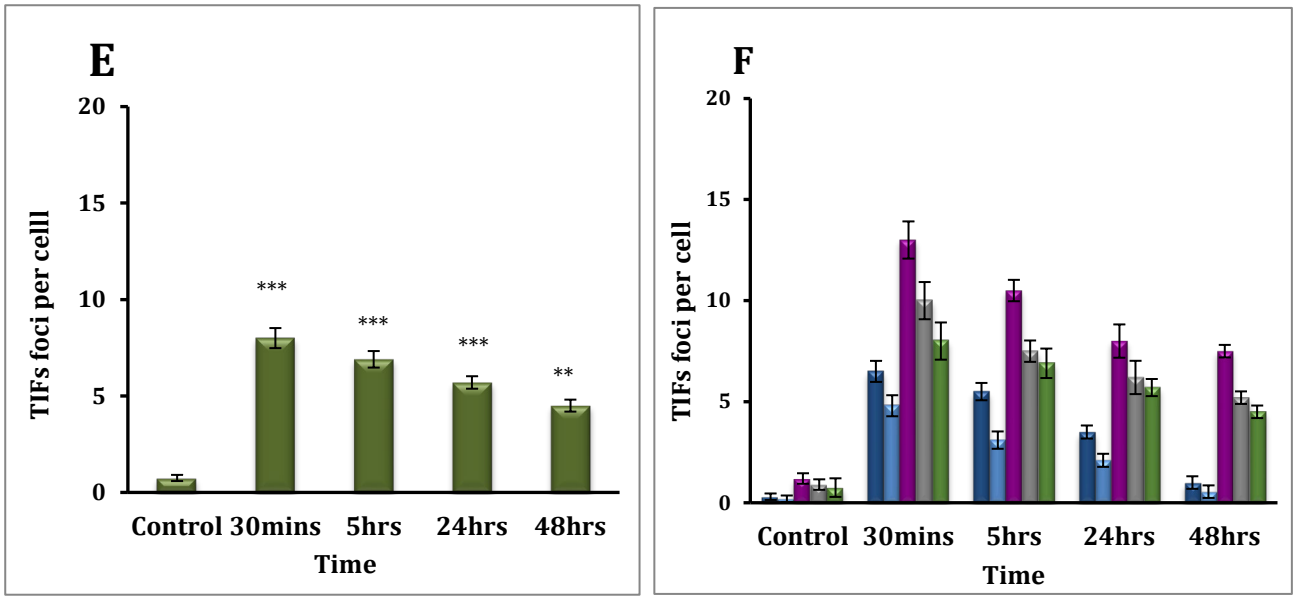

Figure 4.11. Frequencies of TIFs foci in NHEJ deficient and controls Chinese hamster cell lines **E).** V3 presented higher frequencies of TIFs foci and showed less pronounced DSB repair compared with control cell line, AA8. **F**). The graph showed high levels of TIFs foci in all NHEJ deficient hamster cells, but it can be observed a moderate DSB repair in NHEJ cells that corresponded with the disappearance of TIFs foci in these three NHEJ deficient cells.

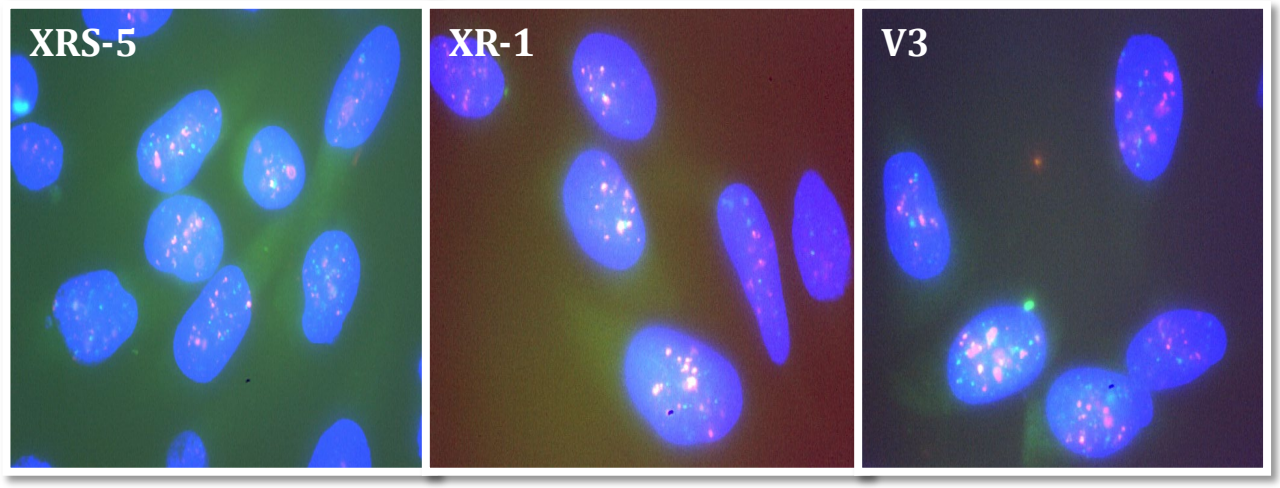

Figure 4.12. Representative image of TIFs foci (yellow spots) in NHEJ deficient Chinese hamster cell lines. The green foci correspond to γ-H2AX that accumulates at the DNA damage site in interphase cells and red foci represent Cy3 telomere probe, which hybridizes ITSs present in hamster cells.

4.5 Discussion

ITSs are found in most vertebrate species, ranging from primates (Ruiz-Herrera *et al.*, 2002), marsupials (Pagnozzi, Ditchfield and Yonenaga-Yassuda, 2002), birds (Nanda and Schmid, 1994) to rodents (Bertoni *et al.*, 1996) including, Chinese hamster. In the Chinese hamster genome ITSs exist in two forms. One form is large blocks of het-ITS located at the pericentromeric regions of chromosomes. The second form is s-ITS, located at intrachromosomal sites (Faravelli *et al.*, 2002; Bertoni *et al.*, 1996). It has been suggested that het-ITSs in Chinese hamster represented the remnants of evolutionary chromosomal rearrangements during speciation, and s-ITSs during the repair of DNA DSBs within AT rich DNA and possibly telomerase was used as the stabilizing mechanism (Ruiz et al., 2008; Faravelli *et al.*, 2002; Harrington, 1991). The het-ITSs represent the major component of satellite DNA sequence in the Chinese hamster genome and they are organized as extended continuous arrays of $(TTAGGG)_n$ with poor in restriction sites (Faravelli *et al.*, 2002). In addition, ITSs exhibit heterogeneous pattern of distribution within the same specie and, also ITSs presented length-based polymorphisms with high prevalence of spontaneous amplification in CHO cell lines (Mondello, 2000; Bolzan, 2017).

The predominant ITSs present in human genome are s-ITSs and found in all human chromosomes. In contrast to s-ITSs in Chinese hamster, human s-ITSs are not preferential sites for spontaneous and induced chromosomal rearrangements on chromosome 2q31 and 4q (Desmaze *et al.*, 2004). Azzalin *et al.*, (2001) have identified 50 s-ITS in human cells and shown that they are not preferential breakage regions.

Moreover, it has been thought that s-ITSs arise from DSBs and that telomerase repairs and stabilizes the broken ends, thus constituting telomere sequence insertions in the human genome (Azzalin, Nergadze and Giulotto, 2001). Furthermore, some authors have suggested that some s-ITS in human cells are sources of genome instability and are associated with colon and gastric carcinomas (Kashima *et al.*, 2006).

In this chapter we employed NHEJ deficient Chinese hamster cell lines to examine the effects of DNA damage within ITSs in these defective cells. From results presented in this chapter it is clear that mutations in the NHEJ core proteins do no abolish DNA damage repair in the NHEJ deficient Chinese hamster cell lines. In mammalian cells, C-NHEJ is the predominant mechanism for repair of DSBs. It involves a set of core proteins that stabilize breaks and ligate the broken ends, in an error prone process often resulting in deletions and insertions. It is known that NHEJ pathway has a biphasic kinetics; fast component which repairs 80 % of DSBs within minutes mediated by C-NHEJ, whereas the slow component repairs 10-20% of breaks within hours and is processed by A-NHEJ (Iliakis, 2009; Iliakis *et al.*, 2004).

As shown in Figure 4.2 and Figure 4.3, the deficient NHEJ hamster cell lines were found to exhibit DSB repair kinetics of chromatid breaks. These three NHEJ deficient hamster cells were shown higher frequencies of CAs compared with the wild-type (parental) cells. Results obtained are in line with previous studies (Bryant, Peter, Mozdarani and Marr, 2008; Mateos *et al.*, 1994). However, the disappearance or rejoining of chromatid breaks with time in these deficient cell lines can be attributed to the activation of A-NHEJ pathway.

Consistent with this view, Mansour et al., (2010) has reported that the A-NHEJ, efficient system that dependent completely on PARP1, rescued NHEJ deficient repair phenotype and been linked to high mutation rate in Chinese hamster cells (Mansour et al., 2010).

As shown in figure 4.10 and Figure 4.11, a significant increase of chromatid breaks within ITSs was observed higher than expected in NHEJ deficient Chinese hamster cells. Our results exhibited differences in the frequencies of chromatid break between hamster cell lines. However, results showed kinetics of repair within ITSs in all NHEJ cell lines and extended throughout the 4hours. These findings suggest that the observed differences may have involved ITSs length heterogeneity arisen from amplification or rearrangements of ITSs blocks within cell lines. Consistent with this view, Ruiz *et al.*, (2005) reported that het-ITSs are located within the constitutive heterochromatin and colocalize with chromosomal fragile sites, inherent break and gap regions, thus constituting preferential sites for DNA integration, amplification and rearrangements (Ruiz *et al.*, 2005). Interestingly, Rivero *et al.*, (2004) also demonstrated that NHEJ, DNA-PKcs, deficient hamster exhibited a slow pattern of DSBs re-joining and indicates that ITSs chromatin conformation enhances the preferential breakage within Chinese hamster genome (Rivero *et al.*, 2004).

In order to investigate whether the DSBs repair kinetics observed at chromosomal levels can be detected at interphase level, we used DNA damage antibody γ-H2AX and TIFs in these NHEJ deficient hamsters. As shown in Figure 4.7 and Figure 4.8, higher γ-H2AX frequencies were found in all NHEJ deficient hamster cell lines compared to their control counterparts. The NHEJ deficient cells exhibit a discreet disappearance of γ-H2AX foci that indicates a reduced DSBs repair system within these cells.

The observations of unresolved DNA DSBs in NHEJ deficient hamsters might corresponded to fact that p53, tumour suppressor protein, is mutated in these cells which may accounts for the slow disappearance of DSB in the nuclei.

As shown in Figure 4.10 and Figure 4.11, initially all three NHEJ deficient hamster cells were shown higher levels of TIFs foci in interphase cells that represented DSBs within ITSs. Unexpectedly, the TIFs foci numbers were found to decrease in these deficient hamster cells corresponded with a moderate disappearance of DSBs within ITS. Several studies have shown that DSB at telomeres "fragile sites" are irreparable and that the DNA damage persists in human cells (Fumagalli *et al.*, 2012; Sfeir *et al.*, 2009). Our results argue that DBSs within ITSs that are located at heterochromatic/centromeric regions can be repaired, regardless whether the NHEJ repair pathway is disrupted in their main core proteins in Chinese hamster cells.

In support of the notion that ITSs are dynamic structures that process and repair DSBs in a different manner in Chinese hamster cells, since ITS is the major DNA satellite present in this specie. There are a number of factors that can influence the behaviour of ITSs either as unstable or stable sequences. For example, length of ITSs (high copy or low copy number, ranging from 20bp to 500kb), the absent or present of telomere binding proteins, such as TRF1, TRF2 and RAP1 and clastogen such as radiation or radiomimetic chemicals, these factors could promote ITSs instability or stability in the chromosome regions present. There are two possible mechanisms involve in DSB repair within ITSs, one is telomerase and the other A-NHEJ. Telomerase can stabilize broken ends near telomeres, a mechanism known as chromosome healing, these broken ends serve as substrate for telomerase in *de novo* telomere addition (Bouffler, 1998).

Given the ITSs abundance in Chinese hamster cells we can speculate that telomerase catalyses the addition of telomeric sequences onto the broken chromosome ends. On the other hand, A-NHEJ repairs breaks in slow fashion kinetics and relies on different set of enzymes, such as DNA ligase III, PARP-1 and H1 to join the broken ends. For instance, histone H1 plays a role in chromatin compaction, folding and gene transcription, and also supports DSB repair by A-NHEJ.

In conclusion, we have shown that both wild type and NHEJ deficient Chinese hamster cells displayed DSB repair kinetics within ITSs regions. However, mechanisms by which ITSs are able to repair remain unclear.

Chapter 5.

Analysis of chromatid type aberrations at interstitial telomeric sites in HR deficient Chinese cell lines

5.1 Introduction

Results presented obtained in the previous chapter 4 indicated that NHEJ defective hamster cell lines show moderate repair kinetics within ITS. We wanted to investigate whether DSBs repair at ITSs in deficient HR hamster cells show similar repair profile observed in NHEJ. Telomeres are specialized nucleoproteins composed of tandem repeats $(TTAGGG)_n$ and located at the linear ends of chromosomes (Blackburn, 2001; Griffith *et al.*, 1999). However, these telomeric sequences have been found at intrachromosomal locations, known as ITSs in many species ranging from yeast to humans (Meyne *et al.*, 1990). Telomeres protect chromosome ends from being recognized as DNA DSBs, recombination and degradation (Jain and Cooper, 2010). Telomere dysfunction results in inappropriate repair of DBSs that leads to DNA ends joined (Tarsounas and West, 2005). These DSBs are resolved either by NHEJ or HR, in which Rad51 and its paralogs are key players in the repair response (Rodrigue *et al.*, 2006). In mammals, HR is the main DNA repair mechanism that restores and maintains the fidelity of the human genome (Hoeijmakers, 2001), predominantly during late S and G2 phases of the cell cycle, when sister chromatid is available and serves as template for accurate repair (Haber, 2000). HR plays a role in the restart and repair of stalled fork during replication (Sengupta *et al.*, 2003), telomeric protection through the formation of t-loop (Tarsounas and West, 2005), telomere maintenance and elongation by the recombination mediated mechanism, ALT (Suwaki, Klare and Tarsounas, 2011; Tarsounas and West, 2005; Dunham *et al.*, 2000). A number of proteins have been associated with HR repair and one of the key HR proteins is Rad51, which mediates strand invasion between the broken strand and its undamaged homologue to promote re-synthesis of the broken strand (West, 2003).

In mammalian cells, there are five Rad51 paralogs (Rad51B, Rad51C, Rad51D, XRCC2 and XRCC3), a family of gene proteins that share 20-30% similarity with each other and present a conserved ATP binding region (Thacker, 2005; Thacker, 1999). In addition, tumour suppressor BRCA2 binds to Rad51 and facilitates the accumulation of Rad51 at the damage site (Tarsounas, Davies and West, 2003), where Rad 51 forms nucleoprotein filaments that proceed into DSB repair (West, 2003). Given that HR mediates the efficient repair of DSB in DNA is crucial for the maintenance of genome and cell survival, therefore a defect or impairment in HR is linked to a group of genetic disorders, including Bloom's syndrome (BLM) (Bugreev *et al.*, 2007), ataxia telangiectasia (AT) (Stewart *et al.*, 1999), and Nijmegen breakage syndrome (NBS) (Suwaki, Klare and Tarsounas, 2011; Khanna and Jackson, 2001). The common features of these syndromes are chromosomal instability, immunodeficiency, neurodegeneration and cancer susceptibility. Moreover, previous studies in chicken and rodent cells have suggested that Rad51 paralog genes are essential in DSB HR repair and maintain chromosome instability. For example, Rad51 paralogs knockout in chicken DT40 cells shows hypersensitivity to cross-linking agents, spontaneous aberrations, and mild sensitivity to IR (Takata *et al.*, 2001), Rad51B, Rad51D and XRCC2 mutations in mice result in early embryonic lethality (Deans *et al.*, 2003; Shu *et al.*, 1999), and XRCC2 and XRCC3 mutations in hamster cells exhibit sensitivity to DNA damage agents, UV and IR, and elevated chromosomal aberrations (Liu *et al.*, 1998; Bishop *et al.*, 1998). Taken together, these genetic events suggest that Rad51 paralogs are key players in early development, DNA repair and preserve genome integrity. In fact, Rad51D deficient cells show chromosome fusion and accelerate telomere attrition therefore Rad51 exhibits a dual role in DNA repair and telomere length protection (Tarsounas *et al.*, 2004).

In this study, we used a group of defective HR Rad51 paralogs genes in Chinese hamster cell lines. The V79 parental line is originated from hamster lung tissue. Irs1 is originated from V79 and is an X-ray sensitive line and complement *XRCC2* gene in humans (Jones, Cox and Thacker, 1988). Irs1-SF is an X-ray hypersensitive cell line and complement *XRCC3* gene in humans (Fuller and Painter, 1988). The XRCC2 is associated in DNA strand pairing activity between sister chromatids and XRCC3 is involved in replication fork progression (Tambini *et al.*, 2010; Yokoyama *et al.*, 2004).

The aim of this chapter is to evaluate the role of XRCC2 and XRCC3 proteins in DSBs repair at telomere sequences in hamster chromosomes. We will examine whether HR deficient hamsters show DSB repair within ITSs.

5.2 Analysis of chromatid type aberrations in HR deficient Chinese hamster cell lines

Results of NHEJ defective Chinese hamster cell lines (see previous chapter) suggested that a mild DNA damage repair mechanism activity in these cells, which is capable of resolving CAs in G2 phase. We next wanted to investigate the DNA damage response at ITSs in HR deficient counterparts (irs1 and irs1-SF) and established the effects of HR repair deficiency. HR mechanism are the predominant repair pathway at S and G2 phases and requires a sister chromatid template, which is found in close proximity to the break and occurs at post-replication of the cell cycle (Suwaki et al 2011). We used G2 assay in Rad51 paralogs deficient hamster cell lines, irs1 (XRCC2-/-) and irs1-SF (XRCC3-/-) to carry out our study. Examples of chromatid type aberrations in HR deficient hamster lines are shown in Figure 5.1. The frequency analysis of chromatid breaks in defective cell lines and their control counterparts are presented in Figure 5.2. Results showed that HR deficient cell lines, irs1 (3.71/cell) and irs1-SF (4.52/cell) presented significantly elevated chromatid breaks compared to control cell line V79 (1.5/cell) (Figure 5.2). Re-joining of chromatid breaks was moderate in deficient lines at 4 hours post-radiation. Overall, HR deficient cell lines showed acute hypersensitivity to IR phenotype and slower DSB repair kinetics compared to the control cell line. Our findings are in line with previous studies of HR deficient irs1 and irs1-SF that exhibited repair kinetics with time (Mateos *et al.*, 1994; MacLeod and Bryant, 1990). The statistical analysis showed significant differences (*t*-test *P<0.05, **P<0.01, ***P<0.001) between untreated and treated samples at different time points (1h-4hrs). Each experiment was repeated twice under same conditions and the results averaged, thus ensuring that the random errors were minimised.

Chromatid type aberrations in HR deficient Chinese hamster cell lines

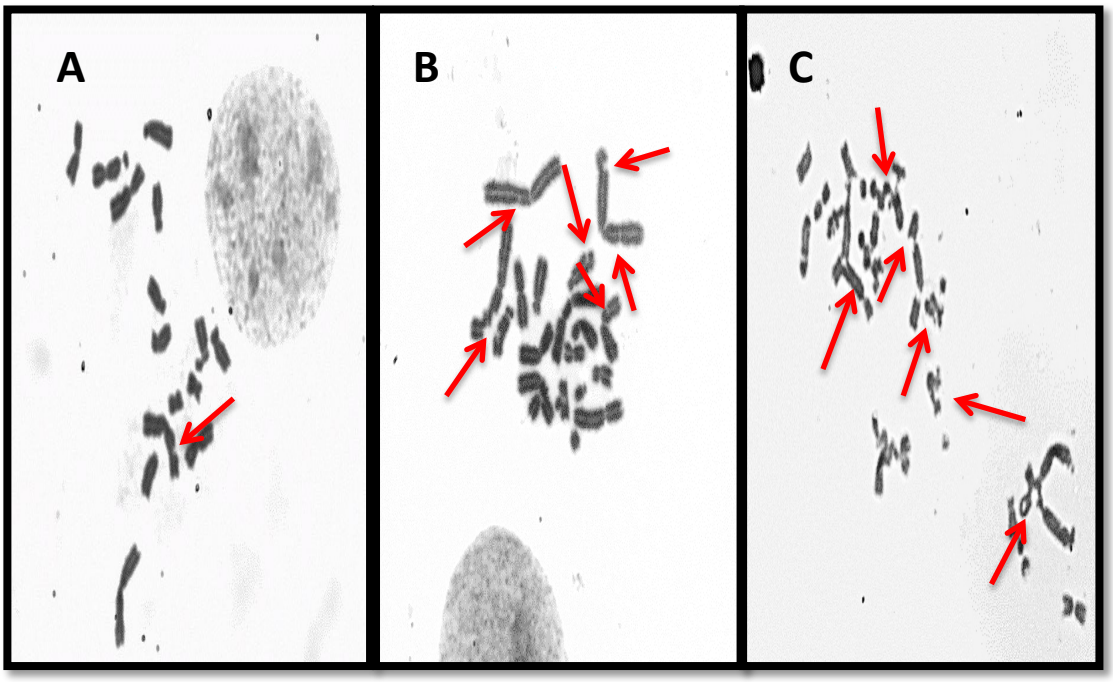

Figure 5.1 Representative images of metaphase chromosomes of HR deficient and control Chinese hamster cell lines. **A)** V79 control cell line showed very few breaks (red arrow) post-irradiation. **B)** Irs-1 cell line exhibited higher breaks and gaps (red arrows) in the metaphase spread. **C)** Irs1-SF cells were displayed complex aberrations including, breaks and exchanges indicated with red arrows. Both cells, Irs-1 and irs1-SF are hypersensitive to IR induced DNA damage.

Chromatid type aberrations in HR deficient Chinese hamster cell lines

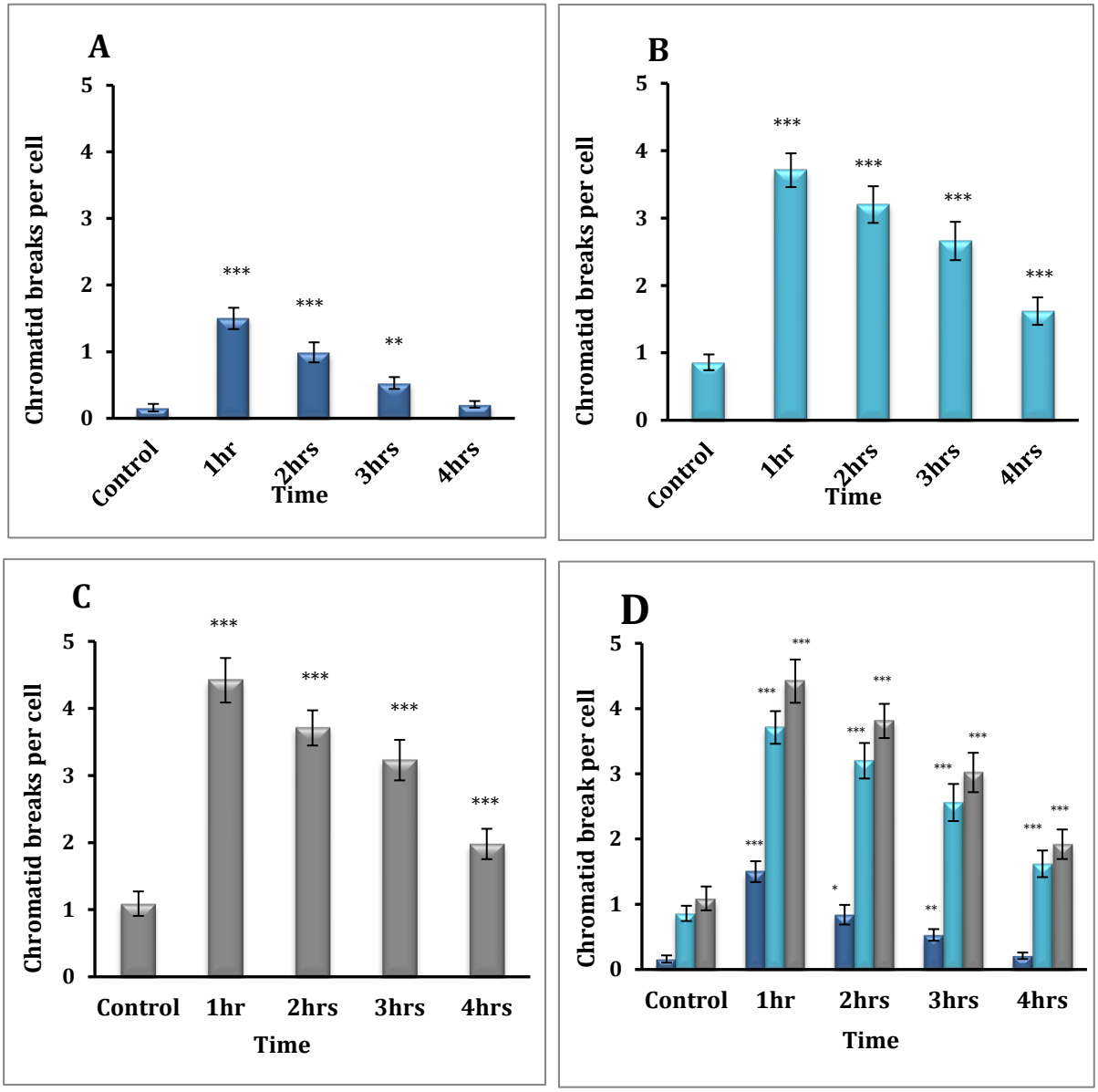

Figure 5.2. Frequencies of chromatid break in HR deficient Chinese hamster cells. **A).** V79 cells were shown low chromatid breaks number compared with irs1 and irs1-SF deficient hamster. **B).** Irs1 showed higher number of breaks post-radiation and exhibited moderate repair kinetics with time. **C).** Irs1-SF cells were shown pronounced hypersentivity to radiation compared with irs1 cells, but can be observed disappearance of breaks with time. **D).** Graph bar showed diffrences in chromatid breaks frequencies between deficient HR cell lines, irs-1 and irs1-SF and control V79 throughout 4 hours post-radiation. The statistical analysis showed significant differences (*t*-test *P<0.05, **P<0.01, ***P<0.001)

5.3 Analysis of chromatid breaks at the ITS in deficient HR hamster cells

We next analysed the chromatid breaks repair within ITSs in deficient HR hamster cells. It has been shown that ITSs in Chinese hamster are formed by large blocks of telomeric DNA in the pericentromeric regions of most hamster chromosomes (Faravelli *et al.*, 2002; Faravelli *et al.*, 1998) and constitute the main satellite DNA and represent 5% of the hamster genome (Day, Limoli and Morgan, 1998). These ITSs are considered "hotspot" for spontaneous and induced chromosomal breakage, recombination and amplification (Slijepcevic *et al.*, 1996; Fernández, Gosálvez and Goyanes, 1995a; Alvarez *et al.*, 1993). To investigate frequencies of chromatid breaks repair within ITSs in HR deficient hamster cells we used cytogenetic FISH analysis. Representative examples of chromatid breaks in HR deficient hamster cells are shown in Figure 5.3. Results of our analysis are shown in Figure 5.4. and table 5.1. Its is clear that frequencies of observed chromatid breaks were higher than expected in all cell lines, based on the percentage of the hamster genome covered by ITS. Our results are in line with previous studies by Fernandez *et al.*, (1995) and Bolzan *et al.*, (2001). However, we observed re-joining of breaks with reduced repair kinetics of DSBs in HR deficient cell lines over time (Figure 5.4). A sudy by Rivero *et al.*, (2004) reported a slow DSBs repair kinetics in Rad51C deficient hamster line and demonstrated that ITSs are alkali sensitive regions formed by short unpaired DNA segments in the hamster genome.

Chromatid aberrations at the ITSs in HR deficient Chinese hamster cell lines using FISH

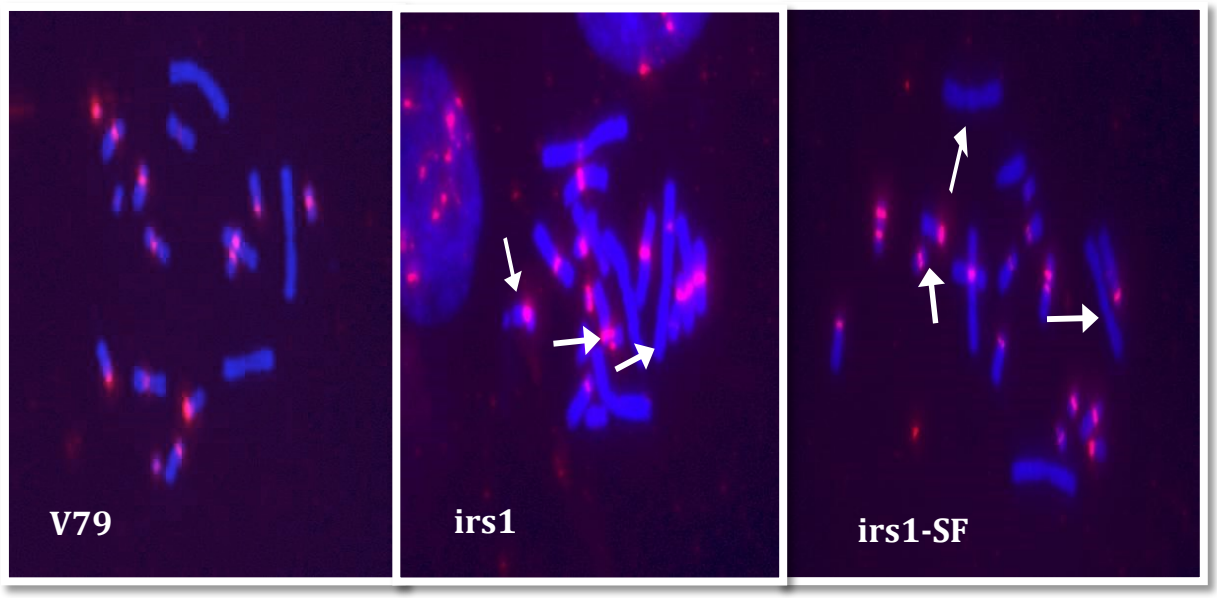

Figure 5.3 Representative image of HR deficient hamster metaphase spreads. Irs1 showed strong telomeric signal in pericentromeric regions and no signal at telomeres. Irs1-SF exhibited condensed metaphase and visible signal at ITSs. It can be observed breaks and gaps indicated in white arrows.

Analysis of chromatid aberrations at ITSs in HR deficient Chinese hamster cell lines using FISH

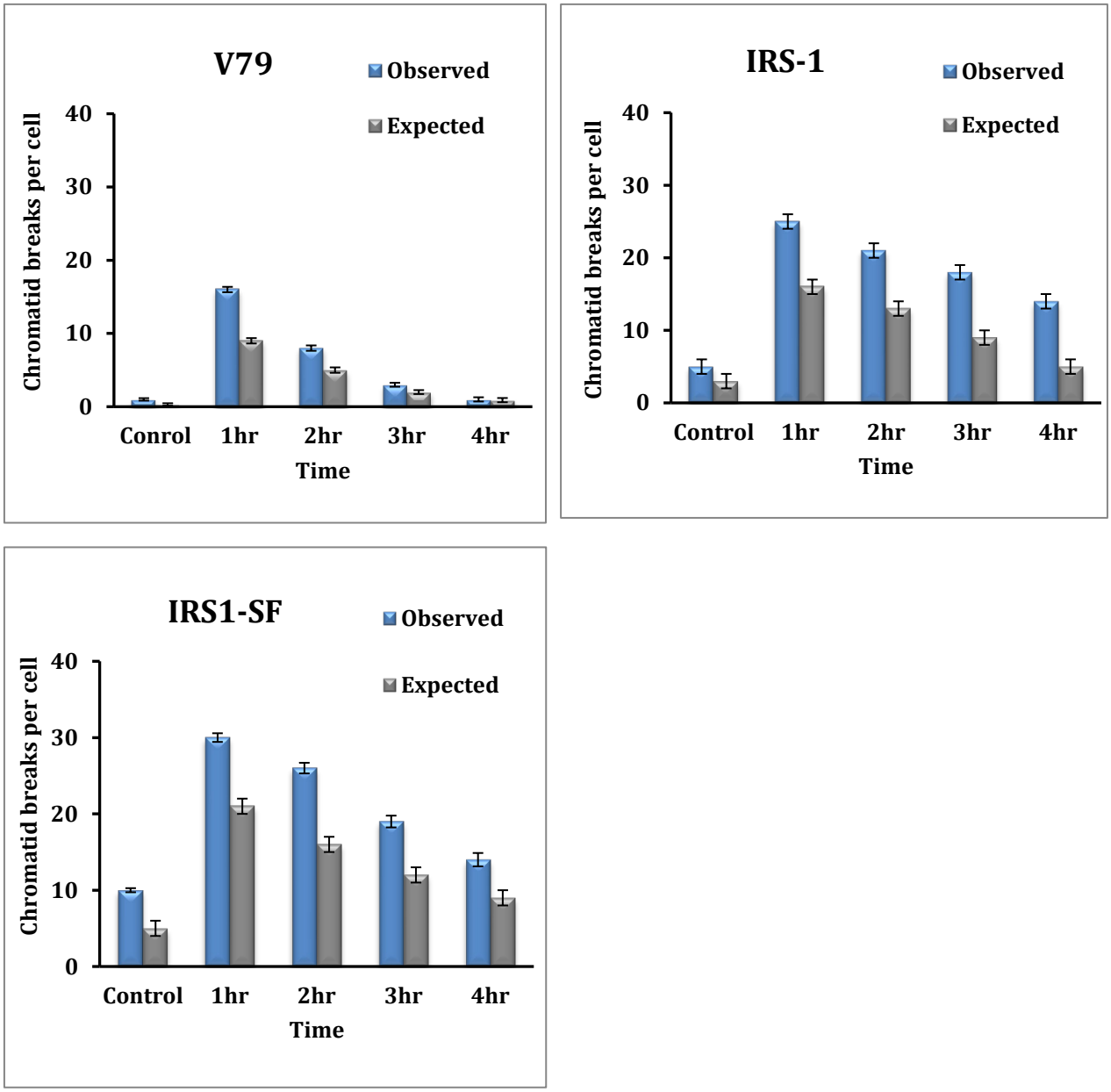

Figure 5.4 Frequencies of chromatid breaks inside and outside ITSs in HR deficient Chinese hamster cell lines. V79 control cell line shows a linear DSB repair kinetics with time. Irs1-SF shows higher breaks than irs-1 cell line at one and two hours post-radiation, and then no much difference in the number of breaks at 3 and 4 hours.

Table 5.1 Distribution of chromatid breaks within ITSs and DSBs repair kinects among HR deficient Chinese hamster cells.

			0h		1hr		2hr		3hr		4hr		
Cell Lines	**Score cells**	**ITS% Ch. Length**	**Obs.**	**Exp.**	**Obs.**	**Exp.**	**Obs.**	**Exp.**	**Obs.**	**Exp.**	**Obs.**	**Exp.**	***p-value (0.05)***
V79	100	9.3	1	0	16	9	8	5	3	2	1	1	p<0.05
irs-1	100	7.5	5	3	25	16	21	13	18	9	14	5	p<0.05
irs1-SF	100	8	10	5	30	21	26	16	19	12	14	9	p<0.05

5.4 Analysis of DNA DSBs in HR deficient hamster cells by H2AX foci

Having analyzed the DNA DSBs repair kinetics in NHEJ deficient Chinese hamster cells (Chapter 4), we next investigated DSBs repair kinetics in HR deficient cells and evaluate the degree of DNA damage response deficiency. H2AX is a key sensor that responses to initial DSBs lesions, undergoes phosphorylation, to form γ-H2AX (Rogakou *et al.*, 1998). γ-H2AX provides a docking site through its chromatin modification, thus enhancing the recruitment of repair factors, repair proteins and amplification of DNA damage signals (Celeste *et al.*, 2002). Detection of γ-H2AX relies upon antibodies raised to the phosphorylated H2AX and the numbers of DBSs are proportional to γ-H2AX foci formation in cultured cells and tissues (Fernandez-Capetillo, Celeste and Nussenzweig, 2003; Rogakou *et al.*, 1999). Representative γH2AX foci images are shown in Figure 5.5. Results of our analysis are presented in Figure 5.6. The results obtained for HR deficient cells indicated higher frequency levels of γ-H2AX foci compared to control cell. The levels of γ-H2AX positive foci in irs1-SF (26.3/cell) were substantially higher than in irs1 (21.5/cell) (Figure 5.6). However, disappearances of γ-H2AX foci were noticeable at 24 and 48 hours in these defective cell lines that may indicate moderate repair kinetics of DNA DSBs. The difference between untreated and treated samples were statistically significant (*t*-test **P<0.01, ***P<0.001) at each time points in the two cell lines. In line with Rothkamm *et al.*, (2003), our results showed reduced DSB kinetics in HR defective Chinese hamster cells. These findings are consistent with the radiosensitivity phenotype present in HR deficient hamster cell lines, hence disruption in the Rad51 paralogs significantly impair DSB repair.

There are differences in sensitivity response to IR and induced DNA DSB damage between the cell lines, which can be due to their specific role in DNA repair. For example, fork progression is decreased or absent in irs1-SF (xrcc3-/-) cells when exposed to cysplatin, indicating that xrcc3 is actively involved in the progression of replication fork after DNA damage presumably through the interaction of Rad51 (Henry-Mowatt *et al.*, 2003). Additionally, the irs1 (xrcc2-/-) deficient line is unable to form Rad51 foci formation after hydroxyurea induced replication arrest (Liu and Lim, 2005). Both mutant cells lines are defective in Rad51 foci formation, therefore HR repair activity is reduced in these cell lines.

γ-H2AX assay to investigate DNA DSB repair in HR deficient Chinese hamster cells

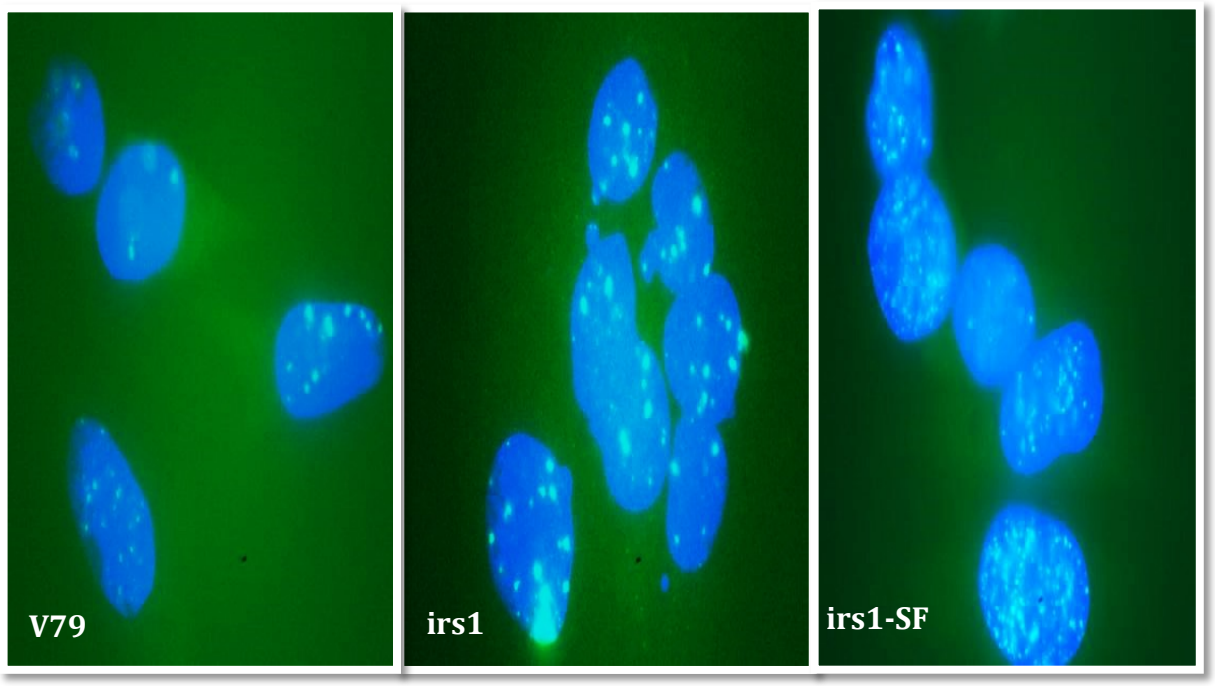

Figure 5.5 Representative images of γ-H2AX Representative image of γ-H2AX detection in HR deficient Chinese hamster cell lines. V79 is a control cell line, irs1 (xrcc2-/-) and irs1-SF (xrcc3-/-) cell lines showed hight levels of positive DNA maker, γ-H2AX green (FITC) foci staining n HR deficient cell lines after 0.5h IR exposure.

DNA DSBs in HR deficient Chinese hamster cell lines using γ-H2AX foci

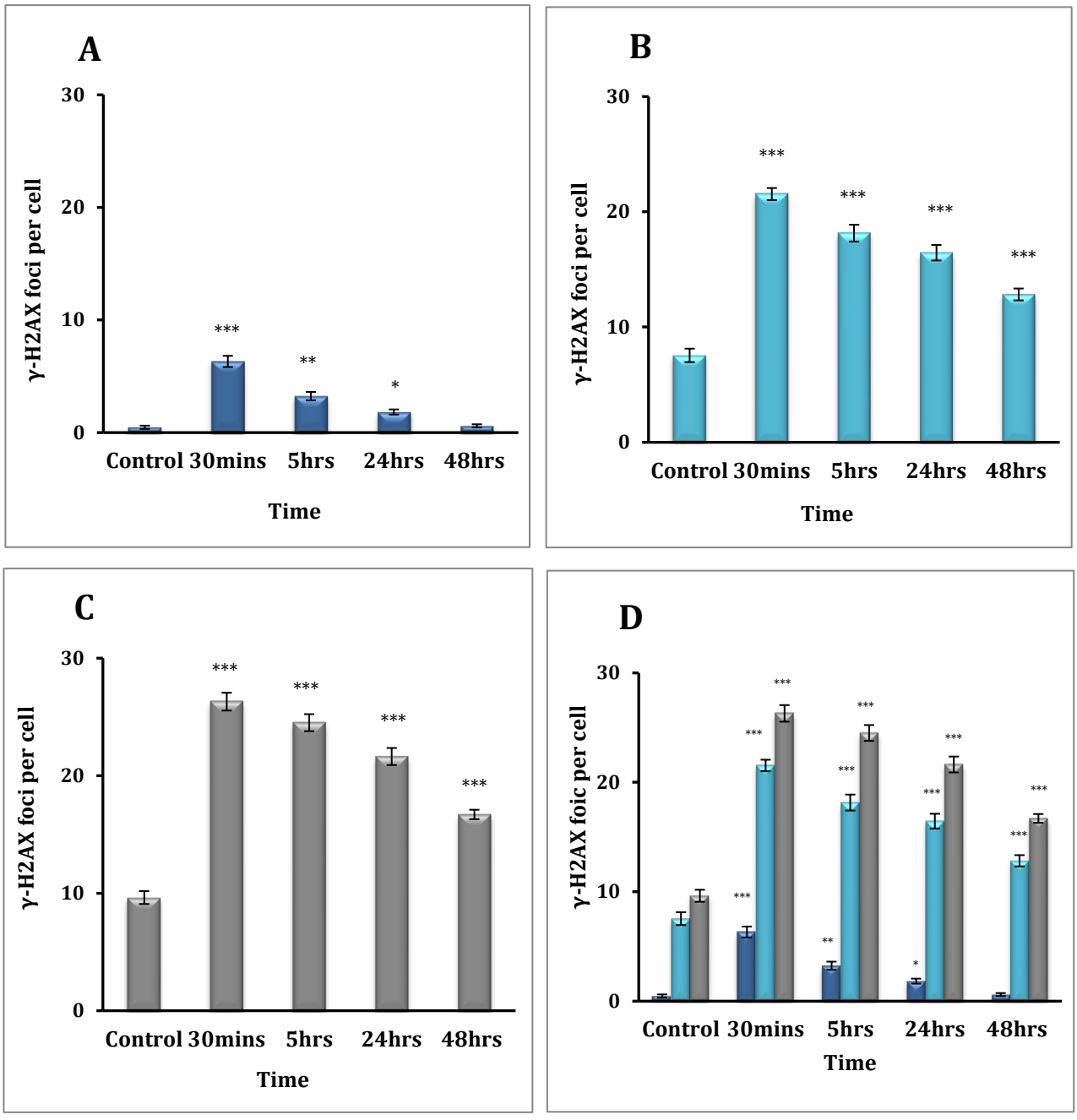

Figure 5.6 Frequencies of γ-H2AX foci in control and HR deficient Chinese hamster cell lines. **A)** V79 control line showed high levels of γ-H2AX accompanied with a significant disappearance γ-H2AX foci at 48 hours post radiation. **B)** irs1 cell line showed higher levels of γ-H2AX throughout the 48 hours compared to counterpart V79. **C)** irs1-SF exhibited significant decrease in the disappearance of γ-H2AX that correlated with the persistence of DNA damage at interphase cells. **D)** The difference between untreated and treated samples were statistically significant (t-test ***P<0.001) at each time points in the two cell lines. Bars represent SEM.

5.5 Analysis of telomere dysfunction (TIF) in HR deficient Chinese hamster cells

In Chapter 4 we presented evidences of reduced DNA repair kinetics within TIFs in NHEJ deficient Chinese hamster cell lines (Figures 4.6). To our knowledge, this study is the first assessment of telomere dysfunction in Chinese hamster cell lines. Next, we used TIF assay to examine repair kinetics in HR deficient hamster cell lines.

When telomeres or shelterin are compromised the capping function is repressed at telomeres and this can lead in chromosomal end-to end fusion and rearrangement, resulting in genome instability (Palm and de Lange, 2008). We performed the TIF assay as in the previous chapter (two independent experiments to ensure consistency of results). The results of our analysis are shown in Figure 5.8. Frequencies of TIFs were higher in HR deficient Chinese hamster cell lines, irs1 (14/cell) and irs1-SF (17.1/cell) at 0.5h post-radiation (Figure 5.7). However, at 48 hours deficient HR cell lines showed a mild decreased in the number of TIFs, but the frequencies were still higher compared to control cell lines (3.5/cell). The difference between untreated samples and treated samples were statistically significant (*t*-test **P<0.01, ***P<0.001). Dr Y. Gozaly thesis (unpublished) has reported a similar finding of TIFs repair kinetics over time in a different set of Chinese hamster cell lines.

Telomere dysfunction in HR deficient Chinese hamster cell lines by TIFs foci

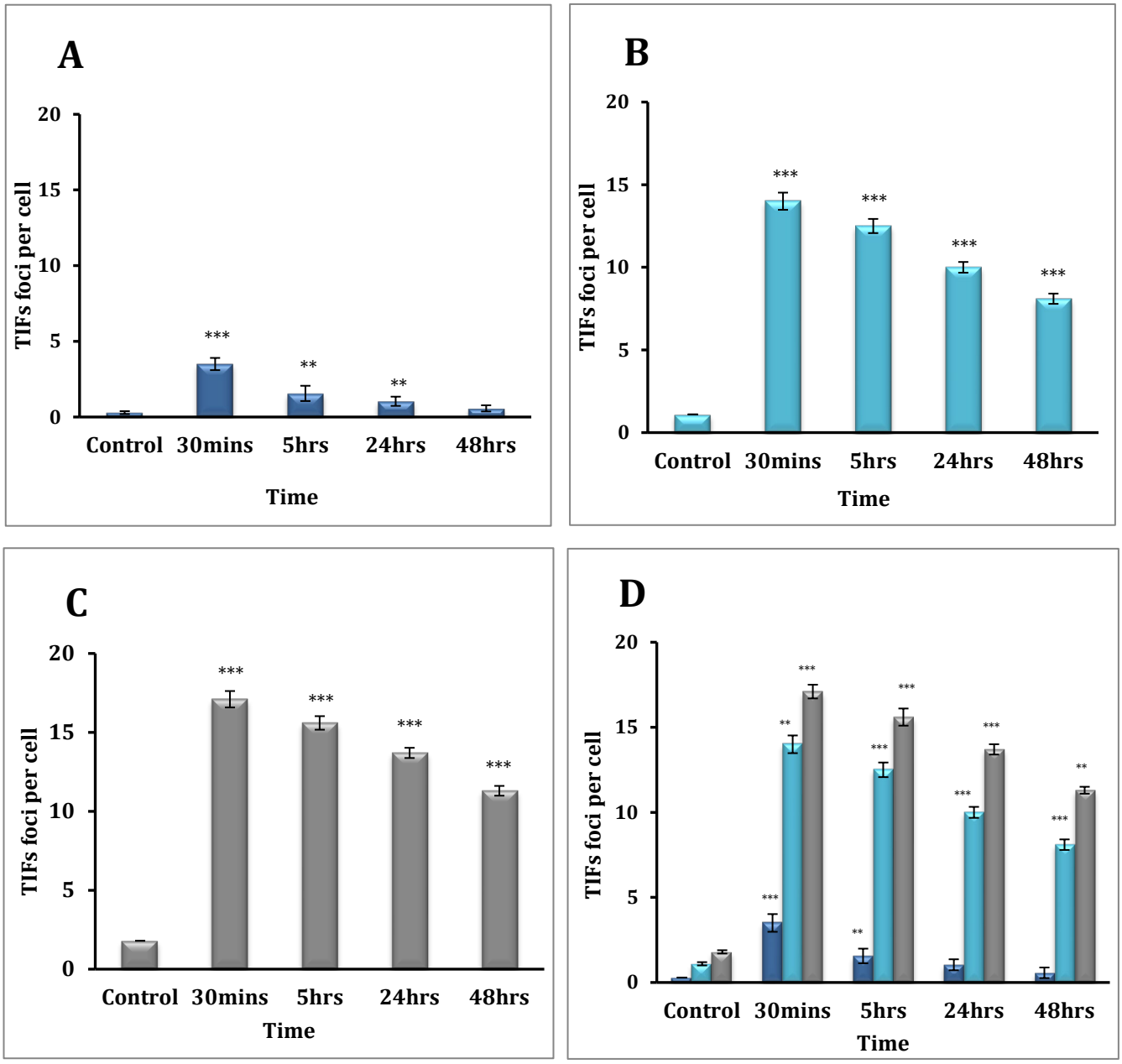

Figure 5.7 Frequencies averages of TIFs foci in HR deficient Chinese cell lines. **A)** V79 control showed lower TIFs levels compared to irs1 and irs1-SF. **B)** irs1 presented higher levels of TIFs at 30 mins and exhibited a reduce disappearance over 24hrs. **C)** irs1-SF showed increased levels of TIFs foci throughout the 48hrs and accompanied with a discreet disappearance of the TIFs foci. **D**) irs1 and irs1-SF cells TIFs levels remained significantly higher compared to V79 but decreased become apparent at 48 hours. The difference between untreated and treated samples were statistically significant (t-test ***P<0.001) at each time points in the two cell lines. Bars represent SEM.

5.6 Discussion

In this chapter we employed HR deficient Chinese hamster cell lines to examine the effects of DNA damage within ITSs in these defective cells. Our results show that chromatid breaks within ITSs are higher than expected and elevated frequencies of DNA damage and telomere dysfunction in interphase cells are observed in these cells (Figure 5.7 and 5.8). Previous studies have shown evidences that ITSs, are hotspots for chromosome breakage and correlate with fragile sites (Day, Limoli and Morgan, 1998; Hastie and Allshire, 1989). Azzalin *et al*. (2001) have cloned human ITS and identified three classes: short ITSs, subtelomeric ITSs, and fusion/inverted ITSs (Azzalin, Nergadze and Giulotto, 2001). In non-human species, such as Chinese hamster, large block of het-ITSs are found within the constitutive heterochromatin, and constitute the main satellite DNA sequence in this species (Faravelli *et al.*, 1998; Balajee, Oh and Natarajan, 1994; Meyne *et al.*, 1990). The cytogenetic studies show that Chinese hamster ITSs regions are prone to spontaneous breakages, recombination, rearrangements and amplification (Day, Limoli and Morgan, 1998; Slijepcevic *et al.*, 1996; Fernández, Gosálvez and Goyanes, 1995b). Alvarez et al. (1993) reported increased frequency of spontaneous and IR-induced breakage within ITSs that was higher than the overall Chinese hamster genome. Our cytogenetic results indicated high frequencies of chromatid break involving ITSs than expected in Chinese hamster cells (Figure 5.4). These findings are in line with results published by Slijepcevic (1996), which showed the telomerase positive Chinese cell lines have a higher sensitivity to breakage compared to telomerase negative Chinese hamster (CHL).

In addition, Jordan et al. (1995) have identified a region in chromosome 5q15 near the GPT gene, to be a preferential site of radiation-induced breakage within ITSs and also integration sites in Chinese hamster cells (Jordan, Oroskar and Sedita, 1995). For example, Kilburn *et al*. (2001) constructed a model of hamster cells containing 800bp of telomeric sequences and integrated it into the APRT gene. Molecular analysis showed up to a 30 folds increase in levels of small deletions and insertions, (microrearrangement) that suggested genomic instability of ITSs in Chinese hamster (Kilburn *et al.*, 2001).

There are no reports in the literature on the DNA damage repair within ITSs in Chinese hamster cells. To the best of our knowledge this is the first report on the DNA damage repair kinetics within ITSs of Chinese hamster cells. (Figure 5.4). We observed that chromatid breaks within ITSs disappeared with time and might suggest that DNA damage response pathway or re-joining mechanism must be active. Interestingly, ITSs contain AT-rich sequences, and low duplex stability. Furthermore, ITSs are comprised of 50 to 60% guanine and *in vitro* studies suggest that this composition can promote the formation of secondary DNA structures such as guanine tetrad pairing. These structures have been proposed as preferential sites for exchanges (W. Sundquist and A. Klug, 1989).

Having established DNA damage repair kinetics within ITSs at chromosomal levels. Next, we wanted to analyse DNA damage at ITSs at cellular level by using H2AX antibody and telomeric probe at interphase cells. Our results evidence that TIFs foci levels were significantly elevated compared to control counterpart Chinese hamster cell line. However, the frequencies of TIFs foci decreased or disappeared at 24 and 48 hours in Chinese hamster cells.

Telomeric DNA damage repair is controversial as previous studies have suggested that telomeric DNA damage is resistant to repair (Fumagalli *et al.*, 2012). Recently, Mao et al. (2016) have reported efficient repair of telomeric DSBs in proliferating cells, including somatic human cells and cancer cells. However, they found that telomeric DSBs are resistant to repair in senesce cells caused by genotoxic stress (Mao *et al.*, 2016).

Our interpretation of the ITSs results suggests that there must be a repair or rejoining mechanism(s) within these sequences that is involved in the repair process (Rivero *et al.*, 2004). Furthermore, the presence of TRF1, TRF2 and RAP1 indicates that these proteins protect and promote stability by reducing unequal HR events between telomeric sequences (C. Mignon-Ravix *et al*., 2002).

Chapter 6.

Analysis of telomerase and ALT activities in Chinese hamster cells and knockdown of ALT-associated proteins ATRX and HDAC9

6.1 Introduction

Previous chapters demonstrated that ITSs in Chinese hamster chromosomes are sensitive to breakage by IR. Various DSB repair mutants established from Chinese hamster cell lines showed elevated sensitivity to ITSs breakage relative to control cell lines. Most observations we made are in line with the previously published studies (Slijepcevic *et al.*, 1996; Fernández, Gosálvez and Goyanes, 1995; Alvarez *et al.*, 1993). The results presented within my study show for the first time, DNA repair kinetics with time in ITS and non-ITS regions using cytological methods. The aim of the present chapter is to make one analytical step further, namely to do molecular analysis of DNA damage response in hamster cells with particular emphasis on how the two mechanisms involved in telomere processing, telomerase and ALT, behave in this process.

Telomeres progressively shorten around 50 to 200 nucleotides with every round of cell division (Levy *et al.*, 1992). This results in the end replication problem, the inability of DNA polymerase to replicate chromosome ends (Kim *et al.*, 1994). Telomere loss is counterbalanced by ribonucleoprotein enzyme telomerase consisting of the catalytic subunit (TERT), an RNA molecule (TERC), and a range of smaller molecules (Zakian, 1997; Blackburn, 1991). Telomerase activity is present in germ line cells, tumours and immortal cell lines but is found at almost undetectable levels in most human somatic cells (Masutomi *et al.*, 2003; Kim *et al.*, 1994). In addition, telomerase activation is thought to be an important step towards cellular immortalization, as the maintenance of telomere length is crucial for tumorigenesis (Carman, Afshari and Barrett, 1998; Counter *et al.*, 1992).

It has been shown that 85 to 90% of human tumour cells acquire immortality through telomerase activity resulting in a stable telomere length. Remaining 10-15% tumours activate an alternative mechanism of telomere maintenance (ALT) (Henson *et al.*, 2002; Counter *et al.*, 1992).

A small subset of tumour cells, such as osteosarcomas cells and lung adenocarcinomas cells are telomerase negative and maintain telomere length by ALT, in which cells show long and heterogeneous telomeres (Bryan *et al.*, 1997) . The ALT pathway is defined as a telomere length maintenance mechanism independent of telomerase activity. It is likely that ALT relies on HR mediated DNA replication mechanism (Bryan *et al.*, 1997). For example, many *S.cerevisiae* and *K. lactis* yeast cells use telomerase to maintain telomere length, but when telomerase is abolished in these cells they can switch to recombinational mechanism mediated by Rad52 (Teng and Zakian, 1999). These *S.cerevisiae* and *K. lactis* telomerase negative cells have long heterogeneous telomeres that resemble human ALT cells lines (Cerone, Londono-Vallejo and Bacchetti, 2001).

The immortalized and tumour ALT cells share common features, long heterogeneous telomeres (T. M. Bryan *et al.*, 1995), extrachromosomal telomeric repeats (ECTRs), mutation of chromatin remodelling factor, ATRX (Tang *et al.*, 2004), increased frequency of T-SCEs (Londono-Vallejo *et al.*, 2004), and presence of Promyelocytic leukaemia nuclear bodies (PML) ALT-associated PML (APBs) (Yeager *et al.*, 1999). APBs are formed by PML nuclear bodies, which associate with telomeric DNA in ALT cells (Yeager *et al.*, 1999). PML bodies are nuclear structures involved in a wide variety of cellular processes, including transcription, DNA repair, DNA replication and tumour suppression (Draskovic *et al.*, 2009; Borden, 2002).

These PMLs are scaffold structures that harbour a number of proteins involved in DNA recombination and repair, such as Rad51 and Rad52 and MRN complex (Yeager *et al.*, 1999), and also directly interact with SUMO1, Sp100, ATRX and DAXX (Ishov *et al.*, 1999).

In human cells, somatic mutations of *ATRX* gene have been found in ALT cancer cells including, glioblastoma multiforme cancers and pancreatic neuroendocrine tumours (Lovejoy *et al.*, 2012; Heaphy *et al.*, 2011). ATRX is a chromatin-remodelling factor of the Snf2 family and closely related to RAD54 (Gibbons *et al.*, 1995). It binds to the protein DAXX, which acts as specific chaperon protein for H3.3 and they together form the ATRX/DAXX/H3.3 complex (Drane *et al.*, 2010).

The cellular function of ATRX is not completely clear; mutated ATRX causes reduced HP1 telomeric loading, telomere dysfunction in mES (Wong *et al.*, 2010), and aberrant mitosis and chromatid bridges. ATRX may also have a role in genome integrity maintenance (Watson *et al.*, 2013; Lovejoy *et al.*, 2012). It has been suggested that loss of ATRX *in vitro* is the surrogate of the ALT phenotype (Lovejoy *et al.*, 2012). A characteristic feature of ALT pathway is the formation of PML nuclear bodies, which co-localize with telomeric DNA and DNA repair proteins, such as Rad51 and Rad52 and MRN complex (Yeager *et al.*, 1999). Interestingly, APBs mediate telomere lengthening in ALT cells by inducing chromatin compaction and restricting TRF2 depletion at telomeres (Osterwald *et al.*, 2015). Therefore, a partial de-protection of telomeres that leads to DNA damage response may promote ALT.

Moreover, it has been demonstrated that depletion of APBs by PML knockdown results in telomere shortening and reduction in the amount of extrachromosomal telomeric repeats, known as c-circles (Osterwald *et al.*, 2015). The RNAi knockdown of heterochromatin proteins, such as histone demethylase LSD1, reduces the number of APBs (Shi *et al.*, 2004).

It has been demonstrated that induction of telomerase activity in the ALT cell line GM847 through expression telomerase (*hTERT*), this significantly results in the lengthening of the shortest telomeres in the majority of cells (Perrem *et al.*, 2001). The GM847 is a Simian Virus 40 transformed skin fibroblast cell line and originated from an individual with Lesch Nyhan syndrome (McDaniel and Schultz, 1992). In addition, the GM847/hTERT hybrid cells have APBs, which is characteristic of ALT cell lines but not telomerase positive cells, suggesting that ALT mechanism can be still functional in the GM847/hTERT hybrid (Perrem *et al.*, 2001). However, ALT activity repressed APBs foci disappearance and reduction of telomere length when GM847 cells were fused with telomerase positive or normal fibroblast cells. This means that ALT repression factors may be present in these cells (Perrem *et al.*, 2001; Perrem *et al.*, 1999).

Moreover, ALT-telomerase cells; GM847/hTERT and WI38-VA13/2RA/hTERT exhibit both telomerase and ALT mechanisms that can co-exist and contribute to telomere maintenance in these human cell lines (Perrem *et al.*, 2001; Cerone, Londono-Vallejo and Bacchetti, 2001). Furthermore, Neumann et al. (2013) have shown ALT activity in mouse somatic tissues *in vivo* (naturally telomerase positive), in which new telomere DNA was synthesized using another telomere as template.

At present ALT activity is detected and quantified by a sensitive and reliable assay, known as the C-circle assay. C-circle is self-priming circular telomeric C-strand template for rolling circle amplification and generating a partially double strand Ccircles molecular intermediate, therefore it is specific in ALT cells and serves as indicator of ALT activity (Henson *et al.*, 2009).

My aim in this chapter is to determine whether telomerase and ALT activity coexist in Chinese hamster cells. If this is confirmed, we aim to manipulate proteins involved in ALT, ATRX and HDAC9, using siRNAs with a view to testing whether this manipulation will affect DNA damage response. This will enable us to obtain a more detailed picture of DNA damage response at ITSs observed in previous chapters.

6.2 Detection of telomerase enzymatic activity in Chinese hamster cell lines

The unlimited proliferative potential of immortal and cancer cells requires the activation of telomere maintenance mechanisms. These are either telomerase or ALT. To measure telomerase activity in Chinese hamster cell lines we used a sensitive PCRbased Telomerase Repeat Amplification Protocol (TRAP) assay (Kim *et al.*, 1994), modified in way to allow quantitation (Wege *et al.*, 2002). Primary Chinese hamster cells have naturally long telomeres estimated to be on average 38kb (Slijepcevic and Hande, 1999). By contrast, all their immortal counterparts show a dramatic reduction in telomere length estimated to be in the region of only 1kb (Slijepcevic and Hande, 1999). In addition, it has been proposed that long telomeres in mouse enhance the chances for spontaneous immortalization, due to telomerase expression in somatic and cultured cells; therefore, mouse cells will escape senescence and acquire indefinite lifespan (Prowse and Greider, 1995). We used protein extracts from the human control cell lines PC-3 and HeLA as telomerase positive controls, and primary human fibroblast cells as telomerase negative controls. Telomerase activity was measured in CHOK-1 and V79 cell lines. We also included a HeLA inactivated sample to exclude false positives from the TRAP assay. The schematic of the analysis by TRAP is shown in Figure 6.1 A. As expected, immortalized Chinese hamster cells showed high levels of telomerase activity comparable to PC3 and HeLA positive telomerase controls (Figure 6.1 B). To exclude false positives, we included all Chinese hamster cell lines (see previous chapters) in our analytics. We observed telomerase activity in all hamster cell lines. Experiments were repeated twice under same conditions and the results averaged, thus ensuring that the random errors were minimised, and statistical analysis showed significant differences (*t*-test **P<0.01, ***P<0.001). Interestingly, all mutant cell lines showed lower telomerase activity relative to control parental lines. It is unclear whether this reduction is due to defective DNA damage response. In contrast

to hamster cells, human primary fibroblast showed significantly low telomerase activity (not completely absent). Our results are consistent with previous studies (Slijepcevic et al. (1996), Pandita et al. (1998) and Carman et al. (1998). Therefore, extensive shortening of telomeres observed in immortalized Chinese hamster cells in spite of telomerase activity suggests that the mechanisms behind these are complex and potentially different from the situation observed in human cells.

In human cells, telomere erosion causes the activation of DNA damage response that leads to chromosome instability and end-to-end chromosome fusions. In contrast to human cells with short telomeres, their Chinese hamsters' counterparts do not exhibit increased frequencies of end-to-end fusion events despite shorten telomeres (Slijepcevic *et al.*, 1997).

Telomerase activity in Chinese hamster cell lines

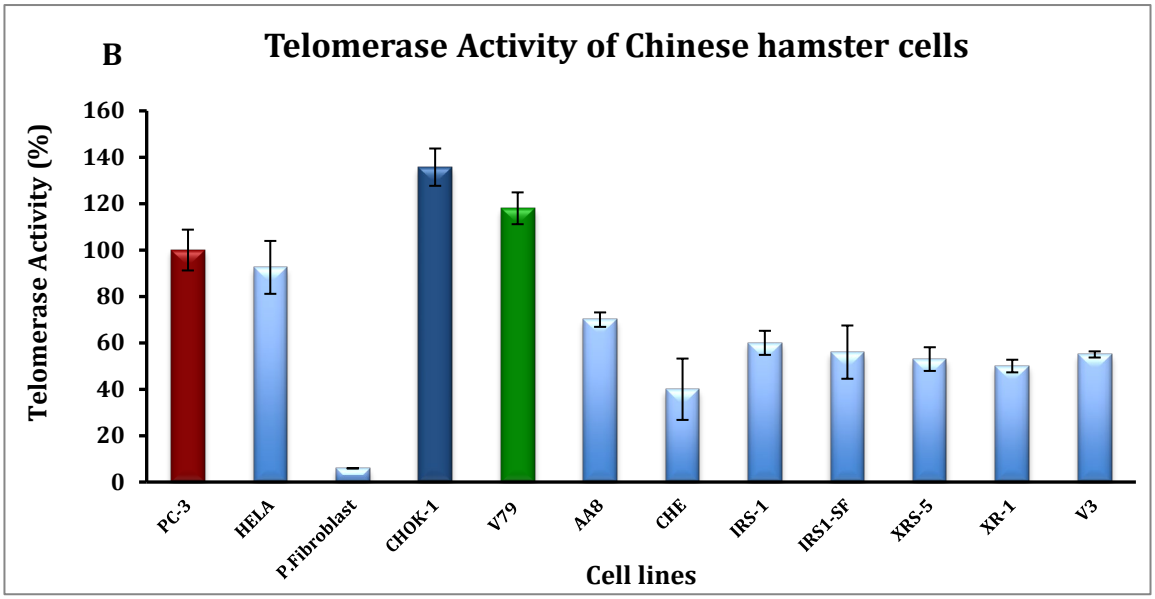

Figure 6.1 Telomere Repeat Amplification Protocol (TRAP) in Chinese hamster cells. **A)** Representative image of RT-PCR amplification of hamster samples. **B)** Telomerase activity of DNA repair proficient and DSB repair deficient hamster cell lines. The control hamster cells, CHOK-1 (dark blue) and V79 (green) were shown higher telomerase activity compared to deficient repair hamster cell lines and PC-3hTERT (red) and HeLA (+controls). Error bars represent SEM.

6.3 Detection of alternative lengthening of telomere activity in Chinese hamster cell lines by C-circle (CC) assay

Having established telomerase activity in all Chinese hamster cells, we next wanted to detect whether Chinese hamster cells express ALT activity. It has been shown that some immortalized human cells are telomerase negative and have a characteristic signature of telomere length, ranging from very short to very long within the same cell (Bryan *et al.*, 1997; Bryan *et al.*, 1995). Telomerase is present in 85% - 90% of tumour cells, while remaining 10-15% of tumour cell lines expressed ALT (Cesare and Reddel, 2010; T. M. Bryan *et al.*, 1997). Interestingly, telomere deficient mouse *mTR-/-* cells are capable of becoming neoplastic, suggesting that the absence of telomerase does not inhibit oncogenic transformation and telomere length is maintained by recombinational mechanisms (Blasco *et al.*, 1997). In addition, ALT cells use recombination as lengthening mechanism and telomeric DNA serves as the template to copy one telomere to another telomere; this system relies on DNA recombination and repair proteins such as the MRN complex and RAD52 (Dunham *et al.*, 2000). Moreover, in recent years telomere maintenance in human tumours or immortalized cells have been classified as either telomerase-dependent or ALT dependent with no possibility that both mechanisms are expressed in the same human cells. However, this has been somewhat revised as the experimental evidence has demonstrated the coexistence of these two mechanisms within the single cell line. For example, human ALT cells, GM847 and VA13, transfected with *hTERT* showed telomerase activity without repressed ALT activity (Perrem *et al.*, 2001; Cerone, Londono-Vallejo and Bacchetti, 2001). Furthermore, in mouse embryonic fibroblasts ALT and telomerase coexist (Neumann *et al.*, 2013; Cerone, Londono-Vallejo and Bacchetti, 2001; Perrem *et al.*, 2001).

The notion of telomerase and ALT coexistence in Chinese hamster cells has not been explored. At present ALT activity is determined and quantified by a sensitive and reliable C-circle (CC) assay. C-circle is self-priming circular telomeric C-strand template for rolling circle amplification and generating a partially double stranded C-circles molecular intermediate. Therefore, the assay is specific for ALT positive cells and an indicator of ALT activity (Henson *et al.*, 2009). The C-circle assay was carried out using gDNA (genomic DNA) from ALT positive human control cells (U2OS), ALT negative human control cells (HELA) and test cell lines, CHOK-1 and V79. All samples were slot blotted onto the nitrocellulose membrane and probed with DNA end-labelled P^{32} $(CCCTAA)_3$ (Figure 6.2 A). To establish that ALT activity is proportional to the gDNA concentration, we performed a serial dilution of U2OS gDNA (ALT positive line) (Figure 6.2 B). The linear regression analysis showed a linear correlation (R^2=0.9737) between concentration of gDNA of U2OS and CC activity.

The results from CC assay showed ALT activity in all Chinese hamster cell lines and U2OS positive control cells but a lack of ALT expression in HELA negative control cells (Figure 6.3 A-C). The results were validated by performing two independent experiments and quantifying the average densitometry of ALT activity on the blots using the Image J software (Figure 6.2 A). Overall, we detected ALT activity in all Chinese hamster cell lines and found small differences in ALT activity between cell lines, which might have corresponded to their specific gene mutation in DNA repair pathways, HR and NHEJ (see previous chapters).

Although the mechanism and causes of ALT are not well known, it has been shown that genes affecting chromatin status could be involved in ALT activation in immortal and cancer cells. We decided to target two genes; ATRX and HDAC9 that modulate chromatin and

histone status respectively, with a view to establishing whether their inactivation would affect DNA damage response.

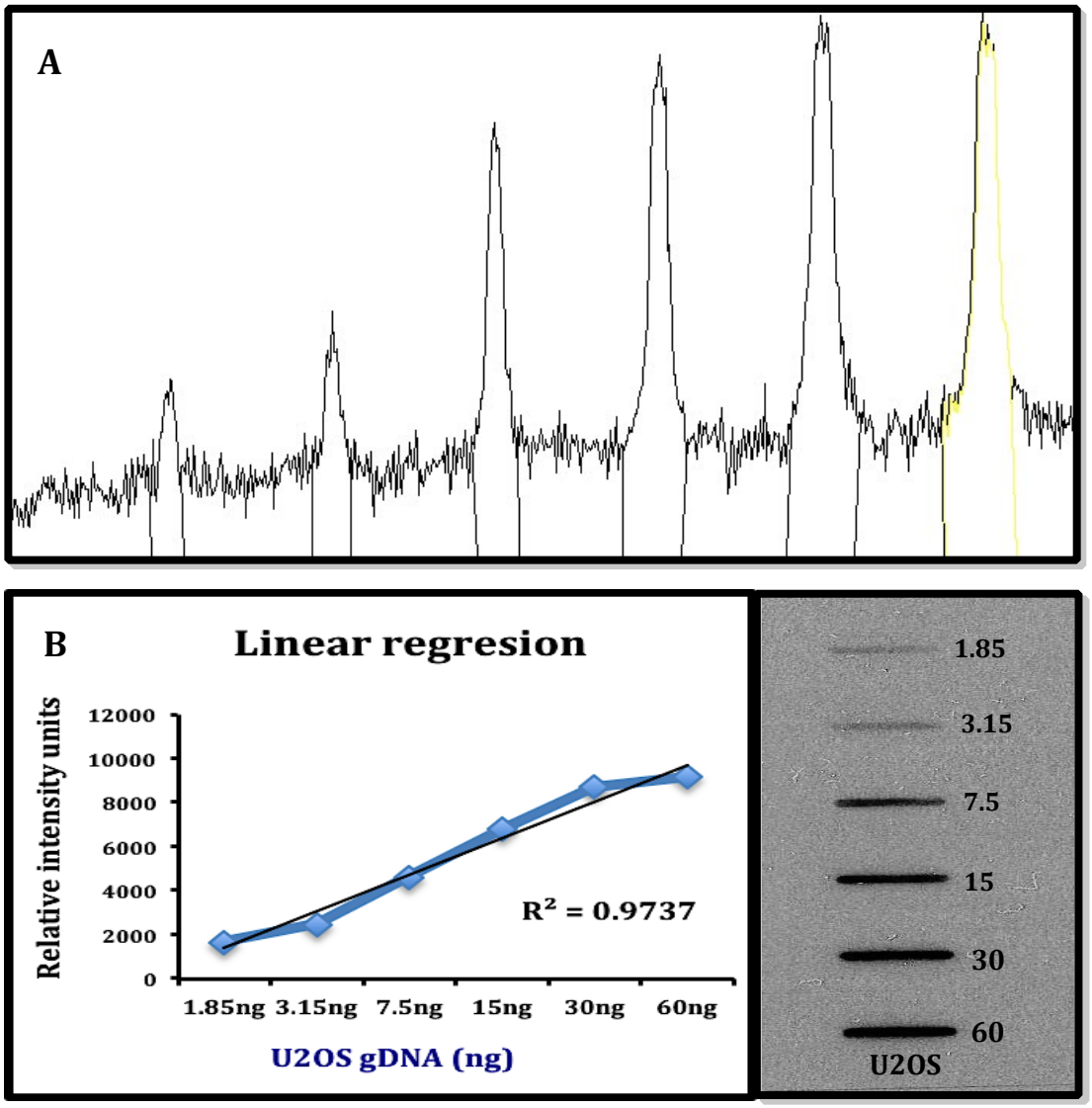

Figure 6.2 Detection of ALT activity in U2OS ($^{+}$ALT) cell line. **A)** Histogram represented U2OS bands (slot blot below) and analysed using Image J software. The bands analysis generated a peak signal in which length-width of each peak is proportional to their intensity. The x-axis represents the gray value and the y-axis represent the pixels, which is then average as the sum of the gray values of all the pixels in the selection divided by the number of pixels. **B)** Slot blot of U2OS serial dilutions ranging from 1.85ng to 60ng gDNA and standard curve were plotted according to histogram values. The linear regression analysis R= 0.9737.

C-circle activit of Chinese hamster cells

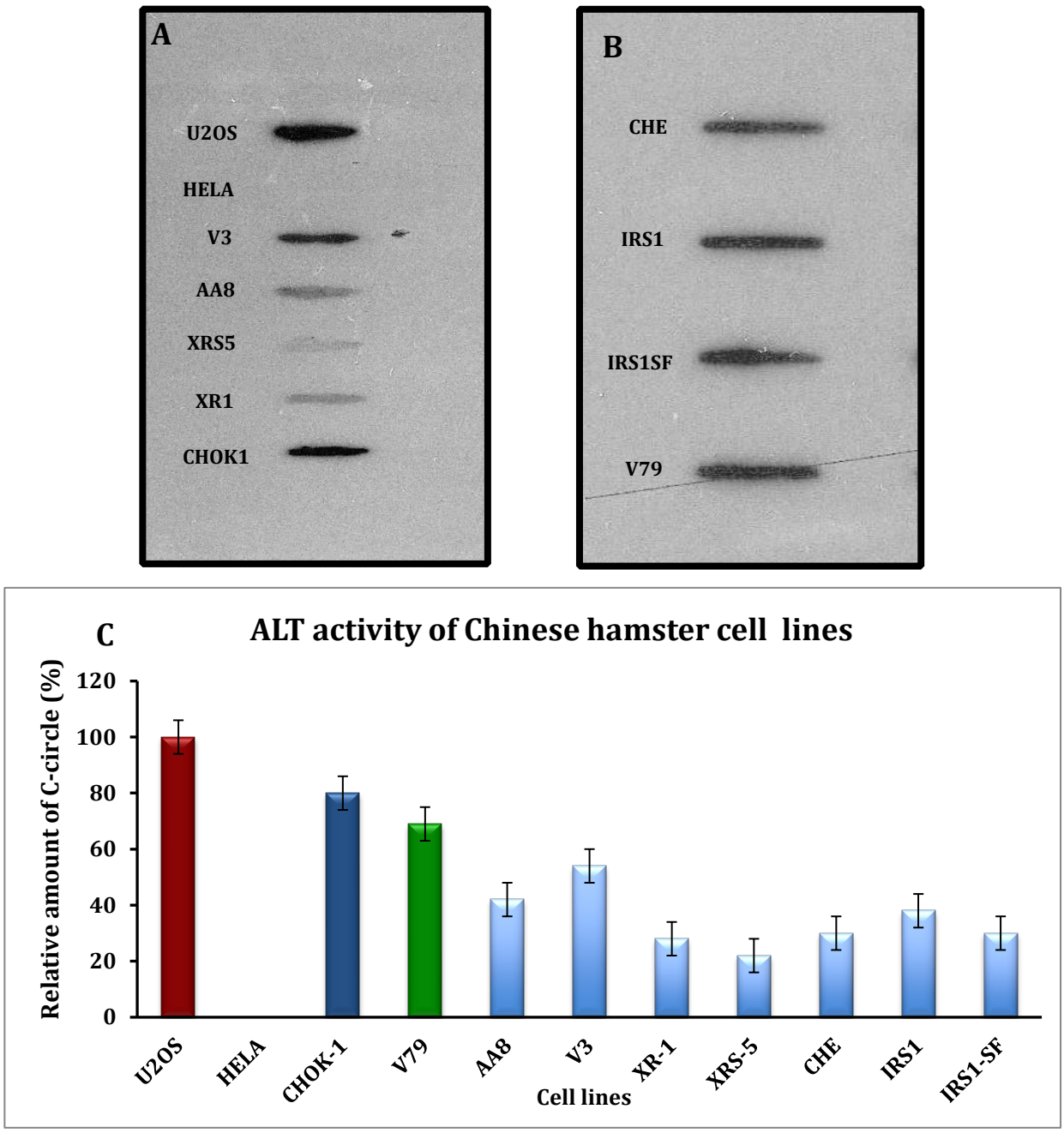

Figure 6.3 C-circle assay in Chinese hamster cell lines. **A-B)** Slot blots showed repair proficient and DSB repair deficient hamster cell lines with human controls U2OS ($^{+}$ALT) and HeLA ($^{-}$ALT). The bands in the blots corresponded to the presence of the ALT activity in each cell line and bands were measured and quantified using Image J, hence bands intensity was proportional to their ALT activity. **C)** The graph showed ALT activity in all hamster cell lines and the activities were converted in percentage having U2OS as 100% ($^{+}$ALT) control. It can be observed from the graph that control hamsters, CHOK-1 and V79 were shown higher ALT activity than DSB deficient hamsters such as xr-1 and xrs-5 lines.

6.4 Effects of ATRX and HDAC9 Knock-down expression using short interfering RNA (siRNA) in Chinese hamster cell lines

We started this chapter by optimizing the siRNA knockdown procedure. Details of the protocol are described in Chapter 2 (Material and methods). We optimised the concentration of siRNA oligonucleotides introduced into cells and quantified the gene expression levels of ATRX and HDAC9 using Taqman real-time qPCR and western blotting. We used GAPDH siRNA as the target gene and quantified GAPDH knockdown gene expression at two separate time points, 48 hours and 72 hours post transfection. As can be seen from Figure 6.4, on average a 90-95% reduction in GAPDH gene expression levels occurred at 48 hours post transfection in two independent experiments.

The lowest level of ATRX was measured 48 hours post-transfection and the percentages of knockdowns were 95% in CHOK-1 and 80% in V79. At 48 hours, HDAC9 showed the lowest levels mRNA expression and the percentages of knockdowns were 95% in CHOK-1 and 80% in V79. Levels of ATRX and HDAC9 showed a slight recovery at 72 hours post-transfection in both, CHOK-1 and V79 cell lines. A scrambled siRNA was used as negative control to shown that the knockdown was not random and was due to degradation of target mRNA (Figure 6.5). To confirm ATRX and HDAC9 knockdowns expression at the protein levels we used western blotting (Figure 6.6 and 6.7) for CHOK-1 and V79 cell lines. Densitometry analysis using ImageJ software showed that there was a reduction of 80% at 48 hours and 60% reduction at 72 hours in ATRX and HDAC9 (Figure 6.6 and 6.7). Taken together, our results show that HDAC9 and ATRX expressions were reduced at 48 hours post-transfection.

siRNA ATRX and HDAC9 knockdown in CHOK-1 cell line

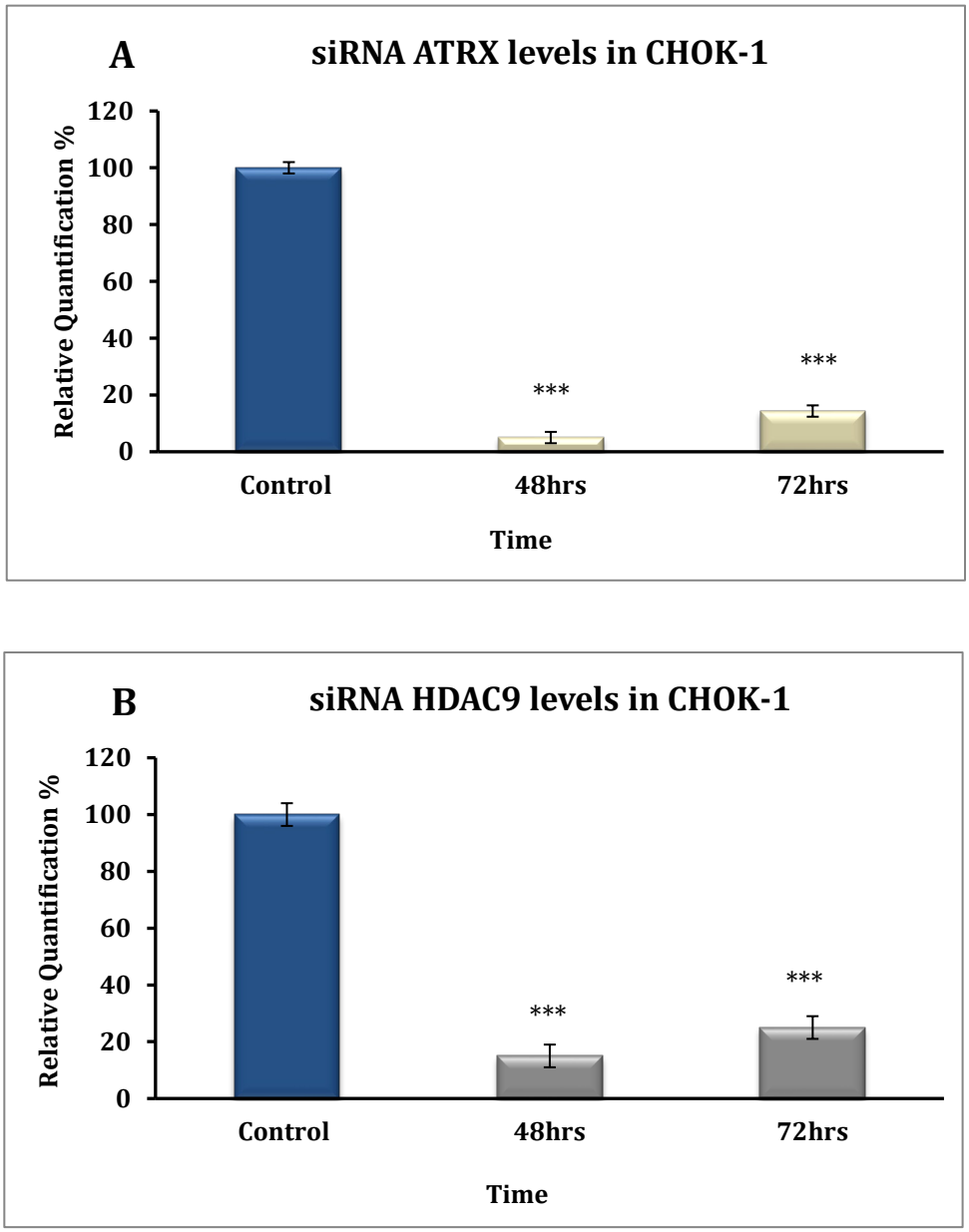

Figure 6.4 Efficient knockdown of mRNA expression of ATRX and HDAC9 genes in CHOK-1 cell line. **A)** ATRX showed a knockdown over >95% in gene expression at 48hrs post-transfection and remained significantly low at 72hrs. **B)** HDAC9 knockdown were achieved at 48hrs >80% efficient and cells began to recover at 72hrs. siRNA gene expression was quantified using Taqman assay and RT-qPRC values plotted as Relative quantities (RQ) in both ATRX and HDAC9 knockdown at different time points, 48hrs and 72 hours post-transfection. Error bars represent SEM. The statistical analysis between untreated vs. treated are significant at 48 hours and 72 hours post-transfection T-test ($p>0.001$***).

siRNA ATRX and HDAC9 knockdown in V79 cell line

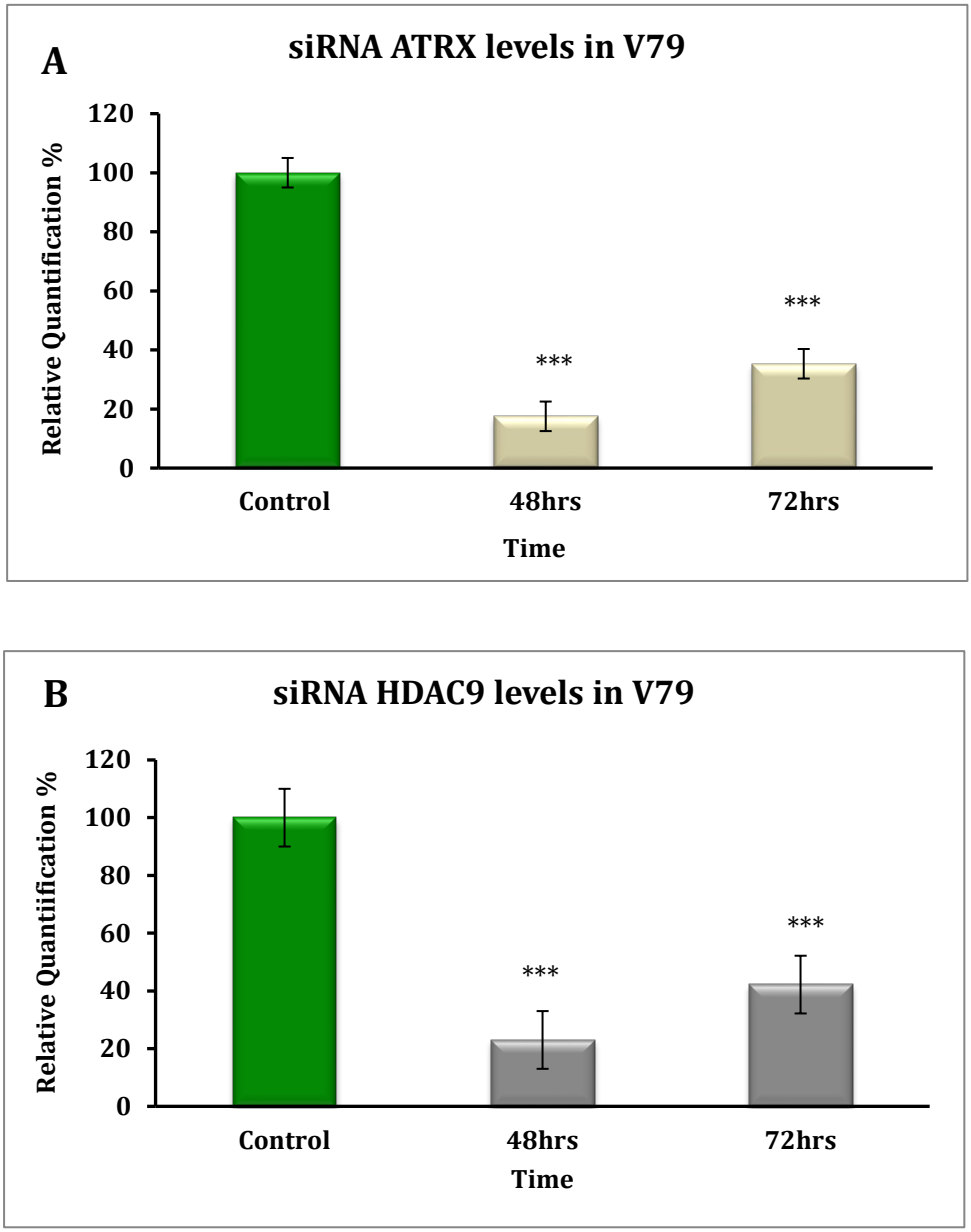

Figure 6.5 Efficient knockdown of mRNA expression of ATRX and HDAC9 genes in V79 cell line. **A)** ATRX mRNA expression over >85% efficient knockdown at 48hrs post-transfection. The expressions were quantified using Taqman assay and RT-qPCR values were expressed as Relative quantities (RQ) percentage. **B)** HDAC9 mRNA efficient knockdown was over >70% at 48hrs and began to recover at 72hrs. Error bars represent SEM. The statistical analysis between untreated vs. treated are significant at 48 hours and 72 hours post-transfection T-test (p>0.001***).

HDAC9 western blot analysis

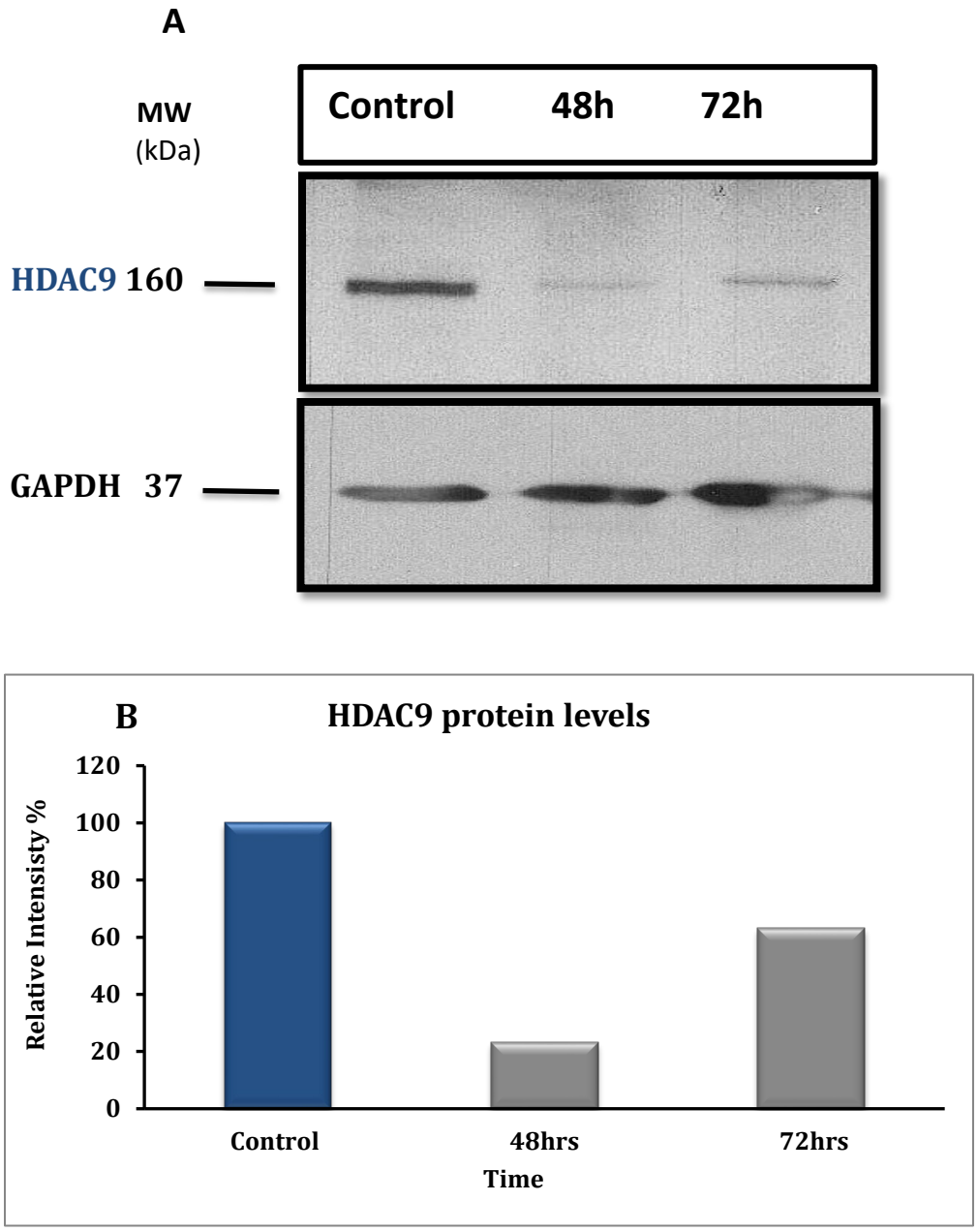

Figure 6.6 Representative image of HDAC9 protein expression by Western blot. **A)** Immunoblot showed a ladder ranging from 350 to 30KDA weight and can be observed protein reduction of HDAC9 at 48hrs and mild increased of protein at 72 hrs. **B)** HDAC9 protein levels were >80% decreased post-transfection at 48hrs but protein began to recover at 72hrs.

ATRX western blot analysis

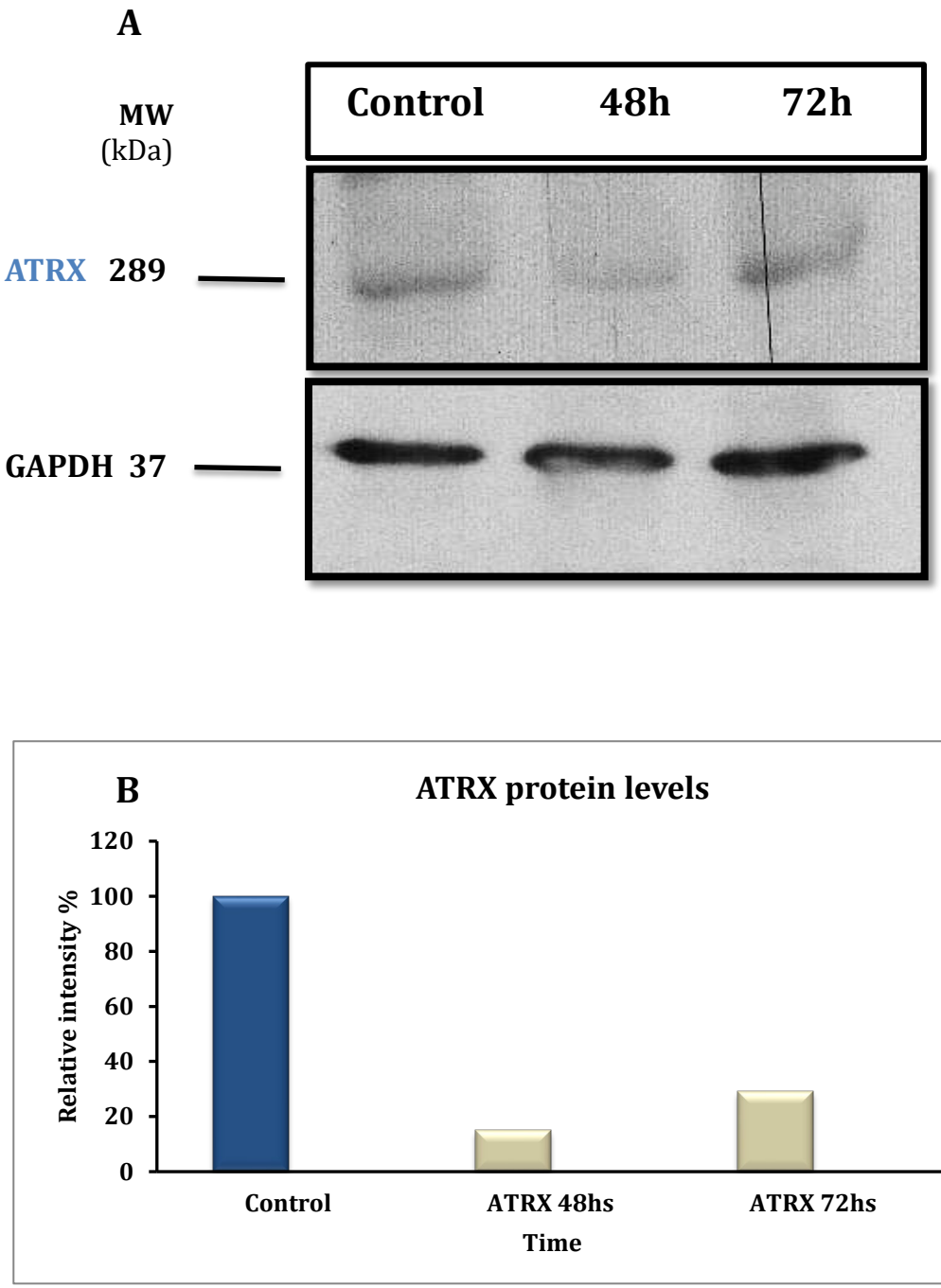

Figure 6.7 Representative image of ATRX protein expression using immunoblot. **A)** ATRX protein showed efficient knockdown at 48hrs and faint band signal at 72 hrs. The molecular weight ladder used was the same used previously for HDCA9 protein. **B)** ATRX protein levels were decreased significantly at 48hrs and remained low at 72hrs.

6.5 Detection of CC activity in Chinese hamster cells post-treatement with ATRX and HDAC9 siRNA

In this study, we analysed 9 Chinese hamster cell lines, including DNA repair proficient cells and NHEJ and HR deficient mutants, and found that all of them express telomerase and ALT simultaneously (Figure 6.1 and Figure 6.2). Given that ATRX is shown to be mutant in most human ALT lines we decide to study this protein in hamster cell lines. We found ATRX positive foci in all Chinese hamster cell lines using immunofluorescence analysis (Figure 6.8).

This prompted us to investigate ATRX in Chinese hamster cells further; given that human ALT cells lack visible ATRX foci (Figure 6.8; (Lovejoy *et al.*, 2012). ATRX is a chromatin remodelling factor, that and forms a dimmer with associated protein DAXX. It also facilitates chromatin assembly and loads histone variant H3.3 at telomeres and pericentromeric chromatin, hence ATRX confers telomere stability (Lewis *et al.*, 2010; Wong *et al.*, 2010; Drane *et al.*, 2010).

To study the relationship between ATRX expression and the ALT activity in Chinese hamster cells. For this purpose, we used siRNA approach and obtained 80% to 90% knockdown efficiency of ATRX. RT-PCR and western blots were used to quantify mRNAs and protein levels in CHOK-1 and V79 cell lines. The results of the CC assay from siRNA ATRX in CHOK-1 showed higher activity of ALT at 48 hours compared to control however at 72 hours, the cells recover too their endogenous levels of ATRX, hence decreased ALT activity. However, V79 did not showed differences between control and treated cells and ALT activity and remains constant throughout 48 hours or 72 hours (Figure 6.9).

Detection of ATRX foci in mammalian cells

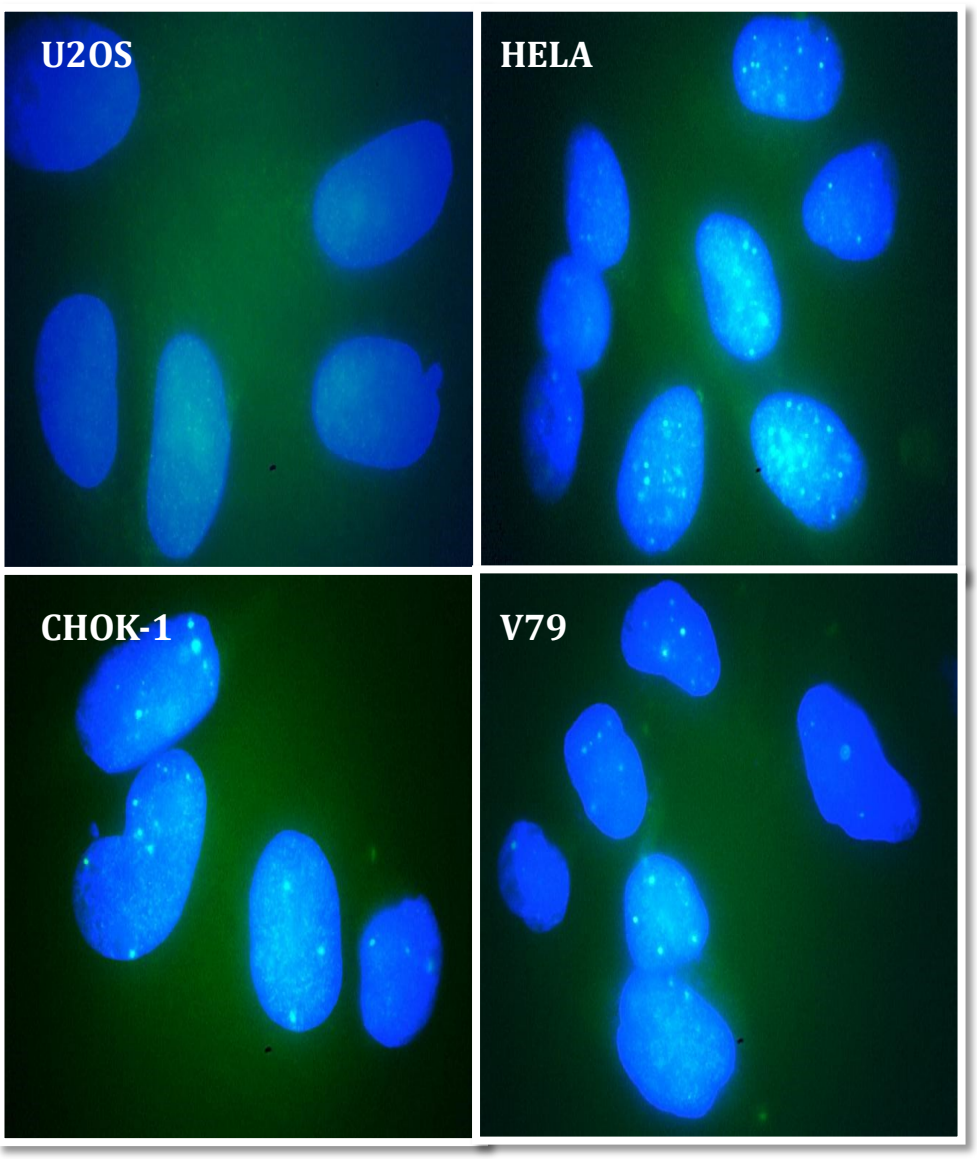

Figure 6.8 Immunofluorescence detection of ATRX in U2OS (ALT+) and HELA (ALT-) and hamster cell lines. ATRX foci are absent in U2OS cell lines while it is present in the telomerase positive tumour cells, HELA. Chinese hamster cells exhibit ATRX positive foci, which is characteristic of their telomerase positive phenotype. It is known that *ATRX* gene mutation is a prerequisite for ALT pathway activation.

ALT activity in siRNA Chinese hamster controls

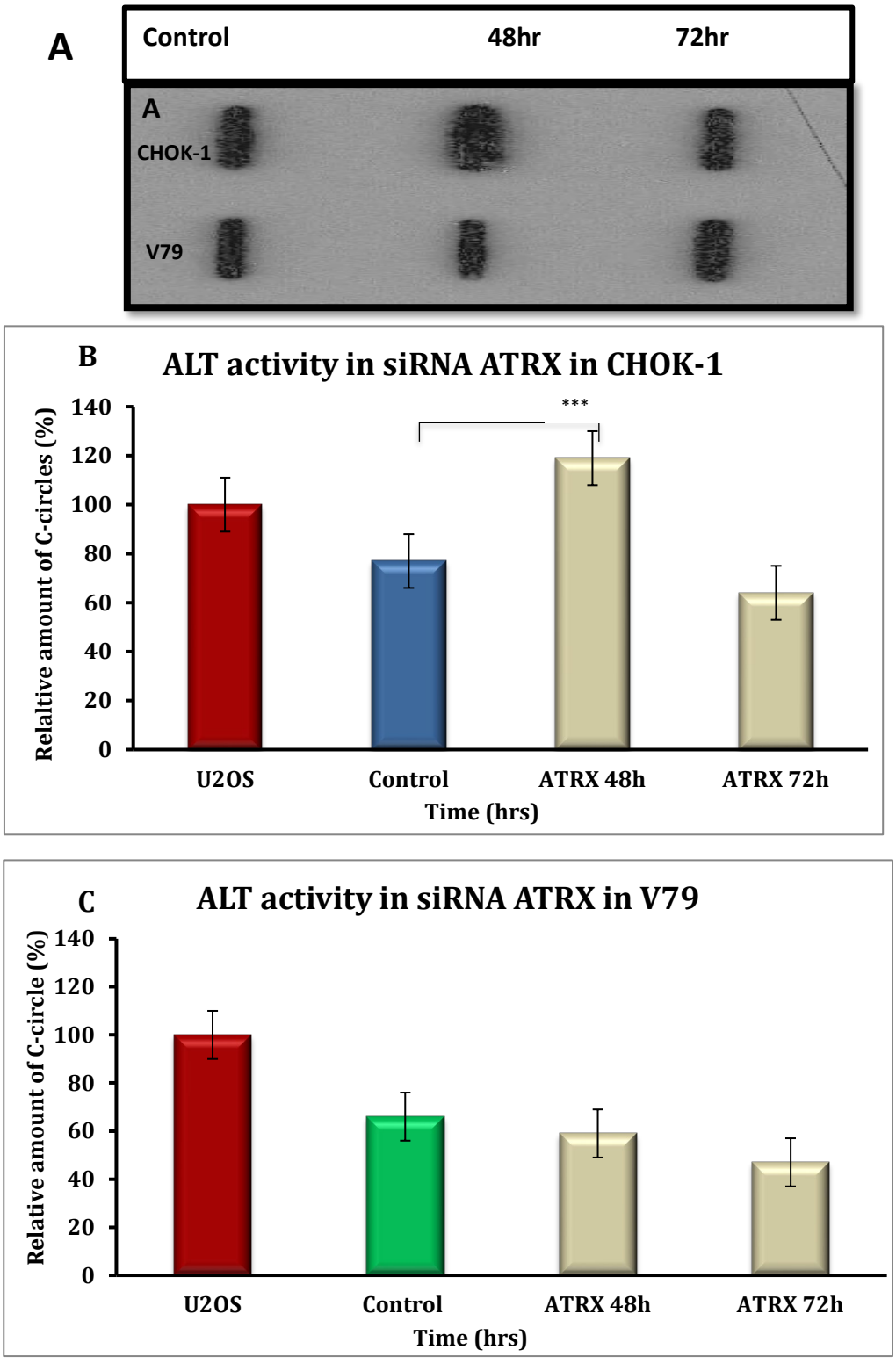

Figure 6.9 C-circle activities of ATRX knockdown in CHOK-1 and V79 cell lines. A) Slot blot using 30ng of CHOK-1 and V79 gDNA. B) siRNA ATRX had effect on ALT activity and increases the activity significantly at 48hr post-transfection but at 72hr activity decreases to control levels in CHOK-1 cells C) ATRX had no effect on C-circle activity at 48hr but slightly effect on activity at 72hr in V79 cells. Error bars represent SEM. The statistical analysis between untreated vs. treated are significant at 48 hours post-transfection T-test ($p>0.01$***).

Interestingly, mutation or loss ATRX correlates with ALT activity particularly in soft tissue sarcomas (Liau *et al.*, 2015). In addition, ALT tumour cell lines such as endocrine tumours and nervous system tumours have mutated ATRX, consistent with the possibility that loss of ATRX is a characteristic of the ALT phenotype (Heaphy *et al.*, 2011; Henson and Reddel, 2010; Henson *et al.*, 2005). The precise molecular mechanism of how ATRX controls ALT pathway remains unclear. However, recent evidences suggest that ATRX loss reduces the time of pre-crisis to immortalization in SV40 transformed fibroblast towards ALT activation (Napier *et al.*, 2015). Furthermore, ATRX loss has been associated with the formation of recombinogenic nucleoprotein structures that included, replication protein A, TERRA and ATR and together favour recombination to maintain telomeres in ALT cells (Flynn *et al.*, 2015). Recently, Clynes et al. (2015) have revealed that ectopic expression of ATRX in U2OS (ALT+ cell line) cells leads to rapid decrease of APBs, T-SCE and C-circles accompanied with telomere shortening and subsequent inhibition of ALT activity. Therefore, these cumulative evidences indicate that ATRX represses ALT mechanism in ALT cell lines.

6.6 Determination of CC assay post siRNA HDAC9 in CHOK-1 and V79 cell lines

In mammalian cells, telomeric chromatin is enriched for constitute heterochromatin marks H3K9me3 and H4K20m3 and low levels of histone acetylation (Schoeftner and Blasco, 2008). Histone deacetylases (HDACs) regulates chromatin formation by removing acetyl group from lysine histones and regulation of gene expression (Ropero and Esteller, 2007). In addition, HDAC5 is recruited to long telomeres in ALT tumour cells, fibrosarcomas, to ensure telomere maintenance, whereas a depletion of HDAC5 leads to short telomeres and homogenous telomere length (Novo *et al.*, 2013). Interestingly, it has been found upregulation of HDAC9 in ALT cell lines and HDAC9 knockdown reduced telomere replicative capacity, therefore HDAC9 regulates ALT activity by APBs formation and increases C-circle in ALT cells (Jamiruddin *et al.*, 2016). For example, HDAC9 is overexpressed in glioblastomas and associated with poor prognosis (Yang *et al.*, 2015).

This prompted us to analyse role of HDAC9 and ALT activity in Chinese hamster cells. For this purpose, we used an HDAC9 siRNA against our hamster cell lines (Figure 6.10). The CC-assay analysis showed ALT activity in both CHOK-1 and V79 at 48 hours and remained activity at 72 hours and not different when compared to controls (Figure 6.10). These findings were unexpected and further suggested that knockdown of HDAC9 has not had any effect on ALT activity in Chinese hamster cells.

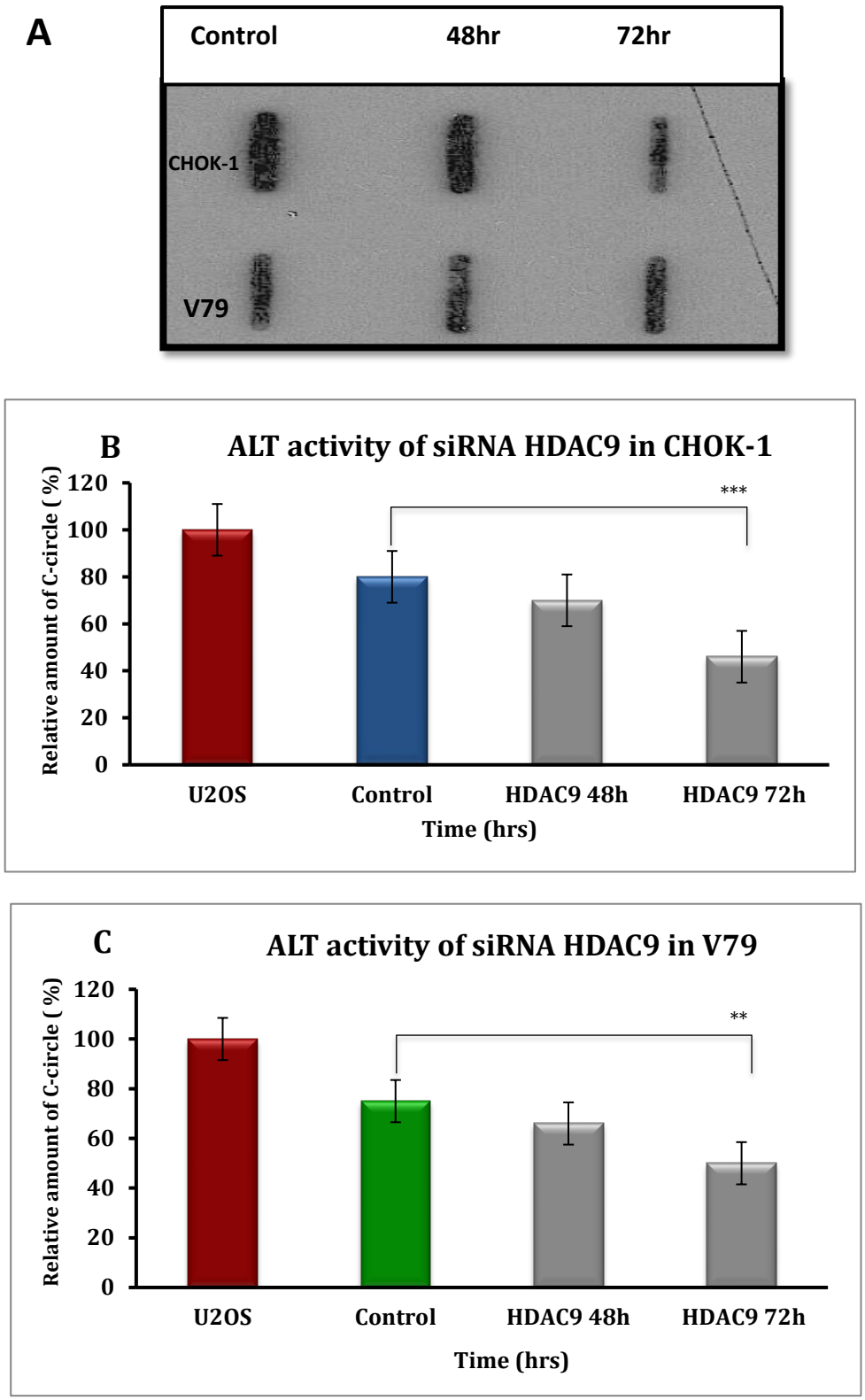

Figure 6.10 C-circle activities of HDAC9 knockdown expression in Chinese hamster cell lines. **A)** Slot blot contained 30ng of CHOK-1 and V79 gDNA post-transfection at 48hrs and 72hrs. **B)** HDAC9 had no effect in C-circle activity at 48hrs but the activity decreased significantly at 72hrs in CHOK-1 cells. **C)** HDAC9 had a mild effect in C-circle activity and levels decreased at 72hrs in V79 cells. Error bars represent SEM. The statistical analysis between untreated vs. treated are significant at 72 hours post-transfection T-test ($p>0.01$**, $p>0.001$***).

6.7 Detection of telomerase activity post siRNA ATRX and HDAC9 in Chinese hamster cell lines

Since above results indicate that ATRX knockdown increases ALT activity and HDAC9 knockdown does not affect ALT activity in Chinese hamster cell lines. We next, wanted to investigate whether knockdown expressions of ATRX and HDAC9 have any effect in telomerase activity. Given that all Chinese hamster cells express telomerase and ALT simultaneously we reasoned that they may affect each other if manipulated.

The TRAP assay revealed that V79 showed a reduction in telomerase activity when ATRX is suppressed (Figure 6.11 A). By contrast, there was no effect in CHO-K1 cells (Figure 6.11 A). Interestingly, the effects were even more pronounced when HDAC9 was suppressed (Figure 6.11 B). These results suggest that CHO-K1 and V79 cells show different responses in telomerase activity when ATRX or HDAC9 proteins are knocked-down. Thus, telomerase and ALT regulation mechanisms may be interrelated. Furthermore, differences between CHO-K1 and V79 cell lines may reflect their tissue origins. Namely, CHOK-1 cells originate from ovaries. By contrast, V79 cells originate from the lung tissue.

Telomerase activity post-siATRX and siHDAC9 in Chinese hamster lines

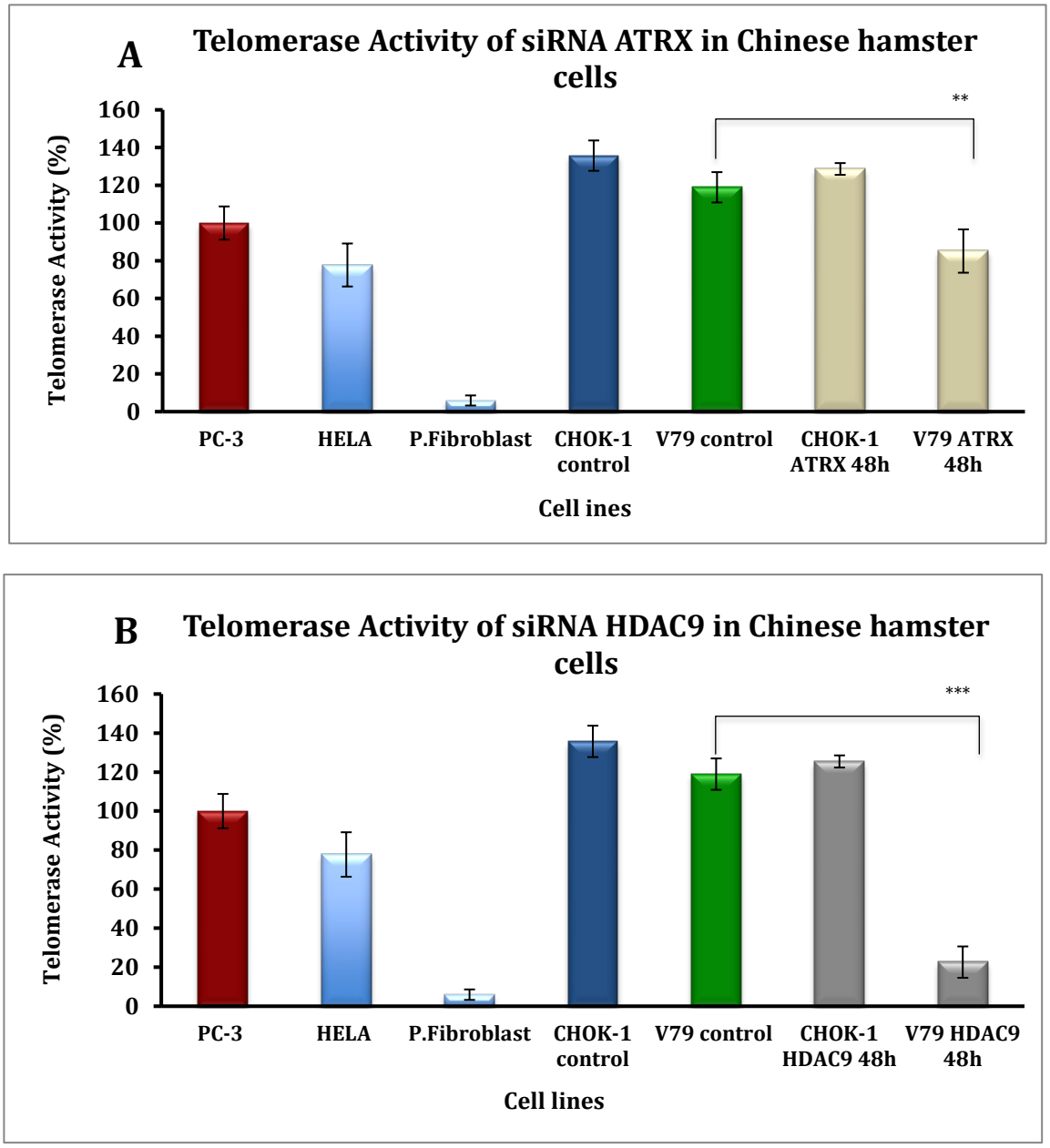

Figure 6.11 TRAP analysis of knockdown siRNA ATRX and HDAC9 in Chinese hamster cell lines. **A)** The siRNA ATRX had no significant effect on the expression of telomerase in CHOK-1 cells, whereas in V79 telomerase activity significantly decreased after ATRX knockdown**. B)** The siRNA HDAC9 caused a significant reduction in telomerase activity in V79 cells and little effect on CHOK-1 cells. Both siRNAs ATRX and HDAC9 were shown significant effects in telomere activity in V79 cells compared with CHOK-1. Error bars represent SEM. The statistical analysis between untreated vs. treated are significant at 72 hours post-transfection T-test (p>0.001***).

γ-H2AX DNA damage response of siRNA ATRX and HDAC9 in Chinese hamster

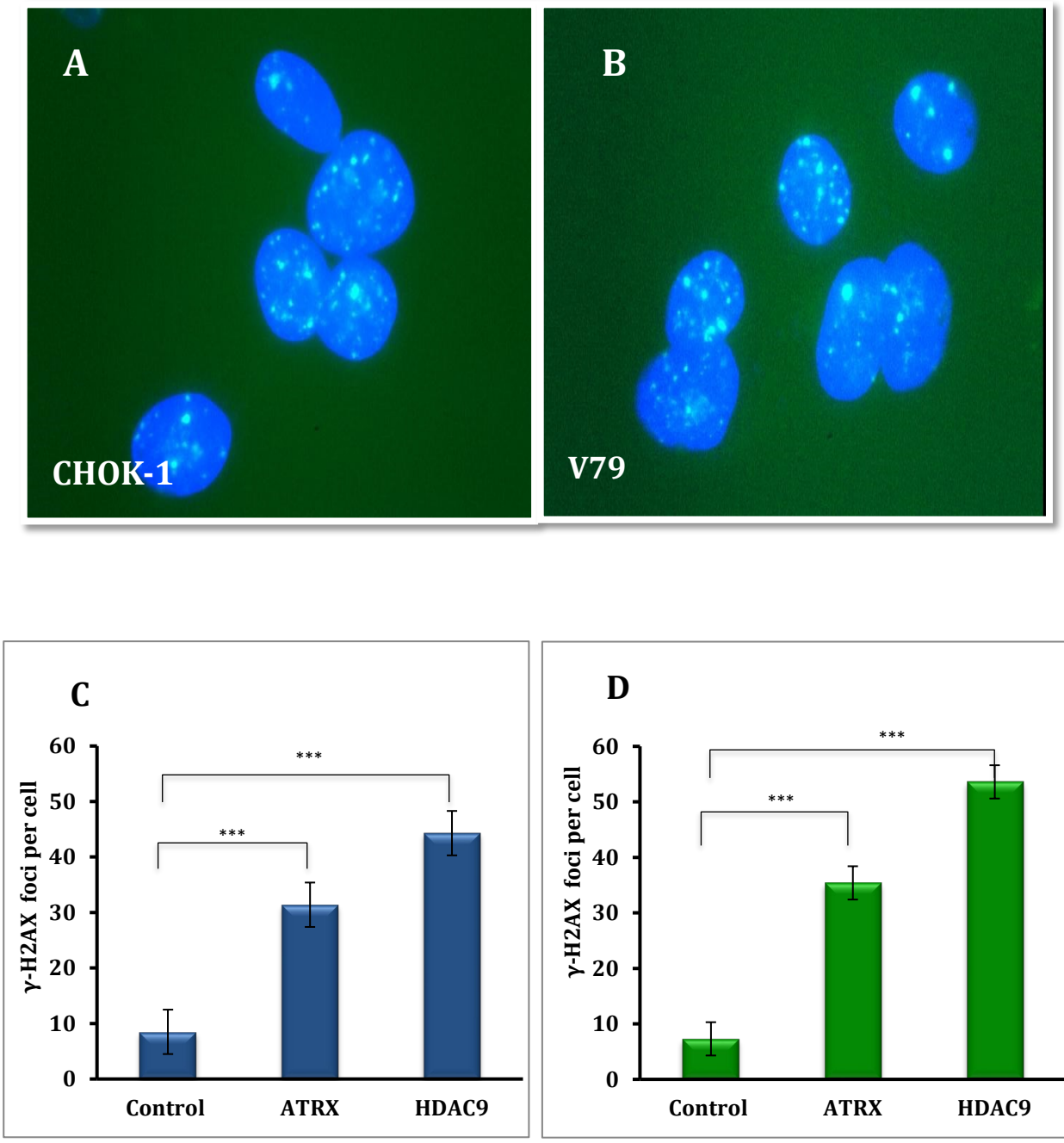

Figure 6.12 Expression of γ-H2AX in knockdown siRNA ATRX and siRNA HDAC9 in Chinese hamster cells. **A)** Representative image of ATRX knockdown and γ-H2AX detection in CHOK-1 line. **B)** Representative image of HDAC9 knockdown resulted in γ-H2AX foci in V79 cell line. **C)** CHOK-1 cells were shown higher frequencies of γ-H2AX foci in knockdown siRNA ATRX and HDAC9. **D)** The γ-H2AX levels were significantly higher in both siRNA ATRX and HDAC9 in V79 cell line. Error bars represent the standard error of the mean. A student t-test was used to compare the untreated and treated.

6.8 Discussion

In this chapter we presented a novel finding. The Chinese hamster cells express ALT activity as telomere maintenance mechanism in parallel with telomerase. The knockdown of ALT related proteins; ATRX and HDAC9 have indeed shown to affect telomerase and ALT activities in Chinese hamster control cells. Supporting for the notion of ALT and telomerase coexistence in mammalian cells have previously been demonstrated by inducing h-TERT ectopic expression in ALT GM847 cells, which lead to telomerase activation and subsequent lengthening of short telomeres (Perrem *et al.*, 2001). These ALT and telomerase positive cells, GM847/hTERT and VA13/hTERT maintain their ALT features such as APBs and heterogeneous telomere length (Cerone, Londono-Vallejo and Bacchetti, 2001). Recently, a human breast cancer study has shown co-expression of both ALT and telomerase mechanisms within the same cells (Xu, Peng and Song, 2014). Moreover, Neumann et al. (2013) have demonstrated that ALT activity occurs in normal mouse somatic cells *in vivo* and telomeres are elongated in dynamic way, telomeres serve as telomeric DNA template, during recombination to copy one telomere to another telomere. Therefore, ALT activity appears as normal component in somatic cells to synthesize new telomeres but is tightly repressed in germline, and the ALT activity becomes upregulated in cancer and immortalized cells *in vitro* (Neumann *et al.*, 2013).

Neumann et al. (2013) findings might allow us to speculate that the coexistence of ALT and telomerase can be extended to all rodents, including hamsters. In fact, ALT may become activated when hamster cells progress from cellular senescence to spontaneously immortalization in Chinese hamster. In notion to coexistence, emerging data from chicken cells have revealed ALT activity and telomerase activity in these cells (O'Hare et al 2011).

One of the aims in this chapter was to established telomerase activity and investigates whether ALT mechanism is active and explores the notion of the coexistence of both mechanisms in Chinese hamster cells. We detected telomerase activity in hamster cells (Figure 6.1), which corresponded with their immortalization process observed in these cells. It is well documented that telomeres in rodent cells are long and also expressed telomerase activity throughout their proliferative lifespan (Serrano and Blasco, 2001; Newbold, 1997).

We next wanted to use a robust and sensitive technique, CC-assay to detect ALT activity in hamster cells. The CC-assay showed strong activity in control cells compared to deficient hamster cells (Figure 6.3). The slot blot bands intensity is proportional to ALT activity in hamster cells. Controls cell lines; CHOK-1 and V79 exhibited strong ALT activity 80% and 70%, respectively (Figure 6.3). These findings were unexpected in hamster cell lines since their telomere lengths are not heterogeneous. In contrast to canonical ALT cells, Chinese hamster cells telomeres length are homogeneously between 1kb.

Supporting the notion of *ATRX* gene supressing ALT activity in ALT cell lines. Theoretically, mutations in ATRX reduce the cellular crisis and facilitate immortalization in fibroblast (Lovejoy *et al.*, 2012). Interestingly, transient ATRX expression repressed ALT mechanism followed by subsequent decreased of APBs and C-circle levels (Napier *et al.*, 2015). To study whether ATRX is present in Chinese hamster cells and from our immunofluorescence results we observed ATRX positive foci in the nuclei (Figure 6.8). Therefore, we reasoned that ATRX knockdown may have altered telomerase and ALT activity in the cells and we achieved 80% to 90% siRNA knockdown expression in hamster cells (Figure 6.4 and Figure 6.5). As expected, ATRX knockdown evidenced that CHOK-1 cell lines showed increased ALT activity

at 48 hours compared to untreated. On the other hand, V79 cell lines did not shown changes in ALT activity (Figure 6.9). Surprisingly, however, no significant changes in telomerase activity in ATRX knockdown in CHOK-1, while moderate reduction was observed in V79 cell line (Figure 6.11).

Recently, it has been shown that HDAC9 inhibits ALT pathway through the APBs formation in U2OS ALT cell line (Jamiruddin *et al.*, 2016), and increased glioblastomas tumours are associated with upregulation of HDAC9 (Yang *et al.*, 2015). HDAC9 knockdown in Chinese hamster cells indicated that ALT activity was not significantly decreased or abolish in hamster cells. There were no significant differences of ALT between cells lines (Figure 6.10). However, we observed a significant change in telomerase activity in V79 HDAC9 knockdown. In contrast to V79, CHOK-1 did not show changes in telomerase activity either in ATRX or HDCA9 knockdowns (Figure 6.11). Interestingly, our observed differences between the levels of telomerase in CHOK-1 and V79 might be associated with telomerase activity being tissue specific. For instance, elevated levels of hTERT in human breast cancer cells are linked to chromosome 3, while prostate cancer is associated to chromosome 11 (H. Linne et al 2017).

It has been reported in mES that ATRX mutation reduced telomere dysfunction by reducing the levels of HP1 at telomeres and chromosome aberrations including, micronuclei and chromatin bridges as well as high levels of γ-H2AX damage at chromosome ends (Lovejoy *et al.*, 2012; Wong *et al.*, 2010; Goldberg *et al.*, 2010).

Chinese hamster cells appear to have functional and detectable levels of ATRX and the subsequent ATRX knockdown may induce the high levels of DSB DNA damage detected by

H2AX (Figure 6.12). A study has suggested that telomerase cancer cells can switch to ALT pathway in specific environments that include, telomeric DNA damage, mutation ATRX/DAXX and telomerase inhibition (Hu *et al.*, 2016).

Taken together our results suggested that Chinese hamster cells express both, telomerase and ALT activity to detectable levels. At this stage one can only speculate that Chinese hamster cells express ALT to maintain telomeres since telomerase has other functions beside telomere maintenance. It is known that Chinese hamster cells contain long arrays of ITSs estimated at 5% of their genome and these regions are prone to spontaneous and IR DBS breakages. It has been shown that telomerase is able to repair DSBs at regions containing ITSs, thereby healed and stabilized chromosomes (Bryant, Peter, 1998; Meltzer, Guan and Trent, 1993).

In regards to ALT related proteins, ATRX and HDAC9 may favour the balance of both mechanisms in the maintenance of telomeres in hamster cells by relaxing and making chromatin accessible to DNA repair and recombination by proteins such as, Rad52. The status of telomeric chromatin is ALT decondensed and reduced nucleosome density, which facilitates HR telomere maintenance at telomeres (Episkopou *et al.*, 2014). Future molecular work is required to demonstrate the role of ALT in telomere maintenance in Chinese hamster cells.

Chapter 7.

General Discussion

The work presented in this thesis aimed to examine DNA damage and repair kinetics at ITSs in Chinese hamster cells in novel ways and identify potential mechanisms behind sensitivity of ITSs to damage.

Our results generated three novel findings. Firstly, DNA damage induced by IR at the ITSs shows competent repair in DNA repair proficient Chinese hamster cell lines and a slow kinetics of repair in DNA repair deficient Chinese hamster cell lines. Secondly, all Chinese hamster cell lines, including DSB repair mutants, exhibit ALT activity but retain telomerase phenotype features. Thirdly, knockdown of ATRX increases ALT activity in the CHOK-1 cell line, whereas the knockdown of HDAC9 decreases telomerase activity in the V79 cell line. These findings are briefly summarized below.

7.1 DNA damage at telomeres and ITSs

Telomere loss causes natural chromosome ends to be recognized by DNA damage response checkpoints and repair proteins as DSB lesions requiring repair. It is clear from numerous studies that DNA damage response proteins are involved in telomere maintenance (Lewandowska and Szumiel, 2002; Smogorzewska *et al.*, 2000). Thus, an unbalance in DNA damage response proteins, as a result of telomere shortening (e.g. due to ageing) may lead to telomere dysfunction and chromosomal instability. It is puzzling why telomeres try to prevent DNA damage, activation in most cells, but at the same times attracts a wide range of signalling and DNA repair proteins. A model called “integrative model” has been proposed which argues in favour of telomere maintenance being an integral part of DNA damage response machinery (Slijepcevic, 2006).

The interaction between ITSs, telomeric sequences present at interstitial genomic sites, and canonical telomeres occurs through interstitial telomere loops (ITLs). In this process, one of the shelterin components, TRF2, interacts with lamin A/C a nuclear matrix protein involved in organismal aging, gene expression and genome stability (Wood *et al.*, 2014). ITSs do not associate with the nuclear matrix directly (Balajee *et al.*, 1996). These ITSs share some shelterin components with telomeres, including TRF1, TRF2 and more recently RAP1 has been detected as an interacting partner, which suggest that telomere binding proteins may protect and stabilize het-ITSs in Chinese hamster cells (Bosco and de Lange, 2012; Krutilina *et al.*, 2003). The ITSs in Chinese hamster represent the main satellite DNA and may arise because of amplification of telomeric repeats during speciation of the Chinese hamster (Faravelli *et al.*, 2002).

The relevance of ITSs in genome instability has been demonstrated by several cytogenetic studies. These studies showed that ITSs acts as hot spots for breakage, amplification, rearrangement, and recombination in Chinese hamster cells (Mosquera *et al.*, 2005; Slijepcevic *et al.*, 1996; Fernández, Gosálvez and Goyanes, 1995).

Our FISH and immunocytochemistry results suggest that ITSs are hypersensitive to IR induced damage (Figures 3.3) in line with previous studies (Fernández, Gosálvez and Goyanes, 1995; Alvarez *et al.*, 1993). Furthermore, we analysed for the first-time damage induction and repair kinetics at ITSs using the TIF assay. Surprisingly, our results show repair proficiency of ITSs in contrast to earlier studies, which suggested that telomeric sequences are essentially irreparable (Fumagalli *et al.*, 2012). However, we cannot rule out the possibility that ITSs in the Chinese hamster genome are interspersed with degenerate sequences, which are reparable per se, and as a result the entire region (i.e. ITS) appear repair proficient. However, it is important to stress that the residual damage at ITSs is still higher than at other genomic locations. This is in line with ITSs being hypersensitive to IR induced damage.

The exact mechanism of DNA repair within ITSs is unknown. We assume that in DNA repair proficient Chinese hamster cell lines, in which the two major DNA repair mechanisms convey and repair the DNA damage. Therefore, the disappearances of DNA damage (H2AX and TIFs foci) from interphase cells correlate with the rejoining and sealing of the broken ends within the ITSs. However, deficient DNA repair cell lines show high levels of DNA DSB within ITSs compared to their control counterparts but they exhibit moderate DSB repair kinetics around 3 hours and 4-hours post-radiation. We can speculate that the repair mechanism within ITSs would be enhanced or repressed by shelterin proteins, TRF1, TRF2 and RAP1 that are presented at ITS in Chinese hamster cells. TRF1 and TRF2 protect and stabilize these hotspot regions from spontaneous CAs (Krutilina *et al.*, 2003; Krutilina *et al.*, 2001).

In the human genome, there are 19 ITSs that coincide with fragile sites in the same chromosome (Ruiz-Herrera *et al.*, 2008). In addition, ITSs have also been associated with end-point of gross chromosomal rearrangements (GCRs) as a result of high levels of recombinational activity within these ITSs (Aksenova *et al.*, 2013). In addition, there are over 100 short ITSs in the human genome that and do not behave as hotspot for spontaneous breakage. However, there are small numbers of human tumours, gastric and colon, associated with ITSs and ITSs are involved in mosaicism (Levy et al., 2014). Therefore, ITSs are relevant from the human disease point of view because they constitute a potential source of genomic instability.

7.2 Telomerase and ALT activity

We detected telomerase activity in all Chinese hamster cell lines (Figure 6.1). It is also known that telomerase can heal and stabilize broken chromosomes. It is therefore tempting to speculate, since ITSs are prone to breakage, they can serve as a substrate for telomerase to add telomeric DNA in order heal the broken ends. If telomerase is exhausted during chromosome healing, there must be another mechanism to compensate for this, suggesting that ALT could act as a replacement. Our results based on the C-circle assay show ALT activity in all Chinese hamster lines examined (Chapter 6.3), and we speculate that ALT and telomerase mechanism may coexist in the same cells for this purpose. This notion is supported by Neumann et al. (2013) who that ALT activity occurs in normal mouse somatic cells *in vivo,* and suggested that ALT activity appears as normal component of telomere maintenance in mouse somatic cells.

We targeted ALT-related proteins that would upregulated and downregulate ALT activity in mammalian cells. Our results showed that the ATRX knockdown upregulated ALT activity in CHOK-1 cell line, whereas there was no HDAC9 effect on ALT activity (Figures 6.9 and Figure 6.10). However, unexpectedly, the HDAC9 knockdown had a strong effect on telomerase activity in V79 (Figure 6.11).

7.3 Future Work

Effects of ATRX and HDAC9 knock-down on ALT and telomerase activity are novel and not previously observed in Chinese hamster cells. Future studies should identify exact mechanisms behind these effects. For example, simultaneous knock-down of telomerase components (TERC or TERT) in cells with ATRX and HDAC9 knockdowns should allow to conclude whether ALT and telomerase cooperate during telomere maintenance in Chinese hamster cells. Furthermore, we have not employed phenotypic assays (TIF, cytogenetics and immunocytochemistry) with a sufficient degree in this study. Thus, future studies should aim to employ a wide range of phenotypic studies to examine effects of knock-down on ITSs repair kinetics and by doing this further elucidate mechanisms behind ITSs sensitivity to breakage.

REFERENCES

Aksenova, A.Y., Greenwell, P.W., Dominska, M., Shishkin, A.A., Kim, J.C., Petes, T.D. and Mirkin, S.M. (2013) 'Genome rearrangements caused by interstitial telomeric sequences in yeast', *Proceedings of the National Academy of Sciences of the United States of America,* 110(49), pp. 19866-19871.

Allshire, R.C., Gosden, J.R., Cross, S.H., Cranston, G., Rout, D., Sugawara, N., Szostak, J.W., Fantes, P.A. and Hastie, N.D. (1988) 'Telomeric repeat from T. thermophila cross hybridizes with human telomeres', *Nature,* 332(6165), pp. 656.

Alvarez, L., Evans, J.W., Wilks, R., Lucas, J.N., Brown, J.M. and Giaccia, A.J. (1993) 'Chromosomal radiosensitivity at intrachromosomal telomeric sites', *Genes, Chromosomes and Cancer,* 8(1), pp. 8-14.

Ashley, T. and Ward, D. (1993) 'A "hot spot" of recombination coincides with an interstitial telomeric sequence in the Armenian hamster', *Cytogenetic and Genome Research,* 62(2-3), pp. 169-171.

Azzalin, C.M., Nergadze, S.G. and Giulotto, E. (2001) 'Human intrachromosomal telomeric-like repeats: sequence organization and mechanisms of origin', *Chromosoma,* 110(2), pp. 75-82.

Azzalin, C.M., Mucciolo, E., Bertoni, L. and Giulotto, E. (1997) 'Fluorescence in situ hybridization with a synthetic (T2AG3)n polynucleotide detects several intrachromosomal telomere-like repeats on human chromosomes', *Cytogenetics and cell genetics,* 78(2), pp. 112.

Bae, N.S. and Baumann, P. (2007) 'A RAP1/TRF2 complex inhibits nonhomologous end-joining at human telomeric DNA ends', *Molecular cell,* 26(3), pp. 323-334.

Bagheri, S., Nosrati, M., Li, S., Fong, S., Torabian, S., Rangel, J., Moore, D.H., Federman, S., Laposa, R.R., Baehner, F.L., Sagebiel, R.W., Cleaver, J.E., Haqq, C., Debs, R.J., Blackburn, E.H. and Kashani-Sabet, M. (2006) 'Genes and pathways downstream of telomerase in melanoma metastasis', *Proceedings of the National Academy of Sciences of the United States of America,* 103(30), pp. 11306-11311.

Bailey, S.M., Brenneman, M.A. and Goodwin, E.H. (2004) 'Frequent recombination in telomeric DNA may extend the proliferative life of telomerase-negative cells', *Nucleic acids research,* 32(12), pp. 3743-3751.

Bailey, S.M., Cornforth, M.N., Kurimasa, A., Chen, D.J. and Goodwin, E.H. (2001) 'Strand-specific postreplicative processing of mammalian telomeres', *Science (New York, N.Y.),* 293(5539), pp. 2462-2465.

Baker, A.M., Fu, Q., Hayward, W., Victoria, S., Pedroso, I.M., Lindsay, S.M. and Fletcher, T.M. (2011) 'The telomere binding protein TRF2 induces chromatin compaction', *PloS one,* 6(4), pp. e19124.

Balajee, A., Dominguez, I., Bohr, V. and Natarajan, A. (1996) 'Immunofluorescent analysis of the organization of telomeric DNA sequences and their involvement in chromosomal aberrations in hamster cells', *Mutation Research/Fundamental and Molecular Mechanisms of Mutagenesis,* 372(2), pp. 163-172.

Balajee, A., Oh, H. and Natarajan, A. (1994) 'Analysis of restriction enzymeinduced chromosome aberrations in the interstitial telomeric repeat sequences of CHO and CHE cells by FISH', *Mutation Research/Fundamental and Molecular Mechanisms of Mutagenesis,* 307(1), pp. 307-313.

Balakin, A.G., Smith, L. and Fournier, M.J. (1996) 'The RNA world of the nucleolus: two major families of small RNAs defined by different box elements with related functions', *Cell,* 86(5), pp. 823-834.

Bender, M.A., Griggs, H.G. and Bedford, J.S. (1974) 'Mechanisms of chromosomal aberration production III. Chemicals and ionizing radiation', *Mutation Research/Fundamental and Molecular Mechanisms of Mutagenesis,* 23(2), pp. 197-212.

Bennardo, N., Cheng, A., Huang, N. and Stark, J.M. (2008) 'Alternative-NHEJ is a mechanistically distinct pathway of mammalian chromosome break repair', *PLoS genetics,* 4(6), pp. e1000110.

Bertoni, L., Attolini, C., Faravelli, M., Simi, S. and Giulotto, E. (1996) 'Intrachromosomal telomere-like DNA sequences in Chinese hamster', *Mammalian Genome,* 7(11), pp. 853-855.

Bertoni, L., Attolini, C., Tessera, L., Mucciolo, E. and Giulotto, E. (1994) 'Telomeric and nontelomeric (TTAGGG) n sequences in gene amplification and chromosome stability', *Genomics,* 24(1), pp. 53-62.

Bessler, M., Wilson, D.B. and Mason, P.J. (2004) 'Dyskeratosis congenita and telomerase', *Current opinion in pediatrics,* 16(1), pp. 23-28.

Bird, A.W., David, Y.Y., Pray-Grant, M.G., Qiu, Q., Harmon, K.E., Megee, P.C., Grant, P.A., Smith, M.M. and Christman, M.F. (2002) 'Acetylation of histone H4 by Esa1 is required for DNA double-strand break repair', *Nature,* 419(6905), pp. 411.

Bishop, D.K., Ear, U., Bhattacharyya, A., Calderone, C., Beckett, M., Weichselbaum, R.R. and Shinohara, A. (1998) 'Xrcc3 is required for assembly of Rad51 complexes in vivo', *The Journal of biological chemistry,* 273(34), pp. 2148221488.

Blackburn, E.H. (2001) 'Switching and signaling at the telomere', *Cell,* 106(6), pp. 661-673.

Blackburn, E.H. (1991) 'Structure and function of telomeres', *Nature,* 350(6319), pp. 569-573.

Blasco, M.A., Lee, H., Hande, M.P., Samper, E., Lansdorp, P.M., DePinho, R.A. and Greider, C.W. (1997) 'Telomere shortening and tumor formation by mouse cells lacking telomerase RNA', *Cell,* 91(1), pp. 25-34.

Bolzán, A.D., Páez, G.L. and Bianchi, M.S. (2001) 'FISH analysis of telomeric repeat sequences and their involvement in chromosomal aberrations induced by radiomimetic compounds in hamster cells', *Mutation Research/Fundamental and Molecular Mechanisms of Mutagenesis,* 479(1), pp. 187-196.

Borden, K.L. (2002) 'Pondering the promyelocytic leukemia protein (PML) puzzle: possible functions for PML nuclear bodies', *Molecular and cellular biology,* 22(15), pp. 5259-5269.

Bosco, N. and de Lange, T. (2012) 'A TRF1-controlled common fragile site containing interstitial telomeric sequences', *Chromosoma,* 121(5), pp. 465474.

Bouffler, S. (1998) 'Involvement of telomeric sequences in chromosomal aberrations', *Mutation Research/Fundamental and Molecular Mechanisms of Mutagenesis,* 404(1), pp. 199-204.

Bouffler, S., Silver, A., Papworth, D., Coates, J. and Cox, R. (1993) 'Murine radiation myeloid leukaemogenesis: Relationship between interstitial telomere-like sequences and chromosome 2 fragile sites', *Genes, Chromosomes and Cancer,* 6(2), pp. 98-106.

Boulton, S.J. and Jackson, S.P. (1996) 'Identification of a Saccharomyces cerevisiae Ku80 homologue: roles in DNA double strand break rejoining and in telomeric maintenance', *Nucleic acids research,* 24(23), pp. 4639-4648.

Bryan, T. and Reddel, R. (1997) 'Telomere dynamics and telomerase activity in in vitro immortalised human cells', *European journal of cancer,* 33(5), pp. 767773.

Bryan, T.M., Englezou, A., Dalla-Pozza, L., Dunham, M.A. and Reddel, R.R. (1997) 'Evidence for an alternative mechanism for maintaining telomere length in human tumors and tumor-derived cell lines', *Nature medicine,* 3(11), pp. 1271.

Bryan, T.M., Englezou, A., Gupta, J., Bacchetti, S. and Reddel, R.R. (1995) 'Telomere elongation in immortal human cells without detectable telomerase activity.', *The EMBO journal,* 14(17), pp. 4240-4248.

Bryant, P.S.P. (1998) 'Review Chromosome healing, telomere capture and mechanisms of radiation-induced chromosome breakage', *International journal of radiation biology,* 73(1), pp. 1-13.

Bryant, P. (1985) 'Enzymatic restriction of mammalian cell DNA: evidence for double-strand breaks as potentially lethal lesions', *International Journal of Radiation Biology and Related Studies in Physics, Chemistry and Medicine,* 48(1), pp. 55-60.

Bryant, P.E. (2004) 'Repair and chromosomal damage', *Radiotherapy and oncology,* 72(3), pp. 251-256.

Bryant, P.E. (1998) 'Mechanisms of radiation-induced chromatid breaks', *Mutation Research/Fundamental and Molecular Mechanisms of Mutagenesis,* 404(1), pp. 107-111.

Bryant, P.E., Mozdarani, H. and Marr, C. (2008) 'G2-phase chromatid break kinetics in irradiated DNA repair mutant hamster cell lines using calyculininduced PCC and colcemid-block', *Mutation Research/Genetic Toxicology and Environmental Mutagenesis,* 657(1), pp. 8-12.

Bryant, P.E., Riches, A.C. and Terry, S.Y. (2010) 'Mechanisms of the formation of radiation-induced chromosomal aberrations', *Mutation Research/Genetic Toxicology and Environmental Mutagenesis,* 701(1), pp. 23-26.

Bugreev, D.V., Yu, X., Egelman, E.H. and Mazin, A.V. (2007) 'Novel pro- and antirecombination activities of the Bloom's syndrome helicase', *Genes & development,* 21(23), pp. 3085-3094.

Callén, E. and Surrallés, J. (2004) 'Telomere dysfunction in genome instability syndromes', *Mutation Research/Reviews in Mutation Research,* 567(1), pp. 85-104.

Camps, J., Grade, M., Nguyen, Q.T., Hormann, P., Becker, S., Hummon, A.B., Rodriguez, V., Chandrasekharappa, S., Chen, Y., Difilippantonio, M.J., Becker, H., Ghadimi, B.M. and Ried, T. (2008) 'Chromosomal breakpoints in primary colon cancer cluster at sites of structural variants in the genome', *Cancer research,* 68(5), pp. 1284-1295.

Carman, T., Afshari, C. and Barrett, J. (1998) 'Cellular senescence in telomeraseexpressing Syrian hamster embryo cells', *Experimental cell research,* 244(1), pp. 33-42.

Celeste, A., Petersen, S., Romanienko, P.J., Fernandez-Capetillo, O., Chen, H.T., Sedelnikova, O.A., Reina-San-Martin, B., Coppola, V., Meffre, E., Difilippantonio,

M.J., Redon, C., Pilch, D.R., Olaru, A., Eckhaus, M., CameriniOtero, R.D., Tessarollo, L., Livak, F., Manova, K., Bonner, W.M., Nussenzweig, M.C. andNussenzweig, A. (2002) 'Genomic instability in mice lacking histone H2AX', *Science (New York, N.Y.),* 296(5569), pp. 922-927.

Cerone, M.A., Londono-Vallejo, J.A. and Bacchetti, S. (2001) 'Telomere maintenance by telomerase and by recombination can coexist in human cells', *Human molecular genetics,* 10(18), pp. 1945-1952.

Cesare, A.J. and Reddel, R.R. (2010) 'Alternative lengthening of telomeres: models, mechanisms and implications', *Nature reviews genetics,* 11(5), pp. 319.

Cesare, A.J. and Griffith, J.D. (2004) 'Telomeric DNA in ALT cells is characterized by free telomeric circles and heterogeneous t-loops', *Molecular and cellular biology,* 24(22), pp. 9948-9957.

Chapman, J.R., Taylor, M.R. and Boulton, S.J. (2012) 'Playing the end game: DNA double-strand break repair pathway choice', *Molecular cell,* 47(4), pp. 497510.

Chen, J., Blasco, M.A. and Greider, C.W. (2000) 'Secondary structure of vertebrate telomerase RNA', *Cell,* 100(5), pp. 503-514.

Chen, L.Y., Liu, D. and Songyang, Z. (2007) 'Telomere maintenance through spatial control of telomeric proteins', *Molecular and cellular biology,* 27(16), pp. 5898-5909.

Chiang, Y.J., Kim, S.H., Tessarollo, L., Campisi, J. and Hodes, R.J. (2004) 'Telomereassociated protein TIN2 is essential for early embryonic development through a telomerase-independent pathway', *Molecular and cellular biology,* 24(15), pp. 6631-6634.

Christmann, M., Tomicic, M.T., Roos, W.P. and Kaina, B. (2003) 'Mechanisms of human DNA repair: an update', *Toxicology,* 193(1), pp. 3-34.

Cleaver, J. (1968) 'Defective repair replication of DNA in xeroderma pigmentosum', *Nature,* 218(5142), pp. 652.

Colgin, L.M., Baran, K., Baumann, P., Cech, T.R. and Reddel, R.R. (2003) 'Human POT1 facilitates telomere elongation by telomerase', *Current biology,* 13(11), pp. 942-946.

Counter, C.M., Avilion, A.A., LeFeuvre, C.E., Stewart, N.G., Greider, C.W., Harley, C.B. and Bacchetti, S. (1992) 'Telomere shortening associated with chromosome instability is arrested in immortal cells which express telomerase activity.', *The EMBO journal,* 11(5), pp. 1921-1929.

Crick, F.H. and Watson, J.D. (1954) 'The complementary structure of deoxyribonucleic acid', *Proceedings of the Royal Society of London.Series A.Mathematical and Physical Sciences,* 223(1152), pp. 80-96.

d'Adda di Fagagna, F., Reaper, P., Clay-Farrace, L., Fiegler, H., Carr, P., Von Zglinicki, T., Saretzki, G., Carter, N. and Jackson, S. (2003) 'A DNA damage checkpoint response in telomere-initiated senescence.', *Nature,* 426(6963), pp. 194-198.

Darroudi, F., Natarajan, A., Van Der Schans, G. and Van Loon, A. (1990) 'Biochemical and cytogenetical characterization of Chinese hamster ovary Xray-sensitive mutant cells xrs 5 and xrs 6 V. The correlation of DNA strand breaks and base damage to chromosomal aberrations and sister-chromatid exchanges induced by X-irradiation', *Mutation Research/DNA Repair,* 235(2), pp. 119-127.

Day, J.P., Limoli, C.L. and Morgan, W.F. (1998) 'Recombination involving interstitial telomere repeat-like sequences promotes chromosomal instability in Chinese hamster cells', *Carcinogenesis,* 19(2), pp. 259-265.

de Lange, T. (2002) 'Protection of mammalian telomeres', *Oncogene,* 21(4), pp. 532.

de Lange, T. (2009) 'How telomeres solve the end-protection problem', *Science (New York, N.Y.),* 326(5955), pp. 948-952.

de Lange, T. (2005) 'Shelterin: the protein complex that shapes and safeguards human telomeres', *Genes & development,* 19(18), pp. 2100-2110.

De Vos, M., Schreiber, V. and Dantzer, F. (2012) 'The diverse roles and clinical relevance of PARPs in DNA damage repair: current state of the art', *Biochemical pharmacology,* 84(2), pp. 137-146.

Deans, B., Griffin, C.S., O'Regan, P., Jasin, M. and Thacker, J. (2003) 'Homologous recombination deficiency leads to profound genetic instability in cells derived from Xrcc2-knockout mice', *Cancer research,* 63(23), pp. 8181-8187.

Dellaire, G., Kepkay, R. and Bazett-Jones, D.P. (2009) 'High resolution imaging of changes in the structure and spatial organization of chromatin, γ-H2A. X and the MRN complex within etoposide-induced DNA repair foci', *Cell Cycle,* 8(22), pp. 3750-3769.

Desmaze, C., Pirzio, L.M., Blaise, R., Mondello, C., Giulotto, E., Murnane, J.P. and Sabatier, L. (2004) 'Interstitial telomeric repeats are not preferentially involved in radiation-induced chromosome aberrations in human cells', *Cytogenetic and genome research,* 104(1-4), pp. 123-130.

Dilley, R.L. and Greenberg, R.A. (2015) 'ALTernative telomere maintenance and cancer', *Trends in cancer,* 1(2), pp. 145-156.

Drane, P., Ouararhni, K., Depaux, A., Shuaib, M. and Hamiche, A. (2010) 'The death-associated protein DAXX is a novel histone chaperone involved in the replication-independent deposition of H3.3', *Genes & development,* 24(12), pp. 1253-1265.

Draskovic, I., Arnoult, N., Steiner, V., Bacchetti, S., Lomonte, P. and LondonoVallejo, A. (2009) 'Probing PML body function in ALT cells reveals spatiotemporal requirements for telomere recombination', *Proceedings of the National Academy of Sciences of the United States of America,* 106(37), pp. 15726-15731.

Dunham, M.A., Neumann, A.A., Fasching, C.L. and Reddel, R.R. (2000) 'Telomere maintenance by recombination in human cells', *Nature genetics,* 26(4), pp. 447.

Edwards, A., Virsik-Peuckert, P. and Bryant, P. (1996) 'Mechanisms of radiationinduced chromosome aberrations', *Mutation Research/Reviews in Genetic Toxicology,* 366(2), pp. 117-128.

Episkopou, H., Draskovic, I., Van Beneden, A., Tilman, G., Mattiussi, M., Gobin, M., Arnoult, N., Londono-Vallejo, A. and Decottignies, A. (2014) 'Alternative lengthening of telomeres is characterized by reduced compaction of telomeric chromatin', *Nucleic acids research,* 42(7), pp. 4391-4405.

Essers, J., Houtsmuller, A.B., van Veelen, L., Paulusma, C., Nigg, A.L., Pastink, A., Vermeulen, W., Hoeijmakers, J.H. and Kanaar, R. (2002) 'Nuclear dynamics of RAD52 group homologous recombination proteins in response to DNA damage', *The EMBO journal,* 21(8), pp. 2030-2037.

Faravelli, M., Azzalin, C.M., Bertoni, L., Chernova, O., Attolini, C., Mondello, C. and Giulotto, E. (2002) 'Molecular organization of internal telomeric sequences in Chinese hamster chromosomes', *Gene,* 283(1), pp. 11-16.

Faravelli, M., Moralli, D., Bertoni, L., Attolini, C., Chernova, O., Raimondi, E. and Giulotto, E. (1998) 'Two extended arrays of a satellite DNA sequence at the centromere and at the short-arm telomere of Chinese hamster chromosome 5', *Cytogenetics and cell genetics,* 83(3-4), pp. 281-286.

Feng, J., Funk, W.D., Wang, S.S., Weinrich, S.L., Avilion, A.A., Chiu, C.P., Adams, R.R., Chang, E., Allsopp, R.C. and Yu, J. (1995) 'The RNA component of human telomerase', *Science (New York, N.Y.),* 269(5228), pp. 1236-1241.

Fernández, J.L. and Gosálvez, J. (2002) 'Application of FISH to detect DNA damage', in *In Situ Detection of DNA Damage.* Springer, pp. 203-216.

Fernández, J.L., Gosálvez, J. and Goyanes, V. (1995a) 'High frequency of mutageninduced chromatid exchanges at interstitial telomere-like DNA sequence blocks of Chinese hamster cells', *Chromosome Research,* 3(5), pp. 281-284.

Fernández, J.L., Gosálvez, J. and Goyanes, V. (1995b) 'High frequency of mutageninduced chromatid exchanges at interstitial telomere-like DNA sequence blocks of Chinese hamster cells', *Chromosome Research,* 3(5), pp. 281-284.

Fernandez-Capetillo, O., Celeste, A. and Nussenzweig, A. (2003) 'Focusing on foci: H2AX and the recruitment of DNA-damage response factors', *Cell cycle,* 2(5), pp. 425-426.

Fernandez-Capetillo, O., Lee, A., Nussenzweig, M. and Nussenzweig, A. (2004) 'H2AX: the histone guardian of the genome', *DNA repair,* 3(8), pp. 959-967.

Finnon, R., Moody, J., Meijne, E., Haines, J., Clark, D., Edwards, A., Cox, R. and Silver, A. (2002) 'A major breakpoint cluster domain in murine radiation-induced acute myeloid leukemia', *Molecular Carcinogenesis: Published in cooperation with the University of Texas MD Anderson Cancer Center,* 34(2), pp. 64-71.

Flint, J., Craddock, C.F., Villegas, A., Bentley, D.P., Williams, H.J., Galanello, R., Cao, A., Wood, W.G., Ayyub, H. and Higgs, D.R. (1994) 'Healing of broken human chromosomes by the addition of telomeric repeats', *American Journal of Human Genetics,* 55(3), pp. 505-512.

Flynn, R.L., Cox, K.E., Jeitany, M., Wakimoto, H., Bryll, A.R., Ganem, N.J., Bersani, F., Pineda, J.R., Suva, M.L., Benes, C.H., Haber, D.A., Boussin, F.D. and Zou, L. (2015) 'Alternative lengthening of telomeres renders cancer cells hypersensitive to ATR inhibitors', *Science (New York, N.Y.),* 347(6219), pp. 273-277.

Fumagalli, M., Rossiello, F., Clerici, M., Barozzi, S., Cittaro, D., Kaplunov, J.M., Bucci, G., Dobreva, M., Matti, V. and Beausejour, C.M. (2012) 'Telomeric DNA damage is irreparable and causes persistent DNA-damage-response activation', *Nature cell biology,* 14(4), pp. 355.

Gall, J.G. (1995) '1 Beginning of the End: Origins of the Telomere Concept', *Cold Spring Harbor Monograph Archive,* 29, pp. 1-10.

Gazy, I. and Kupiec, M. (2013) 'Genomic instability and repair mediated by common repeated sequences', *Proceedings of the National Academy of Sciences of the United States of America,* 110(49), pp. 19664-19665.

Geserick, C., Tejera, A., Gonzalez-Suarez, E., Klatt, P. and Blasco, M. (2006) 'Expression of mTert in primary murine cells links the growth-promoting effects of

telomerase to transforming growth factor-β signaling', *Oncogene,* 25(31), pp. 4310.
Giaccia, A.J., Denko, N., MacLaren, R., Mirman, D., Waldren, C., Hart, I. and Stamato, T.D. (1990) 'Human chromosome 5 complements the DNA doublestrand break-repair deficiency and gamma-ray sensitivity of the XR-1 hamster variant', *American Journal of Human Genetics,* 47(3), pp. 459-469.
Gibbons, R.J., Picketts, D.J., Villard, L. and Higgs, D.R. (1995) 'Mutations in a putative global transcriptional regulator cause X-linked mental retardation with α-thalassemia (ATR-X syndrome)', *Cell,* 80(6), pp. 837-845.
Goldberg, A.D., Banaszynski, L.A., Noh, K., Lewis, P.W., Elsaesser, S.J., Stadler, S., Dewell, S., Law, M., Guo, X. and Li, X. (2010) 'Distinct factors control histone variant H3. 3 localization at specific genomic regions', *Cell,* 140(5), pp. 678691.
Griffith, J.D., Comeau, L., Rosenfield, S., Stansel, R.M., Bianchi, A., Moss, H. and De Lange, T. (1999) 'Mammalian telomeres end in a large duplex loop', *Cell,* 97(4), pp. 503-514.
Guo, A., Salomoni, P., Luo, J., Shih, A., Zhong, S., Gu, W. and Pandolfi, P.P. (2000) 'The function of PML in p53-dependent apoptosis', *Nature cell biology,* 2(10), pp. 730.
GURLEY, L.R., D'ANNA, J.A., BARHAM, S.S., DEAVEN, L.L. and TOBEY, R.A. (1978) 'Histone phosphorylation and chromatin structure during mitosis in Chinese hamster cells', *The FEBS Journal,* 84(1), pp. 1-15.
Haber, J.E. (2000) 'Partners and pathways: repairing a double-strand break', *Trends in Genetics,* 16(6), pp. 259-264.
Hahn, W.C., Stewart, S.A., Brooks, M.W., York, S.G., Eaton, E., Kurachi, A.,Beijersbergen, R.L., Knoll, J.H., Meyerson, M. and Weinberg, R.A. (1999) 'Inhibition of telomerase limits the growth of human cancer cells', *Nature medicine,* 5(10), pp. 1164-1170.
Hall, E.J. and Giaccia, A.J. (2006) *Radiobiology for the Radiologist.* Lippincott Williams & Wilkins.
Han, H. and Hurley, L.H. (2000) 'G-quadruplex DNA: a potential target for anticancer drug design', *Trends in pharmacological sciences,* 21(4), pp. 136-142.
Han, W. and Yu, K.N. (2009) 'Response of cells to ionizing radiation', *Advances in Biomedical Sciences and Engineering.Bentham Science Publishers,* , pp. 204262.
Harley, C.B. (1991) 'Telomere loss: mitotic clock or genetic time bomb?', *Mutation Research/DNAging,* 256(2-6), pp. 271-282.
Harley, C.B., Futcher, A.B. and Greider, C.W. (1990) 'Telomeres shorten during ageing of human fibroblasts', *Nature,* 345(6274), pp. 458.
Harrington, L.A. (1991) 'Telomerase primer specificity and chromosome healing', *Nature,* 353(6343), pp. 451.
Hastie, N.D. and Allshire, R.C. (1989) 'Human telomeres: fusion and interstitial sites', *Trends in Genetics,* 5, pp. 326-331.

Heaphy, C.M., de Wilde, R.F., Jiao, Y., Klein, A.P., Edil, B.H., Shi, C., Bettegowda, C.,

Rodriguez, F.J., Eberhart, C.G., Hebbar, S., Offerhaus, G.J., McLendon, R., Rasheed, B.A., He, Y., Yan, H., Bigner, D.D., Oba-Shinjo, S.M., Marie, S.K., Riggins, G.J., Kinzler, K.W., Vogelstein, B., Hruban, R.H., Maitra, A., Papadopoulos, N. and Meeker, A.K. (2011) 'Altered telomeres in tumors with ATRX and DAXX mutations', *Science (New York, N.Y.),* 333(6041), pp. 425.

Heiss, N.S., Knight, S.W., Vulliamy, T.J., Klauck, S.M., Wiemann, S., Mason, P.J., Poustka, A. and Dokal, I. (1998) 'X-linked dyskeratosis congenita is caused by mutations in a highly conserved gene with putative nucleolar functions', *Nature genetics,* 19(1), pp. 32.

Hemann, M.T. and Greider, C.W. (1999) 'G-strand overhangs on telomeres in telomerase-deficient mouse cells', *Nucleic acids research,* 27(20), pp. 39643969.

Henderson, E.R. and Blackburn, E.H. (1989) 'An overhanging 3' terminus is a conserved feature of telomeres', *Molecular and cellular biology,* 9(1), pp. 345-348.

Henry-Mowatt, J., Jackson, D., Masson, J., Johnson, P.A., Clements, P.M., Benson, F.E., Thompson, L.H., Takeda, S., West, S.C. and Caldecott, K.W. (2003) 'XRCC3 and Rad51 modulate replication fork progression on damaged vertebrate chromosomes', *Molecular cell,* 11(4), pp. 1109-1117.

Henson, J.D., Cao, Y., Huschtscha, L.I., Chang, A.C., Au, A.Y., Pickett, H.A. and Reddel, R.R. (2009) 'DNA C-circles are specific and quantifiable markers of alternative-lengthening-of-telomeres activity', *Nature biotechnology,* 27(12), pp. 1181.

Henson, J.D., Neumann, A.A., Yeager, T.R. and Reddel, R.R. (2002) 'Alternative lengthening of telomeres in mammalian cells', *Oncogene,* 21(4), pp. 598.

Henson, J.D. and Reddel, R.R. (2010) 'Assaying and investigating alternative lengthening of telomeres activity in human cells and cancers', *FEBS letters,* 584(17), pp. 3800-3811.

Henson, J.D., Hannay, J.A., McCarthy, S.W., Royds, J.A., Yeager, T.R., Robinson, R.A., Wharton, S.B., Jellinek, D.A., Arbuckle, S.M., Yoo, J., Robinson, B.G., Learoyd, D.L., Stalley, P.D., Bonar, S.F., Yu, D., Pollock, R.E. and Reddel, R.R. (2005) 'A robust assay for alternative lengthening of telomeres in tumors shows the significance of alternative lengthening of telomeres in sarcomas and astrocytomas', *Clinical cancer research: an official journal of the American Association for Cancer Research,* 11(1), pp. 217-225.

Hoeijmakers, J.H. (2001) 'Genome maintenance mechanisms for preventing cancer', *Nature,* 411(6835), pp. 366.

Hu, Y., Shi, G., Zhang, L., Li, F., Jiang, Y., Jiang, S., Ma, W., Zhao, Y., Songyang, Z. and Huang, J. (2016) 'Switch telomerase to ALT mechanism by inducing telomeric DNA damages and dysfunction of ATRX and DAXX', *Scientific reports,* 6, pp. 32280.

Huffman, K.E., Levene, S.D., Tesmer, V.M., Shay, J.W. and Wright, W.E. (2000) 'Telomere shortening is proportional to the size of the G-rich telomeric 3'overhang', *The Journal of biological chemistry,* 275(26), pp. 19719-19722.

IJdo, J.W., Baldini, A., Wells, R.A., Ward, D.C. and Reeders, S.T. (1992) 'FRA2B is distinct from inverted telomere repeat arrays at 2q13', *Genomics,* 12(4), pp. 833.

IJdo, J.W., Baldini, A., Ward, D.C., Reeders, S.T. and Wells, R.A. (1991) 'Origin of human chromosome 2: an ancestral telomere-telomere fusion', *Proceedings of the*

National Academy of Sciences of the United States of America, 88(20), pp. 9051-9055.
Iliakis, G. (2009) 'Backup pathways of NHEJ in cells of higher eukaryotes: cell cycle dependence', *Radiotherapy and oncology: journal of the European Society for Therapeutic Radiology and Oncology,* 92(3), pp. 310-315.
Iliakis, G., Wang, H., Perrault, A.R., Boecker, W., Rosidi, B., Windhofer, F., Wu, W., Guan, J., Terzoudi, G. and Pantelias, G. (2004a) 'Mechanisms of DNA double strand break repair and chromosome aberration formation', *Cytogenetic and genome research,* 104(1-4), pp. 14-20.
Iliakis, G., Wang, H., Perrault, A.R., Boecker, W., Rosidi, B., Windhofer, F., Wu, W., Guan, J., Terzoudi, G. and Pantelias, G. (2004b) 'Mechanisms of DNA double strand break repair and chromosome aberration formation', *Cytogenetic and genome research,* 104(1-4), pp. 14-20.
Ishov, A.M., Sotnikov, A.G., Negorev, D., Vladimirova, O.V., Neff, N., Kamitani, T., Yeh, E.T., Strauss, J.F.,3rd and Maul, G.G. (1999) 'PML is critical for ND10 formation and recruits the PML-interacting protein daxx to this nuclear structure when modified by SUMO-1', *The Journal of cell biology,* 147(2), pp. 221-234.
Iwano, T., Tachibana, M., Reth, M. and Shinkai, Y. (2004) 'Importance of TRF1 for functional telomere structure', *The Journal of biological chemistry,* 279(2), pp. 1442-1448.
Jain, D. and Cooper, J.P. (2010) 'Telomeric strategies: means to an end', *Annual Review of Genetics,* 44, pp. 243-269.
Jamiruddin, M.R., Kaitsuka, T., Hakim, F., Fujimura, A., Wei, F., Saitoh, H. and Tomizawa, K. (2016) 'HDAC9 regulates the alternative lengthening of telomere (ALT) pathway via the formation of alt-associated pml bodies', *Biochemical and biophysical research communications,* 481(1), pp. 25-30.
Jeggo, P. (1998) 'Identification of genes involved in repair of DNA double-strand breaks in mammalian cells', *Radiation research,* 150(5s), pp. S80-S91.
Jeggo, P. and Kemp, L. (1983) 'X-ray-sensitive mutants of Chinese hamster ovary cell line isolation and cross-sensitivity to other DNA-damaging agents', *Mutation Research/DNA Repair Reports,* 112(6), pp. 313-327.
Johnson, K.L. (1999) 'Radiation-induced breakpoint misrejoining in human chromosomes: random or non-random?', *International journal of radiation biology,* 75(2), pp. 131-141.
Jordan, R., Oroskar, A. and Sedita, B. (1995) 'Characterization of a potential radiation-sensitive fragile site', *Environmental and molecular mutagenesis,* 25(Suppl. 25), pp. 25.
Kanaar, R., Hoeijmakers, J.H. and van Gent, D.C. (1998) 'Molecular mechanisms of DNA double-strand break repair', *Trends in cell biology,* 8(12), pp. 483-489.
Kao, F. and Puck, T.T. (1967) 'Genetics of somatic mammalian cells. IV. Properties of Chinese hamster cell mutants with respect to the requirement for proline', *Genetics,* 55(3), pp. 513.
Kao, F.T. and Puck, T.T. (1968) 'Genetics of somatic mammalian cells, VII. Induction and isolation of nutritional mutants in Chinese hamster cells', *Proceedings of the National Academy of Sciences of the United States of America,* 60(4), pp. 1275-1281.

Kashima, K., Nanashima, A., Yasutake, T., Sawai, T., Tsuji, T., Hidaka, S., Akama, F., Miyashita, K., Tagawa, Y. and Nagayasu, T. (2006) 'Decrease of telomeres and increase of interstitial telomeric sites in chromosomes of short-term cultured gastric carcinoma cells detected by fluorescence in situ hybridization', *Anticancer Research,* 26(4B), pp. 2849-2855.

Khanna, K.K. and Jackson, S.P. (2001) 'DNA double-strand breaks: signaling, repair and the cancer connection', *Nature genetics,* 27(3), pp. 247.

Kim, N.W., Piatyszek, M.A., Prowse, K.R., Harley, C.B., West, M.D., Ho, P.L., Coviello, G.M., Wright, W.E., Weinrich, S.L. and Shay, J.W. (1994) 'Specific association of human telomerase activity with immortal cells and cancer', *Science (New York, N.Y.),* 266(5193), pp. 2011-2015.

Kim, S.H., Han, S., You, Y.H., Chen, D.J. and Campisi, J. (2003) 'The human telomere-associated protein TIN2 stimulates interactions between telomeric DNA tracts in vitro', *EMBO reports,* 4(7), pp. 685-691.

Klieser, E., Urbas, R., Stättner, S., Primavesi, F., Jäger, T., Dinnewitzer, A., Mayr, C., Kiesslich, T., Holzmann, K. and Di Fazio, P. (2017) 'Comprehensive immunohistochemical analysis of histone deacetylases in pancreatic neuroendocrine tumors: HDAC5 as a predictor of poor clinical outcome', *Human pathology,* 65, pp. 41-52.

Knight, S., Heiss, N., Vulliamy, T., Greschner, S., Stavrides, G., Pai, G., Lestringant, G., Varma, N., Mason, P. and Dokal, I. (1999) 'X-linked dyskeratosis congenita is predominantly caused by missense mutations in the DKC1 gene', *The American Journal of Human Genetics,* 65(1), pp. 50-58.

Kramer, K.M. and Haber, J.E. (1993) 'New telomeres in yeast are initiated with a highly selected subset of TG1-3 repeats', *Genes & development,* 7(12A), pp. 2345-2356.

Krutilina, R.I., Oei, S., Buchlow, G., Yau, P.M., Zalensky, A.O., Zalenskaya, I.A., Bradbury, E.M. and Tomilin, N.V. (2001) 'A negative regulator of telomerelength protein trf1 is associated with interstitial (TTAGGG) n blocks in immortal Chinese hamster ovary cells', *Biochemical and biophysical research communications,* 280(2), pp. 471-475.

Krutilina, R.I., Smirnova, A.N., Mudrak, O.S., Pleskach, N.M., Svetlova, M.P., Oei, S., Yau, P.M., Bradbury, E.M., Zalensky, A.O. and Tomilin, N.V. (2003) 'Protection of internal (TTAGGG) n repeats in Chinese hamster cells by telomeric protein TRF1', *Oncogene,* 22(43), pp. 6690-6698.

Lai, T., Zhang, N., Noh, J., Mender, I., Tedone, E., Huang, E., Wright, W.E., Danuser, G. and Shay, J.W. (2017) 'A method for measuring the distribution of the shortest telomeres in cells and tissues', *Nature communications,* 8(1), pp. 1356.

Lamb, J., Harris, P.C., Wilkie, A.O., Wood, W.G., Dauwerse, J.G. and Higgs, D.R. (1993a) 'De novo truncation of chromosome 16p and healing with (TTAGGG)n in the alpha-thalassemia/mental retardation syndrome (ATR16)', *American Journal of Human Genetics,* 52(4), pp. 668-676.

Lamb, J., Harris, P.C., Wilkie, A.O., Wood, W.G., Dauwerse, J.G. and Higgs, D.R. (1993b) 'De novo truncation of chromosome 16p and healing with (TTAGGG)n in the

alpha-thalassemia/mental retardation syndrome (ATR16)', *American Journal of Human Genetics,* 52(4), pp. 668-676.

Levy, M.Z., Allsopp, R.C., Futcher, A.B., Greider, C.W. and Harley, C.B. (1992) 'Telomere end-replication problem and cell aging', *Journal of Molecular Biology,* 225(4), pp. 951-960.

Lewandowska, H. and Szumiel, I. (2002) 'Histone H2AX in DNA repair', *Nukleonika,* 47(4), pp. 127-131.

Lewis, P.W., Elsaesser, S.J., Noh, K.M., Stadler, S.C. and Allis, C.D. (2010) 'Daxx is an H3.3-specific histone chaperone and cooperates with ATRX in replication-independent chromatin assembly at telomeres', *Proceedings of the National Academy of Sciences of the United States of America,* 107(32), pp. 14075-14080.

Li, Q., Zhang, J., Yang, L., Yu, Q., Chen, Q., Qin, X., Le, F., Zhang, Q. and Liu, J. (2014) 'Stabilization of G-quadruplex DNA and inhibition of telomerase activity studies of ruthenium (II) complexes', *Journal of inorganic biochemistry,* 130, pp. 122-129.

Liang, F., Romanienko, P.J., Weaver, D.T., Jeggo, P.A. and Jasin, M. (1996) 'Chromosomal double-strand break repair in Ku80-deficient cells', *Proceedings of the National Academy of Sciences of the United States of America,* 93(17), pp. 8929-8933.

Liau, J., Lee, J., Tsai, J., Yang, C., Liu, T., Ke, Z., Hsu, H. and Jeng, Y. (2015) 'Comprehensive screening of alternative lengthening of telomeres phenotype and loss of ATRX expression in sarcomas', *Modern Pathology,* 28(12), pp. 1545.

Lin, K.W. and Yan, J. (2008) 'Endings in the middle: current knowledge of interstitial telomeric sequences', *Mutation Research/Reviews in Mutation Research,* 658(1), pp. 95-110.

Liu, L., Lai, S., Andrews, L.G. and Tollefsbol, T.O. (2004) 'Genetic and epigenetic modulation of telomerase activity in development and disease', *Gene,* 340(1), pp. 1-10.

Liu, N., Lamerdin, J.E., Tebbs, R.S., Schild, D., Tucker, J.D., Shen, M.R., Brookman, K.W., Siciliano, M.J., Walter, C.A. and Fan, W. (1998) 'XRCC2 and XRCC3, new human Rad51-family members, promote chromosome stability and protect against DNA cross-links and other damages', *Molecular cell,* 1(6), pp. 783793.

Liu, N. and Lim, C. (2005) 'Differential roles of XRCC2 in homologous recombinational repair of stalled replication forks', *Journal of cellular biochemistry,* 95(5), pp. 942-954.

Loayza, D. and de Lange, T. (2003) 'POT1 as a terminal transducer of TRF1 telomere length control', *Nature,* 423(6943), pp. 1013-1018.

Londono-Vallejo, J.A., Der-Sarkissian, H., Cazes, L., Bacchetti, S. and Reddel, R.R. (2004) 'Alternative lengthening of telomeres is characterized by high rates of telomeric exchange', *Cancer research,* 64(7), pp. 2324-2327.

Lovejoy, C.A., Li, W., Reisenweber, S., Thongthip, S., Bruno, J., De Lange, T., De, S., Petrini, J.H., Sung, P.A. and Jasin, M. (2012) 'Loss of ATRX, genome instability, and an altered DNA damage response are hallmarks of the alternative lengthening of telomeres pathway', *PLoS genetics,* 8(7), pp. e1002772.

Lundblad, V. and Blackburn, E.H. (1993) 'An alternative pathway for yeast telomere maintenance rescues est1− senescence', *Cell,* 73(2), pp. 347-360.

MacLeod, R.A. and Bryant, P.E. (1990) 'Similar kinetics of chromatid aberrations in X-irradiated xrs 5 and wild-type Chinese hamster ovary cells', *Mutagenesis,* 5(4), pp. 407-410.
Makarov, V.L., Hirose, Y. and Langmore, J.P. (1997) 'Long G tails at both ends of human chromosomes suggest a C strand degradation mechanism for telomere shortening', *Cell,* 88(5), pp. 657-666.
Mao, P., Liu, J., Zhang, Z., Zhang, H., Liu, H., Gao, S., Rong, Y.S. and Zhao, Y. (2016) 'Homologous recombination-dependent repair of telomeric DSBs in proliferating human cells', *Nature communications,* 7, pp. 12154.
Marcu, L., Bezak, E. and Allen, B. (2012) *Biomedical Physics in Radiotherapy for Cancer.* Csiro publishing.
Mason, P., Wilson, D. and Bessler, M. (2005) 'Dyskeratosis congenita-a disease of dysfunctional telomere maintenance', *Current Molecular Medicine,* 5(2), pp. 159-170.
Masutomi, K., Evan, Y.Y., Khurts, S., Ben-Porath, I., Currier, J.L., Metz, G.B., Brooks, M.W., Kaneko, S., Murakami, S. and DeCaprio, J.A. (2003) 'Telomerase maintains telomere structure in normal human cells', *Cell,* 114(2), pp. 241253.
Mateos, S., Slijepcevic, P., MacLeod, R.A. and Bryant, P.E. (1994) 'DNA doublestrand break rejoining in xrs5 cells is more rapid in the G2 than in the G1 phase of the cell cycle', *Mutation Research/DNA Repair,* 315(2), pp. 181-187.
Meier, U.T. (2005) 'The many facets of H/ACA ribonucleoproteins', *Chromosoma,* 114(1), pp. 1-14.
Meltzer, P.S., Guan, X. and Trent, J.M. (1993) 'Telomere capture stabilizes chromosome breakage', *Nature genetics,* 4(3), pp. 252.
Meyne, J., Baker, R.J., Hobart, H.H., Hsu, T., Ryder, O.A., Ward, O.G., Wiley, J.E., Wurster-Hill, D.H., Yates, T.L. and Moyzis, R.K. (1990) 'Distribution of nontelomeric sites of the (TTAGGG) n telomeric sequence in vertebrate chromosomes', *Chromosoma,* 99(1), pp. 3-10.
Mladenov, E. and Iliakis, G. (2011) 'Induction and repair of DNA double strand breaks: the increasing spectrum of non-homologous end joining pathways', *Mutation Research/Fundamental and Molecular Mechanisms of Mutagenesis,* 711(1), pp. 61-72.
Mosquera, A., Gosálvez, J., Sabatier, L. and Fernández, J.L. (2005) 'Interstitial telomeric DNA sequences of Chinese hamster cells are hypersensitive to nitric oxide damage, and DNA-PKcs has a specific local role in its repair', *Genes, Chromosomes and Cancer,* 44(1), pp. 76-84.
Moyzis, R.K., Buckingham, J.M., Cram, L.S., Dani, M., Deaven, L.L., Jones, M.D., Meyne, J., Ratliff, R.L. and Wu, J.R. (1988) 'A highly conserved repetitive DNA sequence, (TTAGGG)n, present at the telomeres of human chromosomes', *Proceedings of the National Academy of Sciences of the United States of America,* 85(18), pp. 6622-6626.

Mu, Z.M., Le, X.F., Vallian, S., Glassman, A.B. and Chang, K.S. (1997) 'Stable overexpression of PML alters regulation of cell cycle progression in HeLa cells', *Carcinogenesis,* 18(11), pp. 2063-2069.
Muller, H. (1941) 'The remaking of chromosomes. The collecting net. WoodsHole

13: 18 1-1 98, 1938. McClintock B: The stability of broken ends of chromosomes in Zea muys', *Genetics,* 41, pp. 234-282.
Multani, A., Ozen, M., Furlong, C., Zhao, Y., Hsu, T. and Pathak, S. (2001) 'Heterochromatin and interstitial telomeric DNA homology', *Chromosoma,* 110(3), pp. 214-220.
Nabetani, A. and Ishikawa, F. (2009) 'Unusual telomeric DNAs in human telomerase-negative immortalized cells', *Molecular and cellular biology,* 29(3), pp. 703-713.
Nanda, I. and Schmid, M. (1994) 'Localization of the telomeric (TTAGGG) n sequence in chicken (Gallus domesticus) chromosomes', *Cytogenetic and Genome Research,* 65(3), pp. 190-193.
Napier, C.E., Huschtscha, L.I., Harvey, A., Bower, K., Noble, J.R., Hendrickson, E.A. and Reddel, R.R. (2015) 'ATRX represses alternative lengthening of telomeres', *Oncotarget,* 6(18), pp. 16543-16558.
Natarajan, A.T. and Palitti, F. (2008) 'DNA repair and chromosomal alterations', *Mutation Research/Genetic Toxicology and Environmental Mutagenesis,* 657(1), pp. 3-7.
Natarajan, A.T. (2002) 'Chromosome aberrations: past, present and future', *Mutation Research/Fundamental and Molecular Mechanisms of Mutagenesis,* 504(1), pp. 3-16.
Natarajan, A. and Boei, J. (2003) 'Formation of chromosome aberrations: insights from FISH', *Mutation Research/Reviews in Mutation Research,* 544(2), pp. 299-304.
Natarajan, A. and Obe, G. (1984) 'Molecular mechanisms involved in the production of chromosomal aberrations', *Chromosoma,* 90(2), pp. 120-127. Nergadze, S.G., Rocchi, M., Azzalin, C.M., Mondello, C. and Giulotto, E. (2004) 'Insertion of telomeric repeats at intrachromosomal break sites during primate evolution', *Genome research,* 14(9), pp. 1704-1710.
Neumann, A.A. and Reddel, R.R. (2002) 'Telomere maintenance and cancer? look, no telomerase', *Nature Reviews Cancer,* 2(11), pp. 879.
Neumann, A.A., Watson, C.M., Noble, J.R., Pickett, H.A., Tam, P.P. and Reddel, R.R. (2013) 'Alternative lengthening of telomeres in normal mammalian somatic cells', *Genes & development,* 27(1), pp. 18-23.
New, J.H., Sugiyama, T., Zaitseva, E. and Kowalczykowski, S.C. (1998) 'Rad52 protein stimulates DNA strand exchange by Rad51 and replication protein A', *Nature,* 391(6665), pp. 407.
Newbold, R.F. 'Genetic control of telomerase and replicative senescence in human and rodent cells', *Ciba Foundation Symposium 211-Telomeres and Telomerase.* Wiley Online Library, 177-197.
Novo, C.L., Polese, C., Matheus, N., Decottignies, A., Londono-Vallejo, A., Castronovo, V. and Mottet, D. (2013) 'A new role for histone deacetylase 5 in the maintenance of long telomeres', *The FASEB Journal,* 27(9), pp. 36323642.

Obe, G., Pfeiffer, P., Savage, J., Johannes, C., Goedecke, W., Jeppesen, P., Natarajan, A., Martınez-López, W., Folle, G. and Drets, M. (2002) 'Chromosomal aberrations: formation, identification and distribution', *Mutation Research/Fundamental and Molecular Mechanisms of Mutagenesis,* 504(1), pp. 17-36.

Ogiwara, H., Ui, A., Otsuka, A., Satoh, H., Yokomi, I., Nakajima, S., Yasui, A., Yokota, J. and Kohno, T. (2011) 'Histone acetylation by CBP and p300 at doublestrand break sites facilitates SWI/SNF chromatin remodeling and the recruitment of non-homologous end joining factors', *Oncogene,* 30(18), pp. 2135.

Ohki, R., Tsurimoto, T. and Ishikawa, F. (2001) 'In vitro reconstitution of the end replication problem', *Molecular and cellular biology,* 21(17), pp. 5753-5766.

Osterwald, S., Deeg, K.I., Chung, I., Parisotto, D., Worz, S., Rohr, K., Erfle, H. and Rippe, K. (2015) 'PML induces compaction, TRF2 depletion and DNA damage signaling at telomeres and promotes their alternative lengthening', *Journal of cell science,* 128(10), pp. 1887-1900.

Padilla-Nash, H.M., Heselmeyer-Haddad, K., Wangsa, D., Zhang, H., Ghadimi, B.M., Macville, M., Augustus, M., Schröck, E., Hilgenfeld, E. and Ried, T. (2001) 'Jumping translocations are common in solid tumor cell lines and result in recurrent fusions of whole chromosome arms', *Genes, Chromosomes and Cancer,* 30(4), pp. 349-363.

Pagnozzi, J.M., Ditchfield, A.D. and Yonenaga-Yassuda, Y. (2002) 'Mapping the distribution of the interstitial telomeric (TTAGGG)n sequences in eight species of Brazilian marsupials (Didelphidae) by FISH and the correlation with constitutive heterochromatin. Do ITS represent evidence for fusion events in American marsupials', *Cytogenetic and genome research,* 98(4), pp. 278-284.

Palin, A.H., Critcher, R., Fitzgerald, D.J., Anderson, J.N. and Farr, C.J. (1998) 'Direct cloning and analysis of DNA sequences from a region of the Chinese hamster genome associated with aphidicolin-sensitive fragility', *Journal of cell science,* 111 (Pt 12)(Pt 12), pp. 1623-1634.

Palm, W. and de Lange, T. (2008) 'How shelterin protects mammalian telomeres', *Annual Review of Genetics,* 42, pp. 301-334.

Pearson, M., Carbone, R., Sebastiani, C., Cioce, M., Fagioli, M., Saito, S., Higashimoto, Y., Appella, E., Minucci, S. and Pandolfi, P.P. (2000) 'PML regulates p53 acetylation and premature senescence induced by oncogenic Ras', *Nature,* 406(6792), pp. 207.

Perrem, K., Bryan, T.M., Englezou, A., Hackl, T., Moy, E.L. and Reddel, R.R. (1999) 'Repression of an alternative mechanism for lengthening of telomeres in somatic cell hybrids', *Oncogene,* 18(22), pp. 3383.

Perrem, K., Colgin, L.M., Neumann, A.A., Yeager, T.R. and Reddel, R.R. (2001) 'Coexistence of alternative lengthening of telomeres and telomerase in hTERT-transfected GM847 cells', *Molecular and cellular biology,* 21(12), pp. 3862-3875.

Pfeiffer, P., Goedecke, W. and Obe, G. (2000) 'Mechanisms of DNA double-strand break repair and their potential to induce chromosomal aberrations', *Mutagenesis,* 15(4), pp. 289-302.

Phan, A.T. and Mergny, J.L. (2002) 'Human telomeric DNA: G-quadruplex, i-motif and Watson-Crick double helix', *Nucleic acids research,* 30(21), pp. 46184625.

Pisano, S., Galati, A. and Cacchione, S. (2008) 'Telomeric nucleosomes: forgotten players at chromosome ends', *Cellular and molecular life sciences,* 65(22), pp. 3553-3563.

Prowse, K.R. and Greider, C.W. (1995) 'Developmental and tissue-specific regulation of mouse telomerase and telomere length', *Proceedings of the National Academy of Sciences of the United States of America,* 92(11), pp. 4818-4822.
Puck, T.T., Cieciura, S.J. and Robinson, A. (1958) 'Genetics of somatic mammalian cells. III. Long-term cultivation of euploid cells from human and animal subjects', *The Journal of experimental medicine,* 108(6), pp. 945-956.
Puerto, S., Ramirez, M., Marcos, R., Creus, A. and Surralles, J. (2001) 'Radiationinduced chromosome aberrations in human euchromatic (17cen-p53) and heterochromatic (1cen-1q12) regions', *Mutagenesis,* 16(4), pp. 291-296.
Rajavel, M., Mullins, M.R. and Taylor, D.J. (2014) 'Multiple facets of TPP1 in telomere maintenance', *Biochimica et Biophysica Acta (BBA)-Proteins and Proteomics,* 1844(9), pp. 1550-1559.
Rapić-Otrin, V., Navazza, V., Nardo, T., Botta, E., McLenigan, M., Bisi, D.C., Levine, A.S. and Stefanini, M. (2003) 'True XP group E patients have a defective UVdamaged DNA binding protein complex and mutations in DDB2 which reveal the functional domains of its p48 product', *Human molecular genetics,* 12(13), pp. 1507-1522.
Revaud, D., Martins, L.M., Boussin, F.D., Sabatier, L. and Desmaze, C. (2011) 'Different DNA-PKcs functions in the repair of radiation-induced and spontaneous DSBs within interstitial telomeric sequences', *Chromosoma,* 120(3), pp. 309-319.
Revaud, D., Mozziconacci, J., Sabatier, L., Desmaze, C. and Lavelle, C. (2009) 'Sequence-driven telomeric chromatin structure', *Cell Cycle,* 8(7), pp. 10991100.
Rhodes, D. and Giraldo, R. (1995) 'Telomere structure and function', *Current opinion in structural biology,* 5(3), pp. 311-322.
Rivero, M.T., Mosquera, A., Goyanes, V., Slijepcevic, P. and Fernández, J.L. (2004) 'Differences in repair profiles of interstitial telomeric sites between normal and DNA double-strand break repair deficient Chinese hamster cells', *Experimental cell research,* 295(1), pp. 161-172.
Rodrigue, A., Lafrance, M., Gauthier, M.C., McDonald, D., Hendzel, M., West, S.C., Jasin, M. and Masson, J.Y. (2006) 'Interplay between human DNA repair proteins at a unique double-strand break in vivo', *The EMBO journal,* 25(1), pp. 222-231.
Rogakou, E.P., Boon, C., Redon, C. and Bonner, W.M. (1999) 'Megabase chromatin domains involved in DNA double-strand breaks in vivo', *The Journal of cell biology,* 146(5), pp. 905-916.
Rogakou, E.P., Pilch, D.R., Orr, A.H., Ivanova, V.S. and Bonner, W.M. (1998) 'DNA double-stranded breaks induce histone H2AX phosphorylation on serine 139', *The Journal of biological chemistry,* 273(10), pp. 5858-5868.
Ropero, S. and Esteller, M. (2007) 'The role of histone deacetylases (HDACs) in human cancer', *Molecular oncology,* 1(1), pp. 19-25.

Rosidi, B., Wang, M., Wu, W., Sharma, A., Wang, H. and Iliakis, G. (2008) 'Histone H1 functions as a stimulatory factor in backup pathways of NHEJ', *Nucleic acids research,* 36(5), pp. 1610-1623.
Rothkamm, K. and Lobrich, M. (2002) 'Misrepair of radiation-induced DNA double-strand breaks and its relevance for tumorigenesis and cancer treatment', *International journal of oncology,* 21(2), pp. 433-440.

Rouse, J. and Jackson, S.P. (2002) 'Interfaces between the detection, signaling, and repair of DNA damage', *Science (New York, N.Y.),* 297(5581), pp. 547551.
Rovatsos, M.T., Marchal, J., Romero-Fernández, I., Fernández, F., Giagia Athanosopoulou, E. and Sánchez, A. (2011) 'Rapid, independent, and extensive amplification of telomeric repeats in pericentromeric regions in karyotypes of arvicoline rodents', *Chromosome research,* 19(7), pp. 869-882.
Ruiz-Herrera, A.,Garcia, F., Azzalin, C., Giulotto, E., Egozcue, J., Ponsa, M. and Garcia, M. (2002) 'Distribution of intrachromosomal telomeric sequences (ITS) on Macaca fascicularis (Primates) chromosomes and their implication for chromosome evolution', *Human genetics,* 110(6), pp. 578-586.
Ruiz-Herrera, A., Nergadze, S.G., Santagostino, M. and Giulotto, E. (2008) 'Telomeric repeats far from the ends: mechanisms of origin and role in evolution', *Cytogenetic and genome research,* 122(3-4), pp. 219-228.
Samper, E., Flores, J.M. and Blasco, M.A. (2001) 'Restoration of telomerase activity rescues chromosomal instability and premature aging in Terc−/− mice with short telomeres', *EMBO reports,* 2(9), pp. 800-807.
San Filippo, J., Sung, P. and Klein, H. (2008) 'Mechanism of eukaryotic homologous recombination', *Annu.Rev. Biochem.,* 77, pp. 229-257.
Sancar, A., Lindsey-Boltz, L.A., Ünsal-Kaçmaz, K. and Linn, S. (2004) 'Molecular mechanisms of mammalian DNA repair and the DNA damage checkpoints', *Annual Review of Biochemistry,* 73(1), pp. 39-85.
Savage, J.R. (1976) 'Classification and relationships of induced chromosomal structual changes', *Journal of medical genetics,* 13(2), pp. 103-122.
Schoeftner, S. and Blasco, M.A. (2008) 'Developmentally regulated transcription of mammalian telomeres by DNA-dependent RNA polymerase II', *Nature cell biology,* 10(2), pp. 228.
Sedelnikova, O.A., Rogakou, E.P., Panyutin, I.G. and Bonner, W.M. (2002) 'Quantitative detection of 125IdU-induced DNA double-strand breaks with γ-H2AX antibody', *Radiation research,* 158(4), pp. 486-492.
Sengupta, S., Linke, S.P., Pedeux, R., Yang, Q., Farnsworth, J., Garfield, S.H., Valerie, K., Shay, J.W., Ellis, N.A., Wasylyk, B. and Harris, C.C. (2003) 'BLM helicasedependent transport of p53 to sites of stalled DNA replication forks modulates homologous recombination', *The EMBO journal,* 22(5), pp. 12101222.
Serrano, M. and Blasco, M.A. (2001) 'Putting the stress on senescence', *Current opinion in cell biology,* 13(6), pp. 748-753.
Shi, Y., Lan, F., Matson, C., Mulligan, P., Whetstine, J.R., Cole, P.A., Casero, R.A. and Shi, Y. (2004) 'Histone demethylation mediated by the nuclear amine oxidase homolog LSD1', *Cell,* 119(7), pp. 941-953.

Shibata, A., Moiani, D., Arvai, A.S., Perry, J., Harding, S.M., Genois, M., Maity, R., van Rossum-Fikkert, S., Kertokalio, A. and Romoli, F. (2014) 'DNA double-strand break repair pathway choice is directed by distinct MRE11 nuclease activities', *Molecular cell,* 53(1), pp. 7-18.
Shibata, A., Conrad, S., Birraux, J., Geuting, V., Barton, O., Ismail, A., Kakarougkas, A., Meek, K., Taucher-Scholz, G., Lobrich, M. and Jeggo, P.A. (2011) 'Factors

determining DNA double-strand break repair pathway choice in G2 phase', *The EMBO journal,* 30(6), pp. 1079-1092.
Shu, Z., Smith, S., Wang, L., Rice, M.C. and Kmiec, E.B. (1999) 'Disruption of muREC2/RAD51L1 in mice results in early embryonic lethality which can Be partially rescued in a p53(-/-) background', *Molecular and cellular biology,* 19(12), pp. 8686-8693.
Sijen, T., Fleenor, J., Simmer, F., Thijssen, K.L., Parrish, S., Timmons, L., Plasterk, R.H. and Fire, A. (2001) 'On the role of RNA amplification in dsRNA-triggered gene silencing', *Cell,* 107(4), pp. 465-476.
Silver, A. and Cox, R. (1993) 'Telomere-like DNA polymorphisms associated with genetic predisposition to acute myeloid leukemia in irradiated CBA mice', *Proceedings of the National Academy of Sciences of the United States of America,* 90(4), pp. 1407-1410.
Simi, S., Simili, M., Bonatti, S., Campagna, M. and Abbondandolo, A. (1998) 'Fragile sites at the centromere of Chinese hamster chromosomes: a possible mechanism of chromosome loss', *Mutation Research/Fundamental and Molecular Mechanisms of Mutagenesis,* 397(2), pp. 239-246.
Simi, S., Vatteroni, L., Antonio, P., Mariani, T. and Rainaldi, G. (1990) 'Folatesensitive fragile sites in Chinese hamster cell lines', *Cancer genetics and cytogenetics,* 46(2), pp. 209-216.
Simonet, T., Zaragosi, L., Philippe, C., Lebrigand, K., Schouteden, C., Augereau, A., Bauwens, S., Ye, J., Santagostino, M. and Giulotto, E. (2011) 'The human TTAGGG repeat factors 1 and 2 bind to a subset of interstitial telomeric sequences and satellite repeats', *Cell research,* 21(7), pp. 1028.
Singleton, B.K., Torres-Arzayus, M.I., Rottinghaus, S.T., Taccioli, G.E. and Jeggo, P.A. (1999) 'The C terminus of Ku80 activates the DNA-dependent protein kinase catalytic subunit', *Molecular and cellular biology,* 19(5), pp. 32673277.
Slijepcevic, P. and Bryant, P. (1995) 'Absence of terminal telomeric FISH signals in chromosomes from immortal Chinese hamster cells', *Cytogenetic and Genome Research,* 69(1-2), pp. 87-89.
Slijepcevic, P., Hande, M., Bouffler, S., Lansdorp, P. and Bryant, P. (1997) 'Telomere length, chromatin structure and chromosome fusigenic potential', *Chromosoma,* 106(7), pp. 413-421.
Slijepcevic, P. and Natarajan, A. (1994) 'Distribution of X-ray-induced G2 chromatid damage among Chinese hamster chromosomes: influence of chromatin conformation', *Mutation Research Letters,* 323(3), pp. 113-119.
Slijepcevic, P., Xiao, Y., Dominguez, I. and Natarajan, A. (1996) 'Spontaneous and radiation-induced chromosomal breakage at interstitial telomeric sites', *Chromosoma,* 104(8), pp. 596-604.

Slijepcevic, P., Xiao, Y., Natarajan, A. and Bryant, P. (1997) 'Instability of CHO chromosomes containing interstitial telomeric sequences originating from Chinese hamster chromosome 10', *Cytogenetic and Genome Research,* 76(12), pp. 58-60.
Slijepcevic, P. (2006) 'The role of DNA damage response proteins at telomeres— an "integrative" model', *DNA repair,* 5(11), pp. 1299-1306.

Slijepcevic, P. and Hande, M.P. (1999) 'Chinese hamster telomeres are comparable in size to mouse telomeres', *Cytogenetics and cell genetics,* 85(34), pp. 196-199.
Smith, L.L., Coller, H.A. and Roberts, J.M. (2003) 'Telomerase modulates expression of growth-controlling genes and enhances cell proliferation', *Nature cell biology,* 5(5), pp. 474.
Smogorzewska, A., van Steensel, B., Bianchi, A., Oelmann, S., Schaefer, M.R., Schnapp, G. and de Lange, T. (2000) 'Control of human telomere length by TRF1 and TRF2', *Molecular and cellular biology,* 20(5), pp. 1659-1668.
Stampfer, M.R., Garbe, J., Levine, G., Lichtsteiner, S., Vasserot, A.P. and Yaswen, P. (2001) 'Expression of the telomerase catalytic subunit, hTERT, induces resistance to transforming growth factor beta growth inhibition in p16INK4A(-) human mammary epithelial cells', *Proceedings of the National Academy of Sciences of the United States of America,* 98(8), pp. 4498-4503.
Stewart, G.S., Maser, R.S., Stankovic, T., Bressan, D.A., Kaplan, M.I., Jaspers, N.G., Raams, A., Byrd, P.J., Petrini, J.H. and Taylor, A.M.R. (1999) 'The DNA doublestrand break repair gene hMRE11 is mutated in individuals with an ataxiatelangiectasia-like disorder', *Cell,* 99(6), pp. 577-587.
Stuurman, N., de Graaf, A., Floore, A., Josso, A., Humbel, B., de Jong, L. and van Driel, R. (1992) 'A monoclonal antibody recognizing nuclear matrixassociated nuclear bodies', *Journal of cell science,* 101 (Pt 4)(Pt 4), pp. 773784.
Suwaki, N., Klare, K. and Tarsounas, M. (2011) 'RAD51 paralogs: roles in DNA damage signalling, recombinational repair and tumorigenesis', *Seminars in cell & developmental biology.* Elsevier. 898-905.
Takata, M., Sasaki, M.S., Sonoda, E., Morrison, C., Hashimoto, M., Utsumi, H., Yamaguchi-Iwai, Y., Shinohara, A. and Takeda, S. (1998) 'Homologous recombination and non-homologous end-joining pathways of DNA doublestrand break repair have overlapping roles in the maintenance of chromosomal integrity in vertebrate cells', *The EMBO journal,* 17(18), pp. 5497-5508.
Takata, M., Sasaki, M.S., Tachiiri, S., Fukushima, T., Sonoda, E., Schild, D., Thompson, L.H. and Takeda, S. (2001) 'Chromosome instability and defective recombinational repair in knockout mutants of the five Rad51 paralogs', *Molecular and cellular biology,* 21(8), pp. 2858-2866.
Tambini, C.E., Spink, K.G., Ross, C.J., Hill, M.A. and Thacker, J. (2010) 'The importance of XRCC2 in RAD51-related DNA damage repair', *DNA repair,* 9(5), pp. 517-525.
Tang, J., Wu, S., Liu, H., Stratt, R., Barak, O.G., Shiekhattar, R., Picketts, D.J. and Yang, X. (2004) 'A novel transcription regulatory complex containing death domain-associated protein and the ATR-X syndrome protein', *The Journal of biological chemistry,* 279(19), pp. 20369-20377.
Tarsounas, M., Davies, D. and West, S.C. (2003) 'BRCA2-dependent and independent formation of RAD51 nuclear foci', *Oncogene,* 22(8), pp. 1115.
Tarsounas, M., Muñoz, P., Claas, A., Smiraldo, P.G., Pittman, D.L., Blasco, M.A. and West, S.C. (2004) 'Telomere maintenance requires the RAD51 recombination/repair protein', *Cell,* 117(3), pp. 337-347.
Tarsounas, M. and West, S.C. (2005) 'Recombination at mammalian telomeres: an alternative mechanism for telomere protection and elongation', *Cell Cycle,* 4(5), pp. 672-674.

Teng, S.C. and Zakian, V.A. (1999) 'Telomere-telomere recombination is an efficient bypass pathway for telomere maintenance in Saccharomyces cerevisiae', *Molecular and cellular biology,* 19(12), pp. 8083-8093.
Terry, S., Riches, A. and Bryant, P. (2008) 'A role for topoisomerase IIα in the formation of radiation-induced chromatid breaks', *British journal of cancer,* 99(4), pp. 670-674.
Thacker, J. (2005) 'The< i> RAD51 gene family, genetic instability and cancer', *Cancer letters,* 219(2), pp. 125-135.
Thacker, J. (1999) 'The role of homologous recombination processes in the repair of severe forms of DNA damage in mammalian cells', *Biochimie,* 81(1), pp. 77-85.
Trojer, P. and Reinberg, D. (2007) 'Facultative heterochromatin: is there a distinctive molecular signature?', *Molecular cell,* 28(1), pp. 1-13.
Tucker, J.D. and Senft, J.R. (1994) 'Analysis of naturally occurring and radiation induced breakpoint locations in human chromosomes 1, 2 and 4', *Radiation research,* 140(1), pp. 31-36.
Van Attikum, H. and Gasser, S.M. (2005) 'The histone code at DNA breaks: a guide to repair?', *Nature Reviews Molecular Cell Biology,* 6(10), pp. 757.
Van Steensel, B., Smogorzewska, A. and de Lange, T. (1998) 'TRF2 protects human telomeres from end-to-end fusions', *Cell,* 92(3), pp. 401-413.
Vaziri, H. and Benchimol, S. (1999) 'Alternative pathways for the extension of cellular life span: inactivation of p53/pRb and expression of telomerase', *Oncogene,* 18(53), pp. 7676.
Venteicher, A.S., Meng, Z., Mason, P.J., Veenstra, T.D. and Artandi, S.E. (2008) 'Identification of ATPases pontin and reptin as telomerase components essential for holoenzyme assembly', *Cell,* 132(6), pp. 945-957.
Wang, M., Wu, W., Wu, W., Rosidi, B., Zhang, L., Wang, H. and Iliakis, G. (2006) 'PARP-1 and Ku compete for repair of DNA double strand breaks by distinct NHEJ pathways', *Nucleic acids research,* 34(21), pp. 6170-6182.
Wang, C. and Meier, U.T. (2004) 'Architecture and assembly of mammalian H/ACA small nucleolar and telomerase ribonucleoproteins', *The EMBO journal,* 23(8), pp. 1857-1867.
Watson, L.A., Solomon, L.A., Li, J.R., Jiang, Y., Edwards, M., Shin-ya, K., Beier, F. and Bérubé, N.G. (2013) 'Atrx deficiency induces telomere dysfunction, endocrine defects, and reduced life span', *The Journal of clinical investigation,* 123(5), pp. 2049-2063.
Weaver, D.T. (1995) 'What to do at an end: DNA double-strand-break repair', *Trends in Genetics,* 11(10), pp. 388-392.
Wege, H., Chui, M.S., Le, H.T., Tran, J.M. and Zern, M.A. (2002) 'SYBR Green real-time telomeric repeat amplification protocol for the rapid quantification of telomerase activity', *Nucleic acids research,* 31(2), pp. e3-e3.
Wells, R.A., Germino, G.G., Krishna, S., Buckle, V.J. and Reeders, S.T. (1990) 'Telomere-related sequences at interstitial sites in the human genome', *Genomics,* 8(4), pp. 699-704.
West, S.C. (2003) 'Molecular views of recombination proteins and their control', *Nature reviews Molecular cell biology,* 4(6), pp. 435.

Whitmore, G., Varghese, A. and Gulyas, S. (1989) 'Cell cycle responses of two Xray sensitive mutants defective in DNA repair', *International journal of radiation biology,* 56(5), pp. 657-665.
Wilkie, A.O., Lamb, J., Harris, P.C., Finney, R.D. and Higgs, D.R. (1990) 'A truncated human chromosome 16 associated with α thalassaemia is stabilized by addition of telomeric repeat (TTAGGG) n', .
Wong, L.H., McGhie, J.D., Sim, M., Anderson, M.A., Ahn, S., Hannan, R.D., George, A.J., Morgan, K.A., Mann, J.R. and Choo, K.H. (2010) 'ATRX interacts with H3.3 in maintaining telomere structural integrity in pluripotent embryonic stem cells', *Genome research,* 20(3), pp. 351-360.
Wood, A.M., Danielsen, J.M.R., Lucas, C.A., Rice, E.L., Scalzo, D., Shimi, T., Goldman, R.D., Smith, E.D., Le Beau, M.M. and Kosak, S.T. (2014) 'TRF2 and lamin A/C interact to facilitate the functional organization of chromosome ends', *Nature communications,* 5, pp. 5467.
Wood, R.D., Mitchell, M., Sgouros, J. and Lindahl, T. (2001) 'Human DNA repair genes', *Science (New York, N.Y.),* 291(5507), pp. 1284-1289.
Wu, G., Lee, W. and Chen, P. (2000) 'NBS1 and TRF1 Colocalize at Promyelocytic Leukemia Bodies during Late S/G2 Phases in Immortalized Telomerasenegative Cells IMPLICATION OF NBS1 IN ALTERNATIVE LENGTHENING OF TELOMERES', *Journal of Biological Chemistry,* 275(39), pp. 30618-30622.
Wyman, C. and Kanaar, R. (2006) 'DNA double-strand break repair: all's well that ends well', *Annu.Rev. Genet.,* 40, pp. 363-383.
Xu, B., Peng, M. and Song, Q. (2014) 'The co-expression of telomerase and ALT pathway in human breast cancer tissues', *Tumor Biology,* 35(5), pp. 40874093.
Yan, C.T., Boboila, C., Souza, E.K., Franco, S., Hickernell, T.R., Murphy, M., Gumaste, S., Geyer, M., Zarrin, A.A. and Manis, J.P. (2007) 'IgH class switching and translocations use a robust non-classical end-joining pathway', *Nature,* 449(7161), pp. 478.
Yang, L., Wang, W., Hu, L., Yang, X., Zhong, J., Li, Z., Yang, H., Lei, H., Yu, H. and Liao, Z. (2013) 'Telomere-binding protein TPP1 modulates telomere homeostasis and confers radioresistance to human colorectal cancer cells', *PloS one,* 8(11), pp. e81034.
Yang, R., Wu, Y., Wang, M., Sun, Z., Zou, J., Zhang, Y. and Cui, H. (2015) 'HDAC9 promotes glioblastoma growth via TAZ-mediated EGFR pathway activation', *Oncotarget,* 6(10), pp. 7644-7656.
Yeager, T.R., Neumann, A.A., Englezou, A., Huschtscha, L.I., Noble, J.R. and Reddel, R.R. (1999) 'Telomerase-negative immortalized human cells contain a novel type of promyelocytic leukemia (PML) body', *Cancer research,* 59(17), pp. 4175-4179.
Yen, C.-., Pazik, J. and Elliott, R. (1996) 'A polymorphic interstitial telomere array near the center of mouse chromosome 8', *Mammalian Genome,* 7(3), pp. 218221.
Yokoyama, H., Sarai, N., Kagawa, W., Enomoto, R., Shibata, T., Kurumizaka, H. and Yokoyama, S. (2004) 'Preferential binding to branched DNA strands and strand-annealing activity of the human Rad51B, Rad51C, Rad51D and Xrcc2 protein complex', *Nucleic acids research,* 32(8), pp. 2556-2565.
Yu, S., Mangelsdorf, M., Hewett, D., Hobson, L., Baker, E., Eyre, H.J., Lapsys, N., Le Paslier, D., Doggett, N.A. and Sutherland, G.R. (1997) 'Human chromosomal

fragile site FRA16B is an amplified AT-rich minisatellite repeat', *Cell,* 88(3), pp. 367-374.

Zakian, V.A. (1997) 'Life and cancer without telomerase', *Cell,* 91(1), pp. 1-3.

Zakian, V.A. (1995) 'Telomeres: beginning to understand the end', *Science (New York, N.Y.),* 270(5242), pp. 1601-1607.

Zimmermann, S., Voss, M., Kaiser, S., Kapp, U., Waller, C. and Martens, U. (2003) 'Lack of telomerase activity in human mesenchymal stem cells', *Leukemia,* 17(6), pp. 1146.